pathogens

Special Issue Reprint

Parasitic Diseases of Fish

Identification, Host-Parasite Interactions and Molecular Biology

Edited by
Gokhlesh Kumar, Arun Sudhagar and Kandasamy Saravanan

mdpi.com/journal/pathogens

MDPI

Parasitic Diseases of Fish: Identification, Host-Parasite Interactions and Molecular Biology

Parasitic Diseases of Fish: Identification, Host-Parasite Interactions and Molecular Biology

Guest Editors

Gokhlesh Kumar
Arun Sudhagar
Kandasamy Saravanan

MDPI

Basel • Beijing • Wuhan • Barcelona • Belgrade • Novi Sad • Cluj • Manchester

Guest Editors

Gokhlesh Kumar
ICAR–Central Marine
Fisheries Research Institute
Kochi
India

Arun Sudhagar
The Peninsular and Marine
Fish Genetic Resources Centre
ICAR–National Bureau of Fish
Genetic Resources
Kochi
India

Kandasamy Saravanan
ICAR—Central Institute of
Brackishwater Aquaculture
Chennai
India

Editorial Office
MDPI AG
Grosspeteranlage 5
4052 Basel, Switzerland

This is a reprint of the Special Issue, published open access by the journal *Pathogens* (ISSN 2076-0817), freely accessible at: https://www.mdpi.com/journal/pathogens/special_issues/parasitic_diseases_of_fish.

For citation purposes, cite each article independently as indicated on the article page online and as indicated below:

Lastname, A.A.; Lastname, B.B. Article Title. *Journal Name* **Year**, *Volume Number*, Page Range.

ISBN 978-3-7258-5605-3 (Hbk)
ISBN 978-3-7258-5606-0 (PDF)
https://doi.org/10.3390/books978-3-7258-5606-0

Contents

About the Editors

Gokhlesh Kumar

Gokhlesh Kumar is a Senior Scientist at the ICAR–Central Marine Fisheries Research Institute (CMFRI), Kochi, India. Prior to joining ICAR–CMFRI, Kochi, he served as a prominent researcher at the University of Veterinary Medicine, Vienna, Austria. With more than 15 years of research experience, he is a distinguished expert in fish biotechnology and fish health. Dr. Kumar has dedicated his career to advancing the understanding of fish molecular biology using proteomic and transcriptomic approaches. His research interests include the molecular biology of freshwater and marine fishes, as well as broader issues related to fish health and disease management. His scientific contributions are widely acknowledged, and his work continues to influence practices in aquaculture and fishery management. He has authored more than 60 research papers in peer-reviewed international journals and maintains active national and international research collaborations. Through his expertise and dedication, Dr. Kumar has played a pivotal role in shaping the discourse on fish biotechnology and health. His ongoing research remains instrumental in developing innovative strategies for biotechnology applications, disease prevention, and the sustainable management of aquatic environments.

Arun Sudhagar

Arun Sudhagar is currently working as a Scientist at the ICAR–National Bureau of Fish Genetic Resources, Kochi, India. With over 11 years of experience in fish health management, Dr. Sudhagar has established himself as a leading expert in the field. He earned his B.F.Sc. degree from the Fisheries College and Research Institute, Tamil Nadu Veterinary and Animal Sciences University, India, and his M.F.Sc. in Fish Pathology and Microbiology from the Central Institute of Fisheries Education, India. Dr. Sudhagar's academic journey was further distinguished by receiving the prestigious Netaji Subhas ICAR-International Fellowship, which enabled him to pursue a PhD at the Clinical Division of Fish Medicine, University of Veterinary Medicine, Vienna, Austria. His doctoral research focused on unraveling the transcriptomic changes during host–pathogen interactions in brown trout during *Tetracapsuloides bryosalmonae* infection. Dr. Sudhagar's research interests are centered on understanding the molecular mechanisms that govern host–pathogen interactions in fish, with the aim of developing innovative strategies for disease prevention and control in aquaculture.

Kandasamy Saravanan

Kandasamy Saravanan is a Senior Scientist at the ICAR-Central Institute of Brackishwater Aquaculture, Chennai, India. He earned his Ph.D. from the ICAR-Central Institute of Fisheries Education, Mumbai, India, where his research focused on the adaptive immune system of rohu (Labeo rohita), elucidating its immunocompetence, secretory IgM gene, and adaptive immune responses. With over a decade of professional experience in research and development, he has led several projects in fish health management and made significant contributions to the field. Earlier in his career, he served as a Scientist at the ICAR–Central Island Agricultural Research Institute, Port Blair, where his research encompassed aquatic animal disease surveillance, diagnostics, fish health management, antimicrobial resistance, and molecular immunology.

Preface

In aquaculture and fisheries, maintaining fish health is crucial for sustainable production, ensuring food security and supporting the economic viability of these industries. Parasitic diseases present a significant challenge, often leading to reduced growth rates, increased mortality, and compromised fish quality. These impacts can result in substantial economic losses for the fish farmers and fishery operations. Beyond the immediate economic effects, parasitic infections can also disrupt the balance of aquatic ecosystems, as infestations may spread to wild fish populations, altering species interactions and potentially reducing biodiversity. Effective management and control of parasitic diseases are therefore essential to the long-term success and sustainability of aquaculture and fisheries.

This Reprint compiles a series of insightful chapters originally published in the Special Issue of the journal *Pathogens* by MDPI publishers. These chapters explore various aspects of parasitic diseases in fish, ranging from the identification of specific parasites to the intricate host–parasite interactions and the application of molecular biology in understanding these relationships. The content spans a broad spectrum of parasitic groups, including protozoans, dinoflagellates, myxozoans, trematodes, copepods, and leeches, addressing specific research problems. Additionally, the Reprint addresses related topics such as the impact of environmental factors on parasitic infections and innovative approaches for disease management. By bringing together these diverse studies, this volume aims to serve as a valuable resource for researchers, educators, and professionals engaged in the study and management of fish health.

We express our deepest gratitude to all the authors who contributed their exceptional work to the Special Issue in *Pathogens*. Their dedication, expertise, and insights have been instrumental in the creation of this comprehensive volume on parasitic diseases in fish. Without their contributions, this Reprint would not have been possible. We also extend our sincere thanks to the Editor-in-Chief and handling staff from *Pathogens* for their guidance and meticulous oversight throughout the publication process. Their commitment to maintaining the highest standards of scientific rigor has greatly enriched this collection. Additionally, we acknowledge the invaluable efforts of our reviewers, whose critical evaluations have enhanced the quality and clarity of each chapter. We are also grateful to our colleagues and institutions for their unwavering support, and to the broader scientific community for fostering an environment of collaboration and knowledge-sharing. It is our hope that this Reprint will serve as a vital resource for researchers, educators, and practitioners in the field of fish health, inspiring ongoing research and innovation in combating parasitic diseases in fish.

Gokhlesh Kumar, Arun Sudhagar, and Kandasamy Saravanan
Guest Editors

pathogens

MDPI

Article

Proteins of the Ciliated Protozoan Parasite *Ichthyophthirius multifiliis* Identified in Common Carp Skin Mucus

Mona Saleh [1,*], Abdel-Azeem S. Abdel-Baki [2,3], Mohamed A. Dkhil [2,4], Mansour El-Matbouli [1] and Saleh Al-Quraishy [2]

1 Clinical Division of Fish Medicine, University of Veterinary Medicine, 1210 Vienna, Austria; Mansour.el-matbouli@vetmeduni.ac.at
2 Zoology Department, College of Science, King Saud University, Riyadh 11451, Saudi Arabia; aabdelbaki@science.bsu.edu.eg (A.-A.S.A.-B.); mdkhil@ksu.edu.sa (M.A.D.); squraishy@ksu.edu.sa (S.A.-Q.)
3 Zoology Department, Faculty of Science, Beni-Suef University, Beni-Suef 62521, Egypt
4 Department of Zoology and Entomology, Faculty of Science, Helwan University, Cairo 11795, Egypt
* Correspondence: mona.saleh@vetmeduni.ac.at; Tel.: +43-(12)-5077-4736

Abstract: The skin mucus is the fish primary defense barrier protecting from infections via the skin epidermis. In a previous study, we have investigated the proteome of common carp (*Cyprinus carpio*) skin mucus at two different time points (1 and 9 days) post-exposure to *Ichthyophthirius multifiliis*. Applying a nano-LC ESI MS/MS technique, we have earlier revealed that the abundance of 44 skin mucus proteins has been differentially regulated including proteins associated with host immune responses and wound healing. Herein, in skin mucus samples, we identified six proteins of *I. multifiliis* associated with the skin mucus in common carp. Alpha and beta tubulins were detected in addition to the elongation factor alpha, 26S proteasome regulatory subunit, 26S protease regulatory subunit 6B, and heat shock protein 90. The identified proteins are likely involved in motility, virulence, and general stress during parasite growth and development after parasite attachment and invasion. Two KEGG pathways, phagosome and proteasome, were identified among these parasite proteins, mirroring the proteolytic and phagocytic activities of this parasite during host invasion, growth, and development, which represent a plausible host invasion strategy of this parasite. The results obtained from this study can support revealing molecular aspects of the interplay between carp and *I. multifiliis* and may help us understand the *I. multifiliis* invasion strategy at the skin mucus barrier. The data may advance the development of novel drugs, vaccines, and diagnostics suitable for the management and prevention of ichthyophthiriosis in fish.

Keywords: aquaculture; ciliate; common carp; ichthyophthiriosis; infection; proteomics

1. Introduction

The ciliated protozoan parasite *Ichthyophthirius multifiliis* is one of the highly virulent pathogens in freshwater aquaculture and ornamental fish industries. It infects the skin and gill epithelia of virtually all species of freshwater fish. Among the main disease characteristics of fish infected with ciliates are black coloration; increased production of mucus; damage of scales; hemorrhagic, decolorized areas on the skin; and dermal necrotic lesions that ultimately damage tissues leading to high mortalities [1]. It has been proposed that theronts invade fish epithelia via moving between two cells [2,3]. Because exactly at this site the mucus cells are exposed to the fish surface, the invasive stages apparently get access to the epidermis by entering mucous cells and in this way stimulate the mucus secretion [4,5]. This was potentiated by noticing that theronts were attracted and chemotactically reacting to serum constituents in fish mucus [6]. Pathogen invasion can elicit immune reactions in the skin mucosal barrier, and fish that endure a primary infection develop resistance to re-infection [7]. Various approaches including

immunoprophylaxis and chemotherapeutics were applied for disease management. Yet, none of those methods turned into a great success, and no vaccine to control the disease triggered by *I. multifiliis* successfully had been reported [7–9]. Hence, it is crucial to monitor novel drug and vaccine opportunities for the parasite. A profounder knowledge of host parasite communication at the spot of infection may also help the development of effective management tools against *I. multifiliis* [9].

The carp skin mucus exhibits key functions in stimulating vital immune reactions that are necessary for defending fish tissues against self and parasite proteases. Actually, the protein content of fish skin mucus provides its anti-inflammatory and protective characteristics. Indeed, proteomic analyses reveal proteins related to virulence, which are produced by invaders to conquer the fish host's immune responses and to assess the composition of the protein of different fish tissues in response to environmental stressors and diseases [10]. For instance, the infection with the ectoparasite sea lice (*Lepeophtheirus salmonis*) results in excessive mucus secretion from fish skin. The alterations in the protein profile of Atlantic salmon skin mucus were assessed using proteomic analysis in response to sea lice. The identified protein component of the skin mucus included intracellular proteins, calmodulin, actin, hemopexin, plasma proteins (apolipoproteins, lectin, plasminogen, and transferrin), and ß-actin, which is the significant component [11].

Recently, the common carp skin mucus proteome profile has been assessed at 1 day and 9 days after infection with *I. multifiliis* [5,12]. A variety of proteins were differentially modulated. Several proteins essential for metabolism were upregulated, whereas multiple downregulated proteins were predominantly structural. Additionally, novel proteins were detected and could act as possible biomarkers for injuries caused during parasitic infection such as olfactomedin 4, lumican, dermatopontin, papilin, and I cytoskeletal 18 [12]. In addition, the abundance of 19 immune-related and signal transduction proteins was altered, comprising the epithelial chloride channel protein, galactose specific lectin nattection, high choriolytic enzyme 1, lysozyme C, granulin, and protein-glutamine gamma-glutamyltransferase 2 [5]. Moreover, several lectins and a varied collection of different serpins with protease inhibitory characteristics were recognized. These apparently activate the lectin pathway and regulate proteolysis, increasing the carp innate immunity and providing defensive features of the skin mucus of fish [5].

Understanding host-pathogen interactions may enable illuminating key regulators and invasion mechanisms of the parasite and fish protective strategies that can pave the way for further studies aimed at developing novel drugs for disease control in aquaculture. In the present study, we identified proteins of *Ichthyophthirius multifiliis* associated with skin mucus in infected common carp.

2. Results and Discussion

Following protein separation using SDS-PAGE (Figure 1) and in-gel digestion [13,14], six proteins of *I. multifiliis* were identified in infected carp skin mucus.

The identified proteins were: tubulins (alpha and beta), elongation factor alpha, 26S proteasome regulatory subunit, 26S protease regulatory subunit 6B, and heat shock protein 90 (Table 1) and were connected to each other and to the previously identified common carp proteins to identify the protein-protein interaction network (Figure 2).

Two KEGG pathways, phagosome and proteasome, were identified among these parasite proteins. Indeed, keratin I cytoskeletal 18 proteins were differentially modulated in common carp after exposure to *I. multifiliis*, pointing to the actions they may perform in the carp immunity when infected [12]. Keratin is a cytoskeletal protein with a key role in cell protection against mechanical and non-mechanical damage. In fish mucus, the pore formation ability of keratin provides antibacterial effects. Keratin turnover is reliant on the ubiquitin-proteasome pathway. In addition, it could be modulated in response to tissue damages due to parasite proteolytic and phagocytic activities during host invasion and development. Further, several lectins and multiple serpins with protease inhibitory effects were previously identified in *I. multifiliis*-infected carp mucus hinting at their

involvement in the activation of the lectin pathway, a cascade of serine proteases, and fine tuning of proteolysis [5].

Parasite proteins showed a protein-protein interaction with carp mucus proteins such as thioredoxin, ras GTPase-activating protein-binding protein, PDZ and LIM domain protein 1-like, lumican, and collagen alpha-1(XIV) chain-like (Figure 2). These parasite proteins are apparently involved in motility, virulence, and the general stress response during parasite growth and development after parasite attachment and host invasion.

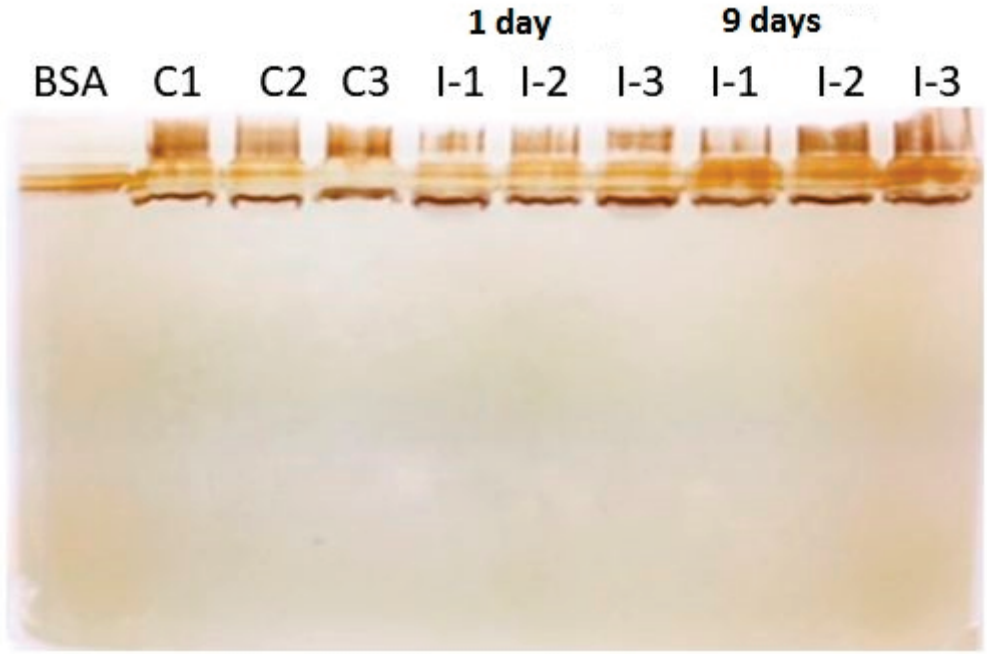

Figure 1. Silver stained 1D-gel of carp mucus protein samples. BSA: bovine serum albumin, C1–C3: control mucus samples, and I-1-3: Ichthyophthirius multifiliis-infected carp mucus samples at 3 and 9 days post exposure.

Table 1. Identified *Ichthyophthirius multifiliis* proteins in the skin mucus of infected common carp.

UniProt Accession Number	Protein	Confident Peptides	Coverage (%)	Function
G0QTP1_ICHMG	Tubulin alpha chain	12	25.4	Microtubule-based process
G0QMB0_ICHMG	Tubulin beta chain	9	33.0	Microtubule-based process
G0QQR6_ICHMG	Elongation factor 1-alpha	8	18.2	Translation elongation factor activity
G0R170_ICHMG	26S proteasome regulatory subunit	3	5.3	Protein catabolic process
G0QY27_ICHMG	26S protease regulatory subunit 6B/AAA domain-containing protein	3	10.1	Protein catabolic process
G0QRA5_ICHMG	Heat shock protein 90/HATPase_c domain-containing protein	3	5.8	Protein folding

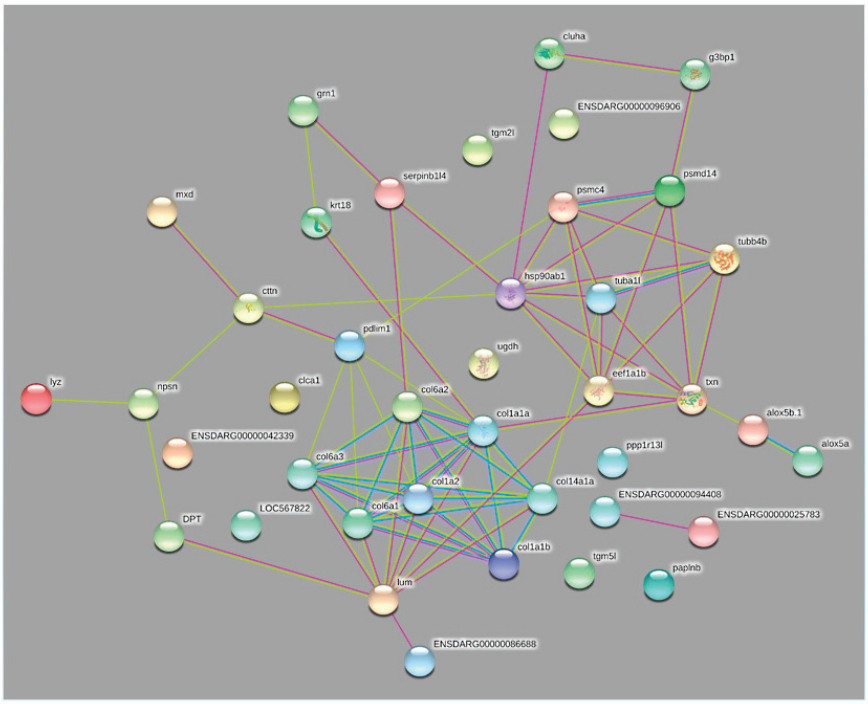

Figure 2. Parasite proteins showing protein-protein interaction with carp mucus proteins. The protein-protein interaction network of carp mucus and *Ichthyophthirius multifiliis* identified proteins. Parasite proteins (tuba1 (alpha tubulin), tubb4b (beta tubulin), eef1a1b (elongation factor 1-alpha; EF-1α), psmd14 (26S proteasome regulatory subunit), psmc4 (26S protease regulatory subunit 6B), and hsp90ab1 (heat shock protein 90; hsp90)) are connected to each other and showed protein-protein interaction with carp mucus proteins thioredoxin, ras GTPase-activating protein-binding protein, PDZ and LIM domain protein 1-like, lumican, and collagen alpha-1(XIV) chain-like. In this network, nodes are proteins; the predicted functional associations are shown as lines, and the strength of predicted functional interactions between proteins is shown as the number of lines. The yellow lines show text-mining evidence; the purple lines denote experimental evidence, and the database evidence is shown as light blue lines.

2.1. The 26S Proteosome

The 26S proteosome complex and 26S protease regulatory subunit 6B were identified in the infected carp skin mucus. Proteases in parasitic protozoa have drawn much attention as prospective drug targets owing to their crucial functions in growth and pathogenicity, and because of the possibility of constructing specific inhibitors [15–18]. Two cathepsin L cysteine proteases (Icp1 and Icp2) of the C1 papain peptidase family have been described in *I. multifiliis* and suggested to be involved in the disease progression. The cathepsin L cysteine proteases were found to be differentially modulated between all life-stages of *I. multifiliis* and likely involved in host-pathogen interactions [19]. Parasitic protozoa proteases have been shown to play important roles in the overwhelming of host cells and development, encystment and excystment, cytoadherence, and stimulation and evasion of host immune responses, as well as catabolism of host proteins for a nutrient purpose [20,21]. In fish pathogenic ciliates, proteases are key to overcome host immune defenses and lysis of host cells [19] and the marine ciliate *Philasterides dicentrarchi* [22]. Fish parasites generate proteolytic enzymes to lyse collagen and other structural particles to induce deterioration of external epithelia to weaken host defenses [12,22]. In fact, the prevalent increased upregulation of cathepsin L cysteine protease was seen in the infectious stages [19,23]. The proteolytic protein collection (degradome) of the *I. multifiliis* consists of 254 protease homologs, approximately 3.1% of the proteome. The massive retention of duplicates 39 ubiquitin carboxyl-terminal hydrolase family members and 15 members of the threonine proteases occurred due to extensive gene duplication events. This mirrors the fundamental function of the proteasome system in *I. multifiliis* regulating cell-cycle and stress responses [24].

In ciliates, during cell differentiation and transition, prompt alterations in the morphology of cell structure are accompanied with the lysis of numerous proteins. The evidence is increasing that the

proteasome system plays crucial role in the degradation of proteins. Further, the 26S proteasome non-ATPase regulatory subunit gene expression was significantly upregulated during cell differentiation of the freshwater ciliate *Pseudourostyla cristata* [25]. Indeed, the *I. multifiliis* 26S proteosome complex and the 26S protease regulatory subunit 6B proteins were identified in infected carp mucus samples. This highlights the importance of these molecules for the regulation of the degradation process of host cell proteins essential for host invasion.

The protein-protein interaction network presented the *I. multifiliis* 26S proteasome connected to carp mucus thioredoxin and ras GTPase-activating protein-binding protein.

As a component of the antioxidant system in living cells, thioredoxins are key for the regulating of redox potential. The increased value of thioredoxin-like isoform X2 protein of *I. multifiliis* observed in carp was aimed at reducing oxidative stress to protect carp against the proteolytic activity of *I. multifiliis* [5]. Indeed, in the current study, the protein-protein interaction network presented the *I. multifiliis* 26S proteasome connected to ras GTPase-activating protein-binding protein agreeing with the previous finding. Ras GTPase-activating protein-binding protein was also augmented in infected common carp mucus samples. This protein was suggested to activate an immune response in carp against *I. multifiliis* [5]. Ras-related proteins are involved in signal transduction, the regulation of TCR signaling, T cell cytoskeletal reorganization, T cell migration, and T cell apoptosis [26]. The protein-protein interaction network displayed 26S proteasome connected to carp mucus thioredoxin and ras GTPase-activating protein-binding protein and likely activates signal transduction and triggers immune defense in carp.

Further, in the current study, the protein-protein interaction network shows that the 26S protease regulatory subunit 6B of *I. multifiliis* connects to PDZ and LIM domain protein 1-like. LIM proteins have been observed to alter NF-κB-mediated signaling in the cytoplasm. It has been reported that PDLIM1 sequestered p65 subunit of NF-κB in the cytoplasm and inhibited its nuclear translocation in an IκBα-independent way [27]. In an earlier investigation, Saleh et al. (2018) observed that the abundance of PDZ and LIM domain protein 1-like was highly increased in common carp, suggesting a suppressive role in the carp immune response once exposed to *I. multifiliis*. This protein seems to trigger the activation of the PDZ and LIM domain protein 1-like aiming at suppressing common carp immune defense as a part of the *I. multifiliis* invasion strategy.

2.2. Elongation Factor Alpha

The parasite elongation factor alpha (EF-1α) was identified in the skin mucus of *I. multifiliis*-exposed carp mucus samples. Given that EF-1α has a distinct role in protein synthesis, it is involved in the whole course of the heat shock response in mammalian cells. EF-1α is among the best conserved and highly abundant proteins in the eukaryotic cell and was reported to contribute to the activation of heat shock transcription factors (HSFs) [28]. HSFs sustain protein homeostasis via modulating the expression of heat shock proteins, particularly in stress conditions [29]. Upon stress, EF-1α rapidly activates the transcription of heat shock proteins. This process is affected when EF-1α is inhibited [30]. The identified EF-1α *I. multifiliis* in infected carp mucus purposes its involvement in the activation of HSFs during host invasion.

When analyzing the proteome of the protozoan parasite *Leishmania donovani* exosomes, many proteins including EF-1α and heat shock protein 90 (hsp90) previously reported to enter the cytosol of leishmania-infected macrophages were cargos of these exosomes [31]. Leishmania EF-1α is a part of the exosome and can be transported to macrophage cytosol. It interacts with host Src homology region 2 domain-containing phosphatase-1 (SHP-1), resulting in a deactivated macrophage phenotype. Thus, EF-1α has been considered as a novel virulence factor in *L. donovani*. In ciliates, EF-1α has been shown to interact with cytoskeletal proteins, including tubulin and actin, in numerous organisms [32]. Ciliates have a distinctive cytoskeletal organization that primarily consists of microtubules. In *Tetrahymena*, EF-1α has been reported to bind to F-actin [33]. It has been demonstrated that EF-1α directly binds to β-tubulin [34]. EF-1α appears to have numerous functions such as the translation of mRNA and tubulin binding.

The protein-protein interaction network shows that elongation factor alpha connects to carp mucus lumican and thioredoxin proteins. Lumican controls collagen fibrillogenesis, which supports keeping and maintaining clear corneas as well as stimulating corneal epithelial tissue repair and promoting the

structure of numerous other connective tissues such as sclera and skin and as a chemokine gradient maker. It has been reported that lumican contributes to bacterial lipopolysaccharide distinguished by the Toll-like receptor 4 signaling pathway and innate immune response [35]. The abundance of lumican protein was significantly decreased, correlating with the infection and growth of *I. multifiliis*, suggesting that it has a role in immune response and wound healing [12]. Thioredoxins are pivotal in the antioxidant system and a key regulator of redox potential in living cells. The increased value of thioredoxin of *I. multifiliis* observed in carp samples was aimed at reducing oxidative stress to defend carp against the harmful effects of *I. multifiliis* [5]. *I. multifiliis* elongation factor alpha was connected to carp mucus lumican (downregulated) and thioredoxin (increased) proteins likely to affect the carp immune response as a part of a host-manipulating strategy.

2.3. Tubulins

I. multifiliis contains 9 of the 14 highly conserved core proteins associated with centriole and basal body biogenesis and function [24].

Alpha and beta tubulins of *I. multifiliis* were identified in the infected carp skin mucus.

Motility has been reported to be particularly essential for mucus colonizers such as *V. salmonicida*, as this is favorable in viscous environments such as mucus [36]. A high number of proteins was differentially regulated and uniquely abundant in the theronts but not in the trophont stages of *I. multifiliis* [9]. Among these, proteins correlating with and associated with motility were highly abundant in the theronts' stages, which reflect the critical need of these parasite stages for rapid and continued motility concomitant with host finding and the infection process [37–39].

In the current study, alpha and beta tubulins of *I. multifiliis* were identified in the infected carp skin mucus. This reflects the critical need of *I. multifiliis* for proteins associated with movement during host invasion to ensure rapid and continued motility associated with host finding and the infection process. Additionally, the presented protein-protein interaction network demonstrates that tubulin alpha connects to carp mucus collagen alpha-1(XIV) chain-like and thioredoxin proteins, and tubulin beta connects to thioredoxin.

In fact, the abundance of 11 collagen-alpha family members including collagen alpha-1(XIV) chain-like was extremely reduced in a process of the massive degradation of collagen [12]. This was likely aimed at tissue remodeling, wound healing to concur with injures, and tissue damage of common carp during *I. multifiliis* attachment, movement, and growth. In addition, the increased value of *I. multifiliis* thioredoxin in common carp mucus was likely aimed at reducing oxidative stress during parasite movement and development.

2.4. Heat Shock Protein 90

In the present study, hsp90 of *I. multifiliis* was detected in carp skin mucus samples. Heat shock proteins are acknowledged virulence factors in a number of bacteria such as *Vibrio salmonicida* and *Salmonella typhimurium*. A 66 kDa hsp of *S. typhimurium* was reported to be needed for adhesion to mucosal cells [40]. In *V. salmonicida*, the hsps DnaK and GroEL were significantly induced in response to skin mucus [36]. Hsps were also suggested to support the survival of bacteria in their hosts [41]. Heat shock response is a strongly regulated and coordinated response that is indispensable for cell survival under stress. While many hsps mRNAs are present in only very low amounts in unchallenged conditions, their synthesis, stability, and translation increase considerably upon stress [42]. The hsp90 of *Leishmania donovani* plays a key role in homeostasis control and the development of this protozoan parasite. It is also involved in cell cycle control and the cellular stress response [29]. The molecular interaction mediated by hsp90 was suggested to be involved in regulating cortical patterning in *Tetrahymena*, and hsp70 and hsp90 were distinguished in the cilia of *Tetrahymena* [43,44]. Hsp90 chaperones are implicated in intracellular morphogenesis, and hsp90 was found in centrosomes in *Drosophila* and mammalian cell lines and in the basal body region of developing *Drosophila* sperm [45]. In *Tetrahymena thermophila*, at 41 °C, the binding of hsp82p with tubulin at a high temperature (stress) was observed after isolation of an immunoprecipitated hsp82p-hsp73p-tubulin complex from a sucrose density gradient [43]. At the cellular level, both monoclonal and polyclonal antibodies against hsp82p produced general cytoplasmic staining. However, monoclonal antibodies against a 12-amino acid synthetic peptide prepared from a fragment of hsp82p amino acid sequence similarly stained ciliary

basal bodies more intensely than the cytoplasmic background [43]. The binding of hsp82p with cortical microtubules occurs at sublethal elevated temperatures (stress) when this protein becomes more abundant and builds complexes with soluble tubulin and with the increased hsp70. This is likely a mechanism for the protection of many proteins in heat-stressed cells [46].

Many genes were differentially expressed among all three life-cycle stages of *I. multifiliis* [23]. Numerous identified genes have a role in cell structure, cell regulation and genes of protein assembly, folding, and translocation, such as hsp70 and hsp90. Additionally, several transcripts comprised cell structural and regulatory proteins including tubulins. Further, hsps are dominant antigens in the immune response to a variety of pathogens. In a previous study, as an immobilization antigen vaccine adjuvant, heat shock protein 70 showed a high protection in fish against *Cryptocaryon irritans* [47]. It has been also reported that tomonts from vulnerable carp were immobilized in in vitro assays when treated with the serum or mucus of immune fish [48]. Immobilization of *I. multifiliis* by humoral elements in the blood and mucus points to a prospective mechanism of host immunity. Antibodies in the mucus likely hinder entering of the parasite into the host, and re-infection is impeded because of possible direct antibody binding and complement activation, or due to antibody-dependent cell-mediated activities [48]. The identification of serum and cutaneous mucosal antibodies recognizing i-antigen has been reported to be associated with effective immune responses when exposed to *I. multifiliis* [49]. Hence, it was anticipated that vaccination against *I. multifilliis* could be achieved. However, to date, there is no cost-effective vaccine available against *I. multifiliis*.

In the current study, *I. multifiliis* hsp90 protein was detected in infected common carp mucus. Hsp90 in *I. multifiiis*-infected carp mucus samples suggests that it builds complexes with tubulin and hsp70 (highly induced in theronts) in a mechanism for protection of a large number of proteins due to stress during host invasion and growth, agreeing with previous reports in *Tetrahymena* [48]. The protein-protein interaction presented hsp90 connected to carp mucus src substrate cortactin-like, leukocyte elastase inhibitor, clustered mitochondria protein homolog, and thioredoxin proteins. Indeed, the carp Src substrate cortactin-like protein was modulated in response to *I. multifiiis* [12]. Cortactin controls actin assembly by activating actin polymerization. Cortactin was identified as the substrates of Src family kinases. Damage to the surface of intact articular cartilage stimulates Src-like kinases, along with MAPKs and IKK, which regulate o NF-κB [50]. Sea lice infection leads to the presence of cleaved fragments from actin and transferrin, suggesting the proteolytic activity of the parasite [11]. The introduction of *L. major* to fibroblasts l caused inhibition of cortactin [51]. The modulation of cortactin in infected carp mucus likely stimulates NF-κB, directed at decreasing inflammatory responses and tissue destruction triggered by *I. multifiliis*.

LEIs belong to the serpins family of proteins, likely stimulated by invading pathogens and have a role in the inhibition and alteration of protease activity directed at reducing host tissue injuries, inflammatory reactions, and apoptosis caused by damaging pathogens [5,52]. Carp LEI proteins increased in response to *I. multifiliis* exposure were proposed to play a role in the inhibition of endogenous proteases to protect leucocytes from degradation and to limit the effects of exogenous proteases of *I. multifiliis* produced during infection [5]. We suggest that carp LEIs are stimulated and activated by *I. multifiliis* hsp90, and hence it might be useful as a vaccine candidate/adjuvant as these molecules prevent leucocytes from degradation and are essential for their survival. The abundance of clustered mitochondria protein homolog (CLUH) and thioredoxin proteins was induced aiming to coordinate the carp immune response and cope with oxidative stress and adverse effects caused by this ciliate.

3. Materials and Methods

3.1. Ethics Statement

The experiments have been approved by the Animal Experimentation Ethics Committee of Vienna University of Veterinary medicine (BMWFW-68.205/0051-WF/V/3b/2016). The experiments were performed in accordance with relevant guidelines and regulations.

3.2. Common Carp and Collection of Skin Mucus

The details of the common carp experimental setup have been described in our earlier study [12]. Prior to infection, common carp (11 $\pm$ 1 cm) were distributed between 6 aquaria, 6 fish per aquarium. There were two groups, exposed and non-exposed control. The fish were exposed to *I. multifiliis* by

cohabitation with naturally infected giant gouramis (*Osphronemus goramy*) obtained from a pet store—a method that mimics natural exposure. The giant gouramis were certified as free from *Aphanomyces invadans* and the Epizootic Haematopoietic Necrosis Virus. Examinations of the giant gouramis did not reveal the incidence of any other ectoparasite or signs of a secondary bacterial infection. At 1 and 9 days post-exposure (dpe), common carp ($N = 3$) from each of the infected and non-infected control groups were anaesthetized using ethyl 3-aminobenzoate methanesulfonate (Sigma, Darmstadt, Germany) (MS-222; 100 mg/L). Sterile, glass slides were used to collect mucus from fish skin, while avoiding blood contamination, and excluding the ventral body surface close to the anal pore, to prevent fecal contamination. The collected mucus was transferred into 1.5 mL microcentrifuge tubes, immediately placed on ice, then snap-frozen in liquid nitrogen and stored at −80 °C for proteomic analysis.

3.3. Protein Extraction, Separation, and In-Gel Digestion

Mucus samples were solubilized in a denaturing lysis buffer (7 M urea, 2 M thiourea, 4% CHAPS, and 1% DTT) containing a mammalian protease inhibitor cocktail. The samples were subjected to sonication on ice, and supernatants were collected by centrifugation. The protein concentration of each sample was measured using the Pierce 660 nm Protein Assay according to the manufacturer's instructions. The samples were subjected to electrophoresis on 10% SDS-PAGE in biological and technical triplicate, and the gels were stained with silver staining. Protein bands were excised from the gels and were reduced and alkylated [13]. In-gel digestion was performed using trypsin (20 ng/µL) at 37 °C for 8 h according to [14]. Afterwards, peptides were extracted, dried, and redissolved in 0.1% trifluoroacidic acid.

3.4. Mass Spectrometry

Tryptic peptides were separated on a nano-HPLC Ultimate 3000 RSLC system (Dionex, Sunnyvale, CA, USA) and analyzed with a high-resolution hybrid triple quadrupole time of flight mass spectrometer (TripleTOF 5600+, Sciex, Framingham, MA, USA). Details of the LC–MS/MS procedure were described earlier [12]. Acquired raw data were processed with ProteinPilot Software version 5.0 (Sciex). The database consisted of NCBI and UniProt entries of the following taxonomies: *Ichthyophthirius multifiliis* (taxonomy id: 5932) and the common Repository of Adventitious proteins (available online: ftp://ftp.thegpm.org/fasta/cRAP/crap.fasta (accessed on 5 April 2021)). Mass tolerances in MS mode were 0.05 Da, and 0.1 Da in MSMS mode, for the rapid re-calibration search, and 0.0011 Da in MS and 0.01 Da in MSMS mode for the final search. The following parameters were used: trypsin digestion, cysteine alkylation with iodoacetamide, and rapid ID. The false discovery rate analysis was set to <1% on the protein and on the peptide level.

Proteomics data have been deposited in the ProteomeXchange Consortium via the PRIDE (Cambridge, UK) partner repository with the dataset identifier PXD011148.

To determine the protein-protein interaction network of carp mucus and *I. multifiliis* proteins, amino acid sequences of previously identified mucus proteins [5,12] and 6 *I. multifiliis* proteins were analyzed using homologs of *Danio rerio* by using STRING software (version 11.0). A representation of the protein-protein interaction network was performed at confidence score 0.15 in the text-mining, experiment, and databases.

4. Conclusions

The identification of these six *I. multifiliis* proteins in infected common carp skin mucus suggests their possible role in the host invasion strategy of this ciliate to conquer host immune defenses effectively. The identification of hsp90 during infection hints that it is a suitable drug and vaccine target and may function as an antigen vaccine adjuvant in a way similar to that of *C. irritans*. Further, in addition to hsp90, which is likely activated by eEF through HSFs, the identification of b-tubulins (important for ciliary function) suggests roles in mobility and viability of the parasite as well as in homeostasis control and the cellular stress response during host invasion and growth, as previously suggested for other protozoan parasites. The identified proteins are implicated in the heat shock response, suggesting they are likely key for parasite development, virulence, and pathogenicity. However, functional experiments and host-parasite interaction studies are required to confirm and elucidate the precise mechanisms of *I.*

multifiliis pathogenesis. This may help us discover potential vaccine and drug targets, which could support the management of ichthyophthiriosis in aquaculture.

Author Contributions: M.S., M.E.-M., and S.A.-Q. designed the study. M.S. performed the experiments. M.S., A.-A.S.A.-B., and M.A.D. analyzed the data. M.S. drafted the manuscript. A.-A.S.A.-B., M.A.D., M.E.-M., and S.A.-Q. revised the manuscript. All authors have read and agreed to the published version of the manuscript.

Funding: This project was funded by the National Plan for Science, Technology, and Innovation (MAARIFAH), King Abdulaziz City for Science and Technology, Kingdom of Saudi Arabia, Award Number (13-NAN2121-02).

Institutional Review Board Statement: All experiments were approved by the Animal Experimentation Ethics Committee of Vienna University of Veterinary medicine (BMWFW-68.205/0051-WF/V/3b/2016). All experiments were performed in accordance with relevant guidelines and regulations.

Informed Consent Statement: Not applicable.

Data Availability Statement: The data presented in this study are available on request from the corresponding author.

Acknowledgments: The authors would like to thank Ebrahim Razzazi-Fazeli and the vetcore proteomics service unit at the University Veterinary Medicine, Vienna for the proteomic analyses. Many thanks for Gokhlesh Kumar for his help and support during the proteomic analyses.

Conflicts of Interest: The authors declare no conflict of interest.

References

1. Esteban, M.A. An overview of the immunological defenses in fish skin. *ISRN Immunol.* **2012**, 1–29. [CrossRef]
2. Ewing, M.S.; Black, M.C.; Blazer, K.M.; Kocan, K.M. Plasma chloride and gill epithelial response of channel catfish to infection with *Ichrhyophrhirius mulrifiliis*. *J. Aqua. Anim. Health.* **1994**, *6*, 187–196. [CrossRef]
3. Kozel, T.R. Scanning electron microscopy of theronts of *Ichthyophthirius multifiliis*: Their penetration into host tissues. *Trans. Am. Microsc. Soc.* **1986**, *105*, 357–364. [CrossRef]
4. Buchmann, K.; Lindenstrøm, T.; Sigh, J. Partial cross-protection against *Ichthyophthirius multifiliis* in *Gyrodactylus derjavini* immunized rainbow trout. *J. Helminthol.* **1999**, *73*, 189–195. [CrossRef] [PubMed]
5. Buchmann, K.; Nielsen, M.E. Chemoattraction of *Ichthyophthirius multifiliis* (Ciliophora) to host molecules. *Int. J. Parasitol.* **1999**, *29*, 1415–1423. [CrossRef]
6. Buchmann, K.; Sigh, J.; Nielsen, C.V.; Dalgaard, M. Host responses against the fish parasitizing ciliate *Ichthyophthirius multifiliis*. *Vet. Parasitol.* **2001**, *100*, 105–116. [CrossRef]
7. Saleh, M.; Kumar, G.; Abdel-Baki, A.A.; Dkhil, M.A.; El-Matbouli, M.; Al-Quraishy, S. Quantitative proteomic profiling of immune responses to *Ichthyophthirius multifiliis* in common carp skin mucus. *Fish Shellfish Immunol.* **2019**, *84*, 834–842. [CrossRef]
8. Hines, R.S.; Spira, D.T. Ichthyophthiriasis in the mirror carp *Cyprinus carpio* (L.) V. Acquired immunity. *J. Fish Biol.* **1974**, *6*, 373–378. [CrossRef]
9. Yao, J.-Y.; Xu, Y.; Yuan, X.-M.; Yin, W.-L.; Yang, G.-L.; Lin, L.-Y.; Pan, X.-Y.; Wang, C.-F.; Shen, J.-Y. Proteomic analysis of differentially expressed proteins in the two developmental stages of *Ichthyophthirius multifiliis*. *Parasitol. Res.* **2017**, *116*, 637–646. [CrossRef]
10. Ahmed, F.M.; Kumar, G.; Soliman, F.M.; Adly, M.A.; Soliman, H.A.M.; El-Matbouli, M.; Saleh, M. Proteomics for understanding pathogenesis, immune modulation and host pathogen interactions in aquaculture. Comp. Biochem. *Physiol. Part D Genom. Proteom.* **2019**, *32*, 100625.
11. Easy, R.H.; Ross, N.W. Changes in Atlantic salmon (*Salmo salar*) epidermal mucus protein composition profiles following infection with sea lice (*Lepeophtheirus salmonis*). *Comp. Biochem. Physiol. Part D Genom. Proteom.* **2009**, *4*, 159–167. [CrossRef]
12. Saleh, M.; Kumar, G.; Abdel-Baki, A.A.; Dkhil, M.A.; El-Matbouli, M.; Al-Quraishy, S. Quantitative shotgun proteomics distinguishes wound-healing biomarker signatures in common carp skin mucus in response to *Ichthyophthirius multifiliis*. *Vet Res.* **2018**, *49*, 37. [CrossRef]
13. Jiménez, C.R.; Huang, L.; Qiu, Y.; Burlingame, A.L. In-gel digestion of proteins for MALDI-MS fingerprint mapping. *Curr. Protoc. Protein Sci.* **2001**, *16*, 4. [CrossRef] [PubMed]
14. Shevchenko, A.; Wilm, M.; Vorm, O.; Mann, M. Mass spectrometric sequencing of proteins from silver-stained polyacrylamide gels. *Anal. Chem.* **1996**, *68*, 850–858. [CrossRef] [PubMed]
15. Atkinson, H.J.; Babbitt, P.C.; Sajid, M. The global cysteine peptidase landscape in parasites. *Trends Parasitol.* **2009**, *25*, 573–581. [CrossRef] [PubMed]
16. Blackman, M.J. Malarial proteases and host cell egress: An 'emerging' cascade. *Cell Microbiol.* **2008**, *10*, 1925–1934. [CrossRef] [PubMed]

17. Kuang, R.; Gu, J.; Cai, H.; Wang, Y. Improved prediction of malaria degradomes by supervised learning with SVM and profile kernel. *Genetica* **2009**, *136*, 189–209. [CrossRef]
18. Wu, Y.; Wang, X.; Liu, X.; Wang, Y. Data-mining approaches reveal hidden families of proteases in the genome of malaria parasite. *Genome Res.* **2003**, *13*, 601–616. [CrossRef]
19. Jousson, O.; Di Bello, D.; Donadio, E.; Felicioli, A.; Pretti, C. Differential expression of cysteine proteases in developmental stages of the parasitic ciliate *Ichthyophthirius multifiliis*. *FEMS Microbiol. Lett.* **2007**, *269*, 77–84. [CrossRef]
20. Klemba, M.; Goldberg, D.E. Biological roles of proteases in parasitic protozoa. *Annu. Rev. Biochem.* **2002**, *71*, 275–305. [CrossRef]
21. Sajid, M.; McKerrow, J.H. Cysteine proteases of parasitic organisms. *Mol. Biochem. Parasitol.* **2002**, *120*, 1–21. [CrossRef]
22. Parama, A.; Iglesias, R.; Alvarez, M.F.; Leiro, J.; Ubeira, F.M.; Sanmartin, M.L. Cysteine proteinase activities in the fish pathogen *Philasterides dicentrarchi* (Ciliophora: Scuticociliatida). *Parasitology* **2004**, *128*, 541–548. [CrossRef]
23. Abernathy, J.; Xu, D.H.; Peatman, E.; Kucuktas, H.; Klesius, P.; Liu, Z.J. Gene expression profiling of a fish parasite *Ichthyophthirius multifiliis*: Insights into development and senescence-associated avirulence. *Comp. Biochem. Phy. D* **2011**, *6*, 382–392. [CrossRef] [PubMed]
24. Coyne, R.S.; Hannick, L.; Shanmugam, D.; Hostetler, J.B.; Brami, D.; Joardar, V.S.; Johnson, J.; Radune, D.; Singh, I.; Badger, J.H.; et al. Comparative genomics of the pathogenic ciliate *Ichthyophthirius multifiliis*, its free-living relatives and a host species provide insights into adoption of a parasitic lifestyle and prospects for disease control. *Genome Biol.* **2011**, *12*, 100. [CrossRef] [PubMed]
25. Gao, X.; Chen, F.; Niu, T.; Qu, R.; Chen, J. Large-scale identification of encystment-related proteins and genes in *Pseudourostyla cristata*. *Sci. Rep.* **2015**, *5*, 11360. [CrossRef] [PubMed]
26. Timmerhaus, G.; Krasnov, A.; Nilsen, P.; Alarcon, M.; Afanasyev, S.; Rode, M.; Takle, H.; Jørgensen, S.M. Transcriptome profiling of immune responses to cardiomyopathy syndrome (CMS) in Atlantic salmon. *BMC Genom.* **2012**, *12*, 459. [CrossRef] [PubMed]
27. Ono, R.; Kaisho, T.; Tanaka, T. PDLIM1 inhibits NF-κB-mediated inflammatory signaling by sequestering the p65 subunit of NF-κB in the cytoplasm. *Sci. Rep.* **2015**, *5*, 18327. [CrossRef] [PubMed]
28. Shamovsky, I.; Ivannikov, M.; Kandel, E.S.; Gershon, D.; Nudler, E. RNA-mediated response to heat shock in mammalian cells. *Nature* **2006**, *440*, 556–560. [CrossRef] [PubMed]
29. Wiesgigl, M.; Clos, J. Heat shock protein 90 homeostasis controls stage differentiation in *Leishmania donovani*. *Mol. Biol. Cell* **2001**, *12*, 3307–3316. [CrossRef] [PubMed]
30. Vera, M.; Pani, B.; Griffiths, L.A.; Muchardt, C.; Abbott, C.M.; Singer, R.H.; Nudler, E. The translation elongation factor eEF1A1 couples transcription to translation during heat shock response. *eLife* **2014**, *3*, e03164. [CrossRef] [PubMed]
31. Silverman, J.M.; Clos, J.; De'Oliveira, C.C.; Shirvani, O.; Fang, Y.; Wang, C.; Foster, L.J.; Reiner, N.E. An exosome-based secretion pathway is responsible for protein export from Leishmania and communication with macrophages. *J. Cell Sci.* **2010**, *123*, 842–852. [CrossRef]
32. Durso, N.A.; Cyr, R.J. Beyond translation: Elongation factor-1α and the cytoskeleton. *Protoplasma* **1994**, *180*, 99–105. [CrossRef]
33. Kurasawa, Y.; Hanyu, K.; Watanabe, Y.; Numata, O. F-actin bundling activity of *Tetrahymena* elongation factor 1α is regulated by Ca^{2+}/calmodulin. *J. Biochem.* **1996**, *119*, 791–798. [CrossRef]
34. Nakazawa, M.; Moreira, D.; Laurent, J.; Le Guyader, H.; Fukami, Y.; Ito, K. Biochemical analysis of the interaction between elongation factor 1alpha and alpha/beta-tubulins from a ciliate, *Tetrahymena pyriformis*. *FEBS Lett.* **1999**, *453*, 29–34. [CrossRef]
35. Wu, F.; Vij, N.; Roberts, L.; Lopez-Briones, S.; Joyce, S.; Chakravarti, S. A novel role of the lumican core protein in bacterial lipopolysaccharide-induced innate immune response. *J. Biol. Chem.* **2007**, *282*, 26409–26417. [CrossRef]
36. Raeder, I.L.; Paulsen, S.M.; Smalås, A.O.; Willassen, N.P. Effect of fish skin mucus on the soluble proteome of *Vibrio salmonicida* analysed by 2-D gel electrophoresis and tandem mass spectrometry. *Microb. Pathog.* **2007**, *42*, 36–45. [CrossRef] [PubMed]
37. Hennessey, T.M.; Kim, D.Y.; Oberski, D.J.; Hard, R.; Rankin, S.A.; Pennock, D.G. Inner arm dynein 1 is essential for Ca++-dependent ciliary reversals in *Tetrahymena thermophila*. *Cell Motil. Cytoskel.* **2002**, *53*, 281–288. [CrossRef] [PubMed]
38. Wood, C.R.; Hard, R.; Hennessey, T.M. Targeted gene disruption of dynein heavy chain 7 of *Tetrahymena thermophila* results in altered ciliary waveform and reduced swim speed. *J. Cell Sci.* **2007**, *120*, 3075–3085. [CrossRef] [PubMed]
39. Cassidy-Hanley, D.M.; Pratt, C.M.; Pratt, L.H.; Devine, C.; Hossain, M.M.; Dickerson, H.W.; Clark, T.G. Transcriptional profiling of stage specific gene expression in the parasitic ciliate *Ichthyophthirius multifiliis*. *Mol. Biochem. Parasit.* **2011**, *178*, 29–39. [CrossRef] [PubMed]
40. Ensgraber, M.; Loos, M. A 66-kilodalton heat shock protein of *Salmonella typhimuriumis* responsible for binding of the bacterium to intestinal mucus. *Infect. Immun.* **1992**, *60*, 3072–3078. [CrossRef]
41. Johnson, K.; Charles, I.; Dougan, G.; Pickard, D.; Gaora, P.Ó.; Costa, G.; Ali, T.; Miller, I.; Hormaeche, C. The role of a stress–response protein in *Salmonella typhimurium* virulence. *Mol. Microb.* **1991**, *5*, 401–407. [CrossRef] [PubMed]
42. Lindquist, S.; Craig, E.A. The heat-shock proteins. *Ann. Rev. Gen.* **1988**, *22*, 631–677. [CrossRef]
43. Williams, N.E.; Nelsen, E.M. HSP70 and HSP90 homologs are associated with tubulin in hetero-oligomeric complexes, cilia and the cortex of *Tetrahymena*. *J. Cell Sci.* **1997**, *110*, 1665–1672. [CrossRef] [PubMed]
44. Frankel, J.; Williams, N.E.; Nelsen, E.M.; Keeling, P.J. An evaluation of Hsp90 as a mediator of cortical patterning in *Tetrahymena*. *J. Eukaryot. Microbiol.* **2001**, *48*, 147–160. [CrossRef] [PubMed]
45. Lange, B.M.H.; Bachi, A.; Wilm, M.; Gonzalez, C. Hsp90 is a core centrosomal component and is required at different stages of the centrosome cycle in Drosophila and vertebrates. *EMBO J.* **2000**, *19*, 1252–1262. [CrossRef] [PubMed]

46. Freeman, B.C.; Morimoto, R.I. The human cytosolic molecular chaperones, hsp90, hsp70 (hsc-70) and hdj-l have distinct roles in recognition of a non-native protein and protein refolding. *EMBO J.* **1996**, *15*, 2969–2979. [CrossRef]
47. Josepriya, T.A.; Chien, K.H.; Lin, H.Y.; Huang, H.N.; Wu, C.J.; Song, Y.L. Immobilization antigen vaccine adjuvanted by parasitic heat shock protein 70C confers high protection in fish against cryptocaryonosis. *Fish Shellfish Immunol.* **2015**, *45*, 517–527. [CrossRef]
48. Clark, T.G.; Gao, Y.; Gaertig, J.; Wang, X.; Cheng, G. The i-antigens of *Ichthyophthirius multifiliis* are GPI-anchored proteins. *J. Eukaryot. Microbiol.* **2001**, *48*, 332–337. [CrossRef]
49. Gonzalez, S.F.; Chatziandreou, N.; Nielsen, M.E.; Li, W.; Rogers, J.; Taylor, R.; Santos, Y.; Cossins, A. Cutaneous immune responses in the common carp detected using transcript analysis. *Mol. Immunol.* **2007**, *4*, 1664–1679. [CrossRef]
50. Watt, F.E.; Ismail, H.M.; Didangelos, A.; Peirce, M.; Vincent, T.L.; Wait, R.; Saklatvala, J. Src and fibroblast growth factor 2 independently regulate signaling and gene expression induced by experimental injury to intact articular cartilage. *Arthritis Rheum* **2013**, *65*, 397–407. [CrossRef]
51. Halle, M.; Gomez, M.A.; Stuible, M.; Shimizu, H.; McMaster, W.R.; Olivier, M.; Tremblay, M.L. The Leishmania surface protease GP63 cleaves multiple intracellular proteins and actively participates in p38 mitogen-activated protein kinase inactivation. *J. Biol. Chem.* **2009**, *284*, 6893–6908. [CrossRef] [PubMed]
52. Cordero, H.; Brinchmann, M.F.; Cuesta, A.; Meseguer, J.; Esteban, M.A. Skin mucus proteome map of European sea bass (*Dicentrarchus labrax*). *Proteomics* **2015**, *15*, 4007–4020. [CrossRef] [PubMed]

pathogens

MDPI

Communication

Outbreak of Parasitic Dinoflagellate *Piscinoodinium* sp. Infection in an Endangered Fish from India: Arulius Barb (*Dawkinsia arulius*)

Arun Sudhagar [1], Nithianantham Sundar Raj [1], Sowmya Pazhur Mohandas [1], Shaji Serin [1], Konnoth Kuttappan Sibi [1], Nandiath Karayi Sanil [2] and Thangaraj Raja Swaminathan [1,*]

[1] Peninsular and Marine Fish Genetic Resources Centre, ICAR-National Bureau of Fish Genetic Resources, Ernakulam North P.O., Kochi 682 018, Kerala, India
[2] Fish Health Section, Marine Biotechnology Division, ICAR-Central Marine Fisheries Research Institute, Ernakulam North P.O., Kochi 682 018, Kerala, India
* Correspondence: t.swaminathan@icar.gov.in; Tel.: +91-48-4239-5570

Abstract: Freshwater velvet disease is caused by the dinoflagellate parasite, *Piscinoodinium* sp. This parasite has been reported in tropical and subtropical fishes, and it can cause devastating losses. Moreover, *Piscinoodinium* sp. is identified as one of the least studied finfish parasites, and the available molecular information about this parasite is meager. Recently, *Piscinoodinium* sp. was responsible for the 100% cumulative mortality of the captive-bred F1 generation of Arulius barb (*Dawkinsia arulius*), an endangered freshwater fish native to India. The trophont stages of the parasite were observed in the skin and gills of the affected fish. The total DNA was extracted from the trophonts collected from the affected Arulius barb and the partial nucleotide sequence of the rDNA complex region (2334 bp) was amplified using PCR. The amplified PCR product exhibited a high sequence identity (97.61%) with *Piscinoodinium* sp. In the phylogenetic analysis of the SSU rDNA, *Piscinoodinium* sp. emerged as a separate clade from other dinoflagellate species. This is the first report of the infection of *Piscinoodinium* sp. in Arulius barb and the molecular information generated from this study can serve as a baseline to study the diversity of the parasite in India. Furthermore, the impact of this parasite among wild fish stock is not known, and this parasite needs further research focus to generate more molecular information and to understand the host–pathogen interaction.

Keywords: *Piscinoodinium* sp.; parasitic dinoflagellate; indigenous ornamental fish; endangered fish

1. Introduction

The parasitic dinoflagellate *Piscinoodonium* sp. is the causative agent of 'freshwater velvet disease' or 'rust disease', named after the typical clinical sign of a velvety golden dusk-like sheen on the skin of the affected fish [1]. The trophont stages of the parasite are attached to the gills, skin, and fin of the affected fish, which displays a velvet or rust-like appearance. This parasite has a worldwide distribution and a broad host range, particularly in tropical and subtropical fishes [1–6]. Furthermore, the parasite has been reported in both ornamental and food fishes [7]. However, very limited molecular information is available about this parasite. In India, a *Piscinoodonium* sp. outbreak was previously reported in common carp (*Cyprinus carpio*), mahseer (*Tor khudree*), and tilapia (*Oreochromis mossambicus*) [8]. The affected fish exhibit extensive epidermal erosion on the skin. The parasite attaches to the host by means of rhizocysts, which cause necrosis, hypertrophy, and lamellar fusion in the gills, subsequently leading to difficulty in respiration [2,9]. Furthermore, the water temperature can play an important role in the outcome of the infection. A previous report suggested that a sudden drop in water temperature can favor *Piscinoodinium* sp. outbreaks in fish [8]. The life cycle of *Piscinoodonium* sp. involves a trophont stage, which attaches to and feeds on the epithelium of the fish host. The trophont

detaches from the host and loses its rhizoid-like structure to form tomonts. The tomonts undergo division to form motile dinospores, which can readily infect the fish host and subsequently develop as trophonts, and the cycle continues [10,11]. This life cycle is similar to that of *Amyloodinium* sp., which causes similar disease with the same clinical signs in saltwater fishes. Previously, it was believed that *Piscinoodinium* sp. and *Amyloodinium* sp. were closely related. However, a molecular phylogenetic analysis suggested that these parasitic dinoflagellates are distantly related and underwent convergent evolution to adopt parasitism [12]. Even though *Piscinoodinium* sp. can cause deleterious effects on the affected fish, this parasite has been often overlooked by researchers. Only a few reports of this parasite are available and no detailed studies have been undertaken, particularly on the generation of molecular information about the parasite and to understand the host–pathogen interaction.

The indigenous fish hatchery facility, ICAR—National Bureau of Fish Genetic Resources (NBFGR), Kochi, Kerala, India, serves as a live germplasm-resource centre for threatened endemic fishes, such as Arulius barb (*Dawkinsia arulius*), Narayan barb (*Pethia setnai*), sun catfish (*Horabagrus brachysoma*), Nilgiri mystus (*Hemibagrus punctatus*), and naadan mushi (*Clarias dussumieri*). The indigenous aquarium fish, Arulius barb, which is native to the Tungabhadhra riverine system and upper reaches of the Cauvery basin, was bred in this facility for the purpose of ex situ conservation and river ranching. Moreover, Arulius barb is listed as an endangered species by the International Union for Conservation of Nature (IUCN)'s red list of threatened species [13]. In March 2021, an acute disease outbreak was observed in the hatchery-bred F1 generation of Arulius barb in this facility, eventually leading to complete mortality in the affected stock. A subsequent clinical examination identified *Piscinoodinium* sp. as the causative agent of the outbreak, and this is the first documentation of this parasite in Arulius barb supported by molecular data.

2. Materials and Methods

2.1. Case History

Breeding of Arulius barb is routinely performed at the indigenous-fish-hatchery facility, ICAR-NBFGR Kochi centre, for conservation. Captive-bred F1-generation Arulius barb (1+ year old) were maintained in 250-L glass tanks at a stocking density of 25 fish per tank. The water-quality parameters were as follows: water temperature, 25 °C to 26 °C; pH, 6.8 to 7.2; dissolved oxygen, 5.5 to 6.0 ppm; ammonia, nil; nitrite, nil; and nitrate <0.01 ppm. The fish were fed thrice a day and the water exchange was performed at a rate of 50% per day. These fishes encountered severe mortality, which eventually led to 100% cumulative mortality (>100 numbers) in 8 days. A total of five moribund fish with a length of 7.2 ± 0.7 cm and a weight of 4.1 ± 0.4 g were examined. The fish were euthanized in 1 g/L of MS222 (Sigma-Aldrich, Saint Louis, MO, USA) before sampling.

2.2. Examination of Affected Fish and Collection of Parasites

Necroscopy of the affected fish suggested a severe infestation of the trophonts stages of *Piscinoodinium* sp. in the gills, fins, and body surfaces. The gills along, with the arch, were carefully placed on a Petri plate and observed under a stereomicroscope (Olympus SZ61, Olympus, Tokyo, Japan) to examine the parasite burden. The sizes of the trophont stages of the parasites were measured using CellSens Imaging Software version 1.17 (Evident Corporation, Nagano, Japan). Subsequently, the gills were washed and aspirated with distilled water, and the parasites were carefully collected in a sterile Petri plate using a Pasteur pipette under the stereomicroscope. The trophonts were further washed in two changes of distilled water and collected in a 1.5-mL microcentrifuge tube (Eppendorf, Hamburg, Germany). The trophonts from all five fish were pooled together. The tube was centrifuged at 5000 rpm for 10 min and the supernatant water was discarded. The parasites were then preserved in 100% ethanol and stored at −20 °C for molecular analysis. Samples were also collected from the sampled fish for routine bacterial and viral diagnostics. Briefly, nucleic acid (DNA and RNA) was extracted from kidneys, gills, and brains of the

infected animals. DNA was extracted using the salting-out method [14], and RNA was extracted using TRIzol reagent (Invitrogen Carlsbad, USA). The cDNA synthesis was performed from the extracted RNA using the Verso cDNA kit (Thermo Scientific, Vilnius, Lithuania). Subsequently, polymerase chain reaction (PCR) was conducted to check for the presence of viruses, such as cyprinid herpesvirus 2 (CyHV-2) [15], carp edema virus (CEV) [16], infectious-spleen-and-kidney-necrosis virus (ISKNV) [17], and viral nervous necrosis (VNN) [18]. The presence of bacterial infection was examined by aseptically collecting samples from the kidney and spleen of the animals and culturing them in the nutrient medium for bacterial growth.

2.3. Polymerase Chain Reaction and Sequencing of rDNA

DNA extraction from the trophonts was performed by the salting-out method [14]. Subsequently, PCR amplification was undertaken by targeting 2334 bp in the rDNA-complex region using GCG18SF and ITSR8 primer pair (Table 1) [12]. The PCR reaction contained 12.5 µL of 2× Emerald Amp GT PCR master mix (Takara, Shiga, Japan), 0.5 µL of each oligonucleotide primer (10 pmol/µL), 10.5 µL of nuclease-free water, and 1 µL containing 50 ng of template DNA. The reaction mixture was initially denatured at 94 °C for 2 min followed by 35 cycles of denaturation (95 °C for 30 s), annealing (58 °C for 45 s), and extension (72 °C for 60 s), and the reaction was then subjected to final extension at 72 °C for 10 min. Subsequently, cloning of the PCR product was performed in pGEM®-T easy-vector systems (Promega, Madison, USA) and transformed in the DH5α strain of *Escherichia coli*. The recombinant plasmids were sequenced in ABI Prism 3700 Big Dye sequencer platform (Agrigenome, Kochi, India). The complete sequence of the insert was obtained by primer walking in both 5′ and 3′ directions using the primers provided in Table 1. The obtained sequences were further analyzed in Sequence Scanner Software ver. 1.0 (Applied Biosystems, Foster City, CA, USA) and Bioedit ver. 7.2.5 [19] and assembled into a consensus sequence.

Table 1. List of primers used in this study. The primer pair GCG18SF and ITSR8 was used for the PCR amplification of the rDNA of *Piscinoodinium* sp, whereas primers such as INT_F, INT_R, T7, and SP6 were used for sequencing. The primer sequence of GCG18SF was slightly modified compared to the original reference.

Primer ID	Primer Sequence (5′-3′)	Annealing Temperature (°C)	Target Size (bp)	Purpose	Reference
GCG18SF	CTGGTGATCCTGCCAGTAGTC	58	2334	*Piscinoodinium* sp. PCR	[12]
ITSR8	TAACCTGCATTCATGCTGTG				
INT_F	GTCTGGTGCCAGCAGCCGCGG	58	-	Sequencing	Present study
INT_R	GTACAAAGGGCAGGGACGTA	58	-	Sequencing	Present study
T7	TAATACGACTCACTATAGGG	55	-	Sequencing	Universal primer
SP6	ATTTAGGTGACACTATAG	55	-	Sequencing	Universal primer
CyHV_F	CCCAGCAACATGTGCGACGG	55	362	CyHV-2 PCR	[15]
CyHV_R	CCGTARTGAGAGTTGGCGCA				
CEV_F1	GCTGTTGCAACCATTTGAGA	60	548	CEV nested PCR (outer)	[16]
CEV_R1	TGCAGGTTGCTCCTAATCCT				
CEV_F2	GCTGCTGCACTTTTAGGAGG	55	181	CEV nested PCR (inner)	
CEV_R1	TGCAAGTTATTTCGATGCCA				
ISKNVF	ATGTCTGCAATCTCAGGTGC	55	1362	ISKNV PCR	[17]
ISKNVR	TTACAGGATAGGGAAGCCTG				
VNN_F2	CGTGTCAGTCATGTGTCGCT	55	430	VNN PCR	[18]
VNN_R3	CGAGTCAACACGGGTGAAGA				

2.4. Phylogenetic Analysis

A phylogenetic tree was constructed using the small subunit (SSU) rDNA sequence (1801 bp) of the *Piscinoodinium* sp. from the present study and other representatives

(collected from the NCBI database) using MEGA X software [20]. The sequences were aligned using MUSCLE, and the best-fitting model for the construction of the phylogenetic tree was computed to be the Tamura–Nei model with discrete Gamma distribution and invariable sites (T93 + G + I) and a lowest Bayesian Information Criterion score of 15,087.28 and maximum-likelihood value of −6952.84. The maximum-likelihood method was used for constructing the phylogenetic tree with the T93 + G + I model and the test of phylogeny was performed using the Bootstrap method with 1000 replicates. The final tree was visualized with the interactive tree of life (iTOL) [21].

3. Results

3.1. Clinical Signs and Parasitological Examination

The affected fish exhibited erratic swimming, anorexia, dyspnea, and excessive mucus production, which eventually led to death. Necroscopy of affected fish showed redness and pinpoint haemorrhage on the body surfaces and fins (Figure 1B) compared to the non-infected fish (Figure 1A). Furthermore, their gills were slightly pale and no gross pathological changes were observed in their other internal organs.

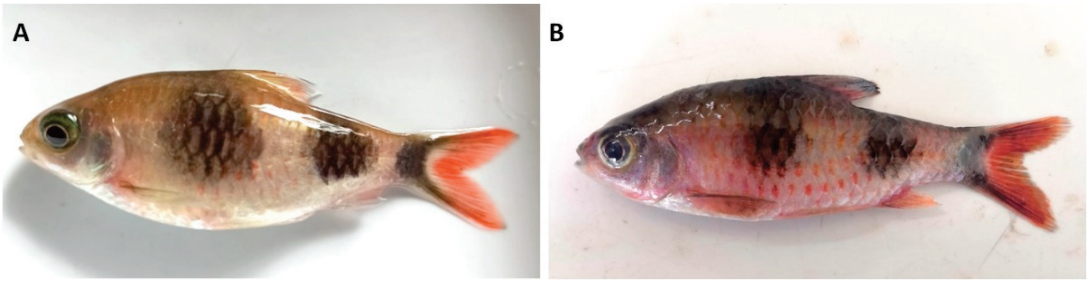

Figure 1. (**A**) Healthy disease-free Arulius barb. (**B**) Arulius barb affected by *Piscinoodinium* sp., showing redness on the body surface.

A microscopic observation of the skin-and-gill smear suggested a heavy infestation of the trophonts of the parasitic dinoflagellate *Piscinoodinium* sp. (Figure 2). The highest parasitic burden was observed on the first-gill arch, ranging from 152 to 232 trophonts. However, the other four gill arches had a relatively lower parasite burden with 82 to 110 trophonts. The size of the trophonts was in the range of 15.87 × 19.63 µm to 60.34 × 94.21 µm. In the routine diagnostics using PCR, the animals were observed to be free of CyHV-2, CEV, ISKNV, and VNN viruses and, moreover, no bacterial growth was observed in the nutrient broth inoculated with the kidney and spleen tissues of the infected animals.

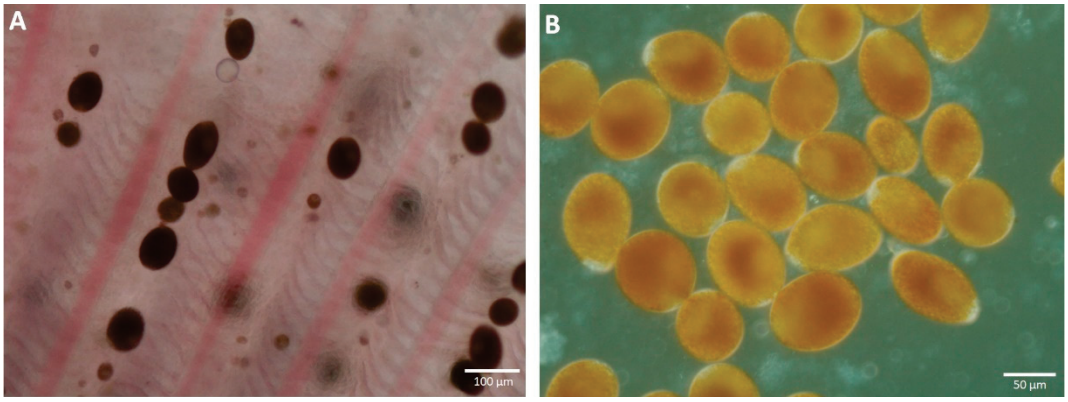

Figure 2. *Piscinoodinium* sp. from Arulius barb visualized under light microscope. (**A**) Trophont attached on the gills. (**B**) Detached trophont collected on a petri plate.

3.2. Polymerase Chain Reaction and Sequence Analysis

About 2334 bp of rDNA complex region spanning small subunit (SSU) rDNA, internal transcribed spacer 1 (ITS 1), 5.8S rDNA, internal transcribed spacer 2 (ITS 2), and partial sequence of the large subunit (LSU) DNA of *Piscinoodinium* sp. were amplified using PCR (Figure S1). The nucleotide sequence of *Piscinoodinium* sp. generated in this study showed 97.61% similarity to the sequence of *Piscinoodinium* sp. already available in the NCBI GenBank (EF016922.1 and EF016917.1). Furthermore, a search for the nucleotide sequences of *Piscinoodinium* sp. in the NCBI GenBank retrieved only eight sequences from the database. The nucleotide sequence generated from the present study was deposited in the NCBI GenBank under the accession numbers OP452934 (SSU rDNA gene) and OP420760 (ITS region) (Table S1).

3.3. Phylogenetic Analysis

The SSU rDNA phylogenetic analysis revealed that the *Piscinoodinium* sp. formed a distinct clade from the other dinoflagellates (Figure 3). The sequence data generated in the present experiment was the first molecular information on *Piscinoodinium* sp. reported from India, and this sequence clustered with seven other sequences of the parasite reported previously from the USA [12]. Moreover, the dinoflagellates belonging to the order Suessiales (*Piscinoodinium* sp., *Asulcocephalium* sp., *Symbiodinium* sp., and *Polarella* sp.) emerged as a separate clade.

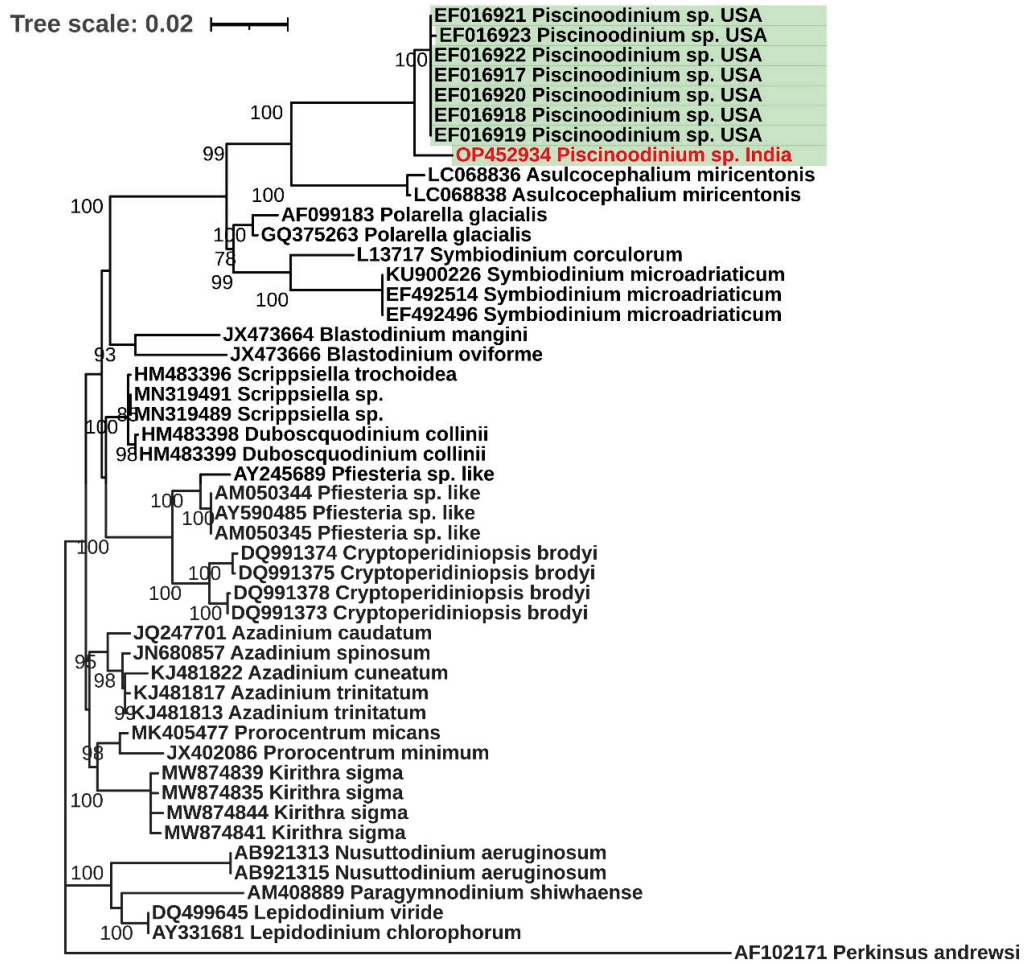

Figure 3. Phylogenetic tree of SSU rDNA gene from selected representatives of dinoflagellates. The maximum likelihood method was used to generate the tree. The green highlights represent the sequences from the parasitic dinoflagellate *Piscinoodinium* sp. and the red font indicates the sequence generated in the present experiment. The SSU rDNA gene sequence from *Perkinsus andrewsi* (accession number AF102171) was used as an outgroup.

4. Discussion

Diseases cause morbidity and mortality in fish in aquaculture operations, causing huge production losses in the industry [22,23]. Moreover, diseases in wild fish can lead to population decline, leading to biodiversity losses [24]. It is important to study and understand disease-causing pathogens at the molecular level to develop strategies to prevent outbreaks. The present document is the first report of *Piscinoodonium* sp. in an endangered fish species, Arulius barb. The high parasite burden in the gills of the infected fish might have been the reason for the reduction in respiratory efficiency, which eventually led to 100% cumulative mortality in the Arulius barb. Moreover, we did not find any bacterial or viral co-infection in the infected fish. Previous reports suggested that the *Piscinoodonium* sp. outbreak occurred when the water temperature dropped from 30 °C to 21 °C [8]. In the present study, the water temperature ranged between 25 °C and 26 °C during the disease outbreak. Laboratory experiments suggest that even a slight variation in water temperature can lead to different outcomes of disease during parasitic infection in fish [25,26]. However, detailed experiments are needed to understand the relationship between the drop-in water temperature and *Piscinoodonium* sp. outbreaks in fish. Moreover, studying the host response during *Piscinoodonium* sp. infection can help to understand the immune defence mechanism of the host against the parasite.

Traditionally, dinoflagellates are characterized and identified based on their morphological features. However, with the advent of molecular taxonomy based on conserved nucleic acid sequences, many of the morphology-based classifications of dinoflagellates were found to be inaccurate. This led to the application of the rDNA sequence as a widely used marker to identify and characterize dinoflagellates [27]. In the present study, we targeted an rDNA-complex region (2334 bp) comprising SSU rDNA, ITS 1, 5.8S rDNA, ITS 2, and a partial sequence of LSU DNA of *Piscinoodinium* sp. for PCR amplification. The generated sequence showed a strong homology with the already existing sequences of *Piscinoodinium* sp. reported from the USA [12]. In spite of the various reports of *Piscinoodinium* sp. from the fish hosts, there are no detailed studies aiming to understand the species diversity, molecular taxonomy, and distribution of the parasite, nor on the host–parasite dynamics. Moreover, the molecular information on the *Piscinoodinium* sp. is scarce. Currently, including the present work, there are only eight nucleotide sequences available for *Piscinoodinium* sp. in the NCBI database. Furthermore, there is only one report of *Piscinoodinium* sp. from India [8]. The disease outbreaks due to this parasite in aquaculture operations and the parasite's prevalence among wild fish populations are poorly documented in India. This overall lack of information about *Piscinoodinium* sp. suggests that the parasite might have been overlooked or poorly studied. There is a need to generate molecular information about this parasite to better understand and develop prophylactic measures against it [28]. Moreover, molecular characterization can help to explore the diversity and evolution of complex parasites [29].

The SSU rDNA gene is identified as one of the most reliable markers with which to determine the phylogenetic relationships among the dinoflagellates. In the phylogenetic analysis of the SSU rDNA gene of *Piscinoodinium* sp. and other representative dinoflagellates, it was observed that the species belonging to the order Suessiales (*Piscinoodinium* sp., *Asulcocephalium* sp., *Symbiodinium* sp., and *Polarella* sp.) emerged as a distinct clade (Figure 3). Among them, only *Piscinoodinium* sp. has a parasitic life cycle with fish as a primary host, and *Symbiodinium* sp. has a symbiotic relationship with a wide range of marine invertebrates. *Asulcocephalium* sp., and *Polarella* sp. are autotrophic dinoflagellates. Moreover, similar to *Piscinoodinium* sp., another parasitic dinoflagellate, *Amyloodinium* sp., causes identical infection and clinical signs in saltwater fishes [1]. However, a phylogenetic analysis suggested that both of these species are genetically distant and might have undergone convergent evolution toward fish ectoparasitism [12].

The affected fish in the present study, Arulius barb, is native to the Cauvery river basin in the Western Ghats region, which is an area of significant biodiversity, harboring diverse fish species [30]. Importantly, Arulius barb is categorized as an endangered species

by IUCN [13]. Furthermore, owing to the broad host range and geographical distribution of *Piscinoodinium* sp., this parasite could be a potential ecological threat to the freshwater ichthyofauna in the wild. In Brazil, *Piscinoodinium pillulare* was highly prevalent among the wild population of *Astronotus ocellatus* sampled from a freshwater lake, and seasonality was observed to influence the parasitism [4]. Parasitic infections among wild fish can even lead to the local extinction of the endemic population of the affected fish species [31]. Further research is required to generate knowledge on the species diversity, infection dynamics, geographical distribution, and genomic information of this parasite. Moreover, OMIC technologies can be used to enhance our understanding of *Piscinoodinium* sp. and its host [32].

5. Conclusions

This study presents the outbreak of *Piscinoodinium* sp. parasitic infection in a captive-bred endangered fish species, Arulius barb. It is evident that *Piscinoodinium* sp. infection can cause mortality as high as 100% in the affected fish stock. We generated molecular information (rDNA complex region) on *Piscinoodinium* sp., and this information could be used for the molecular diagnosis of the parasite. Furthermore, this sequence information can serve as baseline data for future studies to understand the geographical distribution and diversity of *Piscinoodinium* sp. This parasite deserves research attention in order to prevent devastating outbreaks in aquaculture operations, as well as among wild fish populations.

Supplementary Materials: The following supporting information can be downloaded at: https://www.mdpi.com/article/10.3390/pathogens11111350/s1. Figure S1: Detection and amplification of rDNA complex region of *Piscinoodinium* sp. by PCR. Table S1: Nucleotide sequence information of rDNA complex region of *Piscinoodinium* sp. generated in the present experiment.

Author Contributions: A.S. performed the experiment and drafted the manuscript; N.S.R., S.P.M., S.S. and K.K.S. performed the sampling, molecular diagnostics, and laboratory analysis; N.K.S. performed microscopic identification and imaging; T.R.S. conceptualized and supervised the writing of the manuscript. All authors have read and agreed to the published version of the manuscript.

Funding: This research was carried out under the National Surveillance Programme of Aquatic Animal Diseases, under Pradhan Mantri Matsya Sampada Yojana (PMMSY) from the Department of Fisheries, Ministry of Fisheries, Animal Husbandry and Dairying, Government of India [No. 35028/05/2012-Fy (Trade)-Vol II dated 19 June 2020]. The authors also acknowledge the support from the Network Project on Ornamental Fish Breeding and Culture funded by ICAR—National Bureau of Fish Genetic Resources.

Institutional Review Board Statement: Not applicable, as the samples for this study were collected during a natural disease outbreak.

Informed Consent Statement: Not applicable.

Data Availability Statement: The molecular-sequence data generated in this study were deposited in the NCBI database under the accession numbers OP452934 and OP420760.

Acknowledgments: The authors acknowledge the support offered by the Director, ICAR-NBFGR, Lucknow, India, to perform this experiment.

Conflicts of Interest: The authors declare no conflict of interest.

References

1. Noga, E.J. *Fish Disease*; Blackwell Publishing, Inc.: Ames, IA, USA, 2010; ISBN 9781118786758.
2. Martins, M.L.; Moraes, J.R.; Andrade, P.M.; Schalch, S.H.; Moraes, F.R. *Piscinoodinium pillulare* (Schäperclaus, 1954) Lom, 1981 (Dinoflagellida) Infection in Cultivated Freshwater Fish from the Northeast Region of Sao Paulo State, Brazil. Parasitological and Pathological Aspects. *Braz J. Biol.* **2001**, *61*, 639–644. [CrossRef] [PubMed]
3. Zago, A.C.; Franceschini, L.; Garcia, F.; Schalch, S.H.C.; Gozi, K.S.; Silva, R.J. da Ectoparasites of Nile Tilapia (*Oreochromis Niloticus*) in Cage Farming in a Hydroelectric Reservoir in Brazil. *Rev. Bras. Parasitol. Vet.* **2014**, *23*, 171–178. [CrossRef]
4. Neves, L.R.; Pereira, F.B.; Tavares-Dias, M.; Luque, J.L. Seasonal Influence on the Parasite Fauna of a Wild Population of *Astronotus ocellatus* (Perciformes: Cichlidae) from the Brazilian Amazon. *J. Parasitol.* **2013**, *99*, 718–721. [CrossRef] [PubMed]

5. Shaharom-Harrison, F.M.; Anderson, I.G.; Siti, A.Z.; Shazili, N.A.M.; Ang, K.J.; Azmi, T.I. Epizootics of Malaysian Cultured Freshwater Pond Fishes by *Piscinoodinium pillulare* (Schaperclaus 1954) Lom 1981. *Aquaculture* **1990**, *86*, 127–138. [CrossRef]
6. Wilson, J.R.; Saunders, R.J.; Hutson, K.S. Parasites of the Invasive Tilapia *Oreochromis mossambicus*: Evidence for Co-Introduction. *Aquat. Invasions* **2019**, *14*, 332–349. [CrossRef]
7. Noga, E.J.; Levy, M.G. Phylum Dinoflagellata. In *Fish Diseases and Disorders. Volume 1: Protozoan and Metazoan Infections*; CABI: Wallingford, UK, 2006; pp. 16–45.
8. Ramesh, K.S.; Mohan, C.V.; Shankar, K.M.; Ahmed, I. *Piscinoodinium* Sp. Infection in Juveniles of Common Carp (*Cyprinus Carpio*), Mahseer (*Tor Khudree*) and Tilapia (*Oreochromis mossambicus*). *J. Aquac. Trop.* **2002**, *15*, 281–288.
9. Ferraz, E.; Sommerville, C. Pathology of *Piscinoodinium* Sp. (Protozoa: Dinoflagellida), Parasites of the Ornamental Freshwater Catfishes *Corydoras* spp. and *Brochis splendens* (Pisces: Callichthyidae). *Dis. Aquat. Organ.* **1998**, *33*, 43–49. [CrossRef]
10. van Duijn, C. *Diseases of Fish*; Thomas H. Charles: Springfield, MA, USA, 1973.
11. Jacobs, D.L. A New Parasitic Dinoflagellate from Fresh-Water Fish. *Trans. Am. Microsc. Soc.* **1946**, *65*, 1–17. [CrossRef]
12. Levy, M.G.; Litaker, R.W.; Goldstein, R.J.; Dykstra, M.J.; Vandersea, M.W.; Noga, E.J. *Piscinoodinium*, a Fish-Ectoparasitic Dinoflagellate, Is a Member of the Class Dinophyceae, Subclass Gymnodiniphycidae: Convergent Evolution with *Amyloodinium*. *J. Parasitol.* **2007**, *93*, 1006–1015. [CrossRef]
13. Abraham, R. *Dawkinsia Arulius*; The IUCN Red List of Threatened Species 2015: e.T172500A70168511. Available online: https://www.iucnredlist.org/species/172500/70168511 (accessed on 14 July 2022).
14. Miller, S.A.; Dykes, D.D.; Polesky, H.F. A Simple Salting out Procedure for Extracting DNA from Human Nucleated Cells. *Nucleic Acids Res.* **1988**, *16*, 1215. [CrossRef]
15. Jeffery, K.R.; Bateman, K.; Bayley, A.; Feist, S.W.; Hulland, J.; Longshaw, C.; Stone, D.; Woolford, G.; Way, K. Isolation of a Cyprinid Herpesvirus 2 from Goldfish, *Carassius auratus* (L.), in the UK. *J. Fish. Dis.* **2007**, *30*, 649–656. [CrossRef] [PubMed]
16. Oyamatsu, T.; Matoyama, H.; Yamamoto, K.-Y.; Fukuda, H. A Trial for the Detection of Carp Edema Virus by Using Polymerase Chain Reaction. *Aquac. Sci.* **1997**, *45*, 247–251. [CrossRef]
17. Swaminathan, T.R.; Raj, N.S.; Preena, P.G.; Pradhan, P.K.; Sood, N.; Kumar, R.G.; Sudhagar, A.; Sood, N.K. Infectious Spleen and Kidney Necrosis Virus-associated Large-scale Mortality in Farmed Giant Gourami, *Osphronemus Goramy*, in India. *J. Fish. Dis.* **2021**, *44*, 2043–2053. [CrossRef]
18. Nishizawa, T.; Mori, I.K.; Nakai, T.; Furusawa, I.; Muroga, K. Polymerase Chain Reaction (PCR) Amplification of RNA of Striped Jack Nervous Necrosis Virus (SJNNV). *Dis. Aquat. Organ.* **1994**, *18*, 103–107. [CrossRef]
19. Hall, T. BioEdit: A User-Friendly Biological Sequence Alignment Editor and Analysis Program for Windows 95/98/NT. *Nucleic Acids Symp. Ser.* **1999**, *41*, 95–98.
20. Kumar, S.; Stecher, G.; Li, M.; Knyaz, C.; Tamura, K. MEGA X: Molecular Evolutionary Genetics Analysis across Computing Platforms. *Mol. Biol. Evol.* **2018**, *35*, 1547–1549. [CrossRef]
21. Letunic, I.; Bork, P. Interactive Tree Of Life (ITOL) v5: An Online Tool for Phylogenetic Tree Display and Annotation. *Nucleic Acids Res.* **2021**, *49*, W293–W296. [CrossRef]
22. Murray, A.G.; Peeler, E.J. A Framework for Understanding the Potential for Emerging Diseases in Aquaculture. *Prev. Vet. Med.* **2005**, *67*, 223–235. [CrossRef]
23. Lafferty, K.D.; Harvell, C.D.; Conrad, J.M.; Friedman, C.S.; Kent, M.L.; Kuris, A.M.; Powell, E.N.; Rondeau, D.; Saksida, S.M. Infectious Diseases Affect Marine Fisheries and Aquaculture Economics. *Ann. Rev. Mar. Sci.* **2015**, *7*, 471–496. [CrossRef]
24. Russell, R.E.; DiRenzo, G.V.; Szymanski, J.A.; Alger, K.E.; Grant, E.H.C. Principles and Mechanisms of Wildlife Population Persistence in the Face of Disease. *Front. Ecol. Evol.* **2020**, *8*, 569016. [CrossRef]
25. Bailey, C.; Segner, H.; Casanova-Nakayama, A.; Wahli, T. Who Needs the Hotspot? The Effect of Temperature on the Fish Host Immune Response to *Tetracapsuloides bryosalmonae* the Causative Agent of Proliferative Kidney Disease. *Fish Shellfish. Immunol.* **2017**, *63*, 424–437. [CrossRef] [PubMed]
26. Bailey, C.; Schmidt-Posthaus, H.; Segner, H.; Wahli, T.; Strepparava, N. Are Brown Trout *Salmo trutta fario* and Rainbow Trout *Oncorhynchus mykiss* Two of a Kind? A Comparative Study of Salmonids to Temperature-Influenced *Tetracapsuloides bryosalmonae* Infection. *J. Fish. Dis.* **2018**, *41*, 191–198. [CrossRef] [PubMed]
27. Ott, B.M.; Litaker, R.W.; Holland, W.C.; Delwiche, C.F. Using RDNA Sequences to Define Dinoflagellate Species. *PLoS ONE* **2022**, *17*, e0264143. [CrossRef] [PubMed]
28. Shivam, S.; El-Matbouli, M.; Kumar, G. Development of Fish Parasite Vaccines in the OMICs Era: Progress and Opportunities. *Vaccines* **2021**, *9*, 179. [CrossRef]
29. Fariya, N.; Kaur, H.; Singh, M.; Abidi, R.; El-Matbouli, M.; Kumar, G. Morphological and Molecular Characterization of a New Myxozoan, *Myxobolus grassi* sp. Nov. (Myxosporea), Infecting the Grass Carp, *Ctenopharyngodon idella* in the Gomti River, India. *Pathogens* **2022**, *11*, 303. [CrossRef]
30. Sreenivasan, N.; Mahesh, N.; Raghavan, R. Freshwater Fishes of Cauvery Wildlife Sanctuary, Western Ghats of Karnataka, India. *J. Threat. Taxa* **2021**, *13*, 17470–17476. [CrossRef]
31. Sudhagar, A.; Kumar, G.; El-Matbouli, M. The Malacosporean Myxozoan Parasite *Tetracapsuloides bryosalmonae*: A Threat to Wild Salmonids. *Pathogens* **2019**, *9*, 16. [CrossRef]
32. Sudhagar, A.; Kumar, G.; El-Matbouli, M. Transcriptome Analysis Based on RNA-Seq in Understanding Pathogenic Mechanisms of Diseases and the Immune System of Fish: A Comprehensive Review. *Int. J. Mol. Sci.* **2018**, *19*, 245. [CrossRef]

pathogens

MDPI

Article

Morphological and Molecular Characterization of a New Myxozoan, *Myxobolus grassi* sp. nov. (Myxosporea), Infecting the Grass Carp, *Ctenopharyngodon idella* in the Gomti River, India

Naireen Fariya [1], Harpreet Kaur [2], Mahender Singh [3], Rehana Abidi [1], Mansour El-Matbouli [4] and Gokhlesh Kumar [4,*]

[1] Parasitology Laboratory, Fish Health Management Division, National Bureau of Fish Genetic Resources, Lucknow 226002, India; n_fariya@yahoo.com (N.F.); abidinbfgr@gmail.com (R.A.)
[2] Department of Zoology, Panjab University, Chandigarh 160014, India; harpreetbimbra@gmail.com
[3] DNA Barcoding Laboratory, Molecular Biology & Biotechnology Division, National Bureau of Fish Genetic Resources, Lucknow 226002, India; dr.mahendersingh29@gmail.com
[4] Clinical Division of Fish Medicine, University of Veterinary Medicine Vienna, Veterinärplatz 1, 1210 Vienna, Austria; mansour.el-matbouli@vetmeduni.ac.at
* Correspondence: gokhlesh.kumar@vetmeduni.ac.at

Abstract: Myxosporeans are well-known parasites infecting food fishes in fresh and marine water around the globe. Grass carp *(Ctenopharyngodon idella*), a freshwater food fish commonly cultured in India with has significant economic importance. Herein, the study focuses on the description of a new myxosporean species, *Myxobolus grassi* sp. nov. from the gills as primary site and liver as secondary site of infection in grass carp. Both organs (gill and liver) were infected concurrently in the host and the prevalence of grass carp infection was 4.05% in gill filaments and liver, respectively. Identification of species was based on the morphological and morphometric features of the myxospore as well as 18S rDNA sequence data. A smear from gill and liver exhibited hundreds of morphologically similar myxospores. BLAST search revealed 98% sequence similarity and 0.03 genetic distance with *M. catlae* (KM029967) infecting gill lamellae of mrigal carp (*Cirrhinus cirrhosus*) from India and 98–84% sequence similarity with other myxobolids in India, China, Japan, Malaysia, Turkey and Hungary. Phylogenetically, it clustered with other myxobolids infecting gills and related organs (i.e., vital organ) of Indian cyprinid carp species. On the basis of myxospore morphology and 18S sequence, we propose *M. grassi* sp. nov.

Keywords: grass carp; myxozoan; new myxozoan species; *Myxobolus grassi*

1. Introduction

Fishes are considered as a healthy source of animal protein, providing essential nutrients to the human diet. Grass carp (*Ctenopharyngodon idella*) is a cyprinid food fish, having a major contribution in freshwater aquaculture globally. It grows quickly with minimal input cost. The fisheries sector can contribute substantially to the elimination of food insecurity and malnutrition in a responsive way [1]. Traditionally, fish culture has been associated with livelihood and income in India, thereby contributing to the economy. Parasitic infections have always received special attention in food fish and ornamental fishes. Moreover, *C. idella* is easily prone to diseases, which affects the health of the fish [2]. Poor management or lack of awareness on better management practices in fish culture might manifest the risk of extensive harmful parasites. Myxozoans are economically important groups of microscopic parasites among freshwater fishes comprising more than 2000 known species [3,4]. The genus *Myxobolus* (Myxobolidae) encompasses largest number of species worldwide [5]. A synopsis of 744 and 112 nominal *Myxobolus* species was compiled by Eiras et al. [6,7]

respectively. In addition, Kaur and Singh [8] gave a synopsis of 131 species of *Myxobolus* reported from India. As demonstrated by Kaur [9] new myxozoans are emerging and threatening the development of pisciculture causing production losses. Hitherto, globally many myxozoan infections were recorded in carps and cyprinids [6,7] while several studies on prevalence of myxosporidiasis and novel myxozoan species with negative impact reported in grass carp [8,10,11]. With this view, the parasitic investigation was performed for grass carp, an economically significant freshwater food fish commonly cultured in India. The present study reports morphological identification and molecular characterization based on 18S rDNA of *M. grassi* sp. nov. infecting the gill filaments and liver of grass carp.

2. Results

Taxonomic summary of *Myxobolus grassi* sp. nov.
(Cnidaria: Myxozoa: Myxosporea: Bivalvulida: Myxobolidae: Myxobolus)
Host: *Ctenopharyngodon idella* (Grass carp) (Valenciennes, 1844)
Locality: Gomti river (Kaisar Bagh fish market), Lucknow, Uttar Pradesh, India
Type specimen: Holotype with the slide no. M01–05/SN/GC/10.2.2018 was deposited in the museum of the Department of Zoology, Punjab University, Chandigarh, India
Paratypes: Gills fixed in 4% formalin with catalogue no. M/G/GC/10.2.2018 as paratype has been deposited with Dr. Harpreet Kaur, Department of Zoology, Punjab University, Chandigarh, India
Site of infection: Gill filaments (Vascular epithelium) and liver
Prevalence: 4.05%
Etymology: The present species is termed as *M. grassi* sp. nov. after the common name of the fish host i.e., grass carp

2.1. Morphological Description

A total of 74 grass carps measured range 20–35 cm in length were examined, and gills and liver were infected in only 3 specimens (Table 1). However, less intensity of infection was observed in liver smears. Myxospores from both infected gills and liver were morphologically and morphometrically similar. Consequently, the infection in gills and liver were as primary and secondary site of infection respectively. Myxospores ellipsoidal, slightly pointed anteriorly (Figures 1 and 2), measuring 6.0–11.1 (9.8 ± 0.9) µm long and 3.9–7.5 (6.2 ± 0.9) µm wide in valvular view (n = 34). Thickness of myxospore was 4.9–6.0 (5.4 ± 0.3) µm in sutural view. The ratio (LS/WS) of the myxospore was 1.58. The polar capsules were converging, drop-shaped and unequal. A larger polar capsule covers more than half of the myxospore body measuring 3.5–5.6 (4.6 ± 0.5) µm long and 1.5–2.6 (2.1 ± 0.2) µm wide. A smaller capsule length about 1/3rd of the myxospore length measured 2.8–4.5 (3.4 ± 0.4) µm long and 1.0–2.1 (1.5 ± 0.2) µm wide. The larger polar capsule consists of 8 coils while the smaller polar capsule consists of six coils in the polar filament. The range of coils is different according to the size of the polar capsule. The length of the polar filaments is 18.8–22.6 (20.3 ± 1.1) µm. The sporoplasm is homogenous, without iodinophilous vacuole.

Table 1. Comparative morphometric data of myxospores collected from gills and liver of 3 grass carp. (Gill 1 is the type sample for the study as having minimum and maximum range of morphometric measurements).

Tissue	Myxospore		Polar Capsules	
	Length (µm)	Width (µm)	Length (µm)	Width (µm)
Gill 1	6.0–11.1 (9.8 ± 0.9)	3.9–7.5 (6.2 ± 0.9)	3.5–5.6 (4.6 ± 0.5); 2.8–4.5 (3.4 ± 0.4)	1.5–2.6 (2.1 ± 0.2); 1.0–2.1(1.5 ± 0.2)
Gill 2	7.0–10.7 (9.7 ± 1.0)	4.0–7.1 (6.1 ± 0.9)	3.5–5.3 (4.5 ± 0.5); 2.4–4.1 (3.5 ± 0.4)	1.6–2.4 (2.0 ± 0.2); 1.0–2.0 (1.5 ± 0.2)

Table 1. *Cont.*

Tissue	Myxospore		Polar Capsules	
	Length (μm)	**Width (μm)**	**Length (μm)**	**Width (μm)**
Gill 3	6.2–11.0 (9.7 ± 1.2)	4.1–7.3 (6.2 ± 1.0)	3.9–5.6 (4.7 ± 0.4); 3.0–4.1(3.5 ± 0.4)	1.5–2.5 (2.1 ± 0.2); 1.2–1.8 (1.5 ± 0.1)
Liver 1	6.2–10.8 (9.1 ± 1.5)	3.9–7.0 (5.9 ± 1.0)	3.9–5.6 (4.6 ± 0.5); 3.0–4.3 (3.7 ± 0.4)	1.5–2.4 (1.9 ± 0.2); 1.0–1.9 (1.4 ± 0.3)
Liver 2	7.0–10.9 (9.5 ± 1.3)	4.0–7.0 (6.0 ± 0.9)	3.8–5.2 (4.7 ± 0.4); 2.8–4.2 (3.5 ± 0.4)	1.6–2.5 (2.1 ± 0.2); 1.0–1.8 (1.5 ± 0.2)
Liver 3	6.4–10.7 (9.3 ± 1.1)	3.9–6.9 (6.0 ± 0.9)	3.6–5.1 (4.6 ± 0.4); 2.8–4.3 (3.4 ± 0.4)	1.5–2.4 (2.0 ± 0.2); 1.1–1.9 (1.5 ± 0.2)

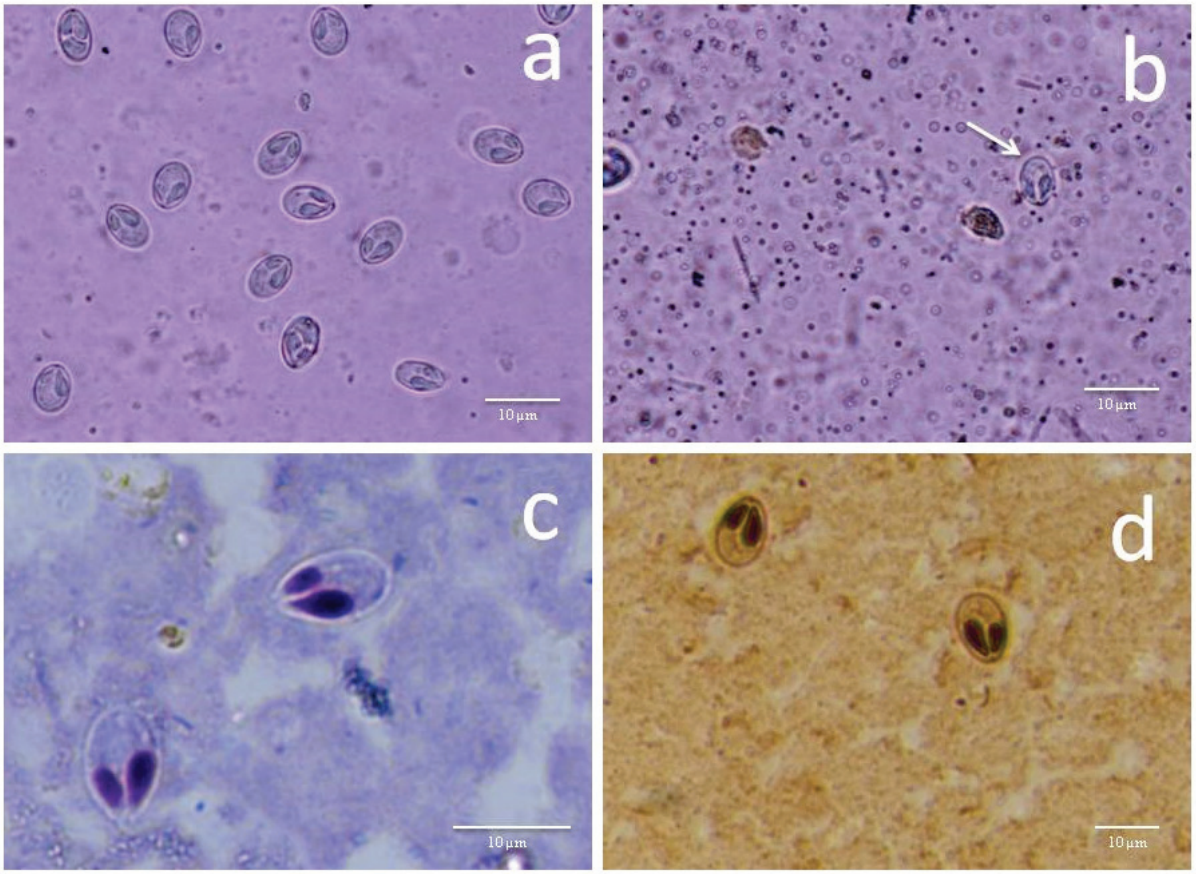

Figure 1. (i) Fresh myxospores of *M. grassi* sp. nov. from grass carp under phase contrast microscope. (**a**) Gill filament (**b**) liver (arrow); (ii) stained myxospores of *M. grassi* sp. nov. from the gill filament of grass carp. (**c**) giemsa stain (**d**) silver-nitrate stain.

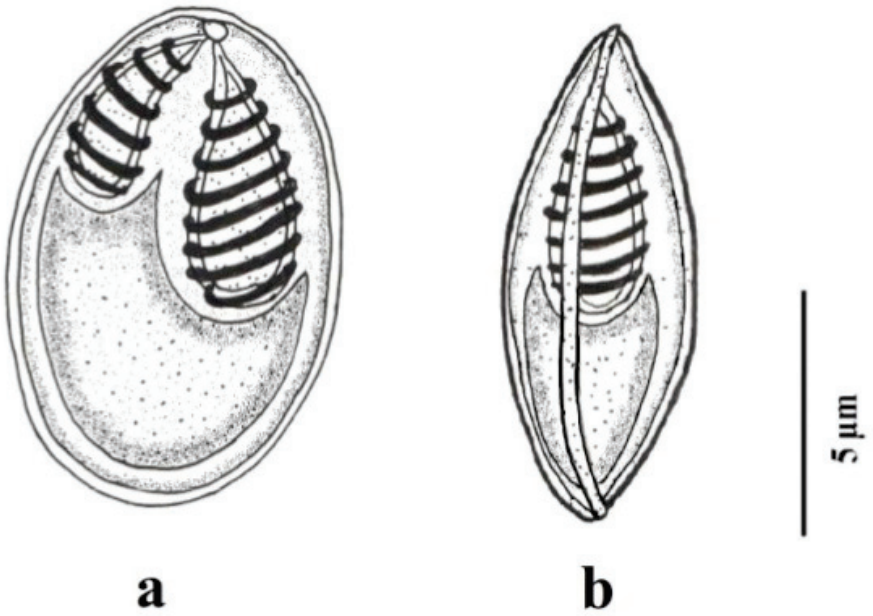

Figure 2. Camera Lucida drawings of the mature myxospore of *M. grassi* sp. nov. from the gill filaments of grass carp showing (**a**) frontal and (**b**) sutural view.

2.2. Remarks on Morphological Analysis

First, it seems that *M. grassi* sp. nov. recorded from the grass carp during the present study resembled various *Myxobolus* species infecting gills and related organs. Besides that, species having ellipsoidal to pyriform myxospores and unequal polar capsules were compared with the present species *M. grassi* sp. nov. Particularly, the closely resembling species were being discussed here in detail: *Myxobolus diversus* and *Myxobolus bhadrensis* were relatively similar to the present species but *M. diversus* myxospores possessed a drop-shape with a pointed tip less wide than the present species while the sporoplasm of *M. bhadrensis* was coarse, uninucleated with extracapsular cavity and iodinophilous vacuole. *M. puntuisii* has smaller polar capsules whereas *M. naini* possessed larger myxospores and polar capsules. In addition, myxospores of *M. buccoroofus* from buccal cavity of *Labeo bata* were longer than the present species. *M. analfinus* myxospores from anal fin of *Heteropneustes fossilis* were bigger in size and has relatively smaller polar capsules while myxospores of *M. debsantus* from tail fin of *Catla catla* and *Labeo rohita* were wider than the present species. Myxospores of *M. burti* from muscles of *Notropis hudsonius* were longer and wider. Myxospores of *M. haldari* from fins and gills of *Cirrhinus mrigala* and *Labeo rohita* were also somewhat smaller and wider in comparison to the present species. *M. grassi* sp. nov myxospores were much wider than *M. intramusculi* from muscle cells of *Percopsis omiscomaycus*. *M. lalithae* from gill filaments of *Labeo calbasu* and *M. mathurii* from gills of *Puntius sarana* have also larger myxospores. Myxospores of *M. tripurensis* from gill filaments and gill rakers of *Labeo calbasu*; *L. bata* and *Cirrhinus reba* differed from *M. grassi* sp. nov. in the length of myxospore and in having sutural markings at the posterior end (Table 2).

Table 2. Comparative description of *M. grassi* sp. nov. with morphologically similar myxobolid species.

Species	Host	Site of Infection	Myxospore		Polar Capsule(s)		Locality	References
			Length (µm)	Width (µm)	Length (µm)	Width (µm)		
M. grassi sp. nov.	*C. idella*	Gills and liver	9.8 ± 0.9 (6.0–11.1)	6.2 ± 0.9 (3.9–7.5)	4.6 ± 0.5 (3.5–5.6); 3.4 ± 0.4 (2.8–4.5)	2.1 ± 0.2 (1.5–2.6); 1.5 ± 0.2 (1.0–2.1)	India	Present Study
M. diversus	*Schizothorax curvifrous*	Gill lamellae	9.1 (8.9–9.3)	5.8 (5.3–6.4)	4.1 (3.9–4.3); 2.5 (2.2–2.8)	1.6 (1.4–1.8); 1.2 (1.0–1.4)	India	[12]
M. bhadrensis	*Labeo rohita*	Muscle	9.5 (8.0–11.0)	7.14 (7.0–8.0)	3.5 (3.0–4.0); 2.5 (2.0–4.0)	2.2 (2.0–3.0); 1.75 (1.0–2.0)	India	[12]

Table 2. *Cont.*

Species	Host	Site of Infection	Myxospore		Polar Capsule(s)		Locality	References
			Length (µm)	Width (µm)	Length (µm)	Width (µm)		
M. puntuisii	*Puntius sophore*	Caudal fin	7.7 (7.5–7.9)	5.3 (5.2–5.4)	3.0 (2.9–3.0); 1.8 (1.7–1.9)	1.7 (1.6–1.8); 0.9 (0.8–0.9)	India	[13]
M. naini	*Labeo bata; L. rohita*	Gill filaments	15.1 (13.6–16.6)	9.2 (7.9–10.5)	6.3 (5.1–7.6); 3.5 (3.1–3.9)	2.9 (2.5–3.4); 2.1 (2.0–2.2)	India	[14]
M. buccoroofus	*Labeo bata*	Buccal cavity	11.6–12.7 (12)	6.4–8.1 (7.1)	4.5–5.3 (4.9); 2.0–2.9 (2.5)	2.7–3.0 (2.9); 1.3–1.7 (1.5)	India	[15]
M. analfnus	*Heteropneustes fossilis*	Anal fin	11.1–13.4 (12.3 ± 0.7)	7.8–9.3 (8.6 ± 0.4)	3.2–4.9 (4.1 ± 0.4); 2.0–3.1 (2.5 ± 0.3)	2.0–2.4 (2.2 ± 0.1); 1.6–2.0 (1.8 ± 0.1)	India	[16]
M. burti	*Notropis hudsonius*	Muscles	9.7–11.3 (10.3 ± 0.6)	7.1–8.4 (7.7 ± 0.4)	4.0–5.8 (5.3 ± 0.5); 4.3–5.2 (4.7 ± 0.3)	2.1–3.2 (2.7 ± 0.3); 2.2–2.7 (2.5 ± 0.2)	Canada	[17]
M. debsantus	*Catla catla; Labeo rohita*	Caudal fin	8.5–9.6 (9.0 ± 0.2)	8.1–8.9 (8.4 ± 0.2)	4.0–4.6 (4.3 ± 0.17); 2.6–2.9 (2.8 ± 0.09)	2.0–2.6 (2.3 ± 0.18); 1.6–1.9 (1.8 ± 0.09)	India	[16]
M. haldari	*Cirrhinus mrigala; Labeo rohita*	Fins and gills	9.0–10.0 (9.3)	7.0–8.5	4.0–5.0 (4.3); 2.5–3.0 (2.9)	2.5–3.0 (2.9); 1.5–2.0 (1.9)	India	[18]
M. intramusculi	*Percopsis omiscomaycus*	Muscle cells	9.9–15.7 (12.5 ± 0.9)	4.6–8.0 (6.2 ± 0.6)	4.0–7.9 (5.8 ± 0.6); 3.4–7.7 (5.8 ± 0.7)	1.0–2.7 (1.7 ± 0.4) 0.9–0.7 (1.7 ± 0.3)	Canada	[19]
M. lalithae	*Labeo calbasu*	Gill filaments	9.0–11.0 (10)	8.0–9.0 (8.4)	5.0–6.0 (5.8); 4.0–5.0 (4.8)	3.0–3.5 (3.0); 2.5–3.0 (2.8)	India	[20]
M. mathurii	*Puntius sarana*	Gills	8.7–23.5	5.1–10.1	2.7–11.9; 2.7–7.8	1.8–4.6; 1.8–4.6	India	[21]
M. tripurensis	*L. calbasu; L. bata; C. reba*	Gill filaments and gill rakers	8.1–9.4 (8.9 ± 0.4)	6.5–7.0 (6.7 ± 0.19)	4.0–4.5 (4.2 ± 0.18); 2.5–2.8 (2.6 ± 0.1)	2.0–2.6 (2.3 ± 0.2); 1.6–1.9 (1.7 ± 0.1)	India	[22]

2.3. Molecular Phylogeny

In the support of morphological study, 970 bp fragment of 18S (SSU rDNA) gene of *M. grassi* sp. nov. was submitted to GenBank with the accession no. KP268649. Although only about half the target gene was amplified, it included coverage of conserved and variable regions. Additionally, there was a lack of intraspecific variation within the three isolates. The present partial sequence showed 98% homology with *M. catlae*, 93% homology to *M. kalavatiae* (Figure 3). In addition, other sequences with less similarity (90–92%) were used for phylogentic study. In phylogentic analysis, the present species was closely related to the gill isolated species *M. catlae* placing it to the same clade with high bootstrap value. Moreover, it also clustered giving the preference on the basal groups of sub clades with *Myxobolus* species infecting gills of Indian carps and numerous cyprinid fishes reported worldwide (Figure 3). This was further supported by the evolutionary divergence values of the present species with other related species. It was 0.03 with *M. catlae*, 0.06 with *M. kalavatae* and 0.20 with *Hennehuya doneci*, 0.26 with *Myxidium streisingeri* and 0.30 with *Chloromyxum cyprinid* (out group). Presumably, the association and connection within tissue-specific myxozoan groups is because of relationship after segregation and conversion into new species from old species. The rate of evolution analysis is usually a comparison where evolutionary change corresponds to a shift in the position of a species.

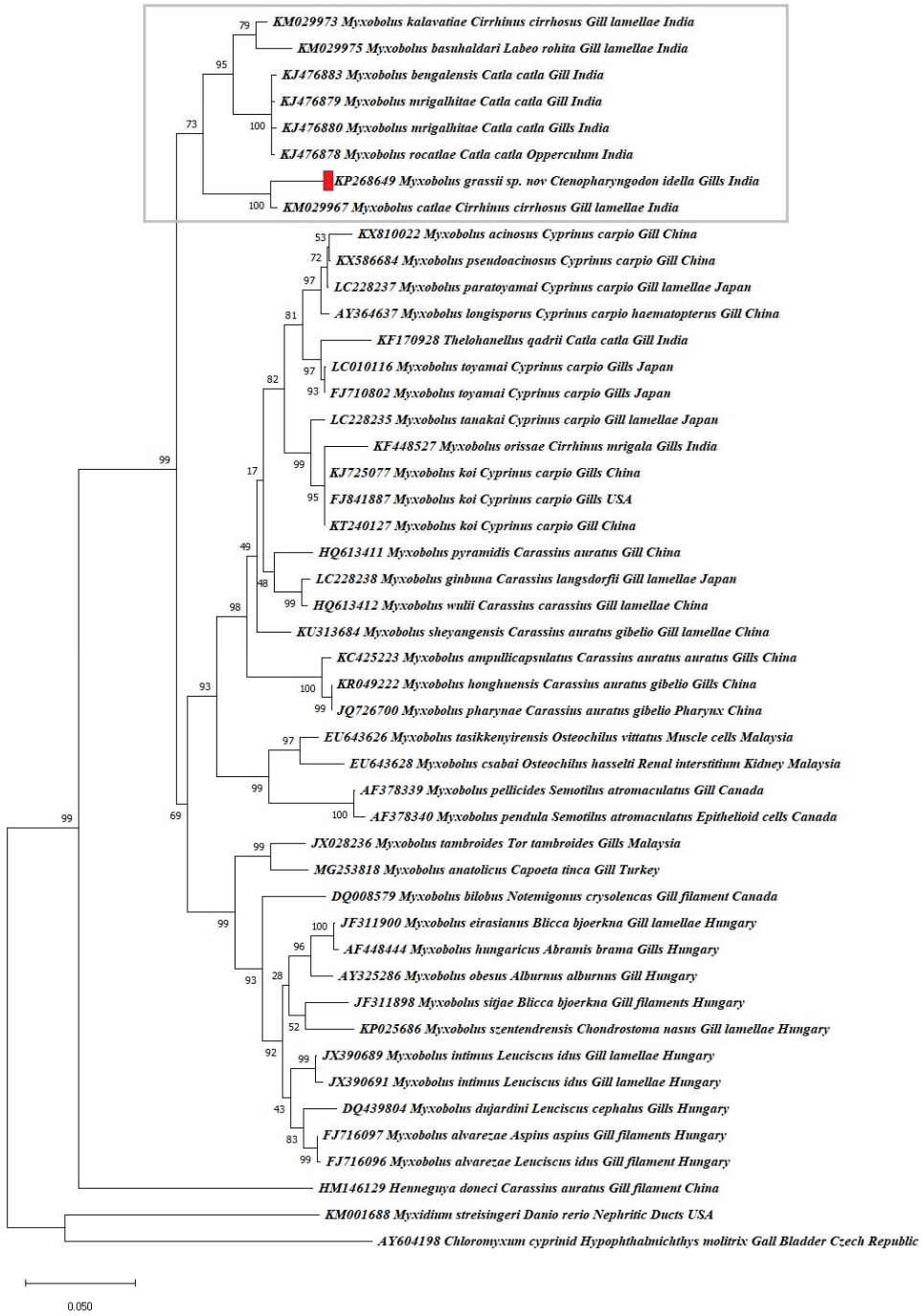

Figure 3. Phylogenetic tree constructed by maximum likelihood displaying *M. grassi* sp. nov. (KP268649) from *C. idella* clustering next to the Indian group of myxosporean. GenBank accession numbers are given before the species and numbers on the nodes represents the bootstrap confidence values.

3. Discussion

The present species was compared with closely resembling species from gills and vital organs but that varied in morphologically. Furthermore, species with unequal, dimorphic myxospores from the synopses of Eiras et al. [6,7] have been compared with present species but all of the species were different in shape and size of myxospore. Moreover, the current species was compared with other Myxobolus species isolated from *C. idella* by earlier workers were as follows: *M. ctenopharyngodoni* from intestine, spleen and kidney; *M. huasaensis* from kidney; *M. microsporus* from almost all organs; *M. tricostatus* from

gills and spleen; *M. pinna* from fins; and *M. edellae* from kidney. *M. ctenopharyngodoni*, *M. huasaensis*, *M. tricostatusis* and *M. edellae* all had comparatively different myxospores and the polar capsules were equal in size. *M. microspores* and *M. pinna* both have unequal polar capsules but were bigger in myxospore size.

The blast analysis of *M. grassi* sp. nov. exhibited 84–98% sequence similarity with as many as 28 myxobolid species infecting gills and related organs in India, Japan, Malaysia, Turkey, Canada, Hungary and Australia. A phylogentic study resulted in *M. grassi* sp. nov. being within the monophyletic clade comprising Indian species having 98% to 91% homology. On the other hand, other species such as *M. csabai* (90%), *M. pendula* (89%) and *M. pellicides* (89%) made a paraphyletic group of gill myxozoans in cyprinids, which indicates the relationship among host and aquatic environment i.e., freshwater fishes (Figure 3). According to Ferguson et al. [23], in the case of *Henneguya*, there is a strong tendency to form clades among species, based on the family of the host fish. The present species represents the Indian intracellular group exhibiting affinity to host family and geographical conditions while manifesting the basal groups of sub clades of *Myxobolus* species infecting intracellular-intramuscular group numerous cyprinid fishes reported worldwide i.e., it included myxosporeans species infecting other internal organs from Japan, Malaysia, Turkey, Canada and Hungary. Consequently, host tissue specificity is strict in myxosporeans, and still different habitats has been demonstrated for some species [24].

However, the difference of the resultant 18S rDNA sequence of *M. grassi* sp. nov. was again compared morphologically with the species assembling in monophyletic group, which indicated incongruence in morphological and molecular data. *M. grassi* sp. nov. clustering in sister clade with *M. catlae* having high bootstrap values differed morphologically and morphometrically with much elongated myxospore (approximately 2/3rd in size) and a sharply pointed thin tip having equal and longer polar capsules. It was well supported by the evolutionary divergence values of 0.03. Easy et al. [19] found 97.9% similarity between intracellular and intercellular plasmodia of *M. procerus*, parasite of *Percopsis omiscomaycus*, and designated a new species—*M. intramusculi* for the intracellular form. While other species clustered in the group of Indian cyprinids origin clade were also morphologically different with the present species. However, *M. kalavatiae* and *M. basuhaldari* were small, ovoid with equal polar capsules covering 1/3rd of the part of the myxospores while myxospores of *M. rocatlae* were elongated with sharply pointed anterior with slender long polar capsules. *M. mrigalhitae* possesses intercapsular process and iodinophilous vacuole whereas *M. bengalensis* comprises pear-shaped myxospores with longer, equal polar capsules and a spherical iodinophilous vacuole.

The present species infecting two organs i.e., gills and liver, can be considered as tissue-specific because maybe the species have developed somewhere else, as there were no developmental stages observed in both organs. Molnar et al. [25] stated site specificity of *M. shaharomae* from liver, testes and intestine was connected to the tissues rather than organs i.e., tissue specific, as the species develops plasmodia in blood vessels. The lower clade comprised of species from Hungary, Canada, Malaysia, Turkey and Australia with a very high bootstrap value indicating a close relationship and connection towards tissue and host tropism [26,27]. In view of close association involving histotropism and genetic distance among groups, the phylogenetic analysis leads us to consider *M. grassi* sp. nov. as a distinct new species after the comparison of the morphological, morphometric and molecular analysis.

4. Materials and Methods

4.1. Morphology and Morphometry

Seventy-four live specimens of grass carps were procured from Kaisar Bagh fish market (latitude 26°50′54.93″ N and longitude 80°55′52.08″ E), Lucknow, Uttar Pradesh, India. Fishes were transported live to the laboratory (in oxygenated plastic buckets and kept in aerated tank temporarily. Fishes were anesthetized with chloroform at a concentration of 40 mg/L and dissected after 2–3 days post capture. All the external and internal organs

were screened for myxozoan infection. Organs were removed from freshly killed fish and placed in a Petri dish with saline, then microscopically examined under a stereo-zoom microscope SMZ-U (Nikon, Japan). Squash preparations of gills and liver were made and examined through a Nikon E600 microscope with 100X objective (plus immersion oil) for the presence of myxospores. Fresh smears revealed numerous myxospores (Figure 1a), however plasmodia were not detected. Fresh wet mount was treated with 10–12% KOH solution to evert the polar filaments. For permanent preparations, air-dried smears were stained with geimsa and silver nitrate [28] (Figure 1b). Fresh myxospores were photographed through a compound binocular microscope Eclipse E600 with Photomicrography digital camera DXM1200F (Nikon, Japan). Morphometric measurements of fresh myxospores (n = 30–34) were done with the help of software NIS-E-Br. Morphological characterization was carried out for the obtained parasite according to the guidelines of Lom and Arthur [29]. Morphometric data are presented in micrometers (μm) with ranges followed by mean ± SD in parentheses. Fresh myxospores from gill filaments (gill 2 and 3) (n = 20) and liver 1, 2, and 3 (n = 20) were measured.

4.2. Molecular Analysis

For molecular analysis, a gill sample from each of the three infected fish were taken. Morphometric measurements were obtained for the liver samples while contamination from host tissue prevented to obtain molecular data from liver. DNA extraction was performed from the myxospores (approximately 500–700) through DNeasy Blood & Tissue Kit (Qiagen, India) following the manufacturer's protocol. DNA concentration was measured through Nano-drop 2000 spectrophotometer (Thermo Scientific, Waltham, MA, USA). Total 970 bp sequence was generated with MC5–MC3 [30] primer sets synthesized by Sigma-Aldrich, India and were used to amplify the partial 18S (SSU rDNA) gene by Polymerase Chain Reaction (PCR) in Eppendorf EP Gradient S Master Cycler (Eppendorf Inc., USA). The final volume of PCR 50 μL containing 1x PCR buffer, 0.2 mM dNTPs, 1.5 mM $MgCl_2$, 0.25 μM of each primer, 2.0 U taq polymerase (Fermentas, Thermo Fisher Scientific) and 100 ng of the genomic DNA template [31]. The PCR amplification protocol consisted of initial denaturation at 94 °C for 4 min, followed by 35 cycles of denaturation at 94 °C for 50 s, at annealing of primers at 56 °C for 50 s, followed by 72 °C for 1 min, final extension at 72 °C for 7 min and then stored at 4 °C prior to sequencing. Aliquots (5 μL) of the amplicons were visualized with 0.02% bromophenol blue (G-Biosciences) after electrophoresis on 1% agarose gel. Amplicon was purified with the QIAquick Gel Extraction Kit (Qiagen), as per manufacturer's instructions. Purified amplicons were sequenced using the ABI BigDye Terminator Cycle Sequencing Ready Reaction Kit v3.1, using the ABI3730xl Genetic Analyzer (Applied Biosystems, Inc. Waltham, MA, USA) for the both directions. The alignment of nucleotide sequences was done with the help of Clustal W and MEGA X [32]. A query search for analogous nucleotide-nucleotide Basic Local Alignment Search Tool (blastn) [33] was conducted for comparison of the present sequence. The genetic distance in phylogenetic evaluation was computed by GTR + G model selected by analysis of best model for Maximum Likelihood (ML) (Figure 3) using MEGA X [31]. Bootstrap analysis (1500 pseudoreplicates) was employed to assess the evolutionary history of the taxa.

5. Conclusions

Grass carp have been reported from many countries and intensive culture practices makes this species susceptible to various parasitic diseases specifically myxozoans. Myxozoans are economically important groups of microscopic parasites among freshwater fishes especially in food and ornamental fishes. With this background, molecular characterization of the parasites is becoming increasingly important in order to identify the complex myxozoan parasites. The evolutionary assessment of present species shows the association of myxozoans species from fish host order and tissue specificity. Hence, details of the present myxospore based on morphological, morphometric and phylogenetic analysis suggest that *M. grassi* sp. nov. is a new species to the scientific world.

Author Contributions: Conceptualization, N.F. and R.A.; methodology, N.F. and H.K.; validation, H.K. and M.S.; formal analysis, N.F. and G.K.; investigation, N.F. and G.K.; data curation, M.S.; writing—original draft preparation, N.F.; writing—review and editing, G.K., H.K. and M.E.-M.; visualization, N.F. and H.K. All authors have read and agreed to the published version of the manuscript.

Funding: This research received no external funding. Open access funding was provided by the Clinical Division of Fish Medicine, University of Veterinary Medicine Vienna, Austria, PP291-ELM to Mansour El-Matbouli.

Institutional Review Board Statement: All experiments and methods were performed as per the guidelines of Committee for the Purpose of Control and Supervision of Experiments on Animals experimentation with relevant guidelines and regulations, India under the permission numbers G/FHM/01/10 and 148/2010.

Informed Consent Statement: Not applicable.

Data Availability Statement: The data supporting the conclusions of this article are included within the article. The sequences have been submitted to the GenBank database under the accession number KP268649.

Acknowledgments: The authors acknowledge the Director, ICAR-National Bureau of Fish Genetic Resources, Lucknow for providing the support to conduct the present study. Open Access Funding by the University of Veterinary Medicine Vienna, Austria.

Conflicts of Interest: The authors declare that there is no conflict of interest.

Nomenclature Acts

The nomenclature act of present work was registered under ZooBank. Identifier for this publication is: http://zoobank.org/urn:lsid:zoobank.org:pub:9306AE87-D87A-47B6-A336-FE0F93A330D6 (accessed on 11 May 2018).

References

1. Thilsted, S.H.; James, D.; Toppe, J.; Subasinghe, R.; Karunasagar, I. Maximizing the contribution of fish to human nutrition. In Proceedings of the ICN2 Second International Conference on Nutrition Better Nutrition Better Lives, Rome, Italy, 19–21 November 2014; FAO: Rome, Italy; UN & WHO: Geneva, Switzerland, 2014.
2. FAO. Food and Agriculture Organization of the United Nations: Fisheries and Aquaculture Department, Cultured Aquatic Species Information Programme: *C. idellus* (Valenciennes, 1844). 2018. Available online: http://www.fao.org/fishery/culturedspecies/Ctenopharyngodon_idellus/en#tcNA00EA (accessed on 11 May 2018).
3. Lom, J.; Dyková, I. Myxozoan genera: Definition and notes on taxonomy, life-cycle terminology and pathogenic species. *Folia Parasitol.* **2006**, *53*, 1–36. [CrossRef]
4. Okamura, B.; Gruhl, A.; Bartholomew, J.L. *Myxozoan Evolution, Ecology and Development*; Springer: London, UK, 2015.
5. Lom, J.; Dykova, I. *Protozoan Parasites of Fishes. Developments in Aquaculture & Fisheries*; Elsevier: Amsterdam, The Netherlands, 1992; Volume 26, p. 328.
6. Eiras, J.C.; Molnar, K.; Lu, Y.S. Synopsis of the species of *Myxobolus* Butschili 1882 (*Myxozoa: Myxosporea: Myxobolidae*). *Syst. Parasitol.* **2005**, *61*, 36–41. [CrossRef] [PubMed]
7. Eiras, J.C.; Zhang, J.; Molnár, K. Synopsis of the species of *Myxobolus* Bütschli, 1882 (*Myxozoa: Myxosporea, Myxobolidae*) described between 2005 and 2013. *Syst. Parasitol.* **2014**, *88*, 11–36. [CrossRef] [PubMed]
8. Kaur, H.; Singh, R. A synopsis of the species of *Myxobolus* Butschli, 1882 (*Myxozoa: Bivalvulida*) parasitizing Indian fishes and a revised dichotomous key to myxosporean genera. *Syst. Parasitol.* **2012**, *81*, 17–37. [CrossRef]
9. Kaur, H. Myxozoan Infestation in Freshwater Fishes in Wetlands and Aquaculture in Punjab (India). *Adv. Anim. Vet. Sci.* **2014**, *2*, 488–502. [CrossRef]
10. Matter, A.F.; Abbass, A.A.; Abd El Gawad, E.A.; El-Asely, A.M.; Shaheen, A.A. Studies on myxosporidiosis in some fresh water fishes. *Benha Vet. Med. J.* **2013**, *25*, 316–325.
11. Kaur, H.; Katoch, A. Prevalence, site and tissue preference of myxozoan parasites infecting gills of cultured fish in Punjab (India). *Dis. Aquat. Org.* **2016**, *118*, 129–137. [CrossRef]
12. Kalavati, C.; Nandi, N.C. *Handbook of Myxosporidean Parasites of Indian Fishes*; Zoological Survey of India: Kolkata, India, 2007; p. 293.
13. Gupta, A.; Kaur, H. Morphological and molecular characterization of *Myxobolus puntiusii* n. sp. (*Cnidaria: Myxosporea*) infecting *Puntius sophore* Hamilton, 1822 from Ranjit Sagar Wetland, Punjab (India). *Turk. J. Zool.* **2017**, *41*, 791–799. [CrossRef]

14. Kaur, H.; Singh, R. Observation on one new species of the genus *Myxobolus* (*Myxozoa: Myxosporea: Bivalvulida*) and redescription of *Myxobolus magauddi* (Bajpai, 1981) Landsberg and Lom, 1991 recorded from freshwater fishes of Kanjali Wetland of Punjab (India). *Proc. Natl. Congr. Parasitol.* **2008**, *81*, 75–79.
15. Basu, S.; Haldar, D.P. Description of three new myxosporean species (*Myxozoa: Myxosporea: Bivalvulida*) of the Genera *Myxobilatus* Davis, 1944 and *Myxobolus* Bütschli, 1882. *Acta Protozool.* **2004**, *43*, 337–343.
16. Basu, S.; Modak, B.K.; Haldar, D.P. Two new species of *Myxobolus* Butschli, 1882 (*Myxozoa: Myxosporea: Bivalvulida*) from food fishes of West Bengal, India- a light and scanning electron microscopy study. *Acta Protozool.* **2009**, *48*, 83–89.
17. Cone, D.; Marcogliese, D.J. Description of a new species of myxozoan from *Notropis hudsonius* in the Great Lakes region of Canada. *J. Parasitol.* **2010**, *96*, 1164–1167. [CrossRef] [PubMed]
18. Gupta, S.; Khera, S. Observations on *Myxobolus haldari* sp. nov. (*Myxozoa: Myxosporea*) from freshwater fishes of North India. *Res. Bull. Punjab Univ. Sci.* **1989**, *40*, 281–291.
19. Easy, R.H.; Johson, S.C.; Cone, D.K. Morphological and molecular comparison of *Myxobolus procerus* (Kudo, 1934) and *M. intramusculi* n. sp (Myxozoa) parasitising muscles of the trout-perc *Percopsis omiscomaycus*. *Syst. Parasitol.* **2005**, *31*, 115–122. [CrossRef]
20. Gupta, S.; Khera, S. On one new and one already known species of the genus *Myxobolus* from freshwater fishes of India. *Res. Bull. Punjab Univ. Sci.* **1988**, *39*, 173–179.
21. Jayasri, M.; Parvateesam, M.; Mathur, P.N. *Myxosoma mathurii* n. sp. (*Protozoa: Myxosporidia*) parasitic on *Puntius sarana* (Ham.). *Curr. Sci.* **1981**, *50*, 736–738.
22. Madhavan, R.; Bandyopadhyay, P.B.; Santosh, B. Observations on two new species of *Myxobolus Butschli*, 1882 from minor carps of Tripura, India. *J. Parasit. Dis.* **2013**, *37*, 56–61. [CrossRef]
23. Ferguson, J.A.; Atkinson, S.D.; Whipps, C.M.; Kent, M.L. Molecular and morphological analysis of *Myxobolus* spp. of salmonid fishes with the description of a new *Myxobolus* species. *J. Parasitol.* **2008**, *94*, 1322–1334. [CrossRef]
24. Zhang, J.Y.; Yokoyama, H.; Wang, J.G.; Li, A.H.; Gong, X.N.; Ryu-Hasegawa, A.; Iwashita, M.; Ogawa, K. Utilization of tissue habitats by *Myxobolus wulii* Landsberg & Lom, 1991 in different carp hosts and disease resistance in allogynogenetic gibel carp: Redescription of *M. wulii* from China and Japan. *J. Fish Dis.* **2010**, *33*, 57–68.
25. Molnar, K.; Eszterbauer, E.; Marton, S.; Cech, G.; Szkely, C. *Myxobolus erythrophthalmi* sp. n. and *Myxobolus shaharomae* sp. n. (Myxozoa: Myxobolidae) from the internal organs of rudd, *Scardinius erythrophthalmus* and bleak, *Alburnus alburnus*. *J. Fish Dis.* **2009**, *32*, 219–231. [CrossRef]
26. Kaur, H.; Gupta, A. Genetic relatedness provides support for a species complex of myxosporeans infecting the Indian major carp, Labeo rohita. *Anim. Biol.* **2015**, *65*, 337–347. [CrossRef]
27. Shivam, S.; El-Matbouli, M.; Kumar, G. Development of Fish Parasite Vaccines in the OMICs Era: Progress and Opportunities. *Vaccines* **2021**, *9*, 179. [CrossRef] [PubMed]
28. Fariya, N. Protocol identification and preservation of myxozoan parasites for microscopy with silver nitrate (Klein's Dry) staining technique. *Microsc. Res. Tech.* **2018**, *81*, 1162–1164. [CrossRef] [PubMed]
29. Lom, J.; Arthur, J.R. A guideline for the preparation of species descriptions in Myxosporea. *J. Fish Dis.* **1989**, *12*, 151–156. [CrossRef]
30. Molnar, K.; Eszterbauer, E.; Szekely, C.; Dan, A.; Harrach, B. Morphological and molecular biological studies on intramuscular Myxobolus spp. of cyprinid fish. *J. Fish Dis.* **2002**, *25*, 643–652. [CrossRef]
31. Abidi, R.; Fariya, N.; Chauhan, U.K. Description and molecular phylogeny of an exotic myxozoan, *Myxobolus arcticus* (Pugachev and Khokhlov, 1979) in kidney of *Clarias batrachus* from river Gomti, Lucknow, India. *Int. J. Curr. Res. (IJCR)* **2016**, *8*, 33209–33216.
32. Kumar, S.; Stecher, G.; Li, M.; Knyaz, C.; Tamura, K. Mega X: Molecular evolutionary Genetics analysis across computing platforms. *Mol. Biol. Evol.* **2018**, *35*, 1547–1549. [CrossRef]
33. Altschul, S.F.; Madden, T.L.; Schäffer, A.A.; Zhang, J.; Zhang, Z.; Miller, W.; Lipman, D.J. Gapped BLAST and PSI-BLAST: A new generation of protein database search programs. *Nucl. Acids Res.* **1997**, *25*, 3389–3402. [CrossRef]

pathogens

MDPI

Article

Host–Parasite Interaction and Phylogenetic of a New Cnidarian *Myxosporean* (Endocnidozoa: Myxobolidae) Infecting a Valuative Commercialized Ornamental Fish from Pantanal Wetland Biome, Brazil

Patrick D. Mathews [1,*], Omar Mertins [2], Anai P. P. Flores-Gonzales [3], Luis L. Espinoza [4], Julio C. Aguiar [1] and Tiago Milanin [5]

[1] Department of Zoology, Institute of Bioscience, University of São Paulo, São Paulo 05508-090, Brazil
[2] Laboratory of Nano Bio Materials, Department of Biophysics, Paulista Medical School, Federal University of Sao Paulo, São Paulo 04023-062, Brazil
[3] Research Institute of Peruvian Amazon (IIAP-AQUAREC), Puerto Maldonado, Madre de Dios 17000, Peru
[4] Laboratory of Biology and Molecular Genetics, Faculty of Veterinary Medicine, Universidad Nacional Mayor de San Marcos, Lima 15021, Peru
[5] Department of Basic Sciences, Faculty of Animal Science and Food Technology, University of São Paulo, Pirassununga 13635-900, Brazil
* Correspondence: patrick.mathews@unifesp.br or patrickmathews83@gmail.com

Abstract: Myxozoans are a diverse group of parasitic cnidarians of wide distribution. A new species, *Myxobolus matogrossoensis* n. sp., is herein described infecting wild specimens of tetra mato-grosso *Hyphessobrycon eques*, caught in the Pantanal biome, the world's largest tropical wetland area. Cysts were found in 3 of the 30 examined fishes. Mature myxospores were ovoid in shape in frontal and measured 6.6 ± 0.4 µm (6.2–7.0 µm) in length and 3.5 ± 0.2 µm (3.3–3.7 µm) in width. The two polar capsules were elongated in shape, equal in size and occupying almost half of the myxospore body. They measured 3.3 ± 0.2 µm (3.1–3.5 µm) in length and 1.8 ± 0.1 µm (1.7–1.9 µm) in width. The polar tubules presented three to four turns. Phylogenetic analysis placed the new species within a clade containing myxobolid species from South American characiforms fish and appears as a close species of *Myxobolus piraputangae* and *Myxobolus umidus*. Nevertheless, the sequences of the new species and *P. umidus* and *P. piraputangae* have a large genetic divergence of 12 and 12.2% in their 18S rDNA gene, respectively. To the best of our knowledge, this is the first report of a *Myxobolus* species parasitizing the tetra fish mato-grosso, thus increasing our knowledge of cnidarian myxosporean diversity from South America.

Keywords: cnidaria; Myxobolus; ornamental fish; Pantanal biome; Brazil

1. Introduction

Myxozoans are a biologically diverse group of microscopic cnidarians of wide distribution around the world [1]. They are parasites mostly innocuous with complex life cycles that include invertebrate and vertebrate hosts [1]. Although the majority of species have fish hosts, they have radiated sporadically into other groups of vertebrates, including amphibians, reptiles, waterfowl and small mammals [2]. Within the myxozoans, *Myxobolus* Bütschli, 1882, is one of the highly rich genera with more than 900 species described taxonomically, infecting a large variety of fishes within a wide geographical range [3–5].

Regarding South America, several studies have described *Myxobolus* species infecting many species of wild and farmed freshwater fish [3,6,7]. Despite this, information on ornamental freshwater fish is still scarce. The Pantanal biome is one the main biodiversity hotspots, harboring around 300 fish species [8], however, the myxozoan fauna are poorly known. Indeed, only 10 *Myxobolus* species were reported in fish from this geographic

region [3,7,9]. With approximately 143 recognized species the genus *Hyphessobrycon* Durbin, 1908, is one of the largest characid genera with a wide distribution in all major watersheds of the Neotropical Region [10]. The *Hyphessobrycon* eques Steindachner, 1882, vernacularly called "tetra mato-grosso", is originally found in the Amazon, Guaporé and Paraguay basins [11] and it is widely found in aquarium stores in several regions of Brazil. It typically inhabits ponds and small lakes, where it forms aggregations around marginal vegetation or submerged tree roots. Despite the commercial importance in the aquarium trade, information about the parasite fauna is still scarce and nothing is known about myxozoan parasites.

In the present study, we describe for the first time a histozoic myxozoan infecting the gills of the body of specimens of H. eques from the Pantanal biome, the largest freshwater wetland in the world, thus increasing our knowledge of cnidarian myxozoan diversity from South America.

2. Material and Methods

In July 2019, 30 specimens of H. eques (ranging from 3.8 to 4 cm in length) were examined for the presence of myxozoan parasites. The fish were acquired from local fisherfolk and were caught in the marginal vegetation beds in the oxbow lakes of Paraguay River near the municipality Porto Murtinho, Brazil. The fish were transported to the field laboratory, where they were euthanized by pit transaction and examined using a light microscope to verify the presence of lesions and myxozoans.

Morphological characterization was performed based on the criteria outlined by Lom and Arthur [12]. Measurements and photographs were taken from 30 randomly selected mature myxospores, using a computer equipped with Axiovision 4.1 image capture software coupled to an Axioplan 2 Zeiss microscope (Carl Zeiss AG, Oberkochen, Germany). The dimensions were given in micrometers (μm) and expressed as the mean ± standard deviation, followed by the range in parentheses and included spore length, thickness, polar capsule length and width. The gill plasmodial index (GPI) was determined based on the criteria established by Kaur and Katock [13] and categorization of plasmodia on the basis of size was calculated according to Kaur and Attri [14]. The plasmodia type localization was determined according to Molnár [15]. Mature myxospores released from ruptured plasmodia were air-dried, fixed with methanol, stained with Giemsa and mounted on permanent slides deposited in the cnidarian collection of the Zoology Museum at the University of São Paulo, São Paulo, Brazil.

For scanning electron microscopy, infected tissues were fixed in 2.5% glutaraldehyde prepared in 0.1 M sodium cacodylate buffer (pH 7.2), then post-fixed in 1% osmium tetroxide overnight, and dehydrated in a graded ethanol series. The samples were dried in a critical point chamber (BALZERSCPD 030, Columbia, South Carolina, SC, USA) using carbon dioxide, and were included in an aluminum stub using double-sided carbon tape and coated with a thin layer of platinum with a thickness of 20–30 nm (SPUTTERING, ©LEICA EM SCD 500, Wetzlar, Germany). Samples were visualized with a DSM 940 scanning electron microscope (Carl Zeiss, Hamburg, Germany) operating at 15 kV.

For molecular analysis, cysts were dissected from the gill lamellae and fixed in absolute ethanol. Extraction of genomic DNA was performed using QIAamp DNA Micro Kit (Qiagen, California, CA, USA). The concentration of the DNA was measured using a NanoDrop 2000 spectrophotometer (Thermo Scientific, Wilmington, North Carolina, NC, USA). Small subunit ribosomal DNA (18S rDNA) was amplified using universal eukaryotic primers ERIB1 (ACCTGGTTGATCCTGCCAG; [16]) with ERIB10 (CTTCCGCAGGTTCACCTACGG; [16]). Polymerase chain reactions were conducted in a final volume reaction of 20 μL, comprised of 1 μL of extracted DNA (10–50 ng), 0.3 μL of each primer (10 μM), and 0.625 U of Qiagen Taq DNA polymerase. Polymerase chain reactions were performed in a Thermocycler (Bio-rad T100) with initial denaturation at 94 °C for 5 min, followed by 39 cycles at 94 °C for 1 min, 58 °C for 1 min, 72 °C for 2 min and then final elongation at 72 °C for 5 min. The amplicons were subjected to electrophoresis in 2% agarose gel in a

TAE buffer (Tris–Acetate EDTA: Tris 40 mM, acetic acid 20 mM, EDTA 1 mM). The size of the amplicons was estimated by comparison with the 1 Kb Plus DNA Ladder (Invitrogen by Life Technologies). Polymerase chain reactions using the original primers and two additional primers, MC5 and MC3 [17], were used in the sequencing to connect the overlapping fragments. Sequencing was performed with a BigDye® Terminator v3.1 cycle sequencing kit (Applied Biosystems Inc., Valencia, CA, USA) in an ABI 3730 DNA sequencing analyzer (Applied Biosystems).

A standard nucleotide BLAST search was conducted to verify the similarity of the sequence obtained in this study with other sequences available in GenBank [18]. Phylogenetic analysis was conducted using the most closely related myxozoans sequences with similarity >80%. The sequences were aligned with ClustalW within BioEdit version 7.1.3.0 [19]. Phylogenetic analysis was performed using Maximum Likelihood method with a Kimura 2-parameter (K2P) evolution sequence model in MEGA 6.0 [20]. Bootstrap analysis with 1000 replicates was employed to assess the relative robustness of the branches in Maximum Likelihood tree. *Ceratomyxa seriolae* sequence was used as outgroup. To evaluate the genetic distance between the myxozoan species clustering together with the new obtained sequence, a pairwise method with the p-distance model in MEGA 6.0 [20] was performed.

3. Results

Out of 30 wild specimens of H. eques examined, three (10%) had the gill infected by a new cnidarian myxozoan species of the genus Myxobolus, described herein.

Taxonomic summary

1. Phylum: Cnidaria Verrill, 1865
2. Class: Myxosporea Bütschli, 1881
3. Order: Bivalvulida Shulman, 1959
4. Family: Myxobolidae Thélohan, 1892
5. Genus: *Myxobolus* Bütschli, 1882
6. Species: Myxobolus matogrossoensis n. sp.
7. Type host: *Hyphessobrycon eques* (Characiformes: Characidae)
8. Site of infection: Gills (Interlamellar-epithelial type, LE2)
9. Gill plasmodium index (GPI): 1 (light infection)
10. Category of plasmodium: Type A (visible under light microscope, size range 40–65 μm)
11. Type of locality: Adjacent area of lakes of Paraguay River near the municipality Porto Murtinho, Mato Grosso do Sul State, Brazil (21°41′56″ S, 57°52′58″ W).
12. Prevalence: From 30 examined fish, three were infected (10%).
13. Type of material: Hapantotype (slides with stained myxospores) were deposited in the cnidarian collection of the Zoology Museum at the University of São Paulo—MZUSP, São Paulo, Brazil (slide no. MZUSP 8695). Partial 18S rDNA sequence gene was deposited in GenBank under accession number OP244900.
14. Etymology: The specific name (*M. matogrossoensis*) is based on host species common name.

Rounded cysts containing large quantities of smaller myxospores, measuring up to 46–55 μm, were found in the gills. Scanning electron microscopy analysis of infected tissues revealed that cyst development occurred in the lamellae (Figure 1a,b).

Mature myxospores were ovoid in shape in frontal and measured 6.6 ± 0.4 μm (6.2–7.0 μm) in length and 3.5 ± 0.2 μm (3.3–3.7 μm) in width (Figure 2a,b). The two polar capsules were elongated in shape, equal in size and occupying almost half of the myxospore body (Figure 2a,b). They measured 3.3 ± 0.2 μm (3.1–3.5 μm) in length and 1.8 ± 0.1 μm (1.7–1.9 μm) in width. The polar tubules presented three to four turns (Figure 2b). Some myxospores were observed with extended polar tubule (Figure 2c). Comparative data of *Myxobolus matogrossoensis* n. sp. with all *Myxobolus* species described in fish from Pantanal wetland biome are showed in Table 1.

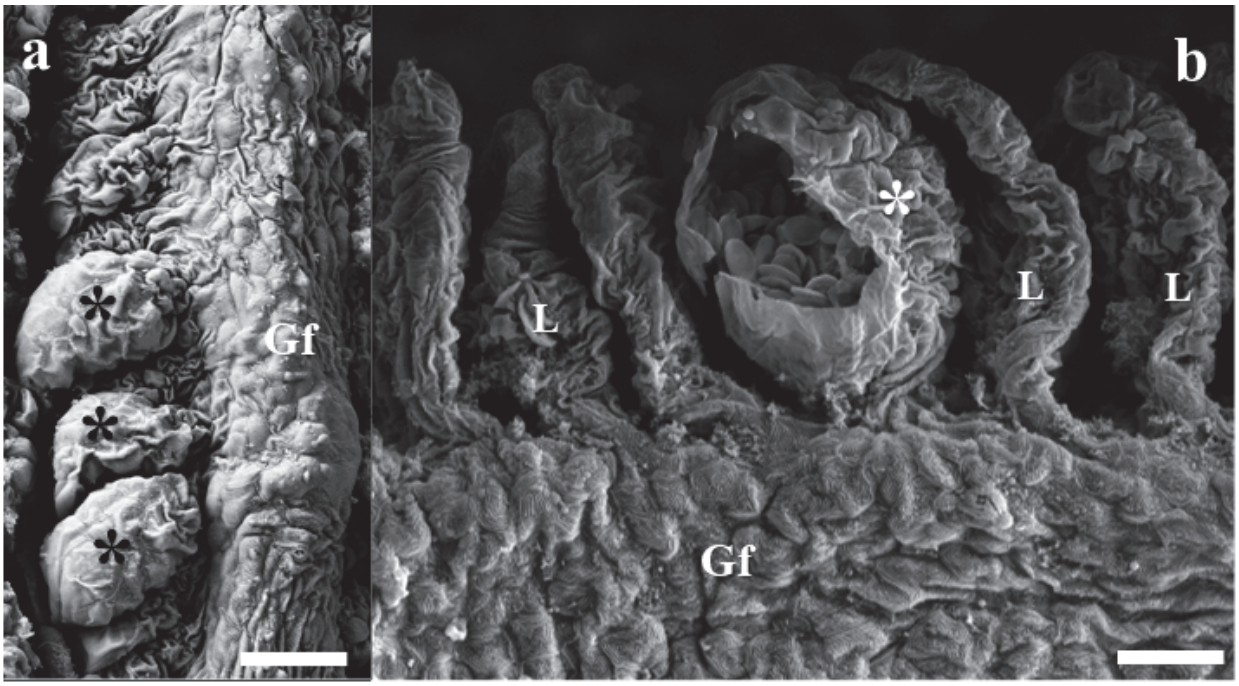

Figure 1. Gill lamellae infected with *M. matogrossoensis* n. sp. (**a**) Gill filament (Gf) showing three cysts (asterisks) in their lamellae (L). (**b**) Ruptured cyst (asterisk) evidencing inside large quantity of smaller myxospores. Scale bars = 20 μm.

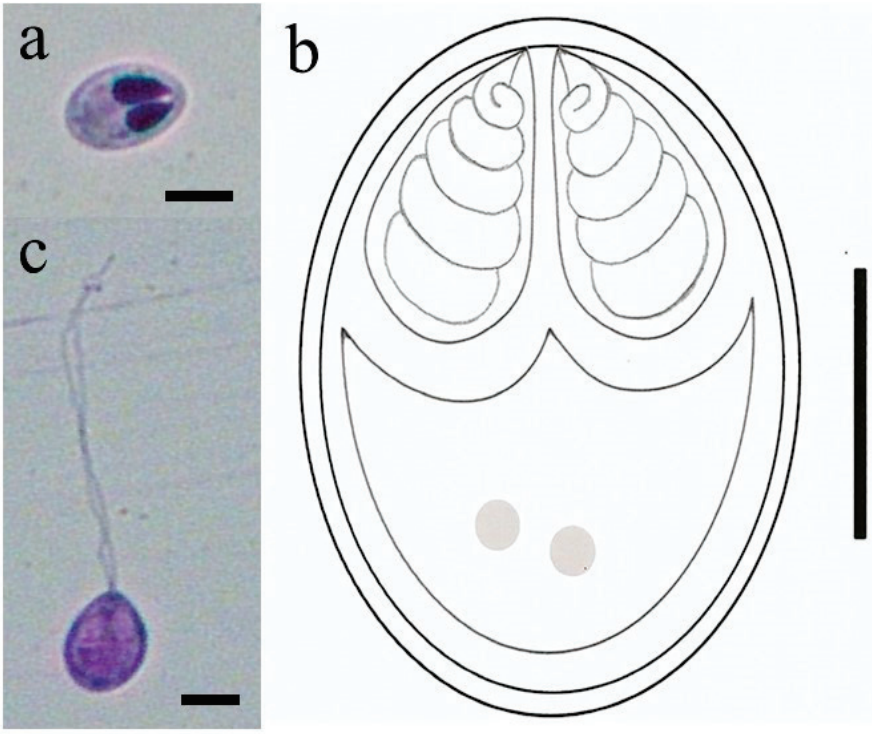

Figure 2. Mature myxospores of *M. matogrossoensis* n. sp. stained with Giemsa. (**a**) Mature myxospore showing two equal-size polar capsules. Scale bar = 5 μm. (**b**) Myxospore with extended polar tubule. Scale bar = 5 μm. (**c**) Schematic representation of a mature myxospore. Scale bar = 2 μm.

Table 1. Comparative data of *Myxobolus matogrossoensis* n. sp. with all *Myxobolus* species described in fish from Pantanal wetland biome. Spore dimensions are given. SL, length of the spore; SW, width of the spore; ST, thickness of the spore; PCL, length of the polar capsules; PCW, width of the polar capsules; NC, number of coils of the polar tubules; -, no data. All measurements are range in μm and/or means ± SD.

Myxobolus Species	SL	SW	ST	PCL	PCW	NC	Site of Infection
This study	6.6 ± 0.4	3.5 ± 0.2	-	3.3 ± 0.2	1.8 ± 0.1	3–4	Gill lamelae
M. sp. Mathews, Mertins, Milanin, Aguiar, Gonzales-Flores, Tavares & Morandini, 2022	22.7 ± 1.2 (21.5–23.9)	12.5 ± 0.4 (12.1–12.9)	11.3 ± 0.5 (10.8–11.8)	4.6 ± 0.3 (3.9 ± 4.3)	2.9 ± 0.1 (2.8–3.0)	4–5	Mandibule
M. cordeiroi. Adriano, Arana, Alves, Silva, Ceccarelli, Henrique-Silva & Maia, 2009	10.8 ± 0.5	7.1 ± 0.2	5.3 ± 0.3	5.2 ± 0.3	1.4 ± 0.1	5–6	Gill arch, skin, body, eye
M. salminus. Adriano, Arana, Carriero, Naldoni, Ceccarelli & Maia, 2009	9.6–10.5 (10.1 ± 0.4)	5.8–6.6 (6.1 ± 0.4)	4.7–5.3 (5.0 ± 0.6)	4.3–4.8 (4.6 ± 0.2)	1.5–1.9 (1.7 ± 0.1)	7–8	Gill filament
M. oliveirai. Milanin, Eiras, Arana, Maia, Alves, Silva, Carriero, Ceccarelli & Adriano, 2010	11.2 ± 0.4	7.4 ± 0.5	4.6 ± 0.6	5.6 ± 0.2	2.3 ± 0.2	6–8	Gill filament
M. brycon. Azevedo, Casal, Marques, Silva & Matos, 2011	6.9 ± 0.6 (6.5–7.2)	3.9–4.8 (4.2 ± 0.5)	1.9–2.8 (2.5 ± 0.7)	3.8–4.7 (4.2 ± 0.6)	1.7–2.5 (1.9 ± 0.6)	8–9	Gill filament
M. flavus. Carriero, Adriano, Silva, Ceccarelli, Maia, 2013	9.2 ± 0.2	6.5 ± 0.3	4.2 ± 0.2	4.5 ± 0.2	1.6 ± 0.1	4–5	Gill arch
M. pantanalis. Carriero, Adriano, Silva, Ceccarelli, Maia, 2013	9.3 ± 0.4	6.5 ± 0.4	-	4.2 ± 0.5	2.0 ± 0.1	4	Gill filament
M. aureus. Carriero, Adriano, Silva, Ceccarelli, Maia, 2013	12.6 ± 0.5	8.3 ± 0.3	5.5 ± 0.3	5.7 ± 0.3	2.9 ± 0.2	7–8	Liver
M. umidus. Carriero, Adriano, Silva, Ceccarelli, Maia, 2013	13.5 ± 0.7	7.8 ± 0.4	7.7 ± 0.1	5.1 ± 0.4	2.7 ± 0.3	5	Spleen
M. piraputungae. Carriero, Adriano, Silva, Ceccarelli, Maia, 2013	10.1 ± 0.5	8.7 ± 0.5	6.7 ± 0.3	5.2 ± 0.4	3.0 ± 0.3	4–5	Kidney

BLAST search performed with the sequencing of the 18S rDNA from the myxospores obtained in the study revealed that this sequence did not match any of myxozoans available in GenBank database. Sequence with the highest similarity identified by BLAST search was from *Myxobolus piraputangae* Carriero, Adriano, Silva, Ceccarelli and Maia, 2013 (query coverage 98%, maximum identities 88.3%), reported in the kidney of *Brycon hilarii*, from the Pantanal National Park, Mato Grosso State, Brazil [9]. Phylogenetic analysis inferred by the Maximum Likelihood method based on the most closely related myxozoan sequences placed the new obtained sequence together with *M. piraputangae* and *M. umidus* Carriero, Adriano, Silva, Ceccarelli and Maia, 2013 (Figure 3). Pairwise analysis of the 18S rDNA sequences of the myxosporean species that cluster in the same clade with the sequence obtained herein revealed an important genetic divergence among these species, with a difference of 12.2% to *M. piraputangae* and 12% to *M. umidus*.

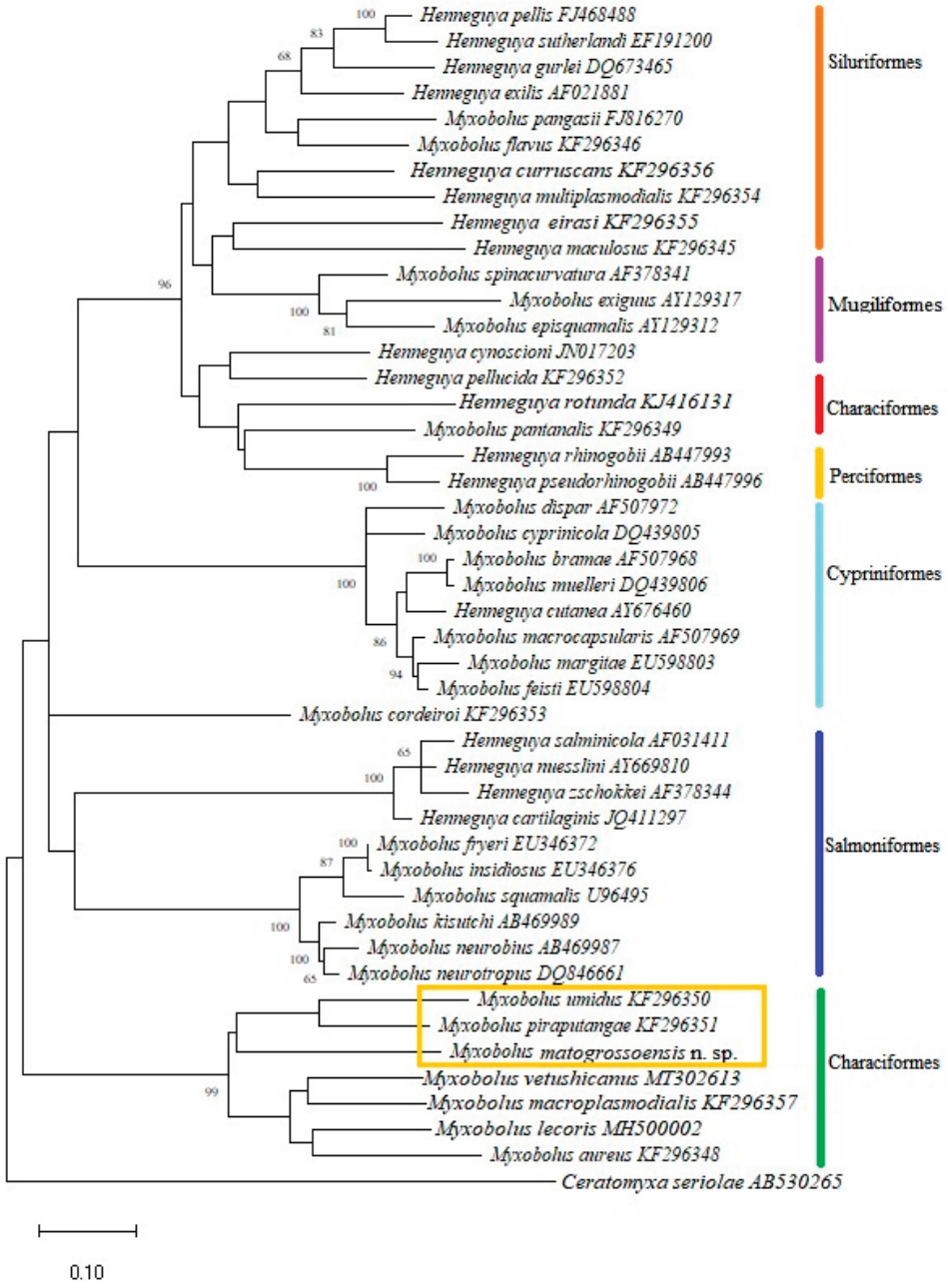

Figure 3. Phylogenetic tree generated based on 18S rDNA sequences of *Myxobolus* species and other closely related myxozoan species. Bootstrap values above 60 are indicated.

4. Discussion

In South America the description of new myxozoan species has been increasing over the years [3], however, myxozoan diversity is still poorly known [21]. Indeed, considering that this biogeographic region harbors the greatest diversity of potential freshwater fish hosts of any continent, it is suggested that many more myxosporean parasites remain to be discovered [22]. This study expands our knowledge about South American myxozoans, with description of a new species from an important ornamental fish from Pantanal biome. To the best of our knowledge, this is the first report of a *Myxobolus* species parasitizing H. eques.

Although molecular tools have revealed great discrepancies between spore-based myxosporean taxonomy and molecular phylogenies inferred from the SSU rDNA [23], mostly myxozoan species have been described exclusively based on myxospore morphology. Thus, morphology-based comparisons remain the main criterion and are necessary

to differentiate the large number of myxozoan species that lack molecular data [24]. Indeed, from South America, considering the around hundred described myxozoans, few species have their SSU rDNA sequences available in Gen-Bank [25]. Taking this issue into account, morphological comparison was performed considering species previously described as infecting fish from the Pantanal biome. The comparison between the mature myxospores of the new isolate and the others showed remarkable differences as evidenced in Table 1. According to Molnár [17] the exact location and tissue specificity is also essential for differentiation of gill-parasitic fish myxosporean species. Accordingly, differences were observed in the infected tissue between the new isolate and the other previously described Myxobolus species from the Pantanal biome.

The molecular phylogenetic analysis performed in our study showed members of genus *Myxobolus* and *Henneguya* grouped together in the produced tree (Figure 3). This is in agreement with previous studies in South America [6,9,26] and other biogeographic regions around the world that showed absence of phylogenetic separation between these two genera [4,27]. Our phylogenetic analysis also showed a strong tendency of myxobolid species to form clusters mainly based on the order and/or family of the host, despite having different geographic origins, as has been previously reported [6,9,27]. According to Carriero et al. [9] the strong tendency of *Myxobolus*/*Henneguya* species to cluster, based on host phylogenies, suggests that the origins and radiations of myxozoans are very ancient, perhaps as old as the hosts themselves that go back to an Osteichthyes Early Silurian origin and Mesozoic radiation. Our topology shows the new isolate placed in a subclade composed exclusively of *Myxobolus* spp. of bryconid fishes from South America, with *M. umidus* and *M. piraputanagae* as the closest related species (Figure 3). However, pairwise similarity analysis revealed the new isolate and these two species have a large genetic divergence of 12.2% to *M. piraputangae* and 12% to *M. umidus*, in their SSU rDNA gene sequences. Taken together, we confidently consider that these data are sufficient to define this isolate as a new freshwater *Myxobolus* species, *Myxobolus matogrossoensis* n. sp. The presence of M. matogrossoensis n. sp. inside a well-supported clade of fish from the family Bryconidae may be attributed to the few sequences available in the GenBank for many yet-to-be-discovered *Myxobolus* species from these underrepresented ornamental characids. Thus, the addition of molecular data from other taxa will enable a better understanding about the evolutionary context of *M. matogrossoensis* n. sp. Conversely, the low occurrence of *M. matogrossoensis* n. sp. in H. eques may suggest accidental infection of these hosts with infective actinospores, especially during the dry season (fish collection season in this study) when the water level is low and fishes are more concentrated. This may have favored the encounter with infective stages. We believe that this new isolate may be found in the future in a bryconid host species still not studied.

Author Contributions: P.D.M.: Conceptualization, Methodology, Investigation, Formal analysis, Data curation, Writing–original draft. O.M.: Formal analysis, Data curation. T.M.: Methodology, Investigation, Formal analysis, Data curation. A.P.P.F.-G.: Methodology. J.C.A.: Methodology. L.L.E.: Investigation, Formal analysis. All authors have read and agreed to the published version of the manuscript.

Funding: This research was funded by São Paulo Research Foundation, FAPESP, Research Grant, number 2018/20482-3.

Institutional Review Board Statement: The study was conducted according to the guidelines of the Declaration of Helsinki, and approved by the Institutional Ethics Committee of Federal University of São Paulo Animal Ethics Committee (protocol code CEUA No. 9209080214).

Informed Consent Statement: Not applicable.

Data Availability Statement: The data set presented in this study are available upon reasonable request to the corresponding author.

Acknowledgments: The authors thank the São Paulo Research Foundation, FAPESP, for Post-Doc fellowship awarded to P.D. Mathews (grant no. 2018/20482–3). The authors are grateful to A.H. Aguillera, P.A. Cortez and R. Sinigaglia-Coimbra from the Electron Microscopy Center (CEME) at UNIFESP for supporting the SEM. P.D. Mathews thanks Edson A. Adriano for his valuable suggestions at this article. The authors thank Christopher George Berger from the Occidental College for revision of the English idiom.

Conflicts of Interest: All the authors declare that there is no conflict of interest in this paper.

References

1. Atkinson, S.D.; Bartholomew, J.L.; Lotan, T. Myxozoans: Ancient metazoan parasites find a home in phylum Cnidaria. *Zoology* **2018**, *129*, 66–68. [CrossRef] [PubMed]
2. Okamura, B.; Gruhl, A.; Bartholomew, J.L. (Eds.) An introduction to Myxozoan evolution, ecology and development. In *Myxozoan Evolution, Ecology and Development*; Springer: Cham, Switzerland, 2015; pp. 1–20.
3. Eiras, J.C.; Cruz, C.F.; Saraiva, A.; Adriano, E.A. Synopsis of the species of Myxobolus (Cnidaria, Myxozoa, Myxosporea) described between 2014 and 2020. *Folia Parasitol.* **2021**, *68*, 012. [CrossRef] [PubMed]
4. Mathews, P.D.; Bonillo, C.; Rabet, N.; Lord, C.; Causse, R.; Keith, P.; Audebert, F. Phylogenetic analysis and characterization of a new parasitic cnidarian (Myxosporea: Myxobolidae) parasitizing skin of the giant mottled eel from the Solomon Islands. *Infec. Genet. Evol.* **2021**, *94*, 104986. [CrossRef] [PubMed]
5. Fariya, N.; Kaur, H.; Singh, M.; Abidi, R.; El-Matbouli, M.; Kumar, G. Morphological and Molecular Characterization of a New Myxozoan, *Myxobolus grassi* sp. nov. (Myxosporea), Infecting the Grass Carp, *Ctenopharyngodon idella* in the Gomti River, India. *Pathogens* **2022**, *11*, 303. [CrossRef] [PubMed]
6. Milanin, T.; Mathews, P.D.; Morandini, A.C.; Mertins, O.; Audebert, F.; Pereira, J.O.L.; Maia, A.A.M. Morphostructural data and phylogenetic relationships of a new cnidarian myxosporean infecting spleen of an economic and ecological important bryconid fish from Brazil. *Microb. Pathog.* **2021**, *150*, 104718. [CrossRef]
7. Mathews, P.D.; Mertins, O.; Milanin, T.; Aguiar, J.C.; Gonzales-Flores, A.P.P.; Tavares, L.E.R.; Morandini, A.C. Ultrastructure, surface topography, morphology and histological observations of a new parasitic cnidarian of the marbled swamp eel from the world's largest tropical wetland area, Pantanal, Brazil. *Tissue Cell* **2022**, *79*, 101909. [CrossRef]
8. Florentino, A.C.; Petrere, M.; Freitas, C.E.D.C.; Toledo, J.J.; Mateus, L.; Súarez, Y.R.; Penha, J. Determinants of changes in fish diversity and composition in floodplain lakes in two basins in the Pantanal wetlands, Brazil. *Environ. Biol. Fish.* **2016**, *99*, 265–274. [CrossRef]
9. Carriero, M.M.; Adriano, E.A.; Silva, M.R.M.; Ceccarelli, P.S.; Maia, A.A.M. Molecular phylogeny of the *Myxobolus* and *Henneguya* genera with several new south American species. *PLoS ONE* **2013**, *8*, e73713. [CrossRef]
10. García-Alzate, C.A.; Urbano-Bonilla, A.; Taphorn, D.C. A new species of Hyphessobrycon (Characiformes, Characidae) from the upper Guaviare River, Orinoco River Basin, Colombia. *ZooKeys* **2017**, *668*, 123–138. [CrossRef]
11. Pelicice, F.M.; Agostinho, A.A. Feeding ecology of fishes associated with *Egeria* spp. patches in a tropical reservoir, Brazil. *Ecol. Freshw. Fish* **2006**, *15*, 10–19. [CrossRef]
12. Lom, J.; Arthur, J.R. A guideline for the preparation of species descriptions in Myxosporea. *J. Fish Dis.* **1989**, *12*, 151–156. [CrossRef]
13. Kaur, H.; Attri, R. Morphological and molecular characterization of *Henneguya bicaudi* n. sp. (Myxosporea: Myxobolidae) infecting gills of *Cirrhinus mrigala* (Ham.) in Harike Wetland, Punjab (India). *Parasitol. Res.* **2015**, *114*, 4161–4167. [CrossRef] [PubMed]
14. Kaur, H.; Katoch, A. Prevalence, site and tissue preference of myxozoan parasites infecting gills of cultured fish in Punjab (India). *Dis. Aquat. Org.* **2016**, *118*, 129–137. [CrossRef] [PubMed]
15. Molnár, K.; Eszterbauer, E.; Sczekely, C.; Benko, M.; Harrach, B. Morphological and molecular biological studies on intramuscular *Myxobolus* spp. *of cyprinid fish. J. Fish Dis.* **2002**, *25*, 643–652. [CrossRef]
16. Barta, J.R.; Martin, D.S.; Liberator, P.A.; Dashkevicz, M.; Anderson, J.W.; Feighner, S.D.; Elbrecht, A.; Perkins-Barrow, A.; Jenkins, M.C.; Danforth, D.; et al. Phylogenetic relationships among eight *Eimeria* species infecting domestic fowl inferred using complete small subunit ribosomal DNA sequences. *J. Parasitol.* **1997**, *83*, 262–271. [CrossRef]
17. Molnár, K. Site preference of fish myxosporeans in the gill. *Dis. Aquat. Org.* **2002**, *48*, 197–207. [CrossRef]
18. Altschul, S.F.; Madden, T.L.; Schaffer, A.A.; Zhang, J.H.; Zhang, Z.; Miller, W.; Lipman, D.J. Gapped BLAST and PSI-BLAST: A new generation of protein database search programs. *Nucleic Acids Res.* **1997**, *25*, 3389–3402. [CrossRef]
19. Hall, T.A. BioEdit: A user-friendly biological sequence alignment editor and analysis program for Windows 95/98/NT. *Nucl. Acids Symp. Ser.* **1999**, *41*, 95–98.
20. Tamura, K.; Stecher, G.; Peterson, D.; Filipski, A.; Kumar, S. MEGA 6: Molecular evolutionary genetics analysis version 6.0. *Mol. Biol. Evol.* **2013**, *30*, 2725–2729. [CrossRef]
21. Okamura, B.; Hartigan, A.; Naldoni, J. Extensive uncharted biodiversity: The parasite dimension. *Integr. Comp. Biol.* **2018**, *58*, 1132–1145. [CrossRef]

22. Naldoni, J.; Arana, S.; Maia, A.A.M.; Silva, M.R.M.; Carriero, M.M.; Ceccarelli, P.S.; Tavares, L.E.R.; Adriano, E.A. Host–parasite–environment relationship, morphology and molecular analyses of *Henneguya eirasi* n. sp. parasite of two wild *Pseudoplatystoma* spp. in Pantanal wetland, Brazil. *Vet. Parasitol.* **2011**, *177*, 247–255. [CrossRef] [PubMed]
23. Fiala, I.; Bartosova-Sojkova, P.; Whipps, C.M. Classification and Phylogenetics of Myxozoa. In *Myxozoan Evolution, Ecology and Development*; Okamura, B., Gruhl, A., Bartholomew, J.L., Eds.; Springer: Cham, Switzerland, 2015; pp. 85–110.
24. Rocha, S.; Azevedo, C.; Alves, Â.; Antunes, C.; Casal, G. Morphological and molecular characterization of myxobolids (Cnidaria, Myxozoa) infecting cypriniforms (Actinopterygii, Teleostei) endemic to the Iberian Peninsula. *Parasite* **2019**, *26*, 48. [CrossRef] [PubMed]
25. Milanin, T.; Atkinson, S.D.; Silva, M.R.; Alves, R.G.; Maia, A.A.; Adriano, E.A. Occurrence of two novel actinospore types (Cnidaria: Myxosporea) in Brazilian fish farms, and the creation of a novel actinospore collective group, Seisactinomyxon. *Acta Parasitol.* **2017**, *62*, 121–128. [CrossRef] [PubMed]
26. Mathews, P.D.; Mertins, O.; Milanin, T.; Espinoza, L.L.; Flores-Gonzales, A.P.; Audebert, F.; Morandini, A.C. Molecular phylogeny and taxonomy of a new Myxobolus species from the endangered ornamental fish, Otocinclus cocama endemic to Peru: A host parasite coextinction approach. *Acta Trop.* **2020**, *210*, 105545. [CrossRef] [PubMed]
27. Liu, Y.; Lovy, A.; Gu, Z.; Fiala, I. Phylogeny of Myxobolidae (Myxozoa) and the evolution of myxospore appendages in the *Myxobolus* clade. *Int. J. Parasitol.* **2019**, *49*, 523–530. [CrossRef]

pathogens

MDPI

Communication

Monogeneans from Catfishes in Lake Tanganyika. II: New Infection Site, New Record, and Additional Details on the Morphology of the Male Copulatory Organ of *Gyrodactylus transvaalensis* Prudhoe and Hussey, 1977

Archimède Mushagalusa Mulega [1,2,3,*], Maarten Van Steenberge [2,4], Nikol Kmentová [2], Fidel Muterezi Bukinga [3], Imane Rahmouni [1], Pascal Mulungula Masilya [3,5], Abdelaziz Benhoussa [1], Antoine Pariselle [1,6] and Maarten P. M. Vanhove [2]

1 Laboratory Biodiversity, Ecology and Genome, Research Center Plant and Microbial Biotechnology, Biodiversity and Environment, Mohammed V University in Rabat, Rabat 10100, Morocco
2 Centre for Environmental Sciences, Research Group Zoology: Biodiversity & Toxicology, Hasselt University, 3590 Diepenbeek, Belgium
3 Département de Biologie, Centre de Recherche en Hydrobiologie, B.P. 73, Uvira, Democratic Republic of the Congo
4 OD Taxonomy and Phylogeny, Royal Belgian Institute for Natural Sciences, 1000 Brussels, Belgium
5 Unité d'Enseignement et de Recherche en Hydrobiologie Appliquée, Département de Biologie-Chimie, ISP/Bukavu, Bukavu, Democratic Republic of the Congo
6 ISEM, Université de Montpellier, CNRS, IRD, 34000 Montpellier, France
* Correspondence: archimedemulega@gmail.com; Tel.: +212-6840298-319

Abstract: The ichthyofauna of Lake Tanganyika consists of 12 families of fish of which five belong to Siluriformes (catfishes). Studies on Siluriformes and their parasites in this lake are very fragmentary. The present study was carried out to help fill the knowledge gap on the monogeneans infesting the siluriform fishes of Lake Tanganyika in general and, more particularly, *Clarias gariepinus*. Samples of gills of *Clarias gariepinus* (Clariidae) were examined for ectoparasites. We identified the monogenean *Gyrodactylus transvaalensis* (Gyrodactylidae). This is the first time this parasite was found infecting gills. We are the first to observe a large spine in the male copulatory organ of this species and to provide measurements of its genital spines; this completes the description of the male copulatory organ, which is important in standard monogenean identification. This is the first monogenean species reported in *C. gariepinus* at Lake Tanganyika and the third known species on a representative of Siluriformes of this lake. It brings the total number of species of *Gyrodactylus* recorded in Lake Tanganyika to four. Knowing that other locations where this species has been reported are geographically remote from Lake Tanganyika, we propose a "failure to diverge" phenomenon for *G. transvaalensis*.

Keywords: Clariidae; *Clarias gariepinus*; gills; Gyrodactylidae; monogenea; parasite; Platyhelminthes; DRC; East Africa; failure to diverge

The distribution of the catfishes (Siluriformes) spans every continent except Antarctica. There are now 4094 recognized species distributed among 497 genera and 39 families in this order. In Africa's freshwaters, Siluriformes are represented by 476 species in 51 genera and nine families [1]. This order contains some of the world's most economically significant freshwater and brackish water fishes. In many nations, they make up a sizeable portion of inland fisheries. Several species are used in aquaculture and have been introduced around the globe. Additionally, many species are valuable to the aquarium industry, where they account for a substantial part of global trade [2]. A typical economically important species is *Clarias gariepinus* (Burchell, 1822) (Clariidae: Siluriformes), a strong, air-breathing catfish

from Africa and the Middle East [3]. It is thought to be the freshwater fish species with the greatest natural geographic distribution in Africa. The most common fish species raised in sub-Saharan Africa seem to be African catfish [4], followed by 'tilapia' [5]. Despite the great diversity and economic importance of catfishes, there is a paucity of knowledge about their parasites [6–8].

Lake Tanganyika is the oldest [9,10] of the East African Rift Lakes. It has a unique ichthyofauna that also contains about 34 catfish species [11] belonging to five families: Bagridae, Clariidae, Claroteidae, Malapteruridae, and Mochokidae [12]. The lack of information on Tanganyikan and East African catfish parasites prompted us to study the monogeneans of representatives of Siluriformes in Lake Tanganyika [13].

Monogeneans (Platyhelminthes) are typically ectoparasitic on the gills, skin, or other external surfaces of fishes or on the exterior surfaces of other cold-blooded vertebrates. Additionally, there are several endoparasitic species. The adults can anchor themselves to the surfaces of their hosts using their conspicuous posterior attachment structure, or haptor. This noticeable organ is equipped with suckers, different types of hooks, or both, and often varies in form between species [14]. Monogenean species identification is not only based on the morphology of the sclerotized structures of the haptor but also on distal sclerotized sections of the reproductive systems: the male copulatory organ (MCO) and the vagina [15]. Monogeneans are known for their potential to negatively impact aquaculture. Recommended treatments include hydrogen peroxide (35%) [16] and formalin (25 ppm), and recommended chemicals for prevention are potassium permanganate (2 ppm), methylene blue (2 ppm), and sodium chloride (0.02%) [17]. This work is part of a series of studies we are conducting on the monogeneans of siluriform representatives in Lake Tanganyika. In particular, this study focuses on the fish *C. gariepinus*.

During a survey in Lake Tanganyika at the mouth of the Mutambala River (29°04.4042′ E, 04°16.4598′ S) in the Democratic Republic of the Congo (DRC), a single individual of *C. gariepinus* (Figure 1) was captured using a gill net. The specimen was killed by severing its spinal cord. Identification was carried out using the key of Fermon et al. [18].

Figure 1. Examined specimen of *Clarias gariepinus* from Lake Tanganyika (Uvira, DRC); picture by Fidel Muterezi Bukinga.

To enable the study of its parasites, the gills of the specimen were stored in 96% ethanol. These gills were examined under a Wild Heerbrugg® M8 binocular. We noted the presence of a single monogenean individual. The parasite specimen was recovered using an entomological needle and mounted on a slide in a drop of Hoyer's medium [19]. The slide was covered with a coverslip to flatten the specimen. It was left for 24 h in a horizontal position before sealing the coverslip with glyceel [20]. Identification was performed using a Leica® DM 2500 microscope equipped with a digital camera (Leica DMC 4500) and phase contrast. The slide was deposited at the Royal Museum for Central Africa, Tervuren, Belgium (accession number RMCA_VERMES_ 43681). Based on Přikrylová et al. [21] the

specimen was identified as belonging to *Gyrodactylus transvaalensis* Prudhoe and Hussey, 1977 (Figure 2). It shares the sturdy hamulus with a root that is wide especially close to where it joins the shaft and finer towards its proximal end. As Přikrylová et al. [21] reported, the inner surface of the anchor root is flattened. These authors also demonstrated some intraspecific diversity, e.g., in the shape of the marginal hook sickle of this species, and also illustrated this for other congeners parasitizing catfishes, e.g., *Gyrodactylus rysavyi* Ergens, 1973 and *Gyrodactylus synodonti* Přikrylová, Blažek, and Vanhove, 2012. In the case of our specimen, the blunt, downward-pointing heel; the triangular toe; and the forward-pointing sickle proper that narrows at the point and of which the point bends at a nearly right angle correspond well with how Přikrylová et al. [21] characterize the marginal hook sickle shape of *G. transvaalensis*.

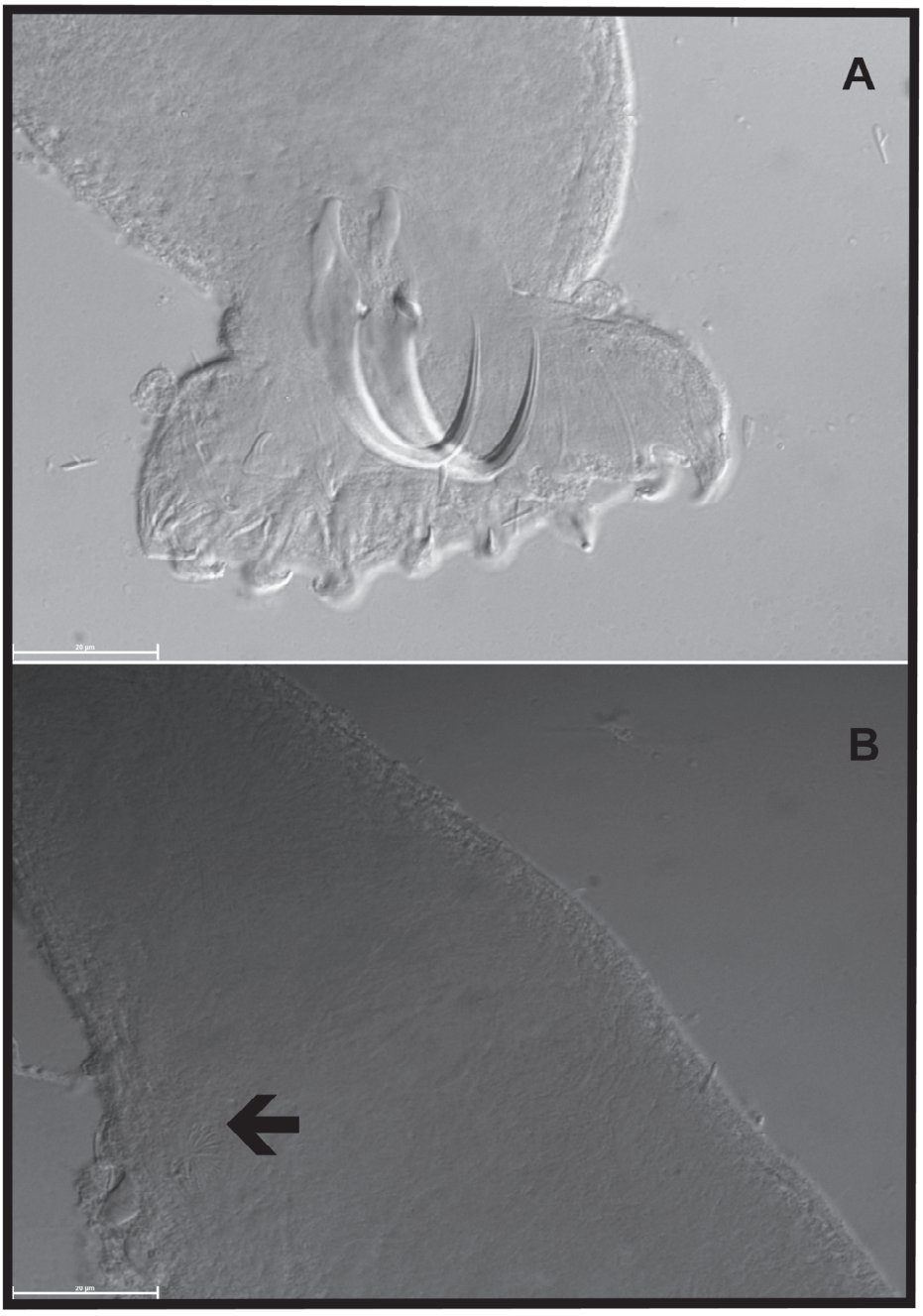

Figure 2. Photomicrographs of the haptoral (**A**) and genital (**B**) hard parts of *Gyrodactylus transvaalensis* from the gills of *Clarias gariepinus* captured in Lake Tanganyika off the mouth of the Mutambala River, DRC (RMCA_VERMES_ 43681). Scalebar measures 20 μm.

The measurements performed on the sclerified parts (Figure 3) of this monogenean follow [22] and are as follows (distances in μm): hamulus total length (HTL) = 44.9; hamulus root length (HRL) = 14.7; hamulus aperture distance (HAD) = 17.1; hamulus proximal shaft width (HPSW) = 6.9; hamulus point length (HPL) = 21.1; hamulus distal shaft width (HDSW) = 2.8; hamulus shaft length (HSL) = 27.9; hamulus inner curve length (HICL) = 1.5; the angle θ between the hamulus point tip through its base and the lower edge of the ventral bar articulation point on the hamulus θ = 44.0°; the angle between the hamulus point tip, its blade, and the vector describing its length and base α = 5.6°; the angle λ between the hamulus point tip through the vector describing its length to the inner curve of the hamulus and the lower edge of the ventral bar articulation point on the hamulus λ = 50.3°; marginal hook total length (MHTL) = 21.5; marginal hook shaft length (MHSL) = 18.2; marginal hook sickle length (MHSL) = 3.7; marginal hook sickle proximal width (MHSPW) = 4.4; marginal hook toe length (MHSTL) = 3.0; marginal hook sickle distal width (MHSDW) = 3.7; marginal hook aperture (MHAD) = 5.6; and marginal hook instep/arch height (MHIH) = 0.5. These measurements are within (or close to) the ranges reported by [21]; these authors also re-examined paratype specimens. Probably because of the fixation in Hoyer's medium, the morphology of the haptoral dorsal and ventral bars was not discernible. The MCO has a diameter of 13.1 with at least six spines (visible) of average length 4.0 (3.6–5.0) arranged in a single row, and a single large one that is 6.2 long. While [21] mentioned a similar MCO diameter (14.5), they found the genital hard parts to be indiscernible on the studied specimen. Conversely, Prudhoe and Hussey [23] did not provide measurements regarding the MCO; they observed a single row with eight spines but saw no large spine. It is important to remember that the number of MCO spines in *Gyrodactylus* may vary within the same species [24,25]. We here provide the first report on the size of the MCO spines of *G. transvaalensis* and on the presence of a large spine in this species' MCO.

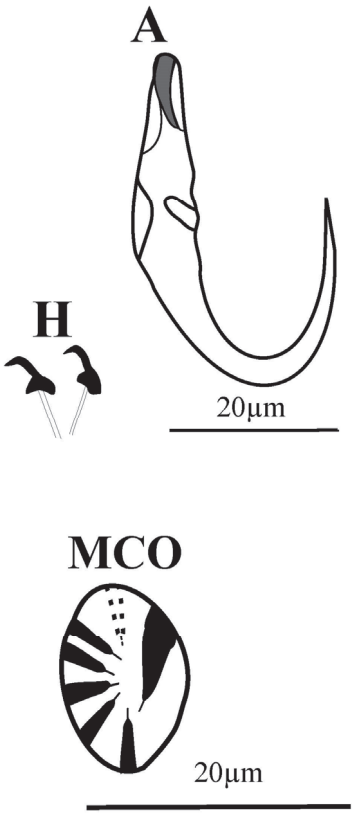

Figure 3. Line drawings of haptoral hard parts of *Gyrodactylus transvaalensis* (RMCA_VERMES_43681) (A = hamulus, H = marginal hooks, MCO = male copulatory organ).

This is the first time that this monogenean species is reported from this infection site, from the DRC, and from the Congo ichthyofaunal province. Indeed, *G. transvaalensis* was described in 1977 by Prudhoe and Hussey [23] on the skin of *C. gariepinus* captured at the confluence of the Elands and Olifants Rivers, about 17 km north of Marble Hall in the central Transvaal (24°48′45.94″ S; 29°21′28.94″ E), currently the Limpopo province, Republic of South Africa. The second report of this species originates from West Africa, where it was found on the fins of *Clarias anguillaris* (Linnaeus, 1758) at Mare Simenti, Niokolo Koba National Park (13°01.79′ N, 13°17.6′ W), Senegal [21] (Figure 4). Since the specimen of *G. transvaalensis* from Lake Tanganyika was found on the type host of this species, it is unlikely that we are dealing with an accidental infection. Additional sampling, however, is needed to ascertain whether this species commonly occurs on the region's clariid catfishes or sporadically.

This study increases the number of species of monogenean flatworms known from representatives of Siluriformes in Lake Tanganyika from two [13] to three and the number of species belonging to *Gyrodactylus* in the lake from three [26] to four. In general, endemicity in Lake Tanganyika is high for a variety of taxa [27,28], including monogenean parasites [29,30]. Currently, 50 monogenean species are known from Lake Tanganyika (see Table 1), including two species of *Bagrobdella* Paperna, 1969; 40 of *Cichlidogyrus* Paperna, 1960; one of *Scutogyrus* Pariselle and Euzet, 1995; one of *Dolicirroplectanum* Kmentová, Gelnar and Vanhove, 2018; four of *Gyrodactylus* von Nordmann, 1832; and two of *Kapentagyrus* Kmentová, Gelnar and Vanhove, 2018.

Table 1. Alphabetical list of monogenean species reported in Lake Tanganyika. The "Reference" column indicates the publication in which the species is reported from Lake Tanganyika, except for those marked by *, which indicates the publications that reported the same species outside of Lake Tanganyika. Species not endemic to Lake Tanganyika are listed in bold.

Species	Authors of Species	Reference
Bagrobdella vanhovei	Mushagalusa Mulega and Pariselle, 2022	[13]
Bagrobdella vansteenbergei	Mushagalusa Mulega and Pariselle, 2022	[13]
Cichlidogyrus adkoningsi	Rahmouni, Vanhove, and Šimková, 2018	[31]
Cichlidogyrus antoineparisellei	Rahmouni, Vanhove, and Šimková, 2018	[31]
Cichlidogyrus aspiralis	Rahmouni, Vanhove, and Šimková, 2017	[32]
Cichlidogyrus attenboroughi	Kmentová et al., 2016	[33]
Cichlidogyrus banyankimbonai	Pariselle and Vanhove, 2015	[34]
Cichlidogyrus brunnensis	Kmentová et al., 2016	[33]
Cichlidogyrus buescheri	Pariselle and Vanhove, 2015	[30]
Cichlidogyrus casuarinus	Pariselle, Muterezi Bukinga and Vanhove, 2015	[35]
Cichlidogyrus centesimus	Vanhove, Volckaert, and Pariselle, 2011	[36]
Cichlidogyrus discophonum	Rahmouni, Vanhove, and Šimková, 2017	[32]
Cichlidogyrus evikae	Rahmouni, Vanhove, and Šimková, 2017	[32]
Cichlidogyrus frankwillemsi	Pariselle and Vanhove, 2015	[34]
Cichlidogyrus franswittei	Pariselle and Vanhove, 2015	[34]
Cichlidogyrus georgesmertensi	Pariselle and Vanhove, 2015	[34]
Cichlidogyrus gillardinae	Muterezi Bukinga et al., 2012	[29]
Cichlidogyrus gistelincki	Gillardin et al., 2012	[37]
Cichlidogyrus glacicremoratus	Rahmouni, Vanhove, and Šimková, 2017	[32]
Cichlidogyrus habluetzeli	Rahmouni, Vanhove, and Šimková, 2018	[31]

Table 1. *Cont.*

Species	Authors of Species	Reference
Cichlidogyrus halli	(Price and Kirk, 1967)	[29]
Cichlidogyrus irenae	Gillardin et al., 2012	[37]
Cichlidogyrus jeanloujustinei	Rahmouni, Vanhove, and Šimková, 2017	[32]
Cichlidogyrus koblmuelleri	Rahmouni, Vanhove, and Šimková, 2018	[31]
Cichlidogyrus makasai	Vanhove, Volckaert, and Pariselle, 2011	[36]
Cichlidogyrus masilyai	Rahmouni, Vanhove, and Šimková, 2018	[31]
Cichlidogyrus mbirizei	Muterezi Bukinga et al., 2012	[29]
		* [38]
		* [39]
		* [40]
Cichlidogyrus milangelnari	Rahmouni, Vanhove, and Šimková, 2017	[32]
Cichlidogyrus mulimbwai	Muterezi Bukinga et al., 2012	[29]
Cichlidogyrus muterezii	Pariselle and Vanhove, 2015	[34]
Cichlidogyrus muzumanii	Muterezi Bukinga et al., 2012	[29]
Cichlidogyrus nshomboi	Muterezi Bukinga et al., 2012	[29]
Cichlidogyrus pseudoaspiralis	Rahmouni, Vanhove, and Šimková, 2017	[32]
Cichlidogyrus raeymaekersi	Pariselle and Vanhove, 2015	[34]
Cichlidogyrus rectangulus	Rahmouni, Vanhove, and Šimková, 2017	[32]
Cichlidogyrus salzburgeri	Rahmouni, Vanhove, and Šimková, 2018	[31]
Cichlidogyrus schreyenbrichardorum	Pariselle and Vanhove, 2015	[30]
Cichlidogyrus sergemorandi	Rahmouni, Vanhove, and Šimková, 2018	[31]
Cichlidogyrus steenbergei	Gillardin et al., 2012	[37]
Cichlidogyrus sturmbaueri	Vanhove, Volckaert, and Pariselle, 2011	[36]
Cichlidogyrus vandekerkhovei	Vanhove, Volckaert, and Pariselle, 2011	[36]
Cichlidogyrus vealli	Pariselle and Vanhove, 2015	[30]
Dolicirroplectanum lacustre	(Thurston and Paperna, 1969)	[41]
Gyrodactylus sturmbaueri	Vanhove, Snoeks, Volckaert, and Huyse, 2011	[26]
		* [42]
Gyrodactylus thysi	Vanhove, Snoeks, Volckaert, and Huyse, 2011	[26]
Gyrodactylus transvaalensis	Prudhoe and Hussey, 1977	* [23]
		* [21]
		Present study
Gyrodactylus zimbae	Vanhove, Snoeks, Volckaert, and Huyse, 2011	[26]
Kapentagyrus limnotrissae	(Paperna, 1973)	[43]
		[44]
		* [45]
Kapentagyrus tanganicanus	Kmentová et al., 2018	[44]
Scutogyrus gravivaginus	(Paperna and Thurston, 1969)	[29]

Eighty six percent of monogenean species (43/50) are endemic to Lake Tanganyika. Non-endemic species include *Kapentagyrus limnotrissae* (Paperna, 1973), which was, together with its host, artificially introduced into Lake Kariba [44]. This species was first described by Paperna in 1973 in Lake Tanganyika, on *Limnothrissa miodon* (Boulenger, 1906), as *Ancyrocephalus limnotrissae*. Kmentová, Gelnar, and Vanhove subsequently redescribed it as *Kapentagyrus limnotrissae* (Paperna, 1973), which is specific to *L. miodon* [44]. *Gyrodactylus sturmbaueri* Vanhove, Snoeks, Volckaert, and Huyse, 2011 infects cichlids. It has been described from Lake Tanganyika on the gills (probably present on the fins and skin as well) of *Simochromis diagramma* (Günther, 1894) [26], but was subsequently reported on the gills of *Pseudocrenilabrus philander* (Weber, 1897) in South Africa and Zimbabwe [42]. *Dolicirroplectanum lacustre* (Thurston and Paperna, 1969) is a parasite of latid fishes throughout Africa [41]. *Cichlidogyrus mbirizei* Muterezi Bukinga, Vanhove, Van Steenberge, and Pariselle, 2012 has been described from the gills of *Oreochromis tanganicae* (Günther, 1894) from Lake Tanganyika [29] (on which the same authors also discovered dactylogyrid species already known from elsewhere [29]) but was later reported in Thailand [38], Malaysia [39], and China [40].

Eight species of monogeneans belonging to *Gyrodactylus* are known from African populations of *C. gariepinus* [46]. These are: *G. alberti* Paperna, 1973; *G. alekosi* Přikrylová, Blažek, and Vanhove, 2012; *G. clarii* Paperna, 1973; *G. gelnari* Přikrylová, Blažek, and Vanhove, 2012; *G. groschafti* Ergens, 1973; *G. rysavyi* Ergens, 1973; *G. transvaalensis* Prudhoe and Hussey, 1977; and *G. turkanaensis* Přikrylová, Blažek, and Vanhove, 2012.

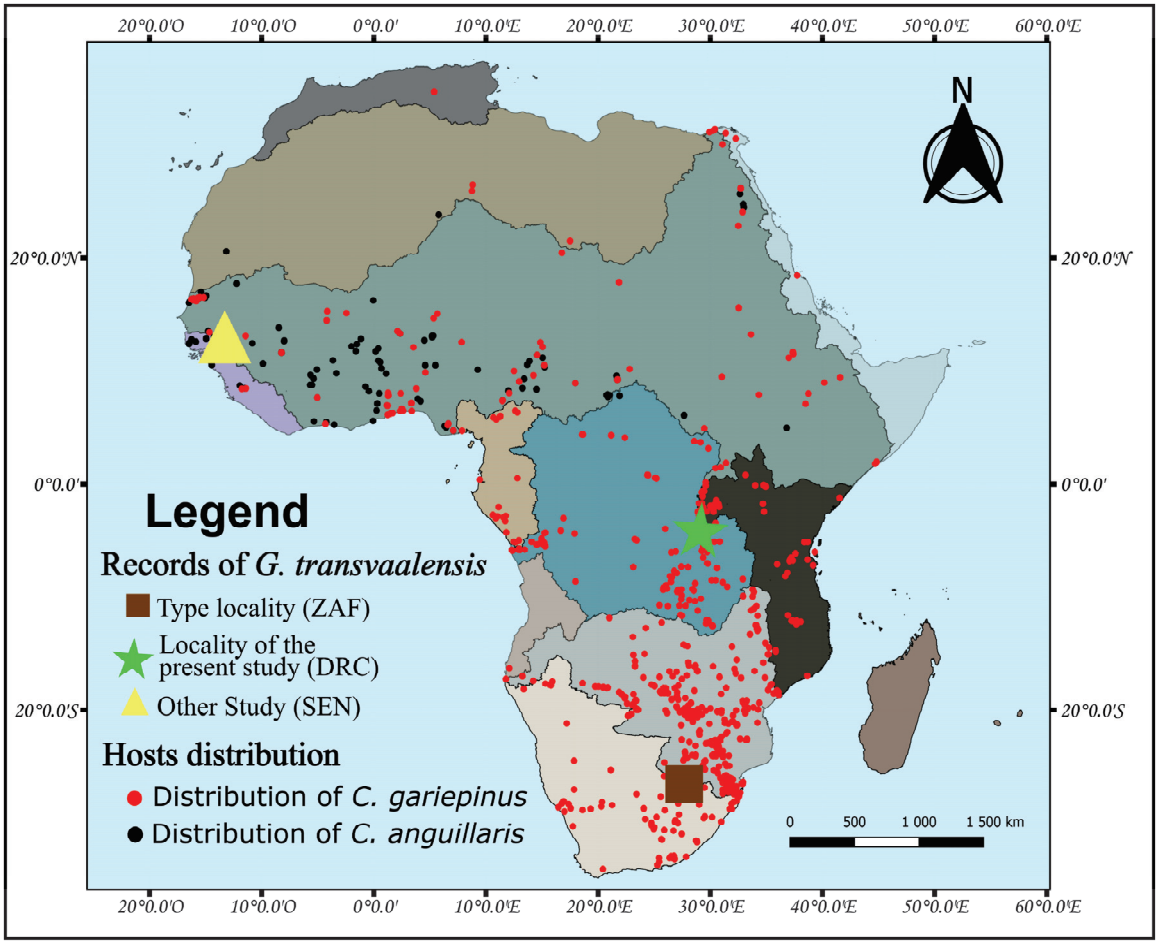

Figure 4. Records of *G. transvaalensis* and distribution range of its hosts. ZAF = South Africa, DRC = Democratic Republic of the Congo, and SEN = Senegal. The map was made with QGIS 3.16. Distribution data of *C. gariepinus* and *C. anguillaris* were downloaded from Fishbase (https://www.fishbase.se/map/OccurrenceMapList.php?genus=Clarias&species=gariepinus, 19 September 2022 and https://www.fishbase.se/map/OccurrenceMapList.php?genus=Clarias&species=anguillaris, 19 September 2022). Colors denote ichthyofaunal provinces, as in [47].

Molecular and morphological data indicate a large amount of variation in *C. gariepinus*, possibly hinting at unrecognized taxic diversity. Additionally, the species as currently defined is paraphyletic with respect to *C. anguillaris* and the species of *Bathyclarias* Jackson, 1959 [48–50]. Because of their often high species specificity, monogenean parasites can be valuable markers to solve problems in fish systematics [50]. Hence, we point out that three of the aforementioned parasite species, *G. gelnari*, *G. rysavyi*, and *G. transvaalensis*, are shared between *C. gariepinus* and *C. anguillaris* and that, apart from these three, no other species of *Gyrodactylus* are known in *C. anguillaris* [46]. Hence, a potential explanation of *G. transvaalensis* (as well as the other two species of *Gyrodactylus* mentioned above) being present on both *C. anguillaris* and *C. gariepinus* is that the fish host speciated and the parasite did not. This is labeled "failure to diverge" [51]. This was also suggested for *D. lacustre* [41], a monogenean infecting a widespread African freshwater fish and the species rendering it paraphyletic [52]. An alternative hypothesis that would require molecular data to be

tested may be related to ongoing diversification in *G. transvaalensis*, driven by, for example, host preference or infection site preference. A further sampling of parasites of *C. gariepinus* and closely related species across their natural range should be undertaken. Combined with molecular studies on these parasites, this may, in view of their marker potential, help resolve uncertainties in the taxonomy and evolutionary history of these clariids.

Author Contributions: Conceptualization, A.M.M., M.V.S. and M.P.M.V.; Methodology: A.M.M., F.M.B., P.M.M. and A.P.; Investigation: A.M.M., M.P.M.V., N.K. and M.V.S.; Data Curation, A.M.M. and A.P.; Writing—original, A.M.M.; Data Preparation, A.M.M.; Review and Editing: A.M.M., M.V.S., N.K., F.M.B., I.R., P.M.M., A.B., A.P. and M.P.M.V. Supervision, M.V.S. and M.P.M.V. All authors have read and agreed to the published version of the manuscript.

Funding: A.M.M. (BOF22BL08) and N.K. (BOF21PD01) are funded by the Special Research Fund of Hasselt University, and M.P.M.V. by the Special Research Fund (BOF) of Hasselt University (BOF20TT06, BOF21INCENT09) and by research grant 1513419N of the Research Foundation—Flanders (FWO-Vlaanderen).

Institutional Review Board Statement: Not applicable.

Informed Consent Statement: Not applicable.

Data Availability Statement: The voucher specimen was deposited in the Royal Museum for Central Africa (Tervuren, Belgium) under accession number RMCA_VERMES_ 43681. The observations here reported were posted on iNaturalist under https://www.inaturalist.org/observations/139872031 (host) and https://www.inaturalist.org/observations/139872032 (parasite).

Acknowledgments: The editors and three referees are thanked for their constructive comments that helped improve this study.

Conflicts of Interest: The authors declare no conflict of interest.

References

1. Fricke, R.; Eschmeyer, W.N.; Fong, D.J. Catalog of Fishes. Available online: https://researcharchive.calacademy.org/research/ichthyology/catalog/SpeciesByFamily.ap (accessed on 15 June 2022).
2. Teugels, G.G. Taxonomy, phylogeny and biogeography of catfishes (Ostariophysi, Siluroidei): An overview. *Aquat. Living Resour.* **1996**, *9*, 9–34. [CrossRef]
3. Bruton, M.N. The food and feeding behavior of *Clarias gariepinus* (Pisces: Clariidae) in Lake Sibaya, South Africa with emphasis on its role as a predator of cichlids. *Trans. Zool. Soc. Lond.* **1979**, *35*, 47–114. [CrossRef]
4. Pouomogne, V. Cultured Aquatic Species Information Programme. *Clarias gariepinus*. Food and Agriculture Organization of the United Nations Fisheries and Aquaculture Department, Rome. Available online: https://www.fao.org/fishery/en/culturedspecies/Clarias_gariepinus/en (accessed on 27 September 2022).
5. Jorissen, M.W.P.; Huyse, T.; Pariselle, A.; Wamuini Lunkayilakio, S.; Muterezi Bukinga, F.; Chocha Manda, A.; Kapepula Kasembele, G.; Vreven, E.J.; Snoeks, J.; Decru, E.; et al. Historical museum collections help detect parasite species jumps after tilapia introductions in the Congo Basin. *Biol. Invasions* **2020**, *22*, 2825–2844. [CrossRef]
6. Mendoza-Palmero, C.A.; Blasco-Costa, I.; Scholz, T. Molecular phylogeny of neotropical monogeneans (Platyhelminthes: Monogenea) from catfishes (Siluriformes). *Parasites Vectors* **2015**, *8*, 164. [CrossRef]
7. de Chambrier, A.; Kuchta, R.; Scholz, T. Tapeworms (Cestoda: Proteocephalidea) of teleost fishes from the Amazon River in Peru: Additional records as an evidence of unexplored species diversity. *Rev. Suisse Zool.* **2020**, *122*, 149–163.
8. Acosta, A.A.; Smit, N.J.; da Silva, R.J. Diversity of helminth parasites of eight siluriform fishes from the Aguapeí River, upper Paraná basin, São Paulo state, Brazil. *Int. J. Parasitol.* **2020**, *11*, 120–128. [CrossRef] [PubMed]
9. Cohen, A.S.; Soreghan, M.J.; Scholz, C.A. Estimating the age of formation of lakes: An example from Lake Tanganyika, East African Rift system. *Geology* **1993**, *21*, 511–514. [CrossRef]
10. Alin, S.; Cohen, A. Lake-level history of Lake Tanganyika, East Africa, for the past 2500 years based on ostracode-inferred water-depth reconstruction. *Palaeogeogr. Palaeoclimatol. Palaeoecol.* **2003**, *199*, 31–49. [CrossRef]
11. Peart, C.R. Detecting a Signature of Adaptive Radiation: Diversification in Lake Tanganyika Catfishes. Ph.D. Thesis, University College London, London, UK, September 2014.
12. Coulter, G.W. *Lake Tanganyika and Its Life*; Oxford University Press: Oxford, UK, 1991.
13. Mushagalusa Mulega, A.; Muterezi Bukinga, F.; Akoumba, J.F.; Masilya, M.P.; Pariselle, A. Monogeneans from catfishes in Lake Tanganyika. I: Two new species of *Bagrobdella* (Dactylogyridae) from *Auchenoglanis occidentalis* (Siluriformes: Claroteidae). *Zoologia* **2022**, *39*, e22016. [CrossRef]

14. Loker, E.S.; Hofkin, B.V. *Parasitology—A Conceptual Approach*; Garland Science, Taylor & Francis Group, LLC: New York, NY, USA, 2015; pp. 1–560.
15. Řehulková, E.; Seifertová, M.; Přikrylová, I.; Francová, K. Monogenea. In *A Guide to the Parasites of African Freshwater Fishes*; Scholz, T., Vanhove, M.P.M., Smit, N., Jayasundera, Z., Gelnar, M., Eds.; CEBioS, Royal Belgian Institute of Natural Sciences: Brussels, Belgium, 2018; Volume 18, pp. 185–243.
16. Boweker, J.D.; Carty, D.; Dotson, M.M. Efficacy of 35% Perox-Aid (Hydrogen Peroxide) in Reducing an Infestation of *Gyrodactylus salmonis* in freshwater-reared rainbow trout. *N. Am. J. Aquac.* **2012**, *74*, 154–159. [CrossRef]
17. Aly, S.; Fathi, M.; Youssef, E.M.; Mabrok, M. Trichodinids and monogeneans infestation among Nile tilapia hatcheries in Egypt: Prevalence, therapeutic and prophylactic treatments. *Aquac. Int.* **2020**, *28*, 1459–1471. [CrossRef]
18. Fermon, Y.; Nshombo, M.V.; Muzumani, R.D.; Jonas, B. *Lac Tanganyika Guide de la Faune des Poissons de la côte Congolaise*; d'Ubwari à la Ruzizi: Aimara, France, 2012; pp. 1–238.
19. Anderson, L.E. Hoyer's solution as a rapid permanent mounting medium for bryophytes. *Bryologist* **1954**, *57*, 242–244. [CrossRef]
20. Bates, J.W. The Slide-Sealing Compound "Glyceel". *J. Nematol.* **1997**, *29*, 565–566.
21. Přikrylová, I.; Blažek, R.; Vanhove, M.P.M. An overview of the *Gyrodactylus* (Monogenea: Gyrodactylidae) species parasitizing African catfishes, and their morphological and molecular diversity. *Parasitol. Res.* **2012**, *110*, 1185–1200. [CrossRef] [PubMed]
22. Shinn, A.P.; Hansen, H.; Olstad, K.; Bechmann, L.; Bakke, T.A. The use of morphometric characters to discriminate specimens of laboratory-reared and wild population of *Gyrodactylus salaris* and *G. thymalli* (Monogenea). *Folia Parasitol.* **2004**, *51*, 239–252. [CrossRef] [PubMed]
23. Prudhoe, S.; Hussey, C.G. Some parasitic worms in freshwater fishes and fish-predators from the Transvaal, South Africa. *Zool. Afr.* **1977**, *12*, 113–147. [CrossRef]
24. King, D.S.; Bentzen, P.; Cone, D.K. *Gyrodactylus patersoni* n.sp. (Monogenean: Gyrodactylidae) infecting Atlantic Silverside (*Menidia menidia*) from Nova Scotia, Canada. *Comp. Parasitol.* **2014**, *81*, 27–32. [CrossRef]
25. Kvach, Y.; Ondračková, M.; Seifertová, M.; Hulak, B. *Gyrodactylus ginestrae* n.sp. (Monogenea: Gyrodactylidae), a parasite of the big-scale sand smelt, *Atherina boyeri* Risso, 1810 (Actinopterygii: Atherinidae) from the Black Sea. *Parasitol. Res.* **2019**, *118*, 3315–3325. [CrossRef]
26. Vanhove, M.P.M.; Snoeks, J.; Volckaert, F.A.M.; Huyse, T. First description of monogenean parasites in Lake Tanganyika: The cichlid *Simochromis diagramma* (Teleostei, Cichlidae) harbours a high diversity of *Gyrodactylus* species (Platyhelminthes, Monogenea). *Parasitology* **2011**, *138*, 364–380. [CrossRef]
27. Salzburger, W.; Van Bocxlaer, B.; Cohen, A.S. Ecology and evolution of the African Great Lakes and their faunas. *Annu. Rev. Ecol. Evol. Syst.* **2014**, *45*, 519–545. [CrossRef]
28. Wilson, A.B.; Glaubrecht, M.; Meyer, A. Ancient lakes as evolutionary reservoirs: Evidence from the thalassoid gastropods of Lake Tanganyika. *Proc. R. Soc. London* **2004**, *271*, 529–536. [CrossRef] [PubMed]
29. Muterezi Bukinga, F.; Vanhove, M.P.M.; Van Steenberge, M.; Pariselle, A. Ancyrocephalidae (Monogenea) of Lake Tanganyika: III: *Cichlidogyrus* infecting the world´s biggest cichlid and the non-endemic tribes Haplochromi, Oreochromini and Tylochromini (Teleostei, Cichlidae). *Parasitol. Res.* **2012**, *111*, 2049–2061. [CrossRef] [PubMed]
30. Pariselle, A.; Van Steenberge, M.; Snoeks, J.; Volckaert, F.A.M.; Huyse, T.; Vanhove, M.P.M. Ancyrocephalidae (Monogenea) of Lake Tanganyika: Does the *Cichlidogyrus* parasite fauna of *Interochromis loocki* (Teleostei, Cichlidae) reflect its host´s phylogenetic affinities? *Contrib. Zool.* **2015**, *84*, 25–38. [CrossRef]
31. Rahmouni, C.; Vanhove, M.P.M.; Šimková, A. Seven new species of *Cichlidogyrus* Paperna, 1960 (Monogenea: Dactylogyridae) parasitizing the gills of Congolese cichlids from northern Lake Tanganyika. *PeerJ* **2018**, *6*, e5604. [CrossRef] [PubMed]
32. Rahmouni, C.; Vanhove, M.P.M. Šimková, A. Underexplored diversity of gill monogeneans in cichlids from Lake Tanganyika: Eight new species of *Cichlidogyrus* Paperna, 1960 (Monogenea: Dactylogyridae) from the northern basin of the lake, with remarks on the vagina and the heel of the male copulatory organ. *Parasites Vectors* **2017**, *10*, 591. [PubMed]
33. Kmentová, N.; Gelnar, M.; Koblmüller, S.; Vanhove, M.P.M. Deep-water parasite diversity in Lake Tanganyika: Description of two new monogenean species from benthopelagic cichlid fishes. *Parasites Vectors* **2016**, *9*, 426. [CrossRef] [PubMed]
34. Van Steenberge, M.; Pariselle, A.; Huyse, T.; Volckaert, F.A.M.; Snoeks, J.; Vanhove, M.P.M. Morphology, molecules, and monogenean parasites: An example of an integrative approach to cichlid biodiversity. *PLoS ONE* **2015**, *10*, e0129987. [CrossRef] [PubMed]
35. Pariselle, A.; Muterezi Bukinga, F.; Van Steenberge, M.; Vanhove, M. Ancyrocephalidae (Monogenea) of Lake Tanganyika: IV: *Cichlidogyrus* parasitizing species of Bathybatini (Teleostei, Cichlidae): Reduced host-specificity in the deepwater realm? *Hydrobiologia* **2015**, *748*, 99–119. [CrossRef]
36. Vanhove, M.P.M.; Volckaert, F.A.M.; Pariselle, A. Ancyrocephalidae (Monogenea) of Lake Tanganyika: I: Four new species of *Cichlidogyrus* from *Ophthalmotilapia ventralis* (Teleostei: Cichlidae), the first record of this parasite family in the basin. *Zoologia* **2011**, *28*, 253–263. [CrossRef]
37. Gillardin, C.; Vanhove, M.P.M.; Pariselle, A.; Huyse, T.; Volckaert, F.A.M. Ancyrocephalidae (Monogenea) of Lake Tanganyika: II: Description of the first *Cichlidogyrus* spp. parasites from Tropheini fish hosts (Teleostei, Cichlidae). *Parasitol. Res.* **2012**, *110*, 305–313. [CrossRef]
38. Lerssutthichawal, T.; Maneepitaksanti, W.; Purivirojkul, W. Gill Monogeneans of potentially cultured Tilapias and first record of *Cichlidogyrus mbirizei* Bukinga et al., 2012, in Thailand. *Walailak J. Sci. Technol.* **2016**, *13*, 543–553.

39. Lim, S.H.; Ooi, A.L.; Wong, W.L. Gill monogeneans of Nile tilapia (*Oreochromis niloticus*) and red hybrid tilapia (*Oreochromis* spp.) from the wild and fish farms in Perak, Malaysia: Infection dynamics and spatial distribution. *SpringerPlus* **2016**, *5*, 1609. [CrossRef]
40. Zhang, S.; Zhi, T.; Xu, X.; Zheng, Y.; Bilong Bilong, C.; Pariselle, A.; Yang, T. Monogenean fauna of alien tilapias (Cichlidae) in south China. *Parasite* **2019**, *26*, 1–16. [CrossRef]
41. Kmentová, N.; Kobmüller, S.; Van Steenberge, M.; Artois, T.; Muterezi Bukinga, F.; Mulimbwa N'sibula, T.; Muzumani, R.D.; Masilya, P.M.; Gelnar, M.; Vanhove, M.P.M. Failure to diverge in African Great Lakes: The case of *Dolicirroplectanum lacustre* gen. nov. comb. nov. (Monogenea, Diplectanidae) infecting latid hosts. *J. Great Lakes Res.* **2020**, *46*, 1113–1130. [CrossRef]
42. Zahradníčková, P.; Barson, M.; Luus-Powell, W.J.; Přikrylová, I. Species of *Gyrodactylus* von Nordmann, 1832 (Platyhelminthes: Monogenea) from cichlids from Zambezi and Limpopo river basins in Zimbabwe and South Africa: Evidence for unexplored species richness. *Syst. Parasitol.* **2016**, *93*, 679–700. [CrossRef]
43. Paperna, I. New species of Monogenea (Vermes) from African freshwater fish. A preliminary report. *Rev. Zool. Bot. Afr.* **1973**, *87*, 505–518.
44. Kmentová, N.; Van Steenberge, M.; Raeymaekers, J.A.M.; Koblmüller, S.; Hablützel, P.I.; Muterezi Bukinga, F.; Mulimbwa N'sibula, T.; Masilya, M.P.; Nzigidahera, B.; Ntakimazi, G.; et al. Monogenean parasites of sardines in Lake Tanganyika: Diversity, origin and intraspecific variability. *Contrib. Zool.* **2018**, *87*, 105–132. [CrossRef]
45. Kmentová, N.; Van Steenberge, M.; Thys van den Audenaerde, D.F.E.; Nhiwatiwa, T.; Muterezi Bukinga, F.; Mulimbwa N'sibula, T.; Masilya Mulungula, P.; Gelnar, M.; Vanhove, M.P.M. Co-introduction success of monogeneans infecting the fisheries target *Limnothrissa miodon* differs between two non-native areas: The potential of parasites as a tag for introduction pathway. *Biol. Invasions* **2019**, *21*, 757–773. [CrossRef]
46. Carvalho Schaeffner, V.C. Host-parasite list. In *A Guide to the Parasites of African Freshwater Fishes*; Scholz, T., Vanhove, M.P.M., Smit, N., Jayasundera, Z., Gelnar, M., Eds.; CEBioS, Royal Belgian Institute of Natural Sciences: Brussels, Belgium, 2018; Volume 18, pp. 185–243.
47. Snoeks, J.; Getahun, A. African fresh and brackish water fish biodiversity and their distribution: More unknowns than knowns. In Proceedings of the 4th International Conference on African Fish and Fisheries, Addis Ababa, Ethiopia, 22–26 September 2008; Snoeks, J., Getahun, A., Eds.; Royal Museum for Central Africa: Tervuren, Belgium, 2013; pp. 69–76.
48. Agnèse, J.F.; Teugels, G.G. The *Bathyclarias–Clarias* species flock. *C. R. Acad. Hebd. Seances Acad. Sci.* **2001**, *324*, 683–688. [CrossRef]
49. Rognon, X.; Teugels, G.G.; Guyomard, R.; Galbusera, P.; Andriamanga, M.; Volckaert, F.; Agnèse, J.F. Morphometric and allozyme variation in the African catfishes *Clarias gariepinus* and *C. anguillaris*. *J. Fish Biol.* **1998**, *53*, 192–207. [CrossRef]
50. Van Steenberge, M.; Vanhove, M.P.M.; Chocha Manda, A.; Larmuseau, M.H.D.; Swart, B.L.; Khang'Mate, F.; Arndt, A.; Hellemans, B.; Van Houdt, J.; Micha, J.L.; et al. Unravelling the evolution of Africa's drainage basins through a widespread freshwater fish, the African sharptooth catfish *Clarias gariepinus*. *J. Biogeogr.* **2020**, *47*, 1739–1754. [CrossRef]
51. Brooks, D.R. Testing the context and extent of host-parasite coevolution. *Syst. Biol.* **1979**, *28*, 299–307. [CrossRef]
52. Koblmüller, S.; Schöggl, C.A.; Lorber, C.J.; Van Steenberge, M.; Kmentová, N.; Vanhove, M.P.M.; Zangl, L. African lates perches (Teleostei, Latidae, *Lates*): Paraphyly of Nile perch and recent colonization of Lake Tanganyika. *Mol. Phylogenet. Evol.* **2021**, *160*, 107141. [CrossRef]

pathogens

MDPI

Article

Morphological and Molecular Identification of *Dactylogyrus gobiocypris* (Monogenea: Dactylogyridae) on Gills of a Model Fish, *Gobiocypris rarus* (Cypriniformes: Gobionidae)

Jiangwen Cheng [1,2], Hong Zou [1], Ming Li [1], Jianwei Wang [1], Guitang Wang [1] and Wenxiang Li [1,3,*]

[1] State Key Laboratory of Freshwater Ecology and Biotechnology and Key Laboratory of Aquaculture Disease Control, Ministry of Agriculture, Institute of Hydrobiology, Chinese Academy of Sciences, Wuhan 430072, China
[2] College of Science, Tibet University, Lhasa 850000, China
[3] University of Chinese Academy of Sciences, Beijing 100049, China
* Correspondence: liwx@ihb.ac.cn

Abstract: The rare minnow *Gobiocypris rarus* is an ideal model organism for toxicological research. *Dactylogyrus* species are usually found on the gills of this rare minnow in laboratory farming systems. Dactylogyrid infection may change the sensibility of fish to toxicants and affect toxicological evaluations. In the present study, dactylogyrid infection was investigated, and species of *Dactylogyrus* collected from rare minnows were determined. Based on the observed '*D. wunderi*' type anchors, with a shorter outer root and elongated inner root, and accessory piece consisting of two parts, the dactylogyrids were identified as *D. gobiocypris*. A partial 18S-ITS1 rDNA sequence was firstly sequenced, and the highest sequence identity (86.7%) was to *D. cryptomeres*. Phylogenetic analysis revealed that *D. gobiocypris* formed a clade with *D. squameus*, *D. finitimus*, and *D. cryptomeres*, all of which have been recorded in the family Gobionidae. Histopathology analysis indicated that a heavy burden of *D. gobiocypris* caused necrosis of gill filaments. Inflammatory responses, such as tumefaction and hyperaemia, were also observed on gills with severe dactylogyrid infection. Supplementary morphological characteristics and 18S-ITS1 rDNA sequence provided basic data for identification of this parasite species.

Keywords: dactylogyrid infection; rare minnow; *Gobiocypris rarus*; *Dactylogyrus gobiocypris*; histopathology

1. Introduction

The rare minnow *Gobiocypris rarus* Ye et Fu, 1983 (Gobionidae) is a small gobionid fish endemic to China, mainly distributed at the edge of the west and northwest area of the Sichuan Basin [1,2]. This rare minnow possesses particular biological characteristics, such as high sensitivity to chemicals, small body size, short life cycle, and being easy to rear in laboratory, which make it an excellent model organism for ecotoxicology studies [3–5]. Since 1995, rare minnows have been widely used in acute and subchronic toxicity experiments on heavy metals [6,7], organics [8–10], and endocrine-disrupting chemicals [11–13].

The monogenean family Dactylogyridae Bychowsky, 1933 is one of the most species-rich groups of helminths, with more than 1000 species recognised worldwide [14]. Forty-one species of *Dactylogyrus* have been recorded from fishes in the family Gobionidae in China [15], and twenty-six species of *Dactylogyrus* are found on fishes in the family Gobionidae in Europe [16]. Species of *Dactylogyrus* were found on gills of rare minnows in a laboratory in China, and *D. gobiocypris* Yao, 1995 was described based on sclerotized parts of the anchor and copulatory complex [17]. No studies have reported *D. gobiocypris* since.

Dactylogyrids can infect the gills of cypriniform fishes [18], causing serious hyperplasia of the gill filament epithelium, copious mucus, and eventually affecting respiratory

function [19,20]. Fish heavily infected with dactylogyrids are also susceptible to bacterial infections [21–23].

The present study provides supplementary morphological characteristics, novel sequences of the 18S ribosomal RNA subunit and the first internal transcribed spacer region of rDNA (ITS1), and histopathological analysis of *D. gobiocypris* parasitizing *G. rarus* specimens reared in the laboratory in the Institute of Hydrobiology, Chinese Academy of Sciences, Wuhan City, Hubei province, China.

2. Materials and Methods

2.1. Parasite Collection

Samples of rare minnow were obtained from the laboratory in the Institute of Hydrobiology, Chinese Academy of Sciences in April 2022. Thirty fish (with total body length of 4.2 ± 0.9 cm) were randomly selected and anesthetized with 0.02% MS-222 (tricaine methanesulfonate) (Sigma, St Louis, MO, USA). Specimens of species of *Dactylogyrus* were then examined and collected using micro surgical needles under a stereoscopic microscope. Worms were rinsed several times with distilled water for further analyses.

2.2. Morphological Identification

A random subsample of dactylogyrids were mounted on a microscope slide and fixed in ammonium picrate glycerine (GAP) as whole mount following the procedure described by Ergens [24] and Malmberg [25] for morphological identification. GAP and Canada balsam were performed according to Ergens [24]. Additional specimens, with opisthaptors excised using a scalpel, were then individually subjected to proteolytic digestion according to the method described by Paladini et al. [26] and Tu et al. [22]. The tissue-free opisthaptoral sclerotized parts were mounted in GAP, and the excised body of each specimen was preserved in 95% ethanol for subsequent molecular analysis. Specimens were photographed using an optical microscope (Axioplan 2 imaging and Axiophot 2, Zeiss, Oberkochen, Germany). Measurements were taken according to Šimková et al. [27], and are given in micrometers (μm) unless otherwise stated. Identification of individual specimens was performed by comparing the morphology and measurements of anchors and the copulatory complex to the literature [17]. Five full worms, embedded in GAP and mounted on Canada balsam, were deposited as voucher specimens (accession nos. CJW-DG 202201-05) in the Museum of the Institute of Hydrobiology, Chinese Academy of Sciences, Wuhan City, Hubei province, China.

2.3. DNA extraction, Amplification and Sequencing

Genomic DNA was extracted from the excised bodies of 12 specimens using a Tissue Cell Genome Kit (TaKaRa, Beijing, China) according to the manufacturer's instructions. The region of rDNA spanning the 3′ end of the 18S ribosomal RNA subunit, the entire ITS1 gene, and the 5′ end of the 5.8S ribosomal RNA subunit were targeted using primers S1 (5′-ATTCCGATAACGAACGAGACT-3′) and H7 (5′-GCTGCGTTCTTCATCGATACTCG-3′) [28,29]. PCR amplification was conducted using LA Taq polymerase (TaKaRa, Beijing, China) with the following profile: 5 min at 95 °C, 35 cycles of 1 min at 94 °C, 1 min at 55 °C, 1 min 30 s at 72 °C, and a final extension of 10 min at 72 °C. After purification, PCR products were cloned into the pGEM-T vector (Promega, Madison, USA), sequenced with the primers described above, produced by Sangon Biotech (Shanghai, China), and assembled manually with DNAStar's SeqMan software (DNAStar, Madison, WI, USA).

2.4. Molecular Analyses

The obtained sequences of partial 18S rDNA, ITS1, and the flanking sequence of 5.8S rDNA were compared using BLAST in GenBank to assess similarity with other *Dactylogyrus* species. From the 12 specimens, 12 sequences of 18S-ITS1 rDNA were obtained to evaluate the intraspecific variation using BLAST. Sequences (Table 1) used for phylogenetic analyses were chosen from *Dactylogyrus* species from closely related hosts. *Thaparocleidus vistulensis*

(Siwak, 1932), in the family Ancylodiscoididae, was used as the outgroup. Sequences were imported into PhyloSuite [30] and aligned with available 18S-ITS1 rDNA sequences of other *Dactylogyrus* spp. in GenBank using MAFFT 7.149 [31]. Ambiguously aligned fragments were trimmed using Gblocks [32] with the following parameter settings: minimum number of sequences for a conserved/flank position (6/6), maximum number of contiguous non-conserved positions (8), minimum length of a block (10), allowed gap positions (with half). Phylogenetic analyses based on the 18S-ITS1 sequences were performed using maximum likelihood (ML) and inference (BI) methods. TNe+G4 and K2P+G4 were chosen as the best-fit partition model for nucleotide evolution for ML and BI analyses, respectively using ModelFinder [33]. ML phylogenies were inferred using IQ-TREE [34], for 1000 standard bootstraps, as well as the Shimodaira–Hasegawa-like approximate likelihood-ratio test. BI phylogenies were inferred using MrBayes 3.2.6 [35], with two parallel runs (2,000,000 generations) in which the initial 25% of sampled data were discarded as burn-in.

2.5. Histopathology Analysis

The first gill arch of each fish was collected and fixed in 10% neutral buffered formalin (Yeasen, Shanghai, China). The fixing solution was diluted to 4% after 4 to 24 h, washed for 24 h and dehydrated in graded ethanol. Gills were embedded in paraffin (Yeasen, Shanghai, China), sliced into 5 µm-thick sections, and stained with the Hematoxylin and Eosin Staining Kit (Yeasen, Shanghai, China) according to Molnár [36]. The slides were mounted on Canada balsam and examined under an optical microscope (Axioplan 2 imaging and Axiophot 2, Zeiss, Oberkochen, Germany).

Table 1. Species included in the phylogenetic analysis.

Parasite Species	Host Species	Locality	GenBank ID	Refs
Dactylogyrus cryptomeres	*Gobio gobio*	Morava River basin, Czech Republic	AJ564123	[28]
Dactylogyrus finitimus	*Romanogobio albipinatus*	Morava River basin, Czech Republic	AJ564133	[28]
Dactylogyrus squameus	*Pseudorasbora parva*	Morava River basin, Czech Republic	AJ564156	[28]
Dactylogyrus gobiocypris	*Gobiocypris rarus*	Wuhan City, China	OP441417	Present study
Dactylogyrus achmerowi	*Cyprinus carpio*	Morava River basin, Czech Republic	AJ564108	[28]
Dactylogyrus extensus	*Cyprinus carpio*	Morava River basin, Czech Republic	AJ564129	[28]
Dactylogyrus vastator	*Carassius auratus*	Liangzi Lake, China	KC876016	[37]
Dactylogyrus intermedius	*Carassius auratus*	Liangzi Lake, China	KC876017	[37]
Dactylogyrus lamellatus	*Ctenopharyngodon idella*	Morava River basin, Czech Republic	AJ564141	[28]
Outgroup *Thaparocleidus vistulensis*	*Silurus glanis*	Morava River basin, Czech Republic	AJ490165	[38]

3. Results

3.1. Taxonomic Summary

Dactylogyrus gobiocypris Yao, 1995

Host: *Gobiocypris rarus* Ye et Fu, 1983 (Cypriniformes: Gobionidae).

Site of infection: gill filaments (Figure 1).

Locality: specimens collected from cultured rare minnow in the laboratory in the Institute of Hydrobiology, Chinese Academy of Sciences (30°54′74.1″ N, 114°35′′04.3″ E), Wuhan City, Hubei province, China.

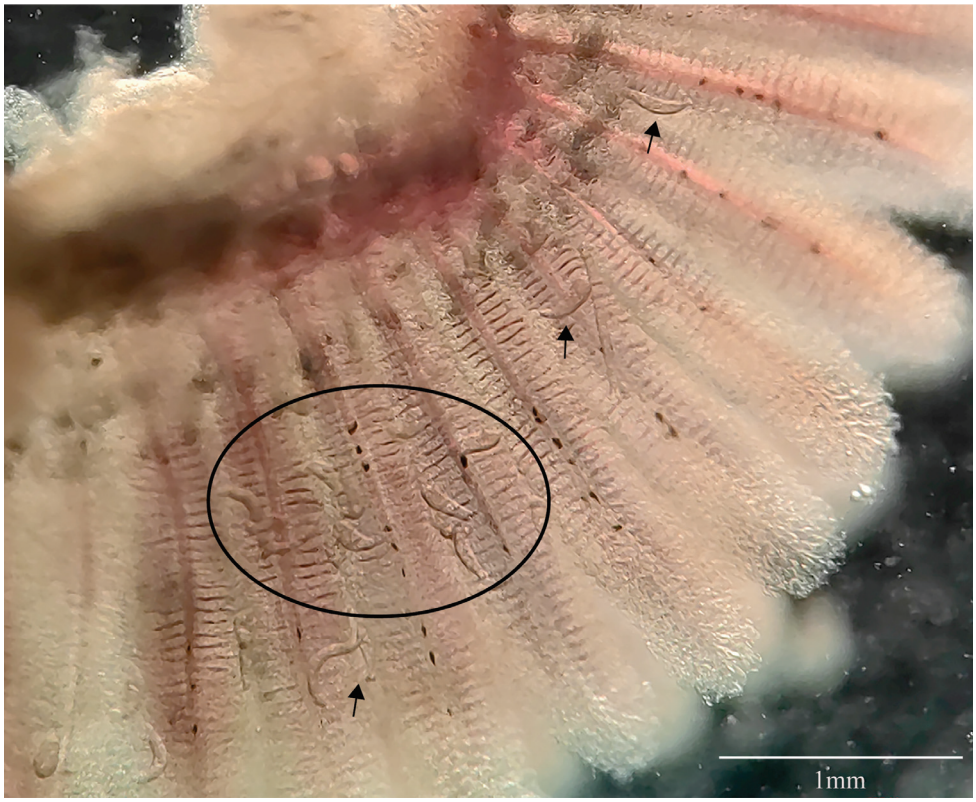

Figure 1. *Dactylogyrus gobiocypris* infection on gills of *Gobiocypris rarus*. Scale-bar: 1 mm.

Prevalence and mean abundance: 96.7% and 60.8 ± 84.5 (3–408), respectively.

Deposition of specimens: deposited in the Museum of the Institute of Hydrobiology (accession nos. CJW-DG 202201–05), Chinese Academy of Sciences, Wuhan City, Hubei province, China.

DNA reference sequences: a sequence (1042 bp) spanning the region of the 3′ end of the 18S ribosomal RNA subunit and ITS1 to the 5′ end of the 5.8S ribosomal RNA subunit was deposited in GenBank (OP441417).

Description: Based on 56 specimens fixed in GAP. Body length, 182 (118–248; n = 32); width, 45 (28–74; n = 32). Eye spots: two pairs. Pharynx diameter, 11 (7–17; n = 33). Copulatory complex: composed of penis and accessory piece, posterior to pharynx. Penis: tubular and well sclerotized; length, 12 (10–14; n = 30). Accessory piece: composed of two parts, one horseshoe-shaped and the other semicapsular; both intersect at the proximal part of the penis; length, 16 (13–17; n = 30). Vaginal armament: absent. Anchor: total length, 26 (24–30; n = 55); base length, 21 (18–24; n = 55); point length, 12 (10–13; n = 55); anchor inner root elongate length, 7 (6–9; n = 55); outer root length, 1 (1–2; n = 55). Ventral bar: rod-shaped, ends slightly enlarged, middle portion slightly convex posteriorly; total length, 4 (2–6; n = 56); median length, 2 (2–5; n = 56); width, 18 (15–21; n = 56). Dorsal bar: V-shaped, slightly extended; total length, 2 (2–4; n = 52); median length, 1 (1–2; n = 52); width, 16 (13–21; n = 52). Marginal hooks: seven pairs; total length, 17 (14–23; n = 55); shaft length, 12 (9–18; n = 55); sickle length, 5 (4–6; n = 55); filament loop length, 8 (7–9; n = 55) (Table 2) (Figures 2 and 3).

Table 2. Morphometric parameters of *Dactylogyrus gobiocypris* in this study, *D. gobiocypris* Yao, 1995 [17] and *D. trullaeformis* Gussev, 1955 [39]. N, the number of *D. gobiocypris* specimens measured.

Source of Data	N	*Dactylogyrus gobiocypris*		*Dactylogyrus trullaeformis*
		Gobiocypris rarus	*G. rarus*	*Gnathopogon strigatus* *Squalidus chankaensis*
		this Study	Yao, 1995 [17] (n = 7)	Gussev, 1955 [39]
Body				
Total length	32	182.0 ± 34.6 (117.7–248.4)	102.5–113.0	150–300
Total width	32	44.8 ± 9.6 (27.8–74.1)	27.5–28.1	30–50
Pharynx diameter	33	11.2 ± 2.2 (7.2–16.8)	34.5	16–19
Anchor				
Total length	55	26.4 ± 1.6 (23.8–30.1)	26.5–30.0	27–30
Base length	55	21.1 ± 1.5 (18.2–24.3)		21–24
Outer root length	55	1.0 ± 0.2 (0.6–1.9)	1.5	1–2
Inner root length	55	7.2 ± 0.7 (5.9–9.0)	7.5–10.0	6–8
Point length	55	11.5 ± 0.8 (9.5–13.4)	12.5–13.0	11–13
Ventral bar				
Total length	56	3.6 ± 0.7 (2.4–5.7)		
Medium length	56	2.3 ± 0.6 (1.5–4.6)	1.8–3.4	1
Width	56	17.9 ± 1.4 (14.8–21.0)	17.5–20.0	14–16
Dorsal bar				
Total length	52	2.4 ± 0.4 (1.5–3.5)		
Medium length	52	1.0 ± 0.2 (0.5–1.5)	1.0	2
Width	52	15.8 ± 1.6 (13.0–20.6)	11.0–15.0	10–19
Marginal hook				
Total length	55	17.1 ± 1.5 (14.3–22.8)	16.5–25.0	15–23
Sickle length	55	5.0 ± 0.4 (4.0–6.3)		
Shaft length	55	12.1 ± 1.5 (9.3–17.7)		
Filament loop length	55	7.7 ± 0.5 (6.9–9.0)		
Copulatory complex				
Penis length	30	11.9 ± 1.2 (10.3–14.4)	15.0–20.0	16–21
Accessory piece	30	15.5 ± 1.1 (13.4–17.1)	17.5–21.3	17

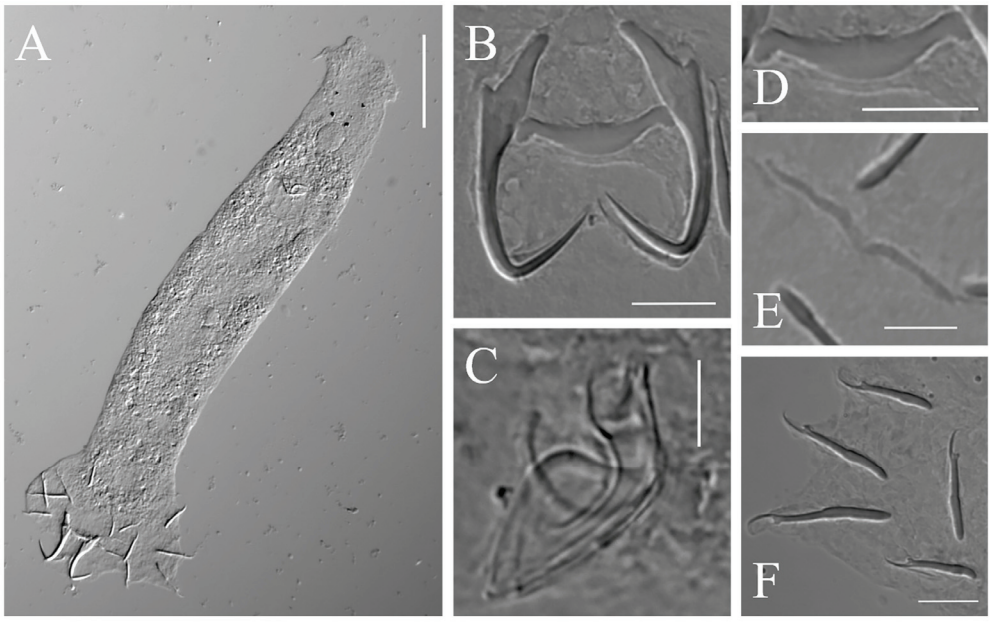

Figure 2. Light micrographs of *Dactylogyrus gobiocypris*: (**A**) whole parasite in ventral view; (**B**) opisthaptoral central hook complex; (**C**) copulatory complex (dorsal view); (**D**) ventral bar; (**E**) dorsal bar; (**F**) marginal hooks. Scale-bars: (**A**) 50 μm; (**B**,**D**,**F**) 10 μm; (**C**,**E**) 5 μm.

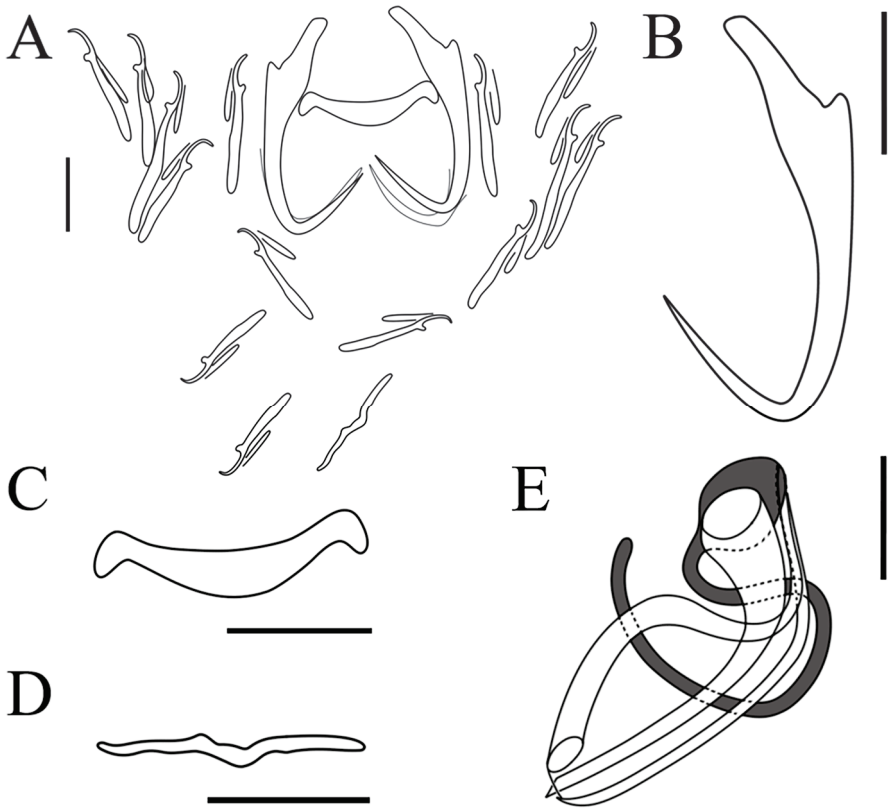

Figure 3. Line drawings of *Dactylogyrus gobiocypris*: (**A**) opisthaptor; (**B**) anchor; (**C**) ventral bar; (**D**) dorsal bar; (**E**) copulatory complex (dorsal view). Scale-bars: (**A**–**D**) 10 μm; (**E**) 5 μm.

3.2. Morphological Characterization

Dactylogyrus gobiocypris Yao, 1995 was the only *Dactylogyrus* species described on the gills of this rare minnow in China [17]. More detailed morphometric measurements are provided herein, since new data on the morphology and phylogeny of *D. gobiocypris* were obtained in the present study. The measurements and shape of the sclerotized parts of the anchors of the specimens collected in the present study were almost identical to the original descriptions of *D. gobiocypris* by Yao [17]. However, the ventral bar was flatter and straighter, and the copulatory complex was shorter, than that of the *D. gobiocypris* described by Yao [17] (penis length 10–14 μm vs. 15–20 μm, and accessory piece 13–17 μm vs. 18–21, respectively). The morphometrical parameters of the sclerotized parts of dactylogyrids sometimes vary over seasons, temperature, and fixation and measurement procedure [29,40,41]. We used a substantial sample size in the present study, while the original descriptions by Yao were based on seven specimens. Thus, these discrepancies are judged to demonstrate intraspecific variation.

According to the studied morphological characteristics, *D. gobiocypris* most closely resembles *D. trullaeformis* in the shape of the anchors, with '*D. wunderi*' type anchors, having a shorter outer root and elongated inner root. However, *D. gobiocypris* differs from *D. trullaeformis* [39] in: (1) the longer length (15–21 μm vs. 14–16 μm, respectively) and shape of the middle portion of ventral bar (slightly convex posteriorly), which is flatter and straighter in *D. trullaeformis*; (2) the accessory piece of *D. gobiocypris* consists of two parts, one of which is horseshoe-shape and the other semicapsular, while the accessory piece of *D. trullaeformis* consists of only one part and is shaped as a heterogeneous groove (Figure 4).

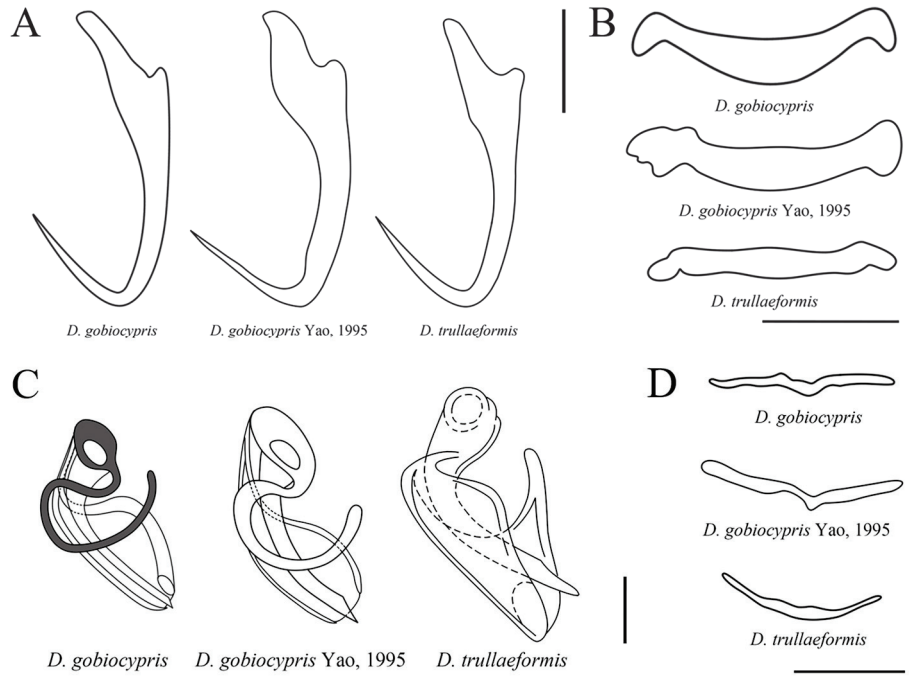

Figure 4. Comparisons of the opisthaptoral and copulatory sclerotized parts among *Dactylogyrus gobiocypris* in the present study, *D. gobiocypris* Yao, 1995 [17] and *D. trullaeformis* Gussev, 1955 [39]: (**A**) anchors; (**B**) ventral bars; (**C**) copulatory complex; (**D**) dorsal bars. Scale-bars: (**A**,**B**,**D**) 10 μm; (**C**) 5 μm.

3.3. Molecular Analyses

Sequences (18S-ITS1) collected from the 12 specimens were identical; the length was 1042 bp. The BLAST search showed that *Dactylogyrus gobiocypris* displayed the highest sequence identity, 86.7%, to *D. cryptomeres*, which was collected from *Gobio gobio* (Linnaeus, 1758) (Cypriniformes: Gobionidae). The sequence of *D. gobiocypris* was then submitted in GenBank for the first time.

Phylogenetic analyses, based on the BI and ML criteria of the 18S rDNA-ITS1 sequence, showed identical topology and only minor differences in statistical support values for some nodes (Figure 5). *Dactylogyrus gobiocypris* formed a clade with *D. squameus*, *D. finitimus*, and *D. cryptomeres*, all of which parasitize on the family Gobionidae. *D. lamellatus*, parasitic on *Ctenopharyngodon Idella* (Valenciennes, 1844) (Cypriniformes: Xenocyprididae), then formed a clade with those *Dactylogyrus* species above.

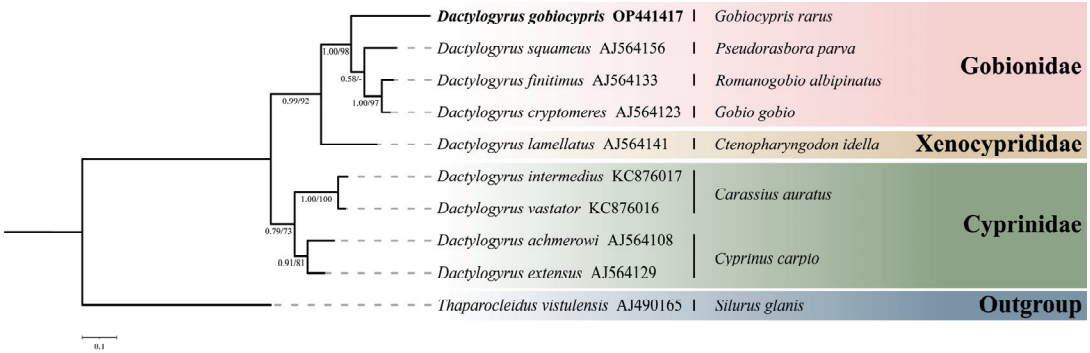

Figure 5. Phylogenetic analysis of *Dactylogyrus gobiocypris* estimated by Bayesian Inference, using 18S-ITS1 rDNA sequences of related species of *Dactylogyrus*. *Thaparocleidus vistulensis* was used as outgroup. Newly generated sequence is in bold. The higher taxa names to the right are for hosts. Posterior probabilities (BI) and bootstrap values (ML) are given below the nodes (posterior probabilities < 0.50 and bootstrap values < 50 are not shown).

3.4. Histopathology Analysis

The histopathological responses of the host to *D. gobiocypris* were investigated by serially sectioning the gills of naturally infected fishes. The gill lamellae of uninfected *G. rarus* were structurally intact, with consistent thickness at the base and end, uniform morphology, and visible gaps between gill lamellae (Figure 6 A,C). Histological examination showed that the infected gills were damaged, to some extent, by necrosis. Additionally, the infection caused hyperplasia of the respiratory epithelium between gill lamellae, with a tendency for adjacent gill filaments to fuse (Figure 6 B). Gill lamellae were affected by the anchors of *D. gobiocypris*, with a breakdown of cell integrity. Cell proliferation was also observed on the base of gill lamellae, which resulted in adhesion of adjacent gill lamellae (Figure 6D).

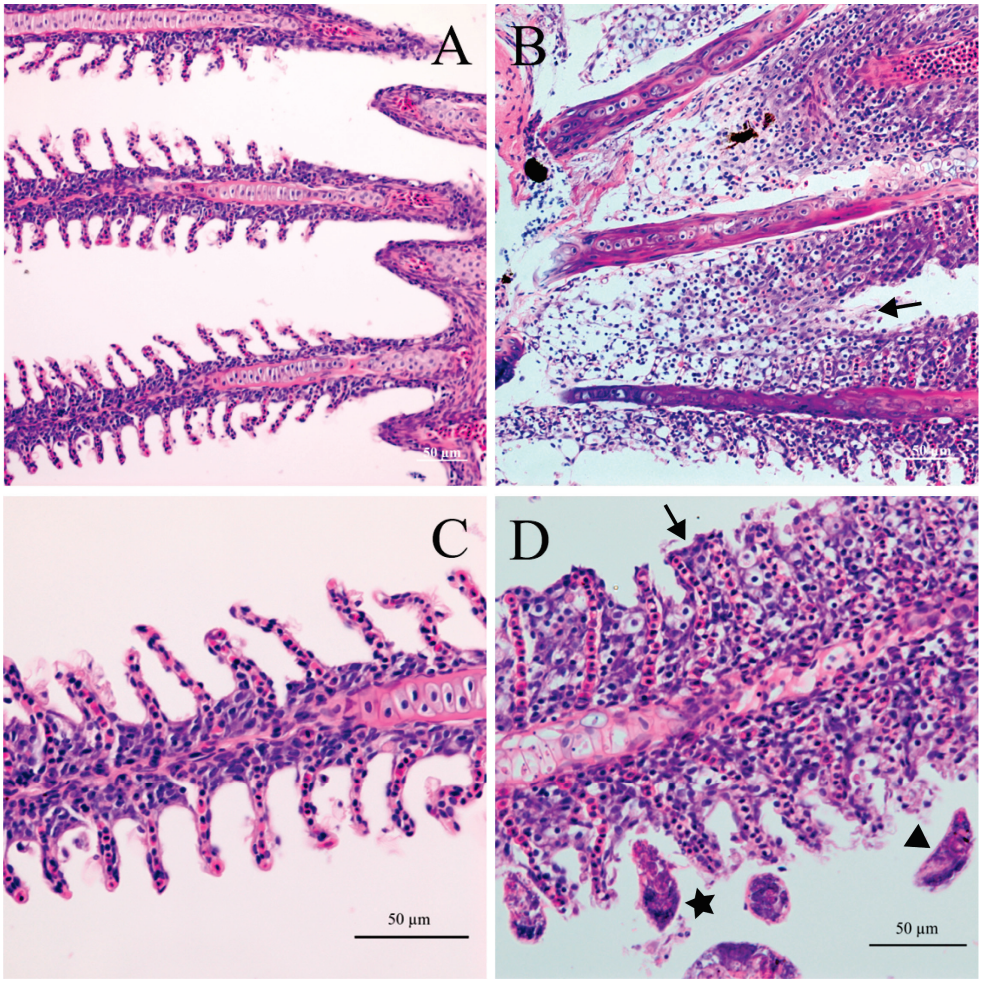

Figure 6. Comparison of histopathological sections of gills of *Gobiocypris rarus,* uninfected (**A**,**C**) and infected (**B**,**D**) with *Dactylogyrus gobiocypris*. The black arrow shows epithelial hyperplasia and the proliferating cells between adjacent gill lamellae. The black triangle indicates the end cells of the gill lamellae are damaged. The five-pointed star points to anchors of *D. gobiocypris* in gill tissues. Scale-bars: (**A**–**D**) 50 µm.

4. Discussion

Species of the genus *Dactylogyrus* are a group of monogenean gill parasites that are highly specific to freshwater fishes of the family Cyprinidae [28]. Basing on the measurements and shape of sclerotized parts of opisthaptor and copulatory complex, the dactylogyrids collected from gills of a rare minnow were identified as *D. gobiocypris*. To date, *D. gobiocypris* represents the only monogenean species reported infecting this rare

minnow in China [17]. The present study provides additional measurements of sclerotized structures of the opisthaptor of this species, along with its molecular characterization and histopathological responses.

In general, the taxonomy of dactylogyrid monogeneans depends on accurate descriptions of the size and shape of the sclerotized parts of the opisthaptor and reproductive organs [29]. The measurements and morphology of the sclerotized parts of the specimens collected in the present study were almost identical to those of *D. gobiocypris* provided by Yao [17]. Of the other species infecting closely related hosts in the Gobionidae family, *D. gobiocypris* most closely resembles *D. trullaeformis* in the shape of the anchors. However, there are distinct differences in the structure of the copulatory complex between the two species. The accessory piece of *D. gobiocypris* consists of two parts, one of which is horseshoe-shaped and the other semicapsular, whereas in *D. trullaeformis* it consists of only one part and is shaped as a heterogeneous groove. The 18S ribosomal RNA subunit and the internal transcribed spacer region (ITS1) are common molecular markers for identification of *Dactylogyrus* species [29,42]. The results of the BLAST search suggested the sequence of *D. gobiocypris* displayed the highest overall identity (86.7%) to *D. cryptomeres*, collected from *Gobio gobio*. The sequence of *D. gobiocypris* was obtained and submitted in GenBank for the first time.

Phylogenetic trees (BI / ML) of *Dactylogyrus* species, constructed based on partial 18S-ITS1 rDNA sequences, are divided into two clades: (1) one clade includes dactylogyrids from *Cyprinus carpio* (Linnaeus, 1758) and *Carassius auratus* Linnaeus, 1758, both representatives of Cyprinidae; (2) the other clade includes parasite species of *C. idella* (Xenocyprididae) and Gobionidae. *Dactylogyrus gobiocypris* exhibited a relatively close phylogenetic relationship with *D. squameus*, *D. finitimus*, and *D. cryptomeres*, all of which parasitize fishes of the Gobionidae family. The molecular phylogeny shows a consistent pattern of relationships among *Dactylogyrus* species. This suggests that there is a high degree of host specificity among the *Dactylogyrus* species that parasitize Gobionidae fishes, which has been displayed in previous molecular phylogenetic studies [28,42,43].

Dactylogyrus gobiocypris was found on all individuals of *G. rarus* investigated, with a high abundance which reached 60.8±84.5 parasites per fish. Prevalence and mean abundance of *Dactylogyrus* infection in cultured rare minnow under laboratory conditions is higher than *Dactylogyrus* spp. in wild and farmed goldfish *Carassius auratus* [42,44]. The IHB rare minnow is a closed laboratory animal colony, the offspring of 50 wild *G. rarus* specimens collected in Hanyuan County of Sichuan Province in 2006 and bred using methods that prevent inbreeding [45]. The higher prevalence and mean abundance of *Dactylogyrus gobiocypris* infection may be related to declining genetic diversity and regular supplementation of the number of susceptible hosts. *Dactylogyrus gobiocypris* can be achieved by in vivo culture under laboratory conditions, and the host is singly infected with *D. gobiocypris*. The rare minnow (*Gobiocypris rarus*)–*D. gobiocypris* artificial infection system can be used as a new host–parasite laboratory model, which will provide support for further investigation.

Observation of histopathological sections of gills of *G. rarus* infected with *D. gobiocypris* indicated that *D. gobiocypris* infection could lead to damage of gill lamellae, causing serious hyperplasia and fusion of the gill filament epithelium. These lesions may reduce the area of gas exchange, affect the respiratory function of gills, and even cause potential secondary infections leading to serious disease with adverse consequences [20,21,46]. In the present study, *G. rarus* infected with a high abundance of *D. gobiocypris* did not have obvious typical clinical symptoms or high mortalities. This lack of symptoms is perhaps caused by decreased parasite virulence or increased host tolerance with a long coevolutionary history.

Parasitic infection may be capable of modifying the resistance of the host to other stressors [46–48]. The susceptibility to toxicants of *G. rarus* may be affected under the stress of high abundance of *D. gobiocypris*, thus interfering with the outcome of toxicological evaluation [49]. Fish hosts infected with parasites have been proven to be more sensitive to toxicants than uninfected conspecifics [50–53]. Most research to date on tolerance to chemicals and environmental pollutants appears to have overlooked the effects of parasites.

Therefore, parasite infection in model organisms should be considered during aquatic toxicity testing and chemical safety assessment.

Author Contributions: Investigation, J.C.; data curation, J.C.; writing—original draft preparation, J.C.; writing—review and editing, H.Z., M.L., J.W., G.W. and W.L.; funding acquisition, G.W. and W.L. All authors have read and agreed to the published version of the manuscript.

Funding: This research was funded by the National Natural Science Foundation of China, grant number 32230109 and the earmarked fund for CARS, grant number CARS-45.

Institutional Review Board Statement: The animal study protocol was approved by the Animal Ethics Committee of the Institute of Hydrobiology, Chinese Academy of Sciences (project identification code: IHB/LL/2020025; date of approval: 27 July 2022).

Informed Consent Statement: Not applicable.

Data Availability Statement: Not applicable.

Acknowledgments: We are very grateful to the anonymous reviewers for their helpful suggestions.

Conflicts of Interest: The authors declare no conflict of interest.

References

1. Ye, M.; Fu, T. Description of a new genus and species of Danioninae from China (Cypriniformes: Cyprinidae). *Acta Zootaxonomica Sin.* **1983**, *8*, 434–437.
2. He, Y.; Wang, J.; Blanchet, S.; Lek, S. Genetic structure of an endangered endemic fish (*Gobiocypris rarus*) in the upper Yangtze River. *Biochem. Syst. Ecol.* **2012**, *43*, 214–225. [CrossRef]
3. Zhou, Y.; Cheng, S.; Hu, W.; Sun, M. A new toxicity test organism-*Gobiocypris rarus*. *Zool. Res.* **1995**, *16*, 59.
4. Zhong, X.; Xu, Y.; Liang, Y.; Liao, T.; Wang, J. The Chinese rare minnow (*Gobiocypris rarus*) as an in vivo model for endocrine disruption in freshwater teleosts: A full life-cycle test with diethylstilbestrol. *Aquat. Toxicol.* **2005**, *71*, 85–95. [CrossRef] [PubMed]
5. Wang, J.; Cao, W. *Gobiocypris rarus* as a Chinese native model organism: History and current situation. *Asian J. Ecotoxicol.* **2017**, *12*, 20–33. [CrossRef]
6. Li, Z.; Chen, L.; Wu, Y.; Li, P.; Li, Y.; Ni, Z. Effects of mercury on oxidative stress and gene expression of potential biomarkers in larvae of the Chinese rare minnow *Gobiocypris rarus*. *Arch. Environ. Contam. Toxicol.* **2014**, *67*, 245–251. [CrossRef] [PubMed]
7. Zhu, B.; Liu, L.; Li, D.; Ling, F.; Wang, G. Developmental toxicity in rare minnow (*Gobiocypris rarus*) embryos exposed to Cu, Zn and Cd. *Ecotoxicol. Environ. Saf.* **2014**, *104*, 269–277. [CrossRef]
8. Wu, W.; Li, W.; Xu, Y.; Wang, J. Long-term toxic impact of 2, 3, 7, 8-tetrachlorodibenzo-p-dioxin on the reproduction, sexual differentiation, and development of different life stages of *Gobiocypris rarus* and *Daphnia magna*. *Ecotoxicol. Environ. Saf.* **2001**, *48*, 293–300. [CrossRef]
9. Zhu, B.; Liu, T.; Hu, X.; Wang, G. Developmental toxicity of 3, 4-dichloroaniline on rare minnow (*Gobiocypris rarus*) embryos and larvae. *Chemosphere* **2013**, *90*, 1132–1139. [CrossRef]
10. Yan, S.; Wang, J.; Zheng, Z.; Ji, F.; Yan, L.; Yang, L.; Zha, J. Environmentally relevant concentrations of benzophenones triggered DNA damage and apoptosis in male Chinese rare minnows (*Gobiocypris rarus*). *Environ. Int.* **2022**, *164*, 107260. [CrossRef]
11. Zha, J.; Sun, L.; Spear, P.A.; Wang, Z. Comparison of ethinylestradiol and nonylphenol effects on reproduction of Chinese rare minnows (*Gobiocypris rarus*). *Ecotoxicol. Environ. Saf.* **2008**, *71*, 390–399. [CrossRef] [PubMed]
12. Wei, Y.; Liu, Y.; Wang, J.; Tao, Y.; Dai, J. Toxicogenomic analysis of the hepatic effects of perfluorooctanoic acid on rare minnows (*Gobiocypris rarus*). *Toxicol. Appl. Pharmacol.* **2008**, *226*, 285–297. [CrossRef] [PubMed]
13. Zhang, Y.; Wu, L.; Zhang, G.; Guan, Y.; Wang, Z. Effect of low-dose malathion on the gonadal development of adult rare minnow *Gobiocypris rarus*. *Ecotoxicol. Environ. Saf.* **2016**, *125*, 135–140. [CrossRef]
14. Gibson, D.I.; Timofeeva, T.A.; Gerasev, P.I. A catalogue of the nominal species of the monogenean genus *Dactylogyrus* Diesing, 1850 and their host genera. *Syst. Parasitol.* **1996**, *35*, 3–48. [CrossRef]
15. Wu, B.; Lang, S.; Wang, J. *Fauna sinica. Platyhelminthes. Monogenea*; Science Press: Beijing, China, 2000; pp. 222–268.
16. Pugachev, O.; Gerasev, P.; Gussev, A.; Ergens, R.; Khotenowsky, I. *Guide to Monogenoidea of Freshwater Fish of Palaearctic and Amur Regions*; Ledizione-LediPublishing: Milan, Italy, 2009; pp. 398–525.
17. Yao, W. A new species of *Dactylogyrus* parasitic from gills of *Gobiocypris rarus*. *Trans. Res. Fish Dis.* **1995**, *2*, 119–120.
18. Wierzbicka, J. Monogenoidea of gills of certain Cyprinidae fish species. *Acta Parasitol. Pol.* **1974**, *22*, 149–163.
19. Jalali, B.; Barzegar, M. Dactylogyrids (Dactylogyridae: Monogenea) on common carp (*Cyprinus carpio* L.) in freshwaters of Iran and description of the pathogenicity of *D. sahuensis*. *J. Agric. Sci. Technol.* **2005**, *7*, 9–16.
20. Rahanandeh, M.; Sharifpour, I.; Jalali, B.; Kazemi, R.; Fatideh, B.; Sabet, S. Survey on Dactylogyrosis in Caspian frisian roach (*Rutilus frisii kutum*) caused by *Dactylogyrus frisii*. *Glob. Vet.* **2010**, *4*, 515–518.

21. Reed, P.; Francis-Floyd, R.; Klinger, R.; Petty, D. Monogenean parasites of fish. In *Publication Series of Fisheries and Aquatic Sciences Department, Institute of Food and Agricultural Sciences, University of Florida*; University of Florida: Gainesville, FL, USA, 2009; pp. 1–10.
22. Tu, X.; Ling, F.; Huang, A.; Wang, G. The first report of *Dactylogyrus formosus* Kulwiec, 1927 (Monogenea: Dactylogyridae) from goldfish (*Carassius auratus*) in central China. *Parasitol. Res.* **2015**, *114*, 2689–2696. [CrossRef]
23. Dove, A.D.; Ernst, I. Concurrent invaders-four exotic species of Monogenea now established on exotic freshwater fishes in Australia. *Int. J. Parasitol.* **1998**, *28*, 1755–1764. [CrossRef]
24. Ergens, R. The suitability of ammonium picrate-glycerin in preparing slides of lower Monogenoidea. *Folia Parasitol.* **1969**, *16*, 320.
25. Malmberg, G. The excretory systems and the marginal hooks as a basis for the systematics of *Gyrodactylus* (Trematoda, Monogenea). *Ark. För Zool.* **1970**, *23*, 1–235.
26. Paladini, G.; Gustinelli, A.; Fioravanti, M.L.; Hansen, H.; Shinn, A.P. The first report of *Gyrodactylus salaris* Malmberg, 1957 (Platyhelminthes, Monogenea) on Italian cultured stocks of rainbow trout (*Oncorhynchus mykiss* Walbaum). *Vet. Parasitol.* **2009**, *165*, 290–297. [CrossRef] [PubMed]
27. Šimková, A.; Pečínková, M.; Řehulková, E.; Vyskočilová, M.; Ondračková, M. *Dactylogyrus* species parasitizing European *Barbus* species: Morphometric and molecular variability. *Parasitology* **2007**, *134*, 1751–1765. [CrossRef] [PubMed]
28. Šimková, A.; Morand, S.; Jobet, E.; Gelnar, M.; Verneau, O. Molecular phylogeny of congeneric monogenean parasites (*Dactylogyrus*): A case of intrahost speciation. *Evolution* **2004**, *58*, 1001–1018. [CrossRef]
29. Sharma, P.; Agarwal, N.; Kumar, S. Ribosomal DNA and morphological analysis of *Dactylogyrus* species from freshwater fishes of India. *J. Parasit. Dis.* **2011**, *35*, 210–214. [CrossRef]
30. Zhang, D.; Gao, F.; Jakovlić, I.; Zou, H.; Zhang, J.; Li, W.; Wang, G. PhyloSuite: An integrated and scalable desktop platform for streamlined molecular sequence data management and evolutionary phylogenetics studies. *Mol. Ecol. Resour.* **2020**, *20*, 348–355. [CrossRef]
31. Nakamura, T.; Yamada, K.D.; Tomii, K.; Katoh, K. Parallelization of MAFFT for large-scale multiple sequence alignments. *Bioinformatics* **2018**, *34*, 2490–2492. [CrossRef]
32. Talavera, G.; Castresana, J. Improvement of phylogenies after removing divergent and ambiguously aligned blocks from protein sequence alignments. *Syst. Biol.* **2007**, *56*, 564–577. [CrossRef]
33. Kalyaanamoorthy, S.; Minh, B.Q.; Wong, T.K.F.; von Haeseler, A.; Jermiin, L.S. ModelFinder: Fast model selection for accurate phylogenetic estimates. *Nat. Methods* **2017**, *14*, 587–589. [CrossRef]
34. Minh, B.Q.; Schmidt, H.A.; Chernomor, O.; Schrempf, D.; Woodhams, M.D.; von Haeseler, A.; Lanfear, R. IQ-TREE 2: New models and efficient methods for phylogenetic inference in the genomic era. *Mol. Biol. Evol.* **2020**, *37*, 1530–1534. [CrossRef] [PubMed]
35. Ronquist, F.; Teslenko, M.; van der Mark, P.; Ayres, D.L.; Darling, A.; Höhna, S.; Larget, B.; Liu, L.; Suchard, M.A.; Huelsenbeck, J.P. MrBayes 3.2: Efficient Bayesian phylogenetic inference and model choice across a large model space. *Syst. Biol.* **2012**, *61*, 539–542. [CrossRef] [PubMed]
36. Molnár, K. Studies on gill parasitosis of the grasscarp (*Ctenopharyngodon idella*) caused by *Dactylogyrus lamellatus* Achmerov, 1952. *Acta Vet. Acad. Sci. Hung.* **1972**, *22*, 9–24. [PubMed]
37. Cheng, J.; Pan, Y.; Ma, X.; Wang, G.; Li, W. Morphological and molecular identification of 7 species of *Dactylogyrus* on gills of the goldfish (*Carassius auratus*). *Acta Hydrobiol. Sin.* **2023**, *47*, 345–354.
38. Šimková, A.; Plaisance, L.; Matějusová, I.; Morand, S.; Verneau, O. Phylogenetic relationships of the Dactylogyridae Bychowsky, 1933 (Monogenea: Dactylogyridea): The need for the systematic revision of the Ancyrocephalinae Bychowsky, 1937. *Syst. Parasitol.* **2003**, *54*, 1–11. [CrossRef]
39. Gusev, A. Monogenetic trematodes of fish from the Amur River system. *Tr. Zool. Inst. Akad. Nauk. SSSR* **1955**, *19*, 171–398.
40. Zolovs, M.; Ozuna, A.; Kirjušina, M. Seasonal variation of attachment apparatus and copulatory organ morphometric variables of *Dactylogyrus crucifer* Wagener, 1857 (Monogenea: Dactylogyridae) on the gills of roach (*Rutilus rutilus* L.) in Latvian water bodies. *Acta Biol. Univ. Daugavp.* **2012**, *12*, 191–198.
41. Vignon, M.; Sasal, P. The use of geometric morphometrics in understanding shape variability of sclerotized haptoral structures of monogeneans (Platyhelminthes) with insights into biogeographic variability. *Parasitol. Int.* **2010**, *59*, 183–191. [CrossRef]
42. Ling, F.; Tu, X.; Huang, A.; Wang, G. Morphometric and molecular characterization of *Dactylogyrus vastator* and *D. intermedius* in goldfish (*Carassius auratus*). *Parasitol. Res.* **2016**, *115*, 1755–1765. [CrossRef]
43. Simkova, A.; Morand, S. Co-evolutionary patterns in congeneric monogeneans: A review of *Dactylogyrus* species and their cyprinid hosts. *J. Fish Biol.* **2008**, *73*, 2210–2227. [CrossRef]
44. Li, W.X.; Zou, H.; Wu, S.G.; Xiong, F.; Li, M.; Ma, X.R.; Marcogliese, D.J.; Locke, S.A.; Wang, G.T. Composition and diversity of communities of *Dactylogyrus* spp. in wild and farmed goldfish *Carassius auratus*. *J. Parasitol.* **2018**, *104*, 353–358. [CrossRef]
45. Li, H.; Wang, C.; Wang, J. Genetic structure of IHB rare minnow (*Gobiocypris rarus*). *J. Hydroecol.* **2018**, *39*, 83–90.
46. Zhang, C.; Li, D.; Chi, C.; Ling, F.; Wang, G. *Dactylogyrus intermedius* parasitism enhances *Flavobacterium columnare* invasion and alters immune-related gene expression in *Carassius auratus*. *Dis. Aquat. Org.* **2015**, *116*, 11–21. [CrossRef] [PubMed]
47. Horoszewicz, L. The influence of parasites, handling of fish and the methods of investigations on the evaluation of their tolerance and thermal resistance. *Rocz Nauk. Roln* **1972**, *94*, 35–53.
48. Sindermann, C.J. Pollution-associated diseases and abnormalities of fish and shellfish: A review. *Fish. Bull.* **1979**, *76*, 717–749.

49. Su, L.; Xu, C.; Cai, L.; Qiu, N.; Hou, M.; Wang, J. Susceptibility and immune responses after challenge with *Flavobacterium columnare* and *Pseudomonas fluorescens* in conventional and specific pathogen-free rare minnow (*Gobiocypris rarus*). *Fish Shellfish. Immunol.* **2020**, *98*, 875–886. [CrossRef]
50. Perevozchenko, I.; Davydov, C. DDT and its metabolites in some cestodes in fishes. *Gidrobiol. Zhurnal* **1974**, *10*, 86–90.
51. Boyce, N.P.; Yamada, S.B. Effects of a parasite, *Eubothrium salvelini* (Cestoda: Pseudophyllidea), on the resistance of juvenile sockeye salmon, *Oncorhynchus nerka*, to Zinc. *J. Fish. Board Can.* **1977**, *34*, 706–709. [CrossRef]
52. Pascoe, D.; Cram, P. The effect of parasitism on the toxicity of cadmium to the three-spined stickleback, *Gasterosteus aculeatus* L. *J. Fish Biol.* **1977**, *10*, 467–472. [CrossRef]
53. Moles, A. Sensitivity of parasitized coho salmon fry to crude oil, toluene, and naphthalene. *Trans. Am. Fish. Soc.* **1980**, *109*, 293–297. [CrossRef]

pathogens

MDPI

Article

Prevalence and Intensity of *Cardicola* spp. Infection in Ranched Southern Bluefin Tuna and a Comparison of Diagnostic Methods

Cecilia Power [1], Shannon Evenden [2], Kirsten Rough [2], Claire Webber [2], Maree Widdicombe [1], Barbara F. Nowak [1] and Nathan J. Bott [1,*]

[1] School of Science, RMIT University, Bundoora, VIC 3083, Australia; s3328980@student.rmit.edu.au (C.P.); s3599119@student.rmit.edu.au (M.W.); b.nowak@utas.edu.au (B.F.N.)
[2] Australian Southern Bluefin Tuna Industry Association, South Quay Blvd, Port Lincoln, SA 5606, Australia; shannon@asbtia.com.au (S.E.); kirstenrough@bigpond.com (K.R.); claire@asbtia.com.au (C.W.)
* Correspondence: Nathan.bott@rmit.edu.au

Abstract: The parasitic blood flukes *Cardicola forsteri* and *C. orientalis* are an ongoing health concern for Southern Bluefin Tuna *Thunnus maccoyii* (SBT) ranched in Australia. In this study we compared the effect of treatment, company, and ranching year on blood fluke infections in ranched SBT. SBT were sampled during the 2018 and 2019 ranching seasons from praziquantel (PZQ) treated pontoons and untreated pontoons managed by two companies. Severity of infection was diagnosed by several criteria including adult fluke counts from hearts, egg counts from gill filaments and the use of specific quantitative polymerase chain reaction (qPCR) for detection of *C. forsteri* and *C. orientalis* ITS-2 DNA in SBT hearts and gills. PZQ treatment remains highly effective against *C. forsteri* infection. Prevalence and intensity of *Cardicola* spp. infection was lower in 2019 than 2018 for Company A in treated pontoons at week 12 and week 17 of ranching, and lower for Company A than Company B in untreated pontoons at month 5 of ranching. Results indicate re-infection may be less likely in the environment near Company A pontoons, and consistent years of treatment may have lowered the parasite load in the environment. qPCR demonstrated higher sensitivity when comparing diagnostic methods for *C. forsteri* in heart, and higher specificity when comparing diagnostic methods for *Cardicola* spp. in gills. Continuing to monitor blood fluke infections in ranched SBT can help to detect changes in drug efficacy over time and help industry to develop a best practice for treatment.

Keywords: *Cardicola*; bluefin tuna; blood fluke; praziquantel; aquaculture; diagnostics

1. Introduction

Southern Bluefin Tuna (SBT), *Thunnus maccoyii*, is a commercially important aquaculture species in Australia [1]. Wild juvenile SBT are caught in the Great Australian Bight via purse seine and slowly towed back to the Spencer Gulf aquaculture zone near Port Lincoln, South Australia, where they are transferred to ranching pontoons. Ranched SBT are fattened on baitfish for 2–7 months before harvesting, enabling industry to add quality and value to their catch quotas [2]. An ongoing health concern in ranched SBT is infection by parasitic blood flukes *Cardicola forsteri* and *Cardicola orientalis* (Trematoda: Aporocotylidae) [3–6].

Cardicola forsteri was first described from the hearts of SBT, and *C. orientalis* reported from the branchial arteries of SBT gills, then detected in SBT samples using molecular techniques [7–9]. Both species can act as serious pathogens by obstructing blood vessels and/or damaging gill epithelium in the circulatory system of SBT [10–12]. Untreated infections with these parasites can lead to mortalities [12]. The anthelmintic praziquantel (PZQ) was shown to be effective against *Cardicola* spp. and introduced by industry in

2012 [13]. Whilst PZQ treatment has reduced ranched SBT mortalities significantly, not all ranched SBT are treated, so ongoing monitoring of parasite loads can be a valuable tool to detect changes in infection severity as new treatment strategies are developed [14].

In 2018, a study was conducted on *Cardicola* spp. infection severity of SBT from a single commercial company from pontoons with different treatment strategies [14]. In 2019, an additional commercial company was sampled with a combination of treated and untreated pontoons. The aim of this paper is to investigate the effect of company, treatment, and ranching year on prevalence and intensity of *Cardicola* spp. infection in commercially ranched SBT.

2. Materials and Methods

2.1. Sample Collection and Processing

Wild SBT were purse seined in the Great Australian Bight (33°27′ S, 132°04′ E) and towed to the Spencer Gulf aquaculture zone near Port Lincoln, South Australia. SBT were sampled from two companies, Company A during the 2018 and 2019 ranching seasons, and Company B during the 2019 ranching season (Table 1). SBT samples collected during transfer from tow pontoon to ranching pontoon were referred to as week 0, and sampling time points thereafter reflect the number of weeks in ranching. Pontoons sampled from each company were from the same tow each year and stocked within 48 hours of arrival. All pontoons in this study were located in an area between 20–25 m water depth.

Table 1. Sampling information including pontoon characteristics and Southern Bluefin Tuna collected from Company A in 2018 and 2019 and Company B in 2019. NA—not applicable.

	Transfer Date	Treatment Date	Treatment Dose (mg/kg)	Sampling Size						
				Week 0	Week 3	Week 8	Week 12	Week 17	Week 21	Week 24
COMPANY A 2018										
Transfer				12	-	-	-	-	-	-
Pontoon 1	28 Feb	9 Mar (Week 2)	15	-	12	12	12	-	-	-
Pontoon 2	28 Feb	3 Apr (Week 6)	15	-	12	12	12	-	-	-
Pontoon 3	28 Feb	NA	NA	-	12	12	12	-	-	-
Pontoon 4	28 Feb	3 Apr (Week 6)	15	-	-	-	-	15	-	-
COMPANY A 2019										
Transfer				12	-	-	-	-	-	-
Pontoon 1	8 Mar	NA	NA	-	10	-	-	-	15	15
Pontoon 2	9 Mar	9 Apr (Week 5)	15-22	-	-	-	12	12	-	-
Pontoon 3	7 Mar	11 Apr (Week 5)	15-22	-	-	-	-	15	-	-
COMPANY B 2019										
Transfer				12	-	-	-	-	-	-
Pontoon 1	28 Mar	NA	NA	-	-	12	12	-	-	-
Pontoon 2	28 Mar	NA	NA	-	-	-	12	15	-	-
Pontoon 3	26 Mar	NA	NA	-	-	-	-	15	-	-
Pontoon 4	27 Mar	29 Apr (Week 5)	15-24	-	-	-	12	15	-	-

SBT from both companies were sampled from some PZQ treated and some untreated pontoons. For Company A in 2018, pontoon 1 was treated week 2 of ranching, pontoon 2 and 4 treated week 6 of ranching, and pontoon 3 was left untreated. For Company A in 2019, pontoon 1 was untreated, and pontoon 2 and pontoon 3 treated week 5 of ranching. Treated SBT from Company A were orally administered PZQ at a dose of 15–22 mg/kg bodyweight. For Company B in 2019, pontoons 1–3 were left untreated and pontoon 4 treated week 5 of ranching. Treated SBT from Company B were orally administered PZQ at a dose of 15–24 mg/kg bodyweight.

SBT were sampled using a baited hook and line from transfer (tow pontoon to ranching pontoon) to week 12. Divers caught SBT from week 17 to week 24. SBT were euthanized using the iki jime method. Fish were then gilled, gutted and wired, the entire process taking under a minute per fish. On shore, weight and total length for each SBT sampled were obtained. This allowed a condition index to be calculated using the South Australian tuna industry formula, whole weight (kg)/length $(m)^3$. As SBT were sampled during commercial operations, whole weights were estimated from the following formula: gilled and gutted weight (kg)/0.87. SBT heart and gills were collected and processed using methods previously described [3,14]. Hearts were dissected 2–4 h after removal and flushed with water

to dislodge adult flukes. Gill filaments were examined for eggs under a 40× compound microscope and quantified as eggs/mm filament length, taking an average from four filaments. Cumulative mortalities for each pontoon sampled were obtained (Table 2).

Table 2. Cumulative mortalities from transfer to harvest of ranched Southern Bluefin Tuna in sampled pontoons from Company A in 2018 and 2019 and Company B in 2019.

	Cumulative Mortality (%)	Weeks in Ranching	Total Stocked Fish
COMPANY A 2018			
Pontoon 1	0.16	16	3128
Pontoon 2	0.31	16	3205
Pontoon 3	0.20	12	2545
Pontoon 4	0.43	17	3108
COMPANY A 2019			
Pontoon 1	0.10	24	2003
Pontoon 2	0.43	17	2082
Pontoon 3	0.43	17	3239
COMPANY B 2019			
Pontoon 1	0.46	15	1525
Pontoon 2	1.82	17	2808
Pontoon 3	0.54	17	2771
Pontoon 4	0.49	17	2849

2.2. DNA Analysis

DNA was extracted from 25 mg of gill and heart samples preserved in RNAlater® using the method and quality controls outlined in Power et al. 2019 [14]. The species-specific primers and probes targeting heterogeneous areas of the internal transcribed spacer-2 (ITS-2) region of rDNA used to detect *C. forsteri* and *C. orientalis* were designed in previous studies, which confirmed their specificity [9,15]. *Cardicola forsteri* and *C. orientalis* DNA was quantified using quantitative polymerase chain reaction (qPCR) techniques previously described [14].

2.3. Statistics

The effects of treatment, ranching year and company on severity of SBT infection with *C. forsteri* and *C. orientalis* were interpreted using GraphPad Prism 8 (GraphPad software, San Diego, CA, USA) as per Power et al. 2019 [14]. Briefly, severity of infection for *C. forsteri* and *C. orientalis* was described by prevalence and intensity as defined by Bush et al., where mean intensity is the average number of parasites per infected host [16]. Data did not meet the assumptions of normality so non-parametric tests were used.

The effect of treatment, ranching year, company and ranching time on infection prevalence was determined using Chi square analysis or Fisher's exact test. Infection intensities were compared using an unpaired t-test or Kruskal–Wallis followed by Dunn's or Mann–Whitney test for pairwise comparisons. The relationship between cumulative mortality and weeks in ranching was determined using simple linear regression. Chi square analysis was used to compare differences in cumulative mortality. Spearman's rank correlation coefficients were used to determine the relationship between condition index and *Cardicola* spp. infection prevalence and intensity. Diagnostic method sensitivity was compared using a two-tailed McNemar χ^2 test.

To determine the effects of treatment, samples from Company B in 2019 were used to directly compare treated and untreated pontoons at week 12 and week 17 of ranching. Samples from Company A in 2018 and 2019 were used to assess the effects of ranching year through direct comparison of untreated pontoons week 0 and week 3, and treated pontoons week 12 and week 17 of ranching. Samples from 2018 and 2019 were also compared over time. To determine the effects of company, samples from Company A in 2019 and Company B in 2019 were used to directly compare treated pontoons week 12 and week 17 of ranching. To compare untreated pontoons from Company A and Company B, samples were directly compared month 0, month 2 and month 5 of ranching. Pontoons from each company sampled within the same week/month were pooled if $p > 0.25$. Samples from

Company A and Company B were also compared over time. Significance for all statistical analysis was assumed at $p \leq 0.05$.

3. Results

3.1. Effect of Treatment

Prevalence and mean intensity of infection with adult *C. forsteri* was higher in untreated pontoons than treated in week 12 and week 17 of ranching (Figure 1). Prevalence increased for Pontoon 1 (untreated) from 33.3% week 8 to 91.7% week 12 and was significantly higher than Pontoon 4 (treated) week 12 with no adult *C. forsteri* detected ($p < 0.0001$). Prevalence for Pontoon 2 (untreated) was 100% week 12 and week 17, significantly higher than Pontoon 4 (treated) week 12 ($p < 0.0001$) and week 17 ($p < 0.0001$). Prevalence for Pontoon 3 (untreated) was 100% week 17, significantly higher than 28.6% prevalence for Pontoon 4 (treated) ($p < 0.0001$). Mean intensity of adult *C. forsteri* infection decreased for Pontoon 1 (untreated), from 4.25 (±1.44) week 8 to 3.18 (±0.72) week 12 and was significantly higher than Pontoon 4 (treated) week 12 with no adult *C. forsteri* detected (H = 26.66, $p = 0.0024$). Mean intensity for Pontoon 2 (untreated) increased from 7.08 (±1.22) week 12 to 18.13 (± 3.48) week 17 and was significantly higher than Pontoon 4 (treated) week 12 (H = 26.66, $p < 0.0001$) and week 17 (H = 10.38, $p = 0.0054$). Mean intensity for Pontoon 3 (untreated) was 16.00 (± 2.60) week 17, significantly higher than 1.50 (±0.29) for Pontoon 4 (treated) (H = 10.38, p =0 0.0094). No significant differences in prevalence or mean intensity were seen between untreated pontoons week 12 and week 17, and no adult *C. forsteri* were detected week 0 (transfer).

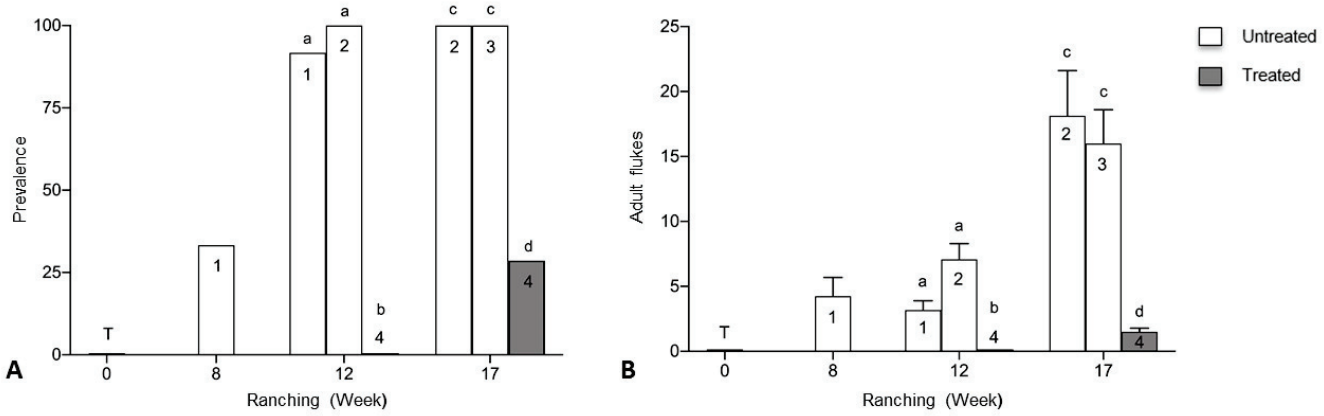

Figure 1. (**A**) Prevalence and (**B**) mean intensity (±SE) of adult *Cardicola forsteri* infection in heart from Company B during 2019 ranching of Southern Bluefin Tuna in Port Lincoln, South Australia (n = 12–15 for each pontoon at each time point). Pontoon 1, Pontoon 2 and Pontoon 3 were left untreated, Pontoon 4 treated with PZQ week 5. Numbers denote pontoon number. Different letters denote statistical differences at $p \leq 0.05$ between pontoons at week 12 and week 17.

Prevalence of *Cardicola* spp. eggs in gill filaments was 50% at week 0 (transfer) (Figure 2A). Prevalence for Pontoon 1 (untreated) decreased from 66.7% week 8 to 60% in week 12. Prevalence for Pontoon 2 (untreated) was 100% in week 12 and week 17, significantly higher than Pontoon 1 (untreated) ($p = 0.0287$) and Pontoon 4 (treated) ($p = 0.0137$) in week 12. Prevalence for Pontoon 4 (treated) increased from 50% in week 12 to 73.3% in week 17. No significant differences in prevalence were seen between Pontoon 1 (untreated) and Pontoon 4 (treated) at week 12, or between Pontoons at week 17. Mean intensity of *Cardicola* spp. eggs/mm gill filament was 0.31 (± 0.19) at week 0 (transfer) (Figure 2B). Mean intensity for Pontoon 1 (untreated) decreased from 0.54 (±0.21) in week 8 to 0.32 (±0.10) in week 12. Mean intensity for Pontoon 2 increased from 1.24 (±0.45) week 12 to 7.24 (±0.87) week 17, significantly higher than Pontoon 4 (treated) (H = 25.18, $p < 0.0001$) week 17. Mean intensity for Pontoon 3 (untreated) was 5.88 (±1.40) in week 17, significantly higher than Pontoon 4 (treated) (H = 25.18, $p = 0.0006$) in week 17. Mean intensity for Pontoon 4 (treated) decreased from 0.33 (±0.10) in week 12 to 0.17 (±0.06) in week 17. No significant differences in mean intensity were seen between pontoons at week 12.

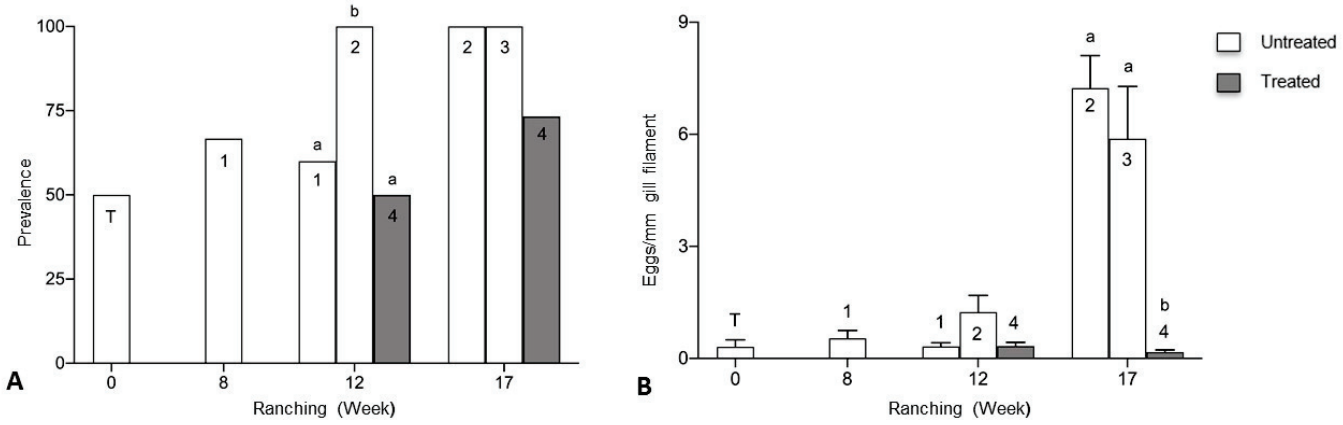

Figure 2. (**A**) Prevalence of *Cardicola* spp. eggs in gill filament; and (**B**) mean intensity (±SE) of *Cardicola* spp. egg/mm of gill filament from Company B during 2019 ranching of Southern Bluefin Tuna in Port Lincoln, South Australia (n = 12–15 for each pontoon at each time point). Pontoon 1, Pontoon 2 and Pontoon 3 were left untreated, Pontoon 4 treated with PZQ week 5. Numbers denote pontoon number. Different letters denote statistical differences at $p \leq 0.05$ between pontoons at week 12 and week 17.

Prevalence of *C. forsteri* (based on positive qPCR of ITS-2) in gill samples was significantly higher in untreated pontoons than treated at week 12 of ranching (Figure 3A). Prevalence increased for Pontoon 1 (untreated) from 66.7% in week 8 to 90.9% in week 12 and was significantly higher than Pontoon 4 (treated) in week 12 at 33.3% (p = 0.0094). Prevalence for Pontoon 2 (untreated) was 100% in week 12 and week 17, significantly higher than Pontoon 4 (treated) in week 12 (p = 0.0013). No differences were seen in prevalence between pontoons at week 17. Mean calculated *C. forsteri* (ITS-2) copy number/mg intensity in gill samples was significantly higher in Pontoon 2 (untreated) than Pontoon 1 (untreated) (H = 16.15, p = 0.0058) and Pontoon 4 (treated) in week 12 (H = 16.15, p = 0.0017) (Figure 3B). Mean intensity was significantly higher in Pontoon 3 (untreated) than Pontoon 2 (untreated) (H = 19.40, p = 0.0003) and Pontoon 4 (treated) in week 17 (H = 19.40, p = 0.0108). No differences were seen between Pontoon 1 (untreated) and Pontoon 4 (treated) in week 12, and Pontoon 2 (untreated) and Pontoon 4 (treated) in week 17.

Cardicola orientalis (ITS-2) was not detected in gill samples at transfer (Figure 3C). Prevalence decreased in Pontoon 1 (untreated) from 41.7% in week 8 to 8.3% in week 12, decreased in Pontoon 2 (untreated) from 33.3% in week 8 to 26.7% in week 12, and decreased in Pontoon 4 (treated) from 16.7% in week 12 to not being detected in week 17. Mean calculated *C. orientalis* (ITS-2) copy number/mg intensity in gill samples decreased in Pontoon 1 (untreated) from 6.81×10^6 in week 8 to 2.70×10^6 in week 12 and increased in Pontoon 2 (untreated) from 2.80×10^6 in week 12 to 5.93×10^7 in week 17 (Figure 3D). No differences were seen in prevalence and mean intensity of *C. orientalis* (ITS-2) in gill samples between pontoons at week 12 and week 17.

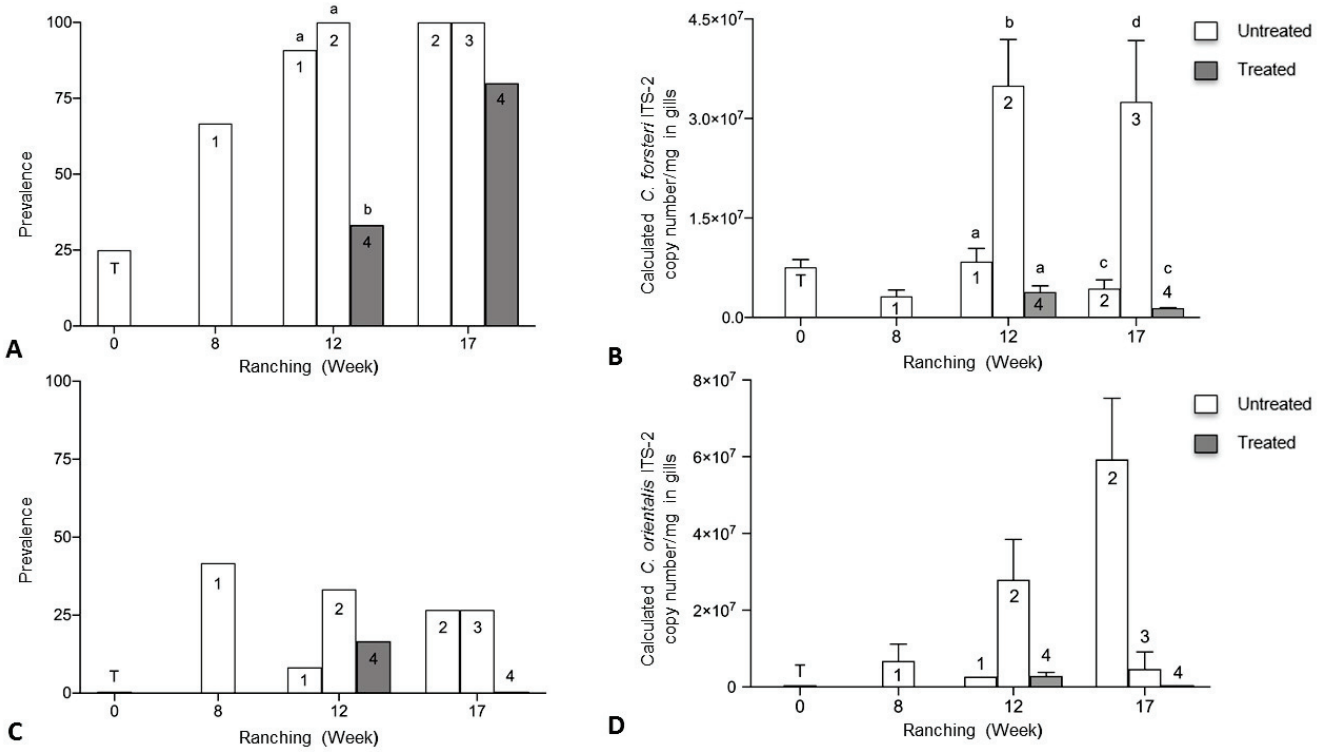

Figure 3. *Cardicola forsteri* (ITS-2) and *Cardicola orientalis* (ITS-2) in gills from Company B during 2019 ranching of Southern Bluefin Tuna in Port Lincoln, South Australia (n = 12–15 for each pontoon at each time point). (**A**) Prevalence of *Cardicola forsteri* (ITS-2) in gills; (**B**) mean calculated *Cardicola forsteri* (ITS-2) copy number/mg intensity (±SE) in gill samples; (**C**) prevalence of *Cardicola orientalis* (ITS-2) in gills; and (**D**) mean calculated *Cardicola orientalis* (ITS-2) copy number/mg intensity (±SE) in gill samples. Numbers denote pontoon number. Pontoon 1, Pontoon 2 and Pontoon 3 were left untreated, Pontoon 4 treated with PZQ week 5. Different letters denote statistical differences at $p \leq 0.05$ between pontoons at week 12 and week 17.

Mean condition index of ranched SBT was 23.5 (±1.32) at week 0 and no data were available at week 8. There was no difference between mean condition index of SBT from Pontoon 2 (untreated) (24.5 ± 0.92) and Pontoon 4 (treated) (23.1 ± 0.32) in week 12 (p = 0.1474). No data were available for Pontoon 1 (untreated) in week 12. There were no differences between mean condition index of SBT from Pontoon 2 (untreated) (24.5 ± 0.23), Pontoon 3 (untreated) (24.7 ± 0.67) and Pontoon 4 (treated) (25.0 ± 0.45) in week 17 (p = 0.5246).

3.2. Effect of Ranching Year

Prevalence of adult *C. forsteri* in heart was significantly higher in 2018 than 2019 week 17 of ranching for Company A treated pontoons (p = 0.0061) (Figure 4A). Mean intensity of adult *C. forsteri* infection was significantly higher in 2018 than 2019 week 12 (U = 30, p = 0.0490) and week 17 (U = 51, p = 0.0416) of ranching for Company A treated pontoons (Figure 4B). No significant differences were seen in prevalence and mean intensity of *C. forsteri* infection between 2018 and 2019 Company A untreated pontoons week 0 and week 3. Prevalence of adult *C. forsteri* increased over time in 2018 treated pontoons (p = 0.0002) but no differences were seen in mean intensity over time in 2018, or in prevalence and mean intensity over time in 2019 treated pontoons.

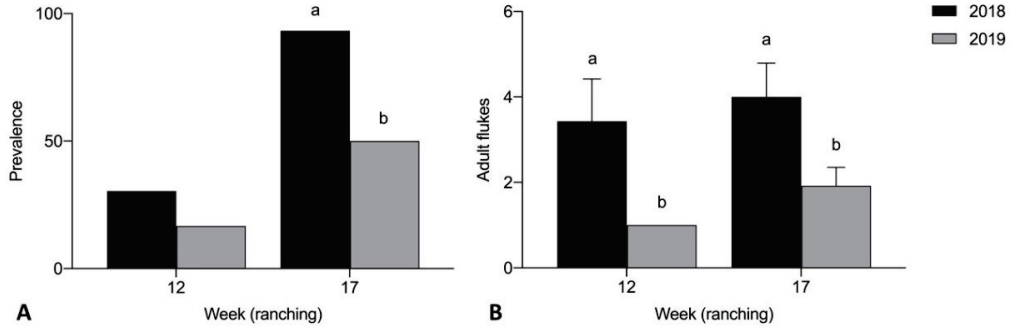

Figure 4. (**A**) Prevalence and (**B**) mean intensity (±SE) of adult *Cardicola forsteri* infection in heart from Company A treated pontoons during 2018 and 2019 ranching of Southern Bluefin Tuna in Port Lincoln, South Australia (week 12 2018 n = 24, week 12 2019 n = 12, week 17 2018 n = 15, week 17 2019 n = 27). Different letters denote statistical differences at $p \leq 0.05$ between ranching years at week 12 and week 17.

Mean intensity of *Cardicola* spp. eggs in gill filament was significantly higher in 2018 than 2019 week 17 of ranching for Company A treated pontoons (U = 19, $p < 0.0001$) (Figure 5B). No significant differences were seen in prevalence of *Cardicola* spp. eggs in gills between Company A treated pontoons week 12 and week 17 (Figure 5A), mean intensity between Company A treated pontoons week 12, and prevalence and mean intensity between Company A untreated pontoons week 0 and week 3. Prevalence and mean intensity of *Cardicola* spp. eggs in gills increased over time in 2018 treated pontoons ($p = 0.0148$, U = 32, $p = 0.0009$) but no differences were seen in prevalence and mean intensity over time in 2019 treated pontoons.

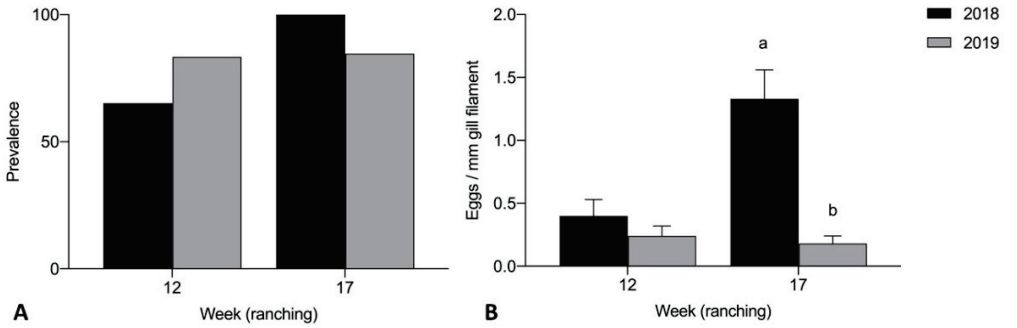

Figure 5. (**A**) Prevalence of *Cardicola* spp. eggs in gill filament; and (**B**) mean intensity (±SE) of *Cardicola* spp. egg/mm of gill filament from Company A treated pontoons during 2018 and 2019 ranching of Southern Bluefin Tuna in Port Lincoln, South Australia (week 12 2018 n = 24, week 12 2019 n = 12, week 17 2018 n = 15, week 17 2019 n = 27). Different letters denote statistical differences at $p \leq 0.05$ between ranching years at week 12 and week 17.

Prevalence of *C. forsteri* (ITS-2) in gill samples was significantly higher in 2018 than 2019 week 12 ($p = 0.0223$) and week 17 ($p = 0.0001$) of ranching for Company A treated pontoons (Figure 6A). Mean calculated intensity of *C. forsteri* (ITS-2) copy number/mg in gill samples was significantly higher in 2019 than 2018 week 12 of ranching for Company A treated pontoons (U = 3, $p = 0.0003$) (Figure 6B). No significant differences were seen in prevalence and mean intensity between 2018 and 2019 Company A untreated pontoons week 0 and week 3. No significant differences were seen in prevalence and mean intensity of *C. orientalis* (ITS-2) in gills between 2018 and 2019 Company A untreated pontoons week 0 and week 3, and between 2018 and 2019 Company A treated pontoons week 12 and week 17. Mean calculated *C. forsteri* (ITS-2) copy number/mg intensity in gill samples increased over time in 2018 treated pontoons (U = 7, $p < 0.0001$). No differences were seen in prevalence over time in 2018 treated pontoons, or in prevalence and mean intensity over time in 2019 treated pontoons.

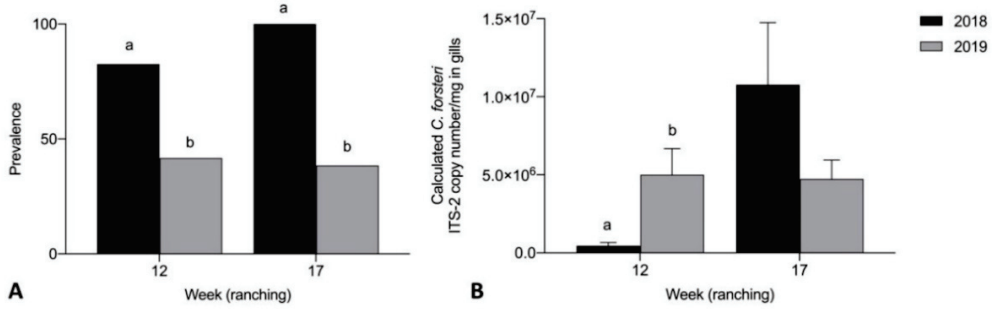

Figure 6. (**A**) Prevalence of *Cardicola forsteri* (ITS-2) in gills; and (**B**) mean calculated *Cardicola forsteri* (ITS-2) copy number/mg intensity (±SE) in gill samples from Company A treated pontoons during 2018 and 2019 ranching of Southern Bluefin Tuna in Port Lincoln, South Australia (week 12 2018 n = 24, week 12 2019 n = 12, week 17 2018 n = 15, week 17 2019 n = 27). Different letters denote statistical differences at $p \leq 0.05$ between ranching years at week 12 and week 17.

Mean condition index of ranched SBT sampled from untreated pontoons in 2018 was 17.6 (±0.19) at week 0, significantly higher than SBT sampled in 2019 with a mean condition index of 16.0 (±0.25) (U = 16, p = 0.0007). At week 3, mean condition index of SBT sampled from untreated pontoons in 2019 was 18.3 (±0.32), significantly higher than SBT sampled in 2018 with a mean condition index of 14.5 (±0.28) (U = 0, $p < 0.0001$). At week 12, mean condition index of SBT sampled in 2019 from treated pontoons was 24.1 (±0.41), significantly higher than SBT sampled in 2018 with a mean condition index of 22.3 (±0.33) (U = 53, p = 0.0023). At week 17, mean condition index of SBT sampled from treated pontoons in 2019 was 25.4 (±0.29), but no results for SBT condition index were obtained from treated pontoons in 2018.

3.3. Effect of Company

No significant differences were seen in prevalence and mean intensity of *Cardicola* spp. infection between Company A and Company B treated pontoons week 12 and week 17 of ranching for any diagnostic method. When comparing untreated pontoons from Company A and Company B, there were no time points (by week) to directly compare, so samples from each company were compared by ranching month. Prevalence and mean intensity of adult *C. forsteri* in 2019 was significantly higher for Company B than Company A untreated pontoons month 5 of ranching (p = 0.0006, U = 22, $p < 0.0001$) (Figure 7). No significant differences were seen in prevalence and mean intensity of *C. forsteri* infection between Company A and Company B untreated pontoons month 0 and month 2. Prevalence of adult *C. forsteri* increased over time for Company A (p = 0.0013) and Company B ($p < 0.0001$) untreated pontoons. Mean intensity of adult *C. forsteri* increased over time for Company B untreated pontoons ($p < 0.0001$), but no differences were seen for Company A.

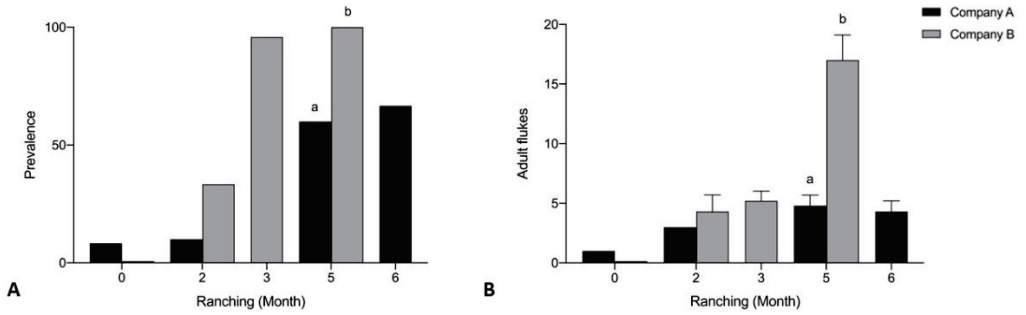

Figure 7. (**A**) Prevalence and (**B**) mean intensity (±SE) of adult *Cardicola forsteri* infection in heart from Company A and Company B untreated pontoons during 2019 ranching of Southern Bluefin Tuna in Port Lincoln, South Australia (A0 n = 12, B0 n = 12, A2 n = 10, B2 n = 12, A2 n = 14, B3 n = 24, A5 n = 15, B5 n = 30, A6 n = 15). Different letters denote statistical differences at $p \leq 0.05$ between companies at each time point.

Mean intensity of *Cardicola* spp. eggs/mm gill filament was significantly higher for Company B than Company A untreated pontoons at month 5 of ranching (U = 143, $p = 0.0489$) (Figure 8). No significant differences were seen in mean intensity of *Cardicola* spp. eggs in gills between Company A and Company B untreated pontoons month 0 and month 2 of ranching, and prevalence of *Cardicola* spp. eggs in gills at any time point. Prevalence of *Cardicola* spp. eggs in gill filaments increased over time for Company A ($p = 0.0158$) and Company B ($p = 0.0003$) untreated pontoons. Mean intensity of *Cardicola* spp. eggs/mm gill filament increased over time for Company B untreated pontoons ($p < 0.0001$), but no differences were seen for Company A.

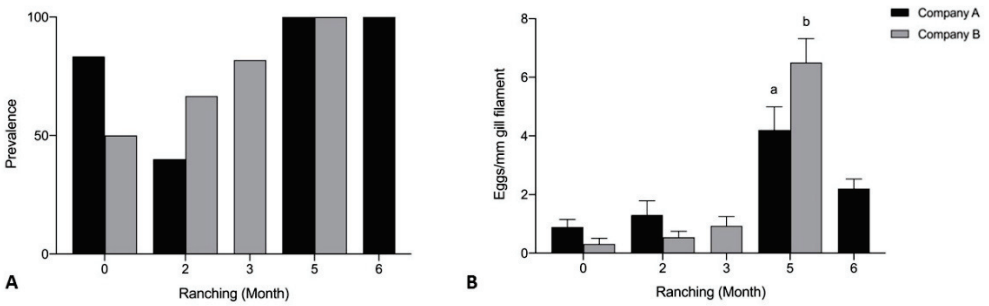

Figure 8. (**A**) Prevalence of *Cardicola* spp. eggs in gill filament; and (**B**) mean intensity (±SE) of *Cardicola* spp. egg/mm of gill filament from Company A and Company B untreated pontoons during 2019 ranching of Southern Bluefin Tuna in Port Lincoln, South Australia (A0 $n = 12$, B0 $n = 12$, A2 $n = 10$, B2 $n = 12$, A2 $n = 14$, B3 $n = 24$, A5 $n = 15$, B5 $n = 30$, A6 $n = 15$). Different letters denote statistical differences at $p \leq 0.05$ between companies at each time point.

Mean calculated *C. forsteri* (ITS-2) copy number/mg in gill samples was significantly higher for Company A than Company B untreated pontoons month 2 of ranching (U = 2, $p = 0.0162$), and significantly higher for Company A than a single Company B untreated pontoon month 5 of ranching (H = 22.47, $p < 0.0001$) (Figure 9B). Company B untreated pontoons could not be pooled at month 5 as one pontoon was significantly higher than the other (H = 22.47, $p = 0.0003$). Mean calculated *C. orientalis* (ITS-2) copy number/mg in gill samples was significantly higher for a single Company B pontoon than Company A untreated pontoons month 5 of ranching (H = 5.07, $p < 0.0001$) (Figure 9D). Company B untreated pontoons could not be pooled at month 5 as one pontoon was significantly higher than the other (H = 3.70, $p < 0.0001$). No significant differences were seen in prevalence of *C. forsteri* (ITS-2) or *C. orientalis* (ITS-2) in gill samples between Company A and Company B untreated pontoons (Figure 9A,C). Prevalence of *C. forsteri* (ITS-2) copy number/mg in gill samples increased over time for Company A ($p = 0.0002$) and Company B ($p < 0.0001$) untreated pontoons. Mean intensity of *C. forsteri* (ITS-2) copy number/mg in gill samples increased over time for Company A (H = 15.89, $p = 0.0022$) and Company B (H = 30.32, $p = 0.0043$) untreated pontoons. Prevalence and intensity of *C. orientalis* (ITS-2) copy number/mg in gill samples did not increase over time for Company A or Company B.

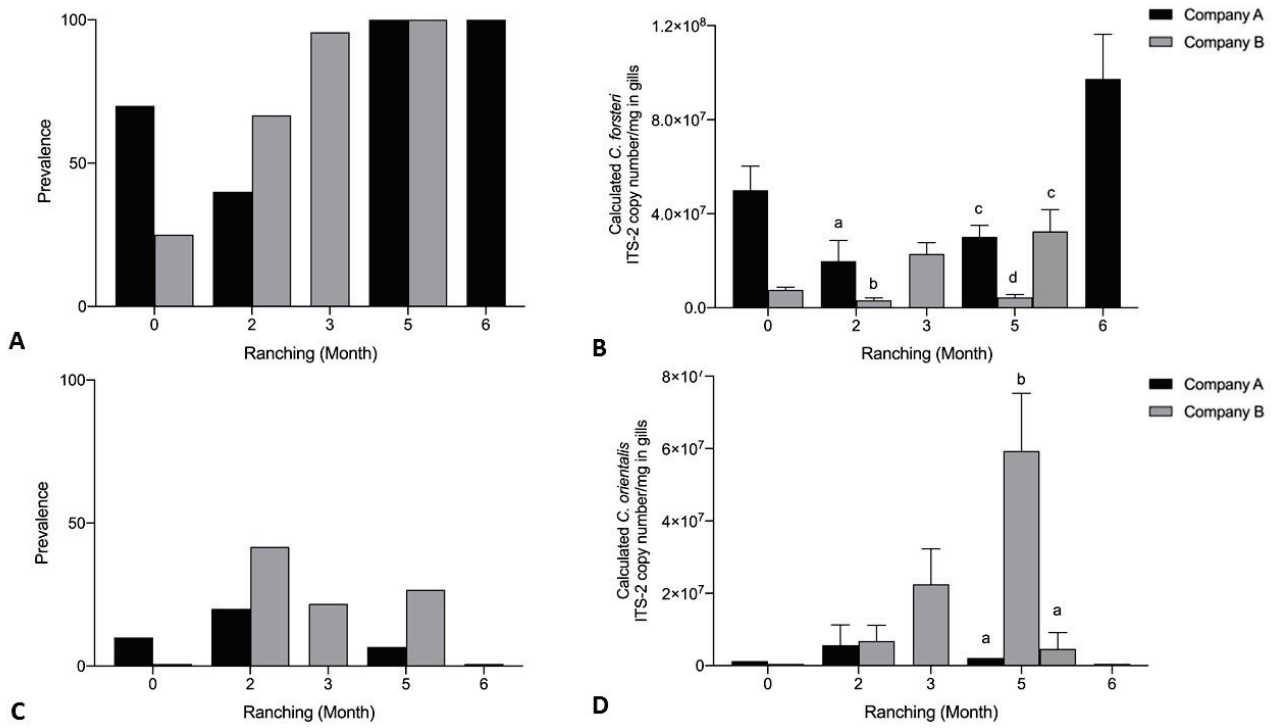

Figure 9. *Cardicola forsteri* (ITS-2) and *Cardicola orientalis* (ITS-2) in gills from Company A and Company B untreated pontoons during 2019 ranching of Southern Bluefin Tuna in Port Lincoln, South Australia (A0 n = 12, B0 n = 12, A2 n = 10, B2 n = 12, A2 n = 14, B3 n = 24, A5 n = 15, B5 n = 30, A6 n = 15). (**A**) Prevalence of *Cardicola forsteri* (ITS-2) in gills; (**B**) mean calculated *Cardicola forsteri* (ITS-2) copy number/mg intensity (±SE) in gill samples; (**C**) prevalence of *Cardicola orientalis* (ITS-2) in gills; and (**D**) mean calculated *Cardicola orientalis* (ITS-2) copy number/mg intensity (±SE) in gill samples. Different letters denote statistical differences at $p \leq 0.05$ between companies at each time point.

There were no significant differences in mean condition index of ranched SBT between Company A and Company B treated pontoons. Mean condition index of ranched SBT sampled from treated pontoons was 24.1 (±0.41) for Company A and 23.1 (±0.32) for Company B week 12. Mean condition index of ranched SBT sampled from treated pontoons was 25.4 (±0.29) for Company A and 25.0 (±0.45) for Company B week 17. When comparing untreated pontoons, mean condition index of ranched SBT sampled from Company B (23.5 ± 1.31) was significantly higher than Company A (17.5 ± 0.25) at month 0 ($p < 0.0001$). No differences were seen between mean condition of ranched SBT from Company A (23.7 ± 0.38) and Company B (24.6 ± 0.35) untreated pontoons month 5 of ranching. Mean condition index could not be compared month 2 of ranching as some results were not available.

3.4. Cumulative Mortality

There was no relationship between cumulative mortality and weeks in ranching for SBT pontoons sampled in this study (d.f. = 9, $R^2 = 0.002$, $p = 0.8738$). Cumulative mortality for Company B, Pontoon 2 (untreated) in 2019 was significantly higher than all other pontoons sampled (Chi-square $X^2 = 40.16$, d.f. = 9, $p < 0.0001$). No differences in cumulative mortality were seen between treated and untreated pontoons in 2019 for Company A, or between 2018 and 2019 pontoons for Company A.

3.5. Effect of Cardicola spp. *Infection Severity on SBT Condition Index*

There was a significant positive correlation between SBT condition index and adult *C. forsteri* numbers in the heart for Company A (Spearman's r = 0.6194, $p < 0.001$) and Company B (Spearman's r = 0.2961, $p = 0.008$). There was a significant positive correlation between SBT condition index and *Cardicola* spp. eggs/mm gill filament for Company A (Spearman's r = 0.2553, $p = 0.007$) and Company B (Spearman's r = 0.2605, $p = 0.019$). A significant positive correlation was also seen between SBT condition index and *C. forsteri* ITS-2 copy number/mg for Company A (Spearman's r = 0.3718, $p <$ 0.001). No correlations were found between SBT condition index and *C. forsteri* ITS-2 copy number/mg

for Company B or between SBT condition index and *C. orientalis* ITS-2 copy number/mg for both companies.

3.6. Comparison between Cardicola spp. *Diagnostic Methods*

For *C. forsteri* in SBT hearts, detection of *C. forsteri* using ITS-2 qPCR had a higher sensitivity than detection of *C. forsteri* using heart flush microscopy (McNemar's test $\chi 2$ test, n = 238, $p < 0.0001$) (Table 3). For the presence of *Cardicola* spp. in SBT gills, detection of *C. forsteri* and *C. orientalis* using ITS-2 qPCR showed similar sensitivity to detection of *Cardicola* spp. eggs using gill microscopy (McNemar's test $\chi 2$ test, n = 308, $p = 0.4185$) (Table 4).

Table 3. Comparison of diagnostic methods for *C. forsteri* in heart of the same individual fish (McNemar's test χ^2, $p < 0.0001$).

		***Cardicola forsteri* (ITS-2) in Heart Samples**		
COMPANY A 2018				
		+	−	Total
Adult *Cardicola forsteri* in heart	+	78	7	85
	−	94	59	153
	Total	172	66	238

Table 4. Comparison of diagnostic methods for *Cardicola* spp. in gills of the same individual fish (McNemar's test χ^2, $p < 0.4185$).

		***Cardicola* spp. (ITS-2) in Gill Samples**		
COMPANY A 2018				
		+	−	Total
Cardicola spp. eggs in gill filament	+	218	24	242
	−	31	35	66
	Total	249	59	308

4. Discussion

Results from this study indicate PZQ remains highly effective against *C. forsteri* infection. When comparing treated and untreated pontoons (Company B) in 2019, prevalence of *C. forsteri* infection in SBT was significantly higher in untreated pontoons week 12 of ranching (7 weeks post treatment), and mean intensity significantly higher in untreated pontoons week 12 and week 17 (12 weeks post treatment). It is likely PZQ is also effective against *C. orientalis* infection, however prevalence was too low to determine its efficacy based on epidemiological data, and the pharmacokinetics of PZQ on adult *C. orientalis* has not been studied previously [13,17]. Results from epidemiological studies help industry to develop the best management strategies for diseases, including treatment, with some companies reducing the number of pontoons treated, thereby reducing their costs. Keeping some pontoons untreated may maintain a population of blood flukes that remain susceptible to anthelmintics in future years [18,19]. Continuing to monitor blood fluke infections in ranched SBT will help to detect changes in drug efficacy over time, and guide future treatment strategies for industry.

When investigating the effect of ranching year, lower prevalence and intensity of *Cardicola* spp. infection was seen in 2019 than 2018 for Company A treated pontoons week 12 and week 17 of ranching. However, when comparing untreated pontoons from earlier in the season (week 0 and week 4), there were no significant differences. Prevalence and intensity of *Cardicola* spp. infection increased from week 12 to week 17 in 2018 treated pontoons, but there were no differences from week 12 to week 17 in 2019. These results may be an indication that consistent years of PZQ treatment have lowered the parasite load in the environment, making re-infection after treatment less likely. Given this study compares only two years of data and other environmental or health factors may be involved, sampling over 3+ years could determine if there are any long-term trends over ranching years in prevalence and intensity of blood fluke infections in ranched SBT or if these results are simply due to annual variation.

There were no differences between treated pontoons for Company A and Company B. Given both companies use similar treatment strategies, their lease sites are located at similar water depths,

and there were no differences in SBT condition, these results are not surprising. When comparing untreated pontoons, prevalence and mean intensity of adult *C. forsteri*, and mean intensity of *Cardicola* spp. eggs was significantly higher for Company B month 5 of ranching. Mean intensity of *C. forsteri* (ITS-2) DNA varied between Company B pontoons at month 5 of ranching, and only one pontoon was significantly higher than Company A. It is interesting to note that mean intensity of adult *C. forsteri* and *Cardicola* spp. eggs increased over time for Company B but not for Company A. These results may be further indication that re-infection is less likely in the environment near Company A pontoons. In a long-term survey of ranched SBT sampled over three ranching seasons (2004–2006), the universal factor explaining *C. forsteri* infection prevalence, abundance and intensity was Company [4]. More specifically, differences between companies may be related to differences in husbandry methods, different sizes of SBT caught for ranching, or the location of lease sites. Our study was completed during commercial operations so was limited with the number of companies and time points included. Given there are now differences in PZQ treatment strategies between companies to consider, another long-term study sampling several companies is warranted.

No differences in cumulative mortality were seen between treated and untreated pontoons, or between ranching years for Company A. However, cumulative mortality for Company B pontoon 2 (untreated) in 2019 was significantly higher than all other pontoons sampled at 1.82%. As the cause of mortality is unknown, it is difficult to determine the reason for this difference. Company B pontoon 2 also had the highest mean intensity of *C. orientalis* ITS-2 DNA in gill samples in this study. In Pacific Bluefin Tuna *Thunnus orientalis*, *C. orientalis* has been shown to have higher pathogenicity than *C. opisthorchis* and *C. forsteri* as it produces significantly more eggs in the gills, and the adults clog the branchial arteries and restrict blood flow [11]. When mortalities peaked in ranched SBT, the dominant species detected was *C. orientalis* [6,9]. It is possible that a higher intensity of *C. orientalis* could contribute to the higher mortality rate seen in Company B pontoon 2.

SBT condition index varied between ranching year and company at certain time points, however no consistent differences were seen. For example, SBT condition index was higher for Company A in 2018 at week 0, but higher in 2019 at week 3 and week 12. This variation may be due to low sample size. There are limitations when studying the relationship between *Cardicola* spp. infection and condition of SBT, as the same fish can only be sampled once throughout the ranching season. Results indicate the severity of infection seen in this study was too low to have an effect on condition of fish.

Molecular diagnostics are crucial when studying infection dynamics of *Cardicola* spp. in ranched SBT. Mean number of *Cardicola* spp. eggs in gills was relatively low in Pontoon 2 (untreated) week 12, but mean intensity of *C. forsteri* (ITS-2) and *C. orientalis* (ITS-2) in gill samples from the same fish was higher in comparison. Egg counts may be low due to the life cycle stage when sampling (miracidia may have hatched from eggs), or due to an uneven distribution of eggs in gill filaments sampled [11,20]. Mean intensity of *Cardicola* spp. eggs in gills was relatively high in Pontoon 2 (untreated) week 17 and in comparison, mean intensity of *C. forsteri* (ITS-2) was relatively low in gill samples but mean intensity of *C. orientalis* (ITS-2) was relatively high. When comparing diagnostic methods, qPCR had higher sensitivity for detection of *C. forsteri* in SBT heart than microscopy. Sensitivity was similar when comparing diagnostic methods for detection of *Cardicola* spp. in gills, but qPCR offers more specificity with *Cardicola* species differentiation [9].

Traditional methods, such as adult counts of *C. forsteri* from SBT heart and egg counts from SBT gills, are simple to perform and can be field based [3,21]. However, traditional methods are laborious, and only detect one life stage—either adults or eggs [10,11]. Additionally, detection of adult *C. orientalis* is difficult using traditional methods [22]. The use of qPCR for detection of *Cardicola* spp. shows greater sensitivity and specificity than traditional methods, but it requires specialised training and equipment, and access to a laboratory [14,16]. These disadvantages negate the potential time advantage afforded by molecular diagnostics. Future research should develop a field-based method that combines the precision of molecular methods with the ease of traditional methods, e.g., use of isothermal amplification assays [23]. Isothermal amplification assays such as recombinase polymerase amplification (RPA), demonstrate optimal temperature at 37 ∘C and can be coupled with a lateral flow strip, making it suitable for rapid diagnosis onshore with limited equipment [23].

Studying infection dynamics of *Cardicola* spp. in ranched SBT is important given there may be differences in pathogenesis between species [11,14]. Since 2013, *C. forsteri* has been the dominant

species documented in ranched SBT populations [14,16]. From 2008 to 2012, *C. orientalis* was identified as the main species in SBT [9]. This change in species dynamic also corresponded with the introduction of PZQ treatment by industry, and a lower rate of mortalities seen during the ranching season [14,16]. Results from this study show *C. forsteri* continues to be the dominant species in ranched SBT, and overall prevalence of *C. orientalis* remains low. The reason for the decline of *C. orientalis* in SBT is unclear, as we do not fully understand the pharmacokinetics of PZQ on *C. orientalis*, and the lifecycle of this species as the intermediate host for *C. orientalis* has not yet been discovered in Australia.

Removal of the intermediate host is another option to control blood fluke infections in ranched SBT [24]. However, there are gaps in our knowledge around life cycles of *Cardicola*. In Australia, the asexual stages of *C. forsteri* were found in a single terebellid polychaete, *Longicarpus modestus*, near SBT pontoon sites [25]. In Japan, life cycles have been elucidated for *C. orientalis*, *C. forsteri* and *C. opisthorchis* with terebellid polychaetes identified as the intermediate host [26–28]. Research has also looked to determine spatial and temporal changes of terebellid polychaetes near tuna pontoons, as this can have different implications for potential efforts to control the parasite [29,30]. Information about the development of *Cardicola* spp. within intermediate hosts is also very limited. Recent work involving transplantation trials of *C. opisthorchis* and *C. orientalis* has opened the possibility for cultivation of *Cardicola* spp. in the laboratory [31,32]. Future work should look to elucidate the life cycle of *C. orientalis* in Australia; in particular, to identify the intermediate host, and determine what factors influence spatial and temporal changes of the intermediate host/s.

Author Contributions: Conceptualization, C.P., B.F.N. and N.J.B.; methodology, C.P., B.F.N. and N.J.B.; validation, C.P., B.F.N. and N.J.B.; formal analysis, C.P. and M.W.; investigation, C.P., S.E., K.R. and C.W.; resources, K.R., C.W. and N.J.B.; data curation, C.P., S.E. and C.W.; writing—original draft preparation, C.P.; writing—review and editing, C.P., B.F.N. and N.J.B.; visualization, C.P.; supervision, B.F.N. and N.J.B.; project administration, C.W. and N.J.B.; funding acquisition, N.J.B. All authors have read and agreed to the published version of the manuscript.

Funding: This research was funded by the Australian Government through the Fisheries Research and Development Corporation (FRDC 2018-170).

Institutional Review Board Statement: Ethical review and approval were waived for this study, as all animals were harvested and euthanized as part of the commercial harvest by aquaculture company personnel in accordance with standards established by the Australian Southern Bluefin Tuna Association.

Acknowledgments: We thank the commercial tuna companies involved for their assistance and support.

Conflicts of Interest: The authors declare no conflict of interest. The funders had no role in the design of the study; in the collection, analyses, or interpretation of data; in the writing of the manuscript, or in the decision to publish the results.

References

1. Ellis, D.; Kiessling, I. Ranching of Southern Bluefin Tuna in Australia. In *Advances in Tuna Aquaculture: From Hatchery to Market*; Elsevier: Oxford, UK, 2016; pp. 217–232. [CrossRef]
2. Power, C.; Nowak, B.F.; Cribb, T.H.; Bott, N.J. Bloody Flukes: A Review of Aporocotylids as Parasites of Cultured Marine Fishes. *Int. J. Parasitol.* **2020**, *50*, 743–753. [CrossRef]
3. Aiken, H.M.; Hayward, C.J.; Nowak, B.F. An Epizootic and Its Decline of a Blood Fluke, Cardicola forsteri, in farmed Southern Bluefin Tuna, Thunnus maccoyii. *Aquaculture* **2006**, *254*, 40–45. [CrossRef]
4. Aiken, H.M.; Hayward, C.J.; Nowak, B.F. Factors Affecting Abundance and Prevalence of Blood Fluke, Cardicola forsteri, Infection in Commercially Ranched Southern Bluefin Tuna, Thunnus maccoyii, in Australia. *Vet. Parasitol.* **2015**, *210*, 106–113. [CrossRef]
5. Balli, J.; Mladineo, I.; Shirakashi, S.; Nowak, B.F. Diseases in Tuna Aquaculture. In *Advances in Tuna Aquaculture: From Hatchery to Market*; Elsevier: Oxford, UK, 2016; pp. 253–272. [CrossRef]
6. Hayward, C.J.; Ellis, D.; Foote, D.; Wilkinson, R.J.; Crosbie, P.B.B.; Bott, N.J.; Nowak, B.F. Concurrent Epizootic Hyper Infections of Sea Lice (Predominantly Caligus chiastos) and Blood Flukes (Cardicola forsteri) in Ranched Southern Bluefin Tuna. *Vet. Parasitol.* **2010**, *173*, 107–115. [CrossRef]
7. Cribb, T.H.; Daintith, M.; Munday, B.L. A New Blood-Luke, Cardicola forsteri (Digenea: Sanguinicolidae) of Southern Bluefin Tuna (Thunnus maccoyii) in Aquaculture. *Trans. R. Soc. S. Aust.* **2000**, *124*, 117–120. [CrossRef]
8. Shirakashi, S.; Tsunemoto, K.; Webber, C.; Rough, K.; Ellis, D.; Ogawa, K. Two Species of Cardicola (Trematoda: Aporocotylidae) Found in Southern Bluefin Tuna Thunnus maccoyii Ranched in South Australia. *Fish Pathol.* **2013**, *48*, 1–4. [CrossRef]
9. Polinski, M.; Hamilton, D.B.; Nowak, B.F.; Bridle, A.R. SYBR, TaqMan, or Both: Highly Sensitive, Non-Invasive Detection of Cardicola Blood Fluke Species in Southern Bluefin Tuna (Thunnus maccoyii). *Mol. Biochem. Parasitol.* **2013**, *191*, 7–15. [CrossRef]

10. Colquitt, S.E.; Munday, B.L.; Daintith, M. Pathological Findings in Southern Bluefin Tuna, Thunnus maccoyii (Castelnau). Infected with Cardicola forsteri (Cribb, Daintith & Munday, 2000) (Digenea: Sanguinicolidae), a Blood Fluke. *J. Fish Dis.* **2001**, *24*, 225–229. [CrossRef]
11. Shirakashi, S.; Kishimoto, Y.; Kinami, R.; Katano, H.; Ishimaru, K.; Murata, O.; Itoh, N.; Ogawa, K. Morphology and Distribution of Blood Fluke Eggs and Associated Pathology in the Gills of Cultured Pacific Bluefin Tuna, Thunnus orientalis. *Parasitol. Int.* **2012**, *61*, 242–249. [CrossRef]
12. Dennis, M.M.; Landos, M.; Antignana, D.T. Case-Control Study of Epidemic Mortality and Cardicola forsteri–Associated Disease in farmed Southern Bluefin Tuna (Thunnus maccoyii) of South Australia. *Vet. Pathol.* **2011**, *48*, 846–855. [CrossRef]
13. Hardy-Smith, P.; Ellis, D.; Humphrey, J.; Evans, M.; Evans, D.; Rough, K.; Valdenegro, V.; Nowak, B.F. In Vitro and In Vivo Efficacy of Anthelmintic Compounds against Blood Fluke (Cardicola forsteri). *Aquaculture* **2012**, *334–337*, 39–44. [CrossRef]
14. Power, C.; Webber, C.; Rough, K.; Staunton, R.; Nowak, B.F.; Bott, N.J. The Effect of Different Treatment Strategies on Cardicola spp. (Trematoda: Aporocotylidae) infection in ranched Southern Bluefin Tuna (Thunnus maccoyii) from Port Lincoln, South Australia. *Aquaculture* **2019**, *513*, 734401. [CrossRef]
15. Neumann, L.; Bridle, A.R.; Leef, M.J.; Nowak, B.F. Annual Variability of Infection with Cardicola forsteri and Cardicola orientalis in Ranched and Wild Southern Bluefin Tuna (Thunnus maccoyii). *Aquaculture* **2018**, *487*, 1–6. [CrossRef]
16. Bush, A.O.; Lafferty, K.D.; Lotz, J.M.; Shostak, A.W. Parasitology Meets Ecology on Its Own Terms: Margolis et al. Revisited. *J. Parasitol.* **1997**, *83*, 575. [CrossRef]
17. Shirakashi, S.; Andrews, M.; Kishimoto, Y.; Ishimaru, K.; Okada, T.; Sawada, Y.; Ogawa, K. Oral Treatment of Praziquantel as an Effective Control Measure against Blood Fluke Infection in Pacific Bluefin Tuna (Thunnus orientalis). *Aquaculture* **2012**, *326–329*, 15–19. [CrossRef]
18. Alsaqabi, S.M.; Lotfy, W.M. Praziquantel: A Review. *J. Vet. Sci. Technol.* **2014**, *5*. [CrossRef]
19. Van Wyk, J.A. Refugia—Overlooked as Perhaps the Most Potent Factor Concerning the Development of Anthelmintic Resistance. *Onderstepoort J. Vet. Res.* **2001**, *68*, 55–67. [PubMed]
20. Norte dos Santos, C.; Leef, M.J.; Jones, B.; Bott, N.J.; Giblot-Ducray, D.; Nowak, B.F. Distribution of Cardicola forsteri Eggs in the Gills of Southern Bluefin Tuna (Thunnus maccoyii) (Castelnau, 1872). *Aquaculture* **2012**, *344–349*, 54–57. [CrossRef]
21. Kirchhoff, N.T.; Leef, M.J.; Ellis, D.; Purser, J.; Nowak, B.F. Effects of the First Two Months of Ranching on the Health of Southern Bluefin Tuna Thunnus maccoyii. *Aquaculture* **2011**, *315*, 207–212. [CrossRef]
22. Ishimaru, K.; Mine, R.; Shirakashi, S.; Kaneko, E.; Kubono, K.; Okada, T.; Sawada, Y.; Ogawa, K. Praziquantel Treatment against Cardicola Blood Flukes: Determination of the Minimal Effective Dose and Pharmacokinetics in Juvenile Pacific Bluefin Tuna. *Aquaculture* **2013**, *402–403*, 24–27. [CrossRef]
23. Ravindran, V.B.; Khallaf, B.; Surapaneni, A.; Crosbie, N.D.; Soni, S.K.; Ball, A.S. Detection of Helminth Ova in Wastewater Using Recombinase Polymerase Amplification Coupled to Lateral Flow Strips. *Water* **2020**, *12*, 691. [CrossRef]
24. Huston, D.C.; Ogawa, K.; Shirakashi, S.; Nowak, B.F. Metazoan Parasite Life Cycles: Significance for Fish Mariculture. *Trends Parasitol.* **2020**, *36*, 1002–1012. [CrossRef] [PubMed]
25. Cribb, T.H.; Adlard, R.D.; Hayward, C.J.; Bott, N.J.; Ellis, D.; Evans, D.; Nowak, B.F. The Life Cycle of Cardicola forsteri (Trematoda: Aporocotylidae), a Pathogen of Ranched Southern Bluefin Tuna, Thunnus maccoyii. *Int. J. Parasitol.* **2011**, *41*, 861–870. [CrossRef]
26. Ogawa, K.; Shirakashi, S.; Tani, K.; Shin, S.P.; Ishimaru, K.; Honryo, T.; Sugihara, Y.; Uchida, H. Developmental Stages of Fish Blood Flukes, Cardicola forsteri and Cardicola opisthorchis (Trematoda: Aporocotylidae), in Their Polychaete Intermediate Hosts collected at Pacific Bluefin Tuna Culture Sites in Japan. *Parasitol. Int.* **2017**, *66*, 972–977. [CrossRef]
27. Shirakashi, S.; Tani, K.; Ishimaru, K.; Shin, S.P.; Honryo, T.; Uchida, H.; Ogawa, K. Discovery of Intermediate Hosts for Two Species of Blood Flukes Cardicola orientalis and Cardicola forsteri (Trematoda: Aporocotylidae) Infecting Pacific Bluefin Tuna in Japan. *Parasitol. Int.* **2016**, *65*, 128–136. [CrossRef]
28. Sugihara, Y.; Yamada, T.; Tamaki, A.; Yamanishi, R.; Kanai, K. Larval Stages of the Bluefin Tuna Blood Fluke Cardicola opisthorchis (Trematoda: Aporocotylidae) Found from Terebella sp. (Polychaeta: Terebellidae). *Parasitol. Int.* **2014**, *63*, 295–299. [CrossRef]
29. Sugihara, Y.; Yamada, T.; Ogawa, K.; Yokoyama, F.; Matsukura, K.; Kanai, K. Occurrence of the Bluefin Tuna Blood Fluke Cardicola opisthorchis in the Intermediate Host *Terebella* sp. *Fish Pathol.* **2015**, *50*, 105–111. [CrossRef]
30. Shirakashi, S.; Tani, K.; Ishimuru, K.; Honryo, T.; Shin, S.P.; Uchida, H.; Ogawa, K. Spatial and Temporal Changes in the Distribution of blood fluke infection in Nicolea gracilibranchis (Polychaeta: Terebellidae), the Intermediate Host for Cardicola orientalis (Digenea: Aporocotylidae), at a Tuna Farming Site in Japan. *J. Parasitol.* **2017**, *103*, 541–546. [CrossRef]
31. Shirakashi, S.; Matsuda, T.; Asai, N.; Honryo, T.; Ogawa, K. In Vivo Cultivation of Tuna Blood Fluke Cardicola orientalis in Terebellid Intermediate Hosts. *Int. J. Parasitol.* **2020**, *50*, 851–857. [CrossRef]
32. Sugihara, Y.; Yamada, T.; Iwanaga, S.; Kanai, K. Transplantation of Cardicola opisthorchis (Trematoda: Aporocotylidae) Sporocysts into the Intermediate Host, Terebella sp. (Polychaeta: Terebellidae). *Parasitol. Int.* **2017**, *66*, 839–842. [CrossRef]

pathogens

MDPI

Article

First Molecular Identification of *Caligus clemensi* on Cultured Crimson Snapper *Lutjanus erythropterus* on Jerejak Island, Penang, Peninsular Malaysia

Zary Shariman Yahaya [1,*], Mohd Nor Siti Azizah [2], Luay Alkazmi [3], Rajiv Ravi [1] and Oluwaseun Bunmi Awosolu [1,4]

[1] School of Biological Sciences, Universiti Sains Malaysia, Penang 11800, Malaysia; rajiv_ravi86@yahoo.com (R.R.); awosolu@student.usm.my (O.B.A.)
[2] Institute of Marine Biotechnology, Universiti Malaysia Terengganu, Kuala Terengganu 21030, Malaysia; sazizah@usm.my
[3] Department of Biology, Umm Al-Qura University, Makkah 21961, Saudi Arabia; lmalkazmi@uqu.edu.sa
[4] Department of Biology, Federal University of Technology, Akure 704, Nigeria
* Correspondence: zary@usm.my; Tel.: +60143497174

Abstract: Fish parasites such as *Caligus clemensi* are a serious concern for cultured fish in many regions of the world, including Malaysia. This study was designed to elucidate the parasites' prevalence and intensity coupled with the morphology and molecular identification of *C. clemensi* on cultured *Lutjanus erythropterus* in Jerejak Island, Penang, Peninsular Malaysia. The study was carried out on 200 fish specimens of cultured *L. erythropterus* obtained from the GST group aquaculture farm. Parasites were collected from the infested part of *L. erythropterus* fish, and their prevalence and intensity were determined. The parasites were identified morphologically using a field emission scanning electron microscope. Molecular studies were performed through PCR amplification and sequencing. MEGA 5 was used to construct a phylogenetic tree using the pairwise distance method. The results showed that only the *C. clemensi* parasite was found prevalent on *L. erythropterus* fish with a prevalence and mean intensity (S.D) of 198 (99%) and 36.4 ± 12.2, respectively. The prevalence varied significantly with respect to fish length ($p < 0.05$). The nucleotide BLAST sequence for 18S ribosomal RNA partial sequences showed 97% with 100% query similarity, E-value 0 with *C. clemensi* with the accession number DQ123833.1. Conclusively, *C. clemensi* remains a major parasite of *L. erythropterus* in the study area.

Keywords: aquaculture industry; aquaculture; fish parasites; morphological identification; phylogenetic tree

1. Introduction

The aquaculture system in floating cages was first established in Penang, Malaysia in 1973. Meanwhile, the snapper fish (Lutjanidae) was the commonest species among marine fish cultures reared in the aquaculture industry [1]. Presently, it is still cultured in many Asian countries including Malaysia. The development of marine cultures has been linked to the emergence of parasitic diseases occasioned by ectoparasites which generally affect fish production [2]. Due to its high infestation rate, the *Caligus* species of copepods are an important threat to the marine culture industry [3]. Thus, diseases caused by parasitic copepods such as Caligids have become widely distributed throughout cultured marine snapper (*Lutjanus* spp.) and other fish species. The *Caligus* species is responsible for causing massive mortalities in cultured *L. erythropterus* due to pathological tissue alterations on the gills and buccal cavity, thereby leading to serious economic loss. They cause serious harm on the host fishes when they feed on the epidermal tissue, blood and mucus of fishes [1,3]. Previous studies in Malaysia have shown that there were five species of copepod from

Caligus general found in marine farmed fishes in Penang and Langkawi Island, according to Maran et al. [3]. These include *Caligus chiastos* from golden snapper, *Lutjanus johni* (Bloch); *Caligus epidemicus* from sea bass, *Lates calcarifer* and *Epinephelus coioides*; *Caligus longipedis* from *Gnathonodon speciosus*; *Corydoras punctatus* from *L. calcarifer*; and *Caligus rotundigenitalis* from *L. erythropterus*, *Epinephelus bleekeri*, *E. fuscoguttatus* and *G. speciosus*. Similarly, a study conducted by Leaw et al. [1] reported a high parasitic infestation rate of 81% in *L. erythropetrus* fish from floating cages off of Penang Island. Besides, reports have indicated that this parasite has a significantly high potential to affect the fish's growth, productiveness and survival rate [4].

Though some findings on the prevalence, mean intensity and veterinary problems caused by the *Caligus* species of copepods have been reported [1,3], the molecular identification of the species is still lacking [1]. Thus, this study is novel since it is the first study to carry out the molecular identification of *C. clemensi* in Malaysia. Moreover, there is a need for adequate updated epidemiological information on the prevalence of the *Caligus* species in Penang to evaluate the impact of *C. clemensi* on cultured crimson snapper and take appropriate action for its control. With this aim, the morphological and molecular identifications of *C. clemensi* on cultured crimson snapper were performed to elucidate the parasite prevalence and mean intensity. In this study, *C. clemensi* was identified for the first time in Malaysia with species confirmation by molecular techniques.

2. Material and Methods

2.1. Parasite Examination on Crimson Snapper

All experimental procedures involving animals were conducted at the Aquatic Research Complex L24, USM, Penang from February to May 2016, in accordance with ethical and practical guidelines [5]. The research was approved by the Universiti Sains Malaysia Animal Ethics Committee (reference number: 1001/PBIOLOGI/855003). The survey was carried out on 200 fish specimens of cultured *L. erythropterus* fish species from aquaculture farm GST group Sdn Bhd on Jerejak Island, Penang, Peninsular Malaysia (5°18′53.2″ N 100°19′29.2″ E). The fish length (cm) was measured prior to parasite examination and categorized into 26–28 cm, 29–31 cm and 32–35 cm according to the authors in [1]. Generally, the fish length was categorized based on growth and development of the fishes with respect to size such that it included the smallest (26–28 cm), the medium (29–31 cm) and the largest (32–35 cm). A solution was prepared containing fresh water and tricaine methane-sulfonate (MS-222) (Sigma–Aldrich) (50 mg/L) to anaesthetize the fish and reduce handling stress. The freshwater medium was used as an anesthetic to reduce the stress as well as for easy handling [6,7]. After the fish had been anaesthetized, parasites were collected from the external skin surfaces of infested areas of the fish such as the head, body and both sides of the inner operculum using surgical dissecting forceps [6,7]. The fish parasites were obtained and measured. All of the *C. clemensi* parasites obtained from the 200 fish samples were calculated based on a morphological field examination [8,9] with the aid of a dissecting microscope (magnification of X50; Leica, Allendale, NJ, USA). The prevalence and mean intensity were calculated according to the method of Bush et al. [10]. The parasite prevalence was defined as the total number (percentage) of infected fishes while mean intensity was defined as the average number of parasites in an infected fish.

2.2. Morphological Identification Using Scanning Electron Microscope

Secondary morphological identification was performed using a Supra 50 VP ultra-high-resolution LEO analytical field emission scanning electron microscope (Carl Zeiss LEO Supra 50 VP field emission equipped with an Oxford INCA system). Sample preparation was carried out according to the Carl Zeiss LEO Supra 50 VP field emission scanning electron microscope manufacturer's procedures and protocol. First, parasite samples were immersed in ethanol and hydrated with 90%, 80% and 70% serial dilutions. After that, the parasite specimens were placed on carbon film-coated 400 mesh copper grids for 1–3 min. Then, filter paper was used to dry the specimens. Grids were then placed

in a desiccator using filter paper-lined petri plates. After three days of preservation, imaging was completed [11,12]. The identification of parasites collected was made by a morphological inspection using appropriate identification keys after the parasite pictures were obtained [3,8,9,11,13–15].

2.3. Molecular Identification

The DNA extraction and purification of each parasite sample were performed using the Qiagen DNeasy blood and tissue kit (Qiagen, Inc., Valencia, CA, USA) following the manufacturer's instructions. Purified genomic DNA was eluted by adding 100 uL of elution buffer AE to the same spin column in a new eppendorf tube and centrifuged at 5200 g for 1 min. The centrifuge step was repeated for a total of 200 uL of the sample volume. DNA sample concentration and quality were measured using an ACT-Gene NanoDrop spectrophotometer (ASP 2680, Taipei, Taiwan). Eluted genomic DNA was stored at −20 °C until the PCR analysis. Subsequently, 18S ribosomal partial sequences were amplified from purified genomic DNA using the Universal Folmer primers LCO 1490 (5′-GGT CAA CAA ATC ATA AAG ATA TTG G-3′) as a forward primer and HCO2198 (5′-TAA ACT TCA GGG TGA CCA AAA AAT CA-3′) as a reverse primer [16,17]. A polymerase chain reaction (PCR) was carried out using a total volume of 25 µL master mix solutions (14 µL of ddH_2O, 2.5 µL of Promega PCR buffer, 3 µL of Promega $MgCl_2$ solutions, 1 µL of Promega dNTP, 1 µL of each forward and reverse primers, 2 µL of DNA template and 0.5 µL of Promega Go Taq DNA polymerase). Standard cycle conditions for the PCR were set accordingly by initial denaturation of 10 min at 95 °C, followed by 35 cycles of 30 s at 95 °C, 30 s at 50 °C, 60 s at 72 °C and final elongation of 7 min at 72 °C. The PCR was carried out in Mycycler thermal cycler Bio-Rad PCR systems (Hercules, CA, USA). Purification of the PCR product was performed using the procedure and materials provided in a QIAquick PCR purification kit (Qiagen, Inc.). Amplification products were sequenced in both directions.

A distance-based tree approach to species identification was conducted using MEGA 5 software (version 5). A BLAST search was conducted with a DNA sequence that was amplified. Using MEGA 5, a distance-based tree approach to species identification was carried out by neighbor-joining the 18S ribosomal partial sequences of the recorded species from the BLAST search and those analyzed in this study. A pairwise distance calculation was completed using MEGA 5 analysis tools and the method of Tajima and Nei [18] served as the substitution model [19]. In addition, the bootstrap method was deployed as a test of phylogeny using 1000 bootstrap replications. DNA barcoding was developed according to bold system web instructions. A character-based diagnostic approach to species delimitation was applied using MEGA 5.

2.4. Statistical Analysis

The statistical analysis was performed using the Statistical Package for Social Sciences software, SPSS version 20. A chi-square analysis was used to compare parasite prevalence. Values at $p < 0.05$ were considered significant.

3. Results

3.1. Prevalence and Mean Intensity of Caligus clemensi

A total of 200 crimson snapper fishes were examined for the prevalence of *C. clemensi*. The fishes were categorized into 26–28 (25%), 29–31 (49%) and 32–35 (26%). The results showed a total prevalence and mean intensity (S.D) of 99% (198) and 36.4 ± 12.2, respectively. Prevalence according to fish length showed that fishes with lengths 26–28 cm and 32–35 cm had a parasite prevalence of 100%, while fishes with 29–31 cm had 97.96%. The result was statistically significant ($p < 0.05$). Similarly, the mean intensity significantly ($p < 0.05$) increased with an increase in fish length such that fishes with 26–28 cm had the lowest mean intensity of 29.48 ± 11.33, followed by fishes with 29–31 cm with a mean intensity of 33.32 ± 10.81 and fishes with the longest length of 32–35 cm had the highest mean intensity of 48.77 ± 4.0 (Table 1).

Table 1. Prevalence and mean intensity of *Caligus clemensi* with regards to the length of crimson snapper.

Parasite	Fish Length (cm)	Number of Fish Examined (%)	Number of Fish Infected (%)	Minimum No. of Parasites Recovered	Maximum No. of Parasite Recovered	Total Number of Parasites Recovered	Mean ± SD
Caligus clemensi	26–28	50 (25)	50 (100.00)	15	53	1474	29.48 ± 11.33
	29–31	98 (49)	96 (97.96)	15	53	3265	33.32 ± 10.81
	32–35	52 (26)	52 (100.00)	42	54	2536	48.77 ± 4.0
Total		200	198 (99.00)			7275	36.4 ± 12.2

3.2. Morphological Analysis of Caligus clemensi

A total of twenty [20] *C. clemensi* were isolated for examination under the scanning electron microscope (SEM). Each of the *C. clemensi* parasites was isolated and viewed on an optical microscope (Figure 1) for the initial minor observations while the detailed observations were observed with a scanning electron microscope (SEM) (Figure 2; Supplementary Table S1). Overall, the total body length was 3.9 to 4.1 mm (Figure 2A). The cephalothorax shield was ovate, with a length of 2.5 to 2.7 mm greater than the width of 1.9 to 2.2 mm (Figure 2A). Furthermore, the mouth tube was carried folded parallel to the body axis (Figure 2D), which showed the tip of the labium for a typical *C. clemensi*. The fourth leg bearing segment measured from 0.3 to 0.2 mm and was located posterior to the cephalothorax (Figure 2B). The genital complex was sub-circular to oval, measuring 0.9 to 1.0 mm (Figure 2A). The abdomen was divided into two segments that were longer than they were wide, measuring 0.7 to 1.0 mm in length (Figure 2A). Leg 4 was positioned on both sides of the genital complex curve (Figure 2E). The furca was carried in a folded position parallel to the body axis, displaying its shape as a flat surface (Figure 2F). All the other organs were labelled as shown in Figures 3 and 4.

Figure 1. *Caligus clemensi* ventral view with the aid of optical microscope, magnification 50X.

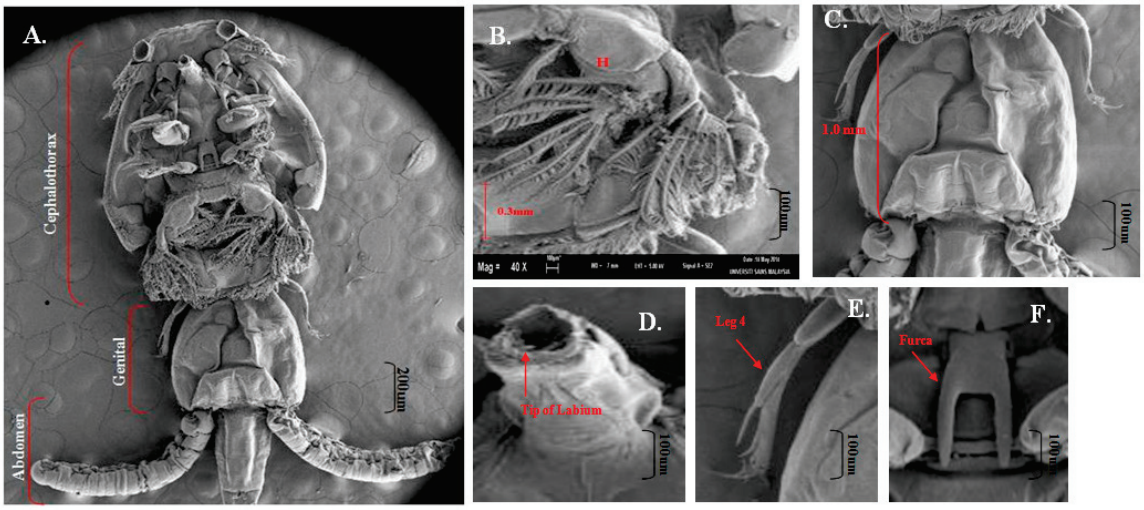

Figure 2. *Caligus clemensi* viewed under SEM. (**A**): Ventral view of adult female with egg sacs; (**B**): leg 2 measured as 0.3 mm; (**C**): genital complex measured as 1.0 mm; (**D**): tip of labium detailed; (**E**): leg 4 detailed; (**F**): furca detailed. Magnifications (**A**) = 35X, (**B**) = 40X, (**C**) = 40X, (**D**) = 80X, (**E**) = 50X and (**F**) = 80X.

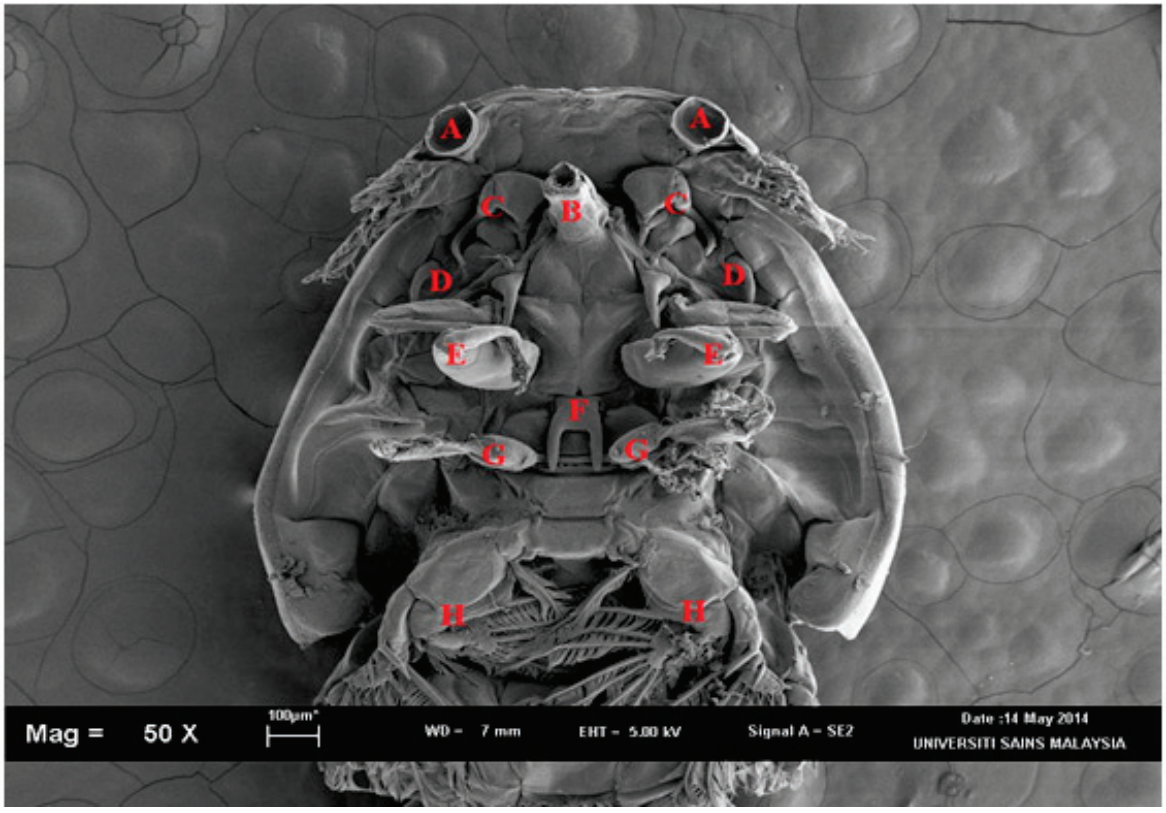

Figure 3. *Caligus clemensi*. in ventral view. A: lunule; B: mouth tube; C: 3-segmented antenna which consists of basal segment (=coxa), middle segment (=basis) and terminal segment (=endpod); D: 1-segmented hook-like post antennal process; E: maxillae; F: sternal furca that has tapering tines; G: leg 1; H: leg 2. Magnification at 50X.

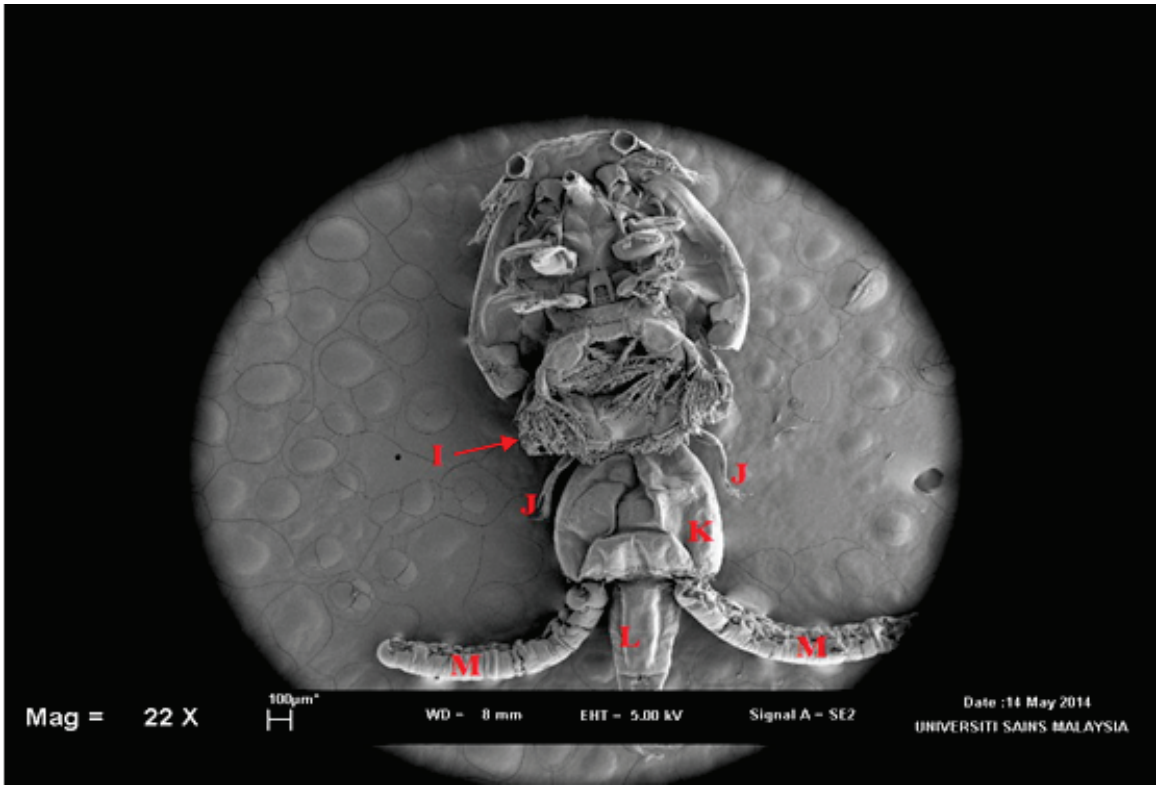

Figure 4. *Caligus clemensi* in ventral view. I: Leg 3; J: leg 4 with 5 setae; K: genital complexes which attach to the posterior portion of the fourth leg-bearing segment without the posterolateral processes; L: 1st abdominal somite that leads to anal somite where caudal ramus originates from it; M: egg sac. Magnification at 22X.

3.3. Molecular Analysis of Caligus clemensi

All the sequences were successfully analyzed and recovered from all *C. clemensi* individuals without any stop codons. The nucleotide BLAST sequence for 18S ribosomal RNA partial sequences showed 97% with 100% query similarity, E-value 0 with *C. clemensi* DQ123833.1 (Figure 5). Moreover, all the sequences from this study have been deposited in GenBank with accession numbers KX808655, KX808656 and KX808657. Additionally, the barcode of Life Data System were obtained and the BOLD submission ID in accordance with species *Caligus clemensi* as shown in Table 2.

Figure 6 shows the constructed phylogenetic tree between species. All of the *C. clemensi* identified in this study shared a close clade relationship with the *C. clemensi* DQ123833.1 sequence. *C. clemensi* was found to be in a closer clade than *C. centrodonti* EF088407, *C. curtus* EF088407 and *C. pelamydis* EF088411.1. This study found distant clades from *C. clemensi* in *C. uniartus* KC569363.1, *C. punctatus* KR048777.1 and *C. fugu* KR048778.1.

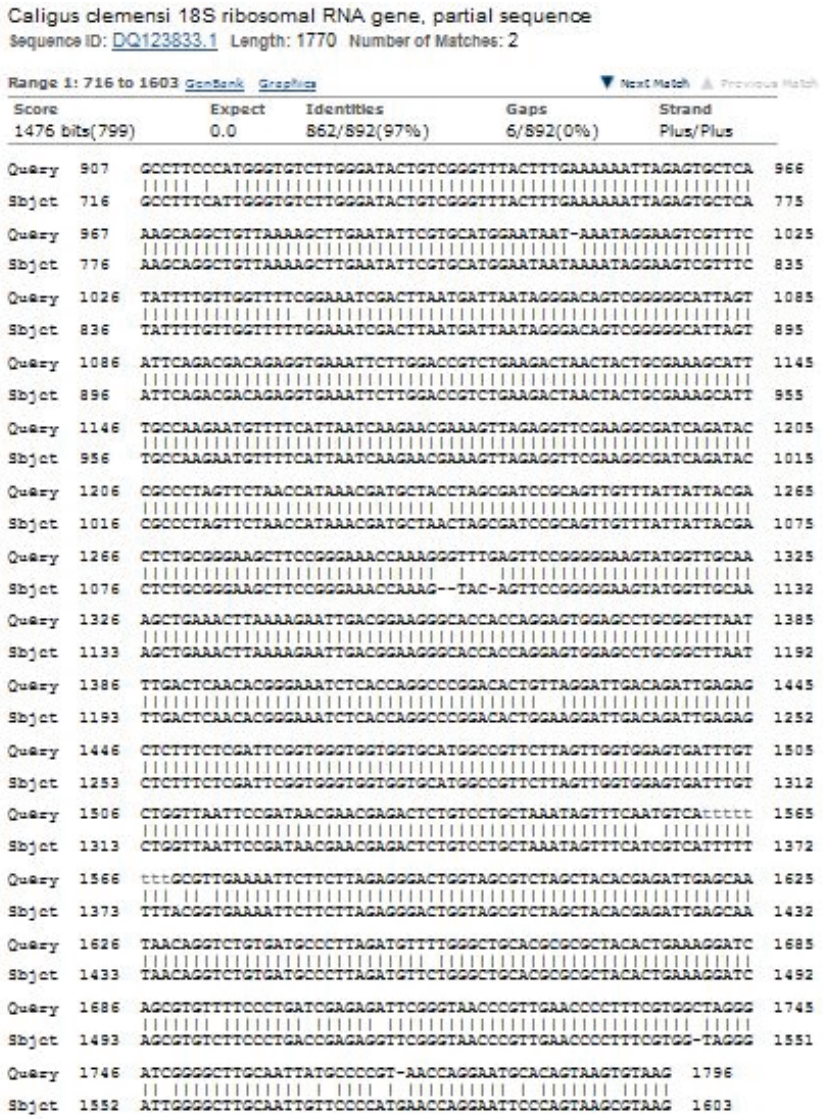

Figure 5. Verification of the obtained sequence of 18S ribosomal RNA partial sequences' comparison with *Caligus clemensi* (DQ123833.1) using ClustalW, multiple sequence alignment software. There is an indication of 97% similarity between both sequences.

Table 2. Barcode of Life Data System, (www.boldsystem.org, accessed on 12 August 2017) BOLD submission ID in accordance with species *Caligus clemensi*.

Identification	Specimen Page	Sequence Page	COI-SP	BIN
Caligus clemensi	Fish Caligus 5	CALIG005-14	671 [0n]	BOLDAC02743
Caligus clemensi	Fish Caligus 4	CALIG004-14	671 [0n]	BOLDAC02743
Caligus clemensi	Fish Caligus 3	CALIG003-14	671 [0n]	BOLDAC02743
Caligus clemensi	Fish Caligus 2	CALIG002-14	671 [0n]	BOLDAC02743
Caligus clemensi	Fish Caligus 1	CALIG001-14	671 [0n]	BOLDAC02743

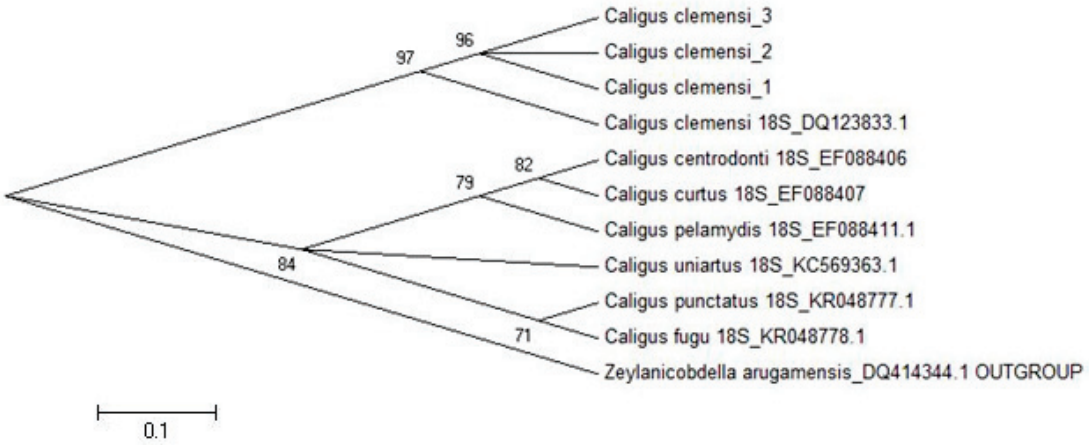

Figure 6. MEGA 5 generated neighbor-joining tree based upon the 18S ribosomal RNA partial sequences of specimens analyzed in this study.

4. Discussion

This study reports the first molecular identification of *C. clemensi* on cultured crimson snapper at Jerejak Island, Penang, Peninsular Malaysia. Previous studies on *Caligus* species from marine finfish cage culture species are few and limited in Malaysia. One of the previous studies conducted by Ahamad Hasmi [20] reported the isolation and identification of three different species of caligids from *Lates calcarifer* cultured in floating net cages in Malaysia. These species were: *C. chiastos*, *C. epidemicus* and *C. rotundigenitalis* [20]. Our findings are substantiated by other studies that were previously reported [1–3]. The *Caligus* species, for example, is known to have a podoplean-type body structure in terms of morphology [21,22]. The *Caligus* species also has one rather than five segments between the cephalothorax shield and the genital segment [9,23]. Moreover, the *Caligus* species is known to be siphonostomatoid due to the presence of a distinctive tubular mouth apparatus. This type of mouth part is characterized by the elongated and tapering structure [21].

Furthermore, the sequence analysis and construction of phylogenetic trees presented in this study reveal the relationship between our study isolates and the others available in the GenBank (Figure 6). The molecular analyses derived from 18S ribosomal RNA partial sequences accurately supported the morphological classification of *C. clemensi*. This is corroborated by the findings of Jones et al. [24]. The phylogenetic tree of *C. clemensi* showed a closer clade of *C. centrodonti*, *C. curtus* and *C. pelamydis*, compared to the distant clade of *C. uniartus*, *C. punctatus* and *C. fugu*, and this is similar to the findings of Øines and Schram [25].

Accurate phylogenetic analyses require the stability of taxonomic classifications, and it is often concluded, based on RNA sequences, that and an increased number of data would result in a higher tree resolution [26]. The taxonomic and systematics of *Caligus* spp. are still very far from complete in their largest genus of Copepoda comprising more than 250 species: Müller, 1785. However, only *C. centrodonti*, *C. curtus*, *C. pelamydis*, *C. uniartus*, *C. punctatus* and *C. fugu* are appropriate to be included in this study. Noticeably, several other taxa, such as *C. elongates* and *C. warlandi*, available in the GenBank, have to be left out since our study was only exploring the published and verified sequences with Refseq.

Vast reports have highlighted the instability and high degree of variations in the phylogeny of *Caligus* spp. [27,28]. The uncertainty of *Caligus* spp. phylogenies is still debatable due to the discrepancy between several varying reports, regardless of whether the 18S, 28S or the mitochondrial genes have been utilized [25]. This is evident from the *C. clemensi* systematics, which revealed uncertainty and instability in the maximum likelihood and maximum parsimony distance analyses, where *C. clemensi* was found to be closely related to *C. pelamydis* as supported by our findings.

To date, only one study on *Caligus rotundigenitalis* infestation on *L. erythropterus* fish has been documented in Malaysia [1]. The report found a high prevalence of *C. rotundigenitalis*

L. erythropterus fish at Bukit Tambun, Penang, Peninsular Malaysia, with an 81% prevalence. This high prevalence has been linked to the species' continuous reproduction and high proliferation capacity throughout the year and its natural life cycle. Additionally, other studies have reported varying degrees of *C. clemensi* prevalence from other parts of the world such as Egypt [29–31] and Canada [32,33]. Similarly, our findings showed a total prevalence of 198 (99.00%) for *C. clemensi* on *L. erythropterus*. This is higher than the report by Leaw et al. [1] who recorded a prevalence of 81.4% for *C. rotundigenitalis*. This variation could be due to the duration of infestation on the fish, fish immune response or the sizes of the fishes examined. Other factors include host response to infestation, interaction of sea temperature, host abundance and distribution in sea cages, according to the report of Costello [34]. Moreover, it was observed in this study that fish length varied significantly with respect to parasite prevalence and mean intensity ($p < 0.05$). The longer the fish, the higher the parasite infestation. The prevalence and mean intensity of *Caligus* spp. have commonly been found to show a positive correlation to the length size of the fish host [11,35]. According to Rohde [35], more investigation revealed that different age stages of fish might have variable infestation levels due to parasite accumulation, the host immune system, size range and feeding habits. Furthermore, as the host's immune system grows over time, the parasite's intensity reduces.

5. Conclusions

Conclusively, this study has successfully identified *C. clemensi* morphologically and through the use of molecular techniques. Additionally, this study showed that crimson snapper cultured at the GST group aquaculture farm had a high prevalence and heavy infestation of *C. clemensi* with the prevalence and mean intensity of 99% and 36.4 $\pm$ 12.2, respectively. This updated information on the prevalence and mean intensity can inform appropriate control measures for the proper management of cultured crimson snapper.

Supplementary Materials: The following are available online at https://www.mdpi.com/article/10.3390/pathogens11020188/s1, Table S1: Measurements of some body parts of *C. clemensi* on cultured Crimson Snapper, *Lutjanus erythropterus* at Jerejak Island, Penang, Peninsular Malaysia.

Author Contributions: Conceptualization, Z.S.Y. and L.A.; methodology, Z.S.Y. and R.R.; software, R.R.; validation, Z.S.Y., L.A. and M.N.S.A.; formal analysis, R.R. and O.B.A.; investigation, Z.S.Y., R.R. and M.N.S.A.; resources, Z.S.Y.; data curation, R.R. and O.B.A.; writing—original draft preparation, R.R. and O.B.A.; writing—review and editing, O.B.A.; visualization, Z.S.Y., R.R. and O.B.A.; supervision, Z.S.Y., L.A. and M.N.S.A.; project administration, Z.S.Y. and L.A.; funding acquisition, Z.S.Y. and R.R. All authors have read and agreed to the published version of the manuscript.

Funding: This research was funded by Universiti Sains Malaysia Research Grant, number 1001/PBIOLOGI/855003.

Institutional Review Board Statement: The study was conducted according to the guidelines of the Declaration of Helsinki, and approved by the Institutional Ethics Committee of Universiti Sains Malaysia Animal Ethics Committee (protocol code 1001/PBIOLOGI/855003).

Informed Consent Statement: Not applicable.

Data Availability Statement: The data set presented in this study are available upon reasonable request from the corresponding author.

Acknowledgments: Funding for the study was provided by the Universiti Sains Malaysia Research University Grant (1001/PBIOLOGI/855003). We acknowledge the GST group of companies for allowing us to perform the experiments at their fish farm. Our appreciation also goes to Johari at the Scanning Electron Microscope (SEM) Unit, School of Biological Sciences, Universiti Sains Malaysia for assisting with the photography sessions.

Conflicts of Interest: All the authors declare that there is no conflict of interest in this paper.

References

1. Leaw, Y.Y.; Faizah, S.; Anil, C.; Kua, B.C. Prevalence, mean intensity and site preference of *Caligus rotundigenitalis* Yü, 1933 (Copepoda: Caligidae) on cage cultured crimson snapper (*Lutjanus erythropterus* Bloch, 1790) from Bukit Tambun, Penang, Malaysia. *Vet. Parasitol.* **2012**, *187*, 505–510. [CrossRef] [PubMed]
2. Nowak, B.F. Parasitic diseases in marine cage culture–an example of experimental evolution of parasites? *Int. J. Parasitol.* **2007**, *37*, 581–588. [CrossRef] [PubMed]
3. Maran, B.V.; Seng, L.T.; Ohtsuka, S.; Nagasawa, K. Records of Caligus (Crustacea: Copepoda: Caligidae) from marine fish cultured in floating cages in Malaysia with a redescription of the male of *Caligus longipedis* Bassett-Smith, 1898. *Zool. Stud.* **2009**, *48*, 797–807.
4. Johnson, S.C.; Blaylock, R.B.; Elphick, J.; Hyatt, K.D. Disease induced by the sea louse (*Lepeophteirus salmonis*) (Copepoda: Caligidae) in wild sockeye salmon (Oncorhynchus nerka) stocks of Alberni Inlet, British Columbia. *Can. J. Fish. Aquat. Sci.* **1996**, *53*, 2888–2897. [CrossRef]
5. See, A.W.L. Animal protection laws of Singapore and Malaysia. *Sing. J. Legal Stud.* **2013**, 125–157.
6. Mc Dermott, T.; D'Arcy, J.; Kelly, S.; Downes, J.K.; Griffin, B.; Kerr, R.F.; Ruane, N.M. Novel use of nanofiltered hyposaline water to control sea lice (*Lepeophtheirus salmonis* and *Caligus elongatus*) and amoebic gill disease, on a commercial Atlantic salmon (*Salmo salar*) farm. *Aquac. Rep.* **2021**, *20*, 100703. [CrossRef]
7. Brookson, C.B.; Krkošek, M.; Hunt, B.P.; Johnson, B.T.; Rogers, L.A.; Godwin, S.C. Differential infestation of juvenile Pacific salmon by parasitic sea lice in British Columbia, Canada. *Can. J. Fish. Aquat. Sci.* **2020**, *77*, 1960–1968. [CrossRef]
8. Ho, J.S.; Lin, C.L. Three species of Caligus Müller, 1785 (Copepoda: Caligidae) parasitic on *Caranx* spp. (Teleostei: Carangidae) off Taiwan. *Syst. Parasit.* **2007**, *68*, 33–43. [CrossRef]
9. Lin, C.L.; Ho, J.S. Two species of rare sea lice (Copepoda, Caligidae) on marine fishes of Taiwan. *J. Fish. Soc. Taiwan* **2003**, *30*, 147–158.
10. Bush, A.O.; Lafferty, K.D.; Lotz, J.M.; Shostak, A.W. Parasitology meets ecology on its own terms: Margolis et al. revisited. *J. Parasitol.* **1997**, *83*, 575–583. [CrossRef]
11. Kua, B.C.; Faizul, H. Scanning electron microscopy of three species of Caligus (Copepoda: Caligidae) parasitized on cultured marine fish at Bukit Tambun, Penang. *Malays. J. Microsc.* **2010**, *6*, 9–13.
12. Ravi, R.; Yahaya, Z.S. *Neobenedenia melleni* parasite of red snapper, *Lutjanus erythropterus*, with regression statistical analysis between fish length, temperature, and parasitic intensity in infected fish, cultured at Jerejak Island, Penang, Malaysia. *J. Parasitol. Res.* **2016**, *2016*, 1–8. [CrossRef] [PubMed]
13. Ho, J.S. Major problem of cage aquaculture in Asia relating to sea lice. In Proceedings of the 1st International Symposium on Cage Aquaculture in Asia, Pingtung, Taiwan, 2–6 November 1999.
14. Whittington, I.D.; Horton, M.A. A revision of Neobenedenia Yamaguti, 1963 (Monogenea: Capsalidae) including a redescription of *N. melleni* (MacCallum, 1927) Yamaguti, 1963. *J. Nat. Hist.* **1996**, *30*, 1113–1156. [CrossRef]
15. Yamaguti, S. Systema helminthum. Vol. IV. Monogenea and Aspidocotylea. Available online: https://www.cabdirect.org/cabdirect/abstract/19642901688 (accessed on 13 November 2021).
16. Folmer, O.; Black, M.; Hoeh, W.R.; Vrijenhoek, R.C. DNA primers for amplification of mitochondrial cytochrome c oxidase subunit I from diverse metazoan invertebrates. *Mol. Mar. Biol. Biotechnol.* **1994**, *3*, 294–299.
17. Kress, W.J.; Erickson, D.L. DNA barcodes: Methods and protocols. *Methods Mol Biol.* **2012**, *858*, 3–8. [PubMed]
18. Tajima, F.; Nei, M. Estimation of evolutionary distance between nucleotide sequences. *Mol. Biol. Evol.* **1984**, *1*, 269–285.
19. Puillandre, N.; Macpherson, E.; Lambourdière, J.; Cruaud, C.; Boisselier-Dubayle, M.C.; Samadi, S. Barcoding type specimens helps to identify synonyms and an unnamed new species in Eumunida Smith, 1883 (Decapoda: Eumunididae). *Invertebr. Syst.* **2011**, *25*, 322–333. [CrossRef]
20. Hasmi, M.F.H.A. Morphological and Phylogenetic Analysis of *Caligus* spp. Isolated from *Lates calcarifer* Cultured in Floating Net Cages in Malaysia/Muhd Faizul Helmi bin Ahamad Hasmi. Ph.D. Thesis, University of Malaya, Kuala Lumpur, Malaysia, 2013.
21. Rohde, K. *Marine Parasitology*; Csiro Publishing: Victoria, Australia, 2005.
22. Roubal, F.R.; Armitage, J.; Rohde, K. Taxonomy of Metazoan ectoparasites of snapper, *Chrysophrys autratus* (Family Sparidae), from southern Australia, eastern Australia and New Zealand. *Aust. J. Zool.* **1983**, *31*, 1–68. [CrossRef]
23. Kabata, Z. Developmental stages of *Caligus clemensi* (Copepoda: Caligidae). *J. Fish. Board Can.* **1972**, *29*, 1571–1593. [CrossRef]
24. Jones, S.R.; Prosperi-Porta, G.; Kim, E.; Callow, P.; Hargreaves, N.B. The occurrence of *Lepeophtheirus salmonis* and *Caligus clemensi* (Copepoda: Caligidae) on three-spine stickleback *Gasterosteus aculeatus* in coastal British Columbia. *J. Parasitol.* **2006**, *92*, 473–480. [CrossRef]
25. Øines, Ø.; Schram, T. Intra-or inter-specific difference in genotypes of *Caligus elongatus* Nordmann 1832? *Acta Parasitol.* **2008**, *53*, 93–105. [CrossRef]
26. Fortey, R.A.; Thomas, R.H. (Eds.) *Arthropod Relationships*; Springer Science & Business Media: Berlin/Heidelberg, Germany, 1997; Volume 55.
27. Mallatt, J.M.; Garey, J.R.; Shultz, J.W. Ecdysozoan phylogeny and Bayesian inference: First use of nearly complete 28S and 18S rRNA gene sequences to classify the arthropods and their kin. *Mol. Phylogenetics Evol.* **2004**, *31*, 178–191. [CrossRef] [PubMed]
28. Turbeville, J.M.; Pfeifer, D.M.; Field, K.G.; Raff, R.A. The phylogenetic status of arthropods, as inferred from 18S rRNA sequences. *Mol. Biol. Evol.* **1991**, *8*, 669–686. [PubMed]

29. El-Deen, N.A.; Hady, A.O.; Shalaby, S.; Zaki, M.S. Field Studies on Caligus disease among cultured *Mugil cephalus* in brackish water fish farms. *Life Sci. J.-Acta Zhengzhou Univ. Overseas Ed.* **2012**, *9*, 733–737.
30. Youssef, E.M. *Caligus lagocephali*, Pillai, 1961 (Copepoda: Caligida: Siphonostomatida) from Morone labrax (as a new host) in Suez Canal area Original. *Egypt. Vet. Med. Soc. Parasitol. J. (EVMSPJ)* **2015**, *11*, 95–98. [CrossRef]
31. Eissa, I.; Derwa, H.; El Lamie, M.; El Raziky, E. Studies on Crustacean Diseases of Seabass and White grouper fishes in Port Said Governorate. *Suez Canal Vet. Med. J. (SCVMJ)* **2016**, *21*, 143–158. [CrossRef]
32. Price, M.H.H.; Morton, A.; Reynolds, J.D. Evidence of farm-induced parasite infestations on wild juvenile salmon in multiple regions of coastal British Columbia, Canada. *Can. J. Fish. Aquat. Sci.* **2010**, *67*, 1925–1932. [CrossRef]
33. Godwin, S.C.; Krkošek, M.; Reynolds, J.D.; Rogers, L.A.; Dill, L.M. Heavy sea louse infection is associated with decreased stomach fullness in wild juvenile sockeye salmon. *Can. J. Fish. Aquat. Sci.* **2018**, *75*, 1587–1595. [CrossRef]
34. Costello, M.J. Ecology of sea lice parasitic on farmed and wild fish. *Trends Parasitol.* **2006**, *22*, 475–483. [CrossRef]
35. Rohde, K. Niche restriction in parasites: Proximate and ultimate causes. *Parasitology* **1994**, *109*, S69–S84. [CrossRef] [PubMed]

pathogens

MDPI

Article

Prevalence, Morpho-Histopathological Identification, Clinical Picture, and the Role of *Lernanthropus kroyeri* to Alleviate the Zinc Toxicity in *Moron labrax*

Attia A. Abou Zaid [1], Rehab R. Abd El Maged [2], Nesma Rasheed [3], Dina Mohamed Mansour [4], Heba H. Mahboub [5], Hany M. Abd El-Lateef [6,7], Jean-Marc Sabatier [8], Hebatallah M. Saad [9,*], Gaber El-Saber Batiha [10,*] and Michel De Waard [11,12,13]

1 Department of Aquaculture, Faculty of Aquatic and Fisheries Sciences, Kafrelsheikh University, Kafrelsheikh 33516, Egypt
2 Department of Parasitology, Animal Health Research Institute (AHRI) (Mansoura Branch), Agriculture Research Center (ARC), Giza 12618, Egypt
3 Department of Pathology, Animal Health Research Institute (AHRI) (Mansoura Branch), Agriculture Research Center (ARC), Giza 12618, Egypt
4 Department of Fish Diseases and Management, Animal Health Research Institute (AHRI), Agriculture Research Center (ARC) (Hurghada Branch), Giza 12618, Egypt
5 Department of Fish Diseases and Management, Faculty of Veterinary Medicine, Zagazig University, Zagazig 44511, Egypt
6 Department of Chemistry, College of Science, King Faisal University, Al-Ahsa 31982, Saudi Arabia
7 Department of Chemistry, Faculty of Science, Sohag University, Sohag 82524, Egypt
8 Aix-Marseille Université, Institut de Neurophysiopathologie (INP), CNRS UMR 7051, Faculté des Sciences Médicales et Paramédicales, 27 Bd Jean Moulin, 13005 Marseille, France
9 Department of Pathology, Faculty of Veterinary Medicine, Matrouh University, Marsa Matrouh 51744, Egypt
10 Department of Pharmacology and Therapeutics, Faculty of Veterinary Medicine, Damanhour University, Damanhour 22511, Egypt
11 Smartox Biotechnology, 6 rue des Platanes, 38120 Saint-Egrève, France
12 L'institut du thorax, INSERM, CNRS, UNIV NANTES, 44007 Nantes, France
13 LabEx «Ion Channels, Science & Therapeutics», Université de Nice Sophia-Antipolis, 06560 Valbonne, France
* Correspondence: heba.magdy@mau.edu.eg (H.M.S.); gaberbatiha@gmail.com (G.E.-S.B.)

Abstract: The present context is a pioneer attempt to verify the ability of copepod, *Lernanthropus kroyeri (L. kroyeri),* to uptake and accumulate heavy metals. We primarily assess the prevalence of the parasite in various seasons and its clinical signs, as well as post-mortem changes in *sea bass* (*Moron labrax*). The morphological features of the parasite using a light microscope, the bioaccumulation of heavy metals in the tissues of both *L. kroyeri* and *M. labrax* (gills, muscles) using Flame Atomic Absorption Spectrometry, and the histopathological alterations were monitored. Fish (n = 200) were obtained from Ezbet Elborg and examined for the parasite, *L. kroyeri*. The results revealed that the total infection was recorded at 86%. The infested fish exhibited excessive mucous and ulceration at the site of attachment. The post-mortem lesion in the gills revealed a marbling appearance with destructed filaments. Various heavy metals (Zn, Co, Cu, and Cd) were detected in the tissues of *L. kroyeri* and *M. labrax* and, surprisingly, *L. kroyeri* had the ability to uptake and accumulate a high amount of Zn in its tissues. Infested fish accumulated a lower concentration of Zn in their tissue compared with the non-infested ones. Within the host tissue, the accumulation of Zn was higher in the gills compared with the muscles. The histopathological findings demonstrated scattered parasitic elements with the destruction of the gill lamellae. Taken together, we highlight the potential role of *L. kroyeri* to eliminate Zn and it can be utilized as a bio-indicator for metal monitoring studies for sustaining aquaculture.

Keywords: *Moron labra*; Lernanthropus parasite; histopathology; heavy metal residues

1. Introduction

Recently, parasitic infestations have induced serious hazards, including higher mortalities and diseases, to the freshwater fish in Egypt [1,2]. Parasitic copepods are commonly present in wild and cultured marine fish [3]. Lernanthropus is the most common genus of copepods and there are more than 100 species isolated from the gills of different species of marine fish [4,5]. Lernanthropus causes the erosion and necrosis of gill filaments [6] with severe desquamation and necrosis of the secondary lamellae and leukocytic infiltration [7]. At the site of parasite attachment, there is complete superficial tissue erosion with exposure of the primary lamellar cartilage, exposure of the blood vessels, and hemorrhage resulting from the grasping action of the mandibles and the maxillae of the parasite [6].

Pollution with heavy metals or toxic pollutants in the aquatic ecosystem is a global problem, with potential concern as it can negatively affect fish with health-inducing physiological, biochemical, molecular, and histopathological alterations [8–10]. Fish absorb heavy metals from the surrounding water and accumulate in different tissues in various amounts [11]. The metals can enter the bloodstream of fish and gradually accumulate in their tissues [12,13], particularly in the hepatic tissue, where they reach the consumers through the food chain or are bio-transformed and excreted [14].

Hence, parasites, as well as heavy metals, induce serious damage to the biochemical and physiological processes that in turn induce severe impairments to the health and physiology status of fish [15]. Recent reports have addressed various methods for heavy metal chelation such as natural extracts, probiotics, and nanoparticles [13,16,17]. Fish parasites are considered extra sensitive to pollution with heavy metals, as they not only uptake and accumulate toxicants in their tissues, but also produce a physiological response to them [18]. Parasites can be used either as effective indicators or as accumulation indicators, because of the different ways in which they react to anthropogenic pollution [19,20]. There is a relationship between parasitism and pollution, and the role of parasites as bio-indicators of heavy metals pollution [21]. Previous reports have addressed the ability of some parasites to accumulate heavy metal concentrations, such as Acanthocephalans, Cestodes [22], and parasitic nematodes [23,24].

Therefore, the current investigation was carried out to assess the impacts of *L. kroyeri* infestation. We addressed the prevalence of the parasite in the different seasons, the clinical signs, and the post-mortem changes. The body surface of *L. kroyeri* using a light microscope was illustrated, besides the bioaccumulation of heavy metals in the tissues of both *L. kroyeri* and *M. labrax*. Furthermore, histopathological alterations on the gills and muscles of infected *M. labrax* were detected.

2. Materials and Methods

2.1. Research Ethics

The protocol of the current study complies with the guidelines and was carried out according to the UK Animals (Scientific Procedures) Act, 1986, and the associated guidelines of the EU Directive for Animal Experiments. The experimental procedures were approved by the Institutional Aquatic Animal Care and Use Committee (IAACUC), Faculty of Aquatic and Fisheries Sciences, Kafrelsheikh University, Kafrelsheikh, Egypt. Approval Code: IAACUC-KSU-038-2022

2.2. Fish Samples

A total number of 200 sea bass (*Moron labrax*) fish samples were collected alive or freshly dead from the market of the Ezbet-El Borg area, Damietta Province, Egypt, during the period between March 2019 until February 2020. The collected fish were transported on thick ice polyethylene bags to the laboratory of the Animal Health Research Institute, El-Mansoura Branch, where they were examined immediately.

2.3. Clinical Examination

The fish were examined for the detection of any clinical abnormalities and external parasites according to Eissa [25].

2.4. Parasitological Examination

Examination of the external surface of the fish body was carried out with naked eyes and a hand lens to detect any abnormalities, the gill opercula were removed using scissors, and the gill filaments were transferred to slides with some normal saline and then covered by a cover slide and examined microscopically [26]. The detected crustacean parasites were carefully collected using a fine brush and special needle, transferred into Petri-dish, and washed several times in distilled water then preserved in 70% ethanol and cleared in lactophenol, and then mounted with polyvol [27].

2.5. Heavy Metals Analysis

The samples were dried at 60 °C for 48 h. Then, the samples were ground to a fine powder and stored in plastic bags until analysis. One gram of each sample was dry-ashed in a muffle furnace at 450 °C for 5 h, and extracted with 20% hydrochloric acid. The samples were measured by Flame Atomic Absorption Spectrometry FAAS (GBC Avanta E, Victoria, Australia; Ser. No. A5616). All of the equipment used was calibrated and uncertainties were calculated. Internal and external quality assurance systems were applied in the Central Laboratory of Environmental Studies at Kafr-Elsheikh University according to ISO/IEC 17025 (2005). All of the measurements, blanks, triplicate measurements of elements in the extracts, and analysis of certified reference materials for each metal (Merck) were routinely included for quality control.

2.6. Histopathological Examination

Tissue specimens were collected from the gills and immediately fixed in 10% neutral buffered formalin solution for at least 24 h, then processed using the conventional paraffin embedding technique. Five-micron sections were prepared and then routinely stained with Hematoxylin and Eosin (H&E) according to Suvarna et al. [28], and then examined microscopically.

3. Results

3.1. Clinical Examination of Infected Fish

The clinical signs of the infected fish were hemorrhagic areas on different parts of the body surface (Figure 1, red arrows) and the gills showed a marbling appearance (area of redness and paleness) (Figure 1, white arrows). The gill tips were attached in some areas with mucous secretion and *L. kroyeri* was seen macroscopically as black filaments (Figure 1, black arrows).

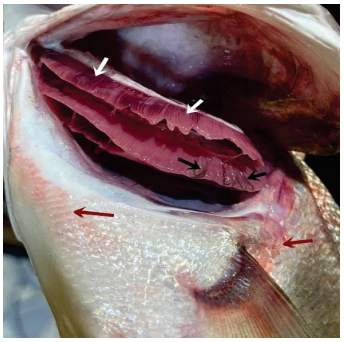

Figure 1. *Moron labrax* showing hemorrhagic areas on different parts of the body surface (red arrows), a marbling appearance (white arrows), and gill tips that were attached in some areas with mucous secretion, and the parasites were seen by naked eyes as black filaments (black arrows).

3.2. Parasitological Examination

3.2.1. Morphological Description of *L. kroyeri* Van Beneden, 1851

The parasite was found to be attached to the gills of *M. labrax*. It appeared to have a white to yellowish color in the fresh samples. The female was easily recognized by the presence of the two egg-sacs, which were clearly seen by the naked eyes (Figure 2). The bodies of isolated copepods appeared elongated in both sexes.

Figure 2. Fresh samples of the parasite, *L. kroyeri*, appeared white to yellowish color in the Petri dish. The female was easily recognized by the presence of the two egg-sacs (arrows).

The cephalothorax had a dorsal shield narrower anteriorly, and was slightly concave on the posterior margin, with rounded posterolateral corners and the anterolateral extended ventrally as prominent, rounded lobes. A deep constriction was found between the cephalothorax and pregenital trunk. There were four pairs of thoracic legs, the first one was biramous (Figure 3).

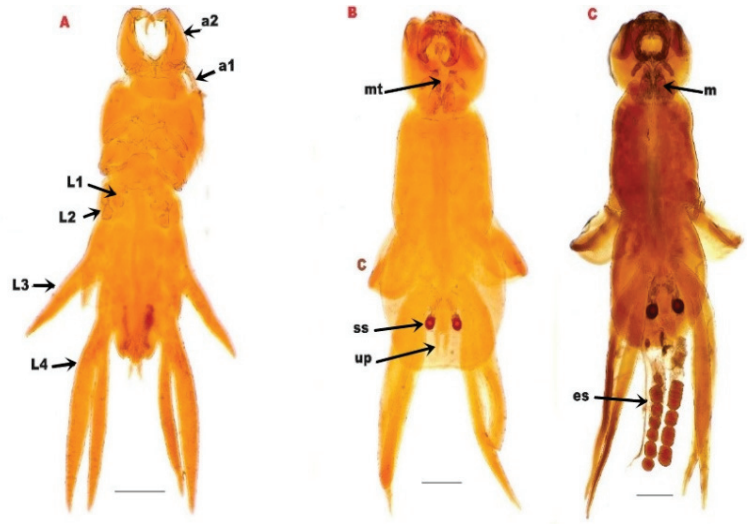

Figure 3. (**A**): *L. kroyeri* premature stage. (**B**): male *L. kroyeri*. (**C**): female *L. kroyeri*. a1; 1st antenna. a2; 2nd antenna. L1; 1st thoracic leg. L2; 2nd thoracic leg. L3; 3rd thoracic leg. L4; 4th thoracic leg. m; maxilliped. mt; mouth tube. es; egg sac. ss; spermatophore sac. up; uropod. *Scale bars = 500 µm*.

3.2.2. Prevalence of *L. kroyeri* in Infected *M. labrax*

One hundred sixty-two out of two hundred examined *M. labrax* were infected with *L. kroyeri* (81%). The highest infection was recorded during spring (94%), followed by summer (90%) and then autumn (78%), and the lowest infections were recorded in winter (31%), as depicted in Table 1 and Figure 4.

Table 1. Prevalence of *L. kroyeri* among examined *M. labrax* along the monitored season.

Winter			Spring			Summer			Autumn			Total		
Nu Ex	Nu In	%	Nu Ex	Nu In	%	Nu Ex	Nu In	%	Nu Ex	Nu In	%	Nu Ex	Nu In	%
50	31	62	50	47	94	50	45	90	50	39	78	200	162	81

Nu.Ex: number of examined *M. labrax*. Nu.In: number of infected *M. labrax*. %: Percentage of infection.

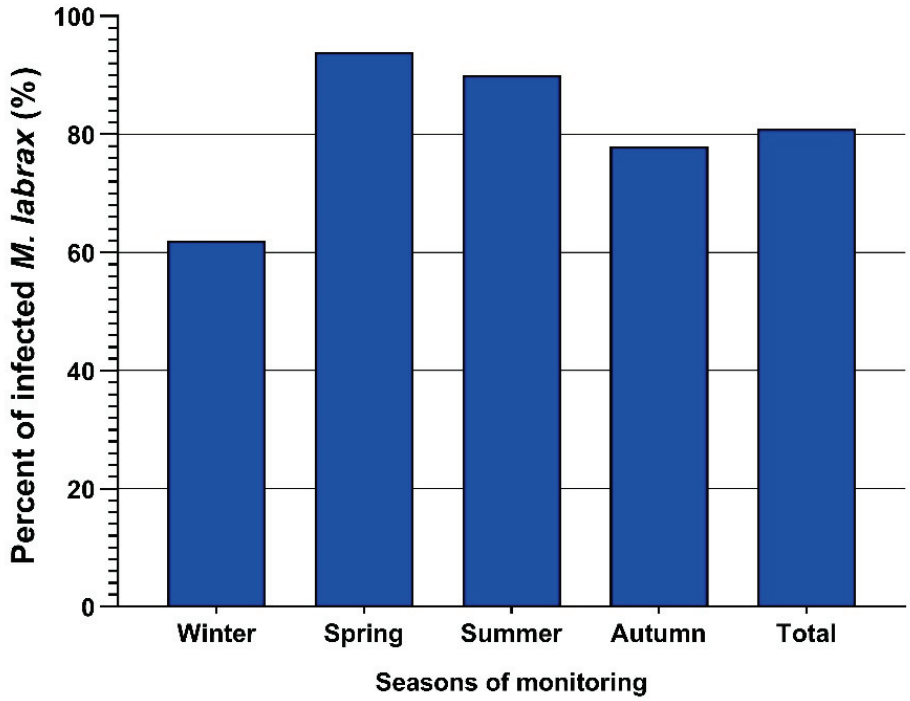

Figure 4. Seasonal prevalence of *L. kroyeri* infestation among the examined *M. lebrax* fish along the monitored seasons. Bars demonstrate the percentage of infested fish in each season.

3.2.3. Heavy Metal Accumulation by *L. kroyeri* and Fish Host

Mean ± SEM of heavy metal concentrations in the gills and muscle of both infected and non-infected fish, as well as in parasitic tissue, are illustrated in Table 2 and Figure 5. Zinc was accumulated in higher levels in the gills (374.0 ± 2.51 mg/kg) and muscles (270.5 ± 3.03 mg/kg) of non-infested fish compared with the gills (275.0 ± 3.11 mg/kg) and muscles (124.8 ± 2.15 mg/kg) of infested fish. Surprisingly, the parasite accumulated Zn in its tissue (237.5 ± 2.86 mg/kg). The differential concentration of Zn in the gills, muscle, and parasitic tissue were analyzed by an unpaired t-test, while the concentrations of other elements were recorded under the detection limit (UDL; <0.3 mg/kg for Co and Cu or <0.03 mg/kg for Cd).

Table 2. Mean of heavy metal concentration in fish tissues and parasites.

Element		Organ	Non-Infected	Infected	*p* Value
Zn	Fish	Gills	374.0 ± 2.51	275.0 ± 3.11	<0.0001
		Muscle	270.5 ± 3.03	124.8 ± 2.15	<0.0001
	Parasite		237.5 ± 2.86		
Co	Fish	Gills	UDL	UDL	-
		Muscle	UDL	UDL	-
	Parasite		UDL		
Cd	Fish	Gills	UDL	UDL	-
		Muscle	UDL	UDL	-
	Parasite		UDL		
Cu	Fish	Gills	UDL	UDL	-
		Muscle	UDL	UDL	-
	Parasite		UDL		

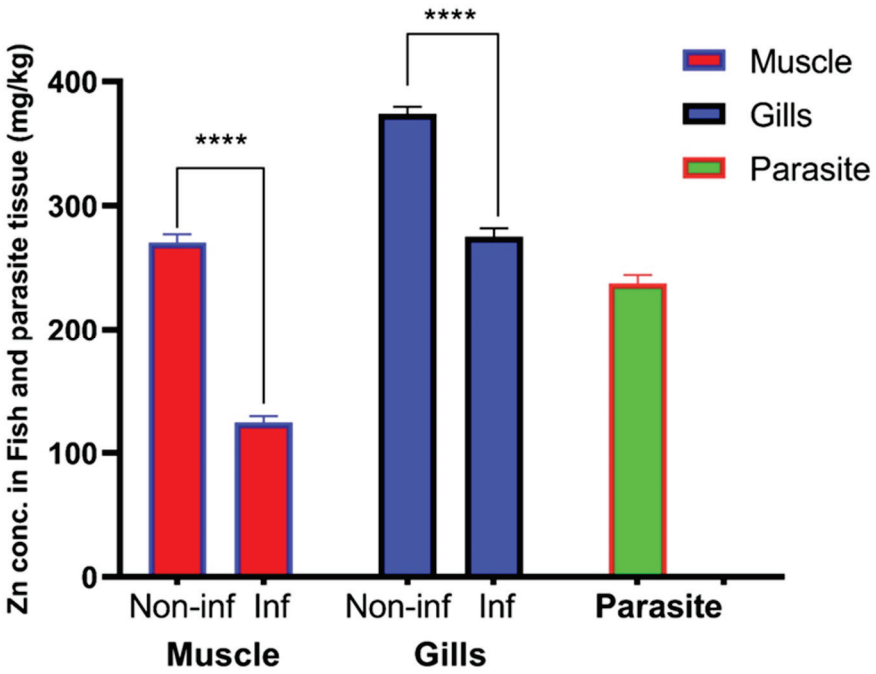

Figure 5. Mean ± SEM concentration of Zn in the gills, muscle, and parasitic tissue. (****) indicates significant differences at *p* value > 0.0001 as reported via *t*-test.

3.3. Histopathological Results

Various sections from crustacean parasitic elements randomly distributed in the gills were noticed (Figure 6A,B). The adjacent primary filaments were bent, stunted, and disorganized with the partial or complete destruction of the secondary lamellar epithelium (Figure 6A,B). Metaplasia of some surface epithelium to goblet cells was evident. Sometimes, intense hemorrhage on the gill surface, excess mucous exudate, and parasites were also observed (Figure 6C). Moreover, complete destruction of the secondary lamellar epithelium from both sides of the gill filaments leaving the primary filaments denuded could be seen (Figure 6D).

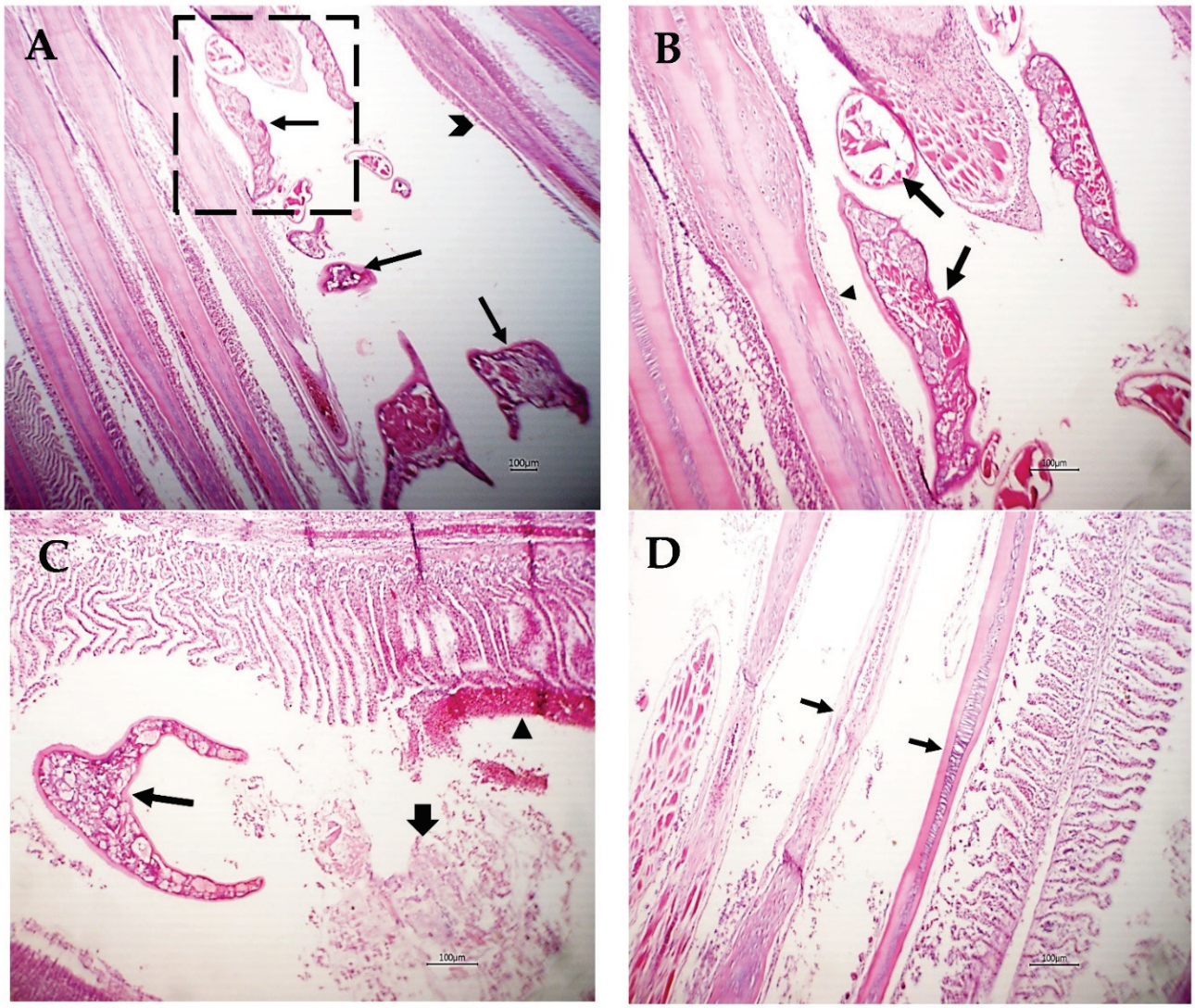

Figure 6. Photomicrograph of *M. labrax* gills stained with H&E. (**A**) Parasitic elements embedded between gill filaments (arrows) with stunted, bent, and disorganized primary filaments (arrowhead). (**B**) High power of the previous picture showing parasitic sections (arrows) with partial destruction of the lamellar epithelium (arrowhead) or metaplasia to mucus-secreting cells. (**C**) Gills showing parasitic sections (thin arrow), intense hemorrhage on the gill surface (arrowhead), and mucous exudate (thick arrow). (**D**) Gills showing denuded of primary filaments (arrow) with complete destruction of the secondary lamellae of some filaments. *Scale bar = 100 µm*.

Other gill filaments showed compensatory hyperplasia and hypertrophy of the secondary lamellar epithelium, which resulted in their fusion (Figure 7A). The blood vessels of the gill filaments and arches revealed telangiectasis beside edema in the surrounding tissue (Figure 7B). Sometimes, lymphocytes and eosinophils granular cells besides melanomacrophage cells were focally scattered in the gill filaments and arches and the sloughing of epidermal tissue of the gill arch in addition to metaplasia to the mucus secretory cells were common (Figure 7C). The gill raker had erosion of its covering epithelium besides necrosis and hyalinization of the muscles (Figure 7D).

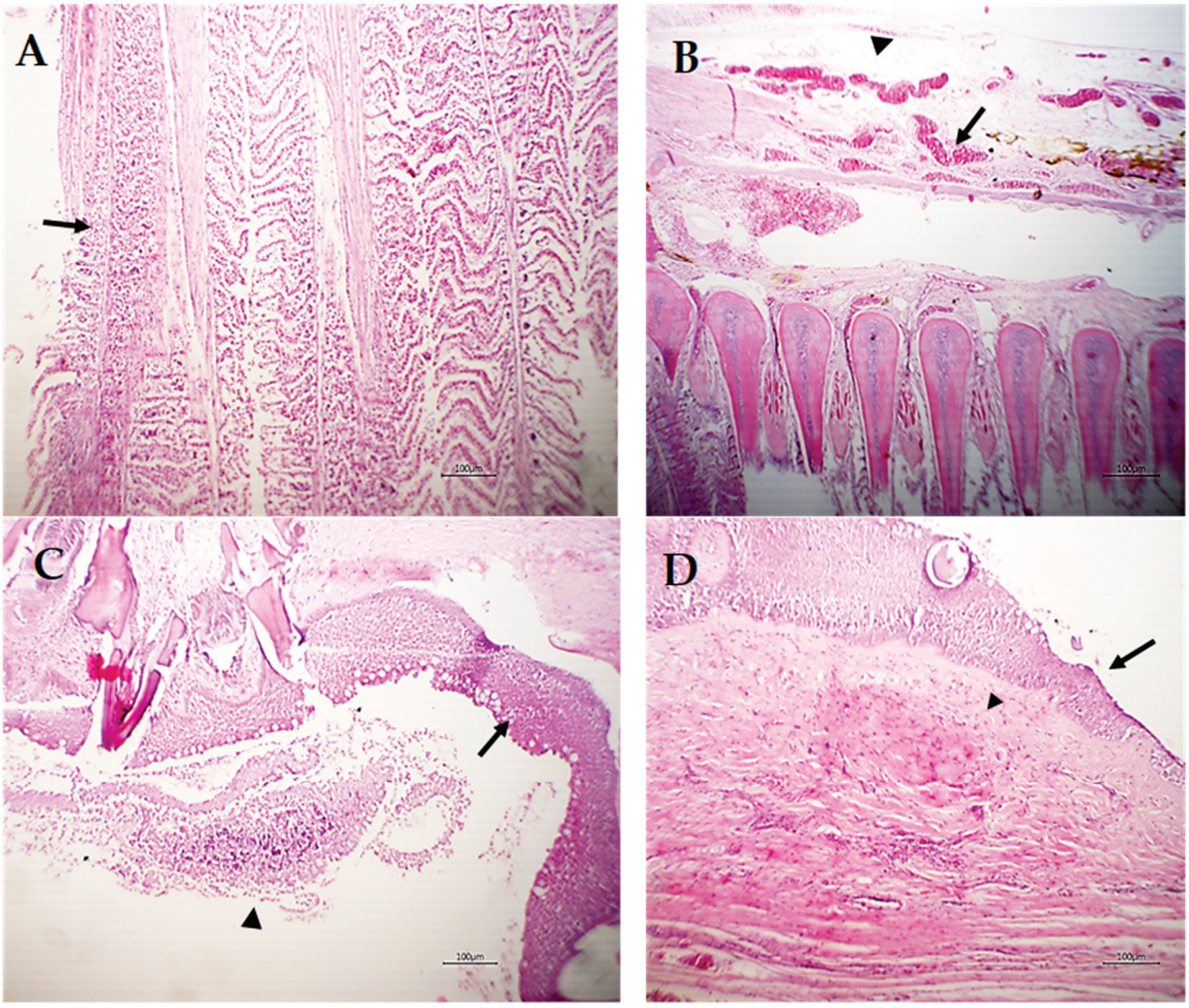

Figure 7. Photomicrograph of *M. labrax* gills stained with H&E. (**A**) Showing compensatory hyperplasia and hypertrophy of the secondary lamellar epithelium (arrow) of some adjacent gill filaments. (**B**) Gill arch showing telangiectasis of blood vessels (arrow) and edema (arrowhead). (**C**) Gill arch showing partial sloughing of the epidermal covering (arrowhead) and metaplasia of the mucus secretory cells (goblet cells) in superficial cells (arrow). (**D**) Gill raker showing erosion of the covering epithelium (arrow) with necrosis and partial hyalinization of muscles (arrowhead). *Scale bar = 100 µm.*

4. Discussion

Lernanthropus is the most common genus of parasitic copepods. There are more than 100 species described from the gills of different marine fish [5]. The current investigation revealed hemorrhagic areas on the body surface with excessive mucous secretion and a marbling appearance of the gills of infected *M. labrax* with *L. kroyeri*. These lesions could be attributed to the attachment of the parasites by their rigid claws, feeding activity, severe irritation caused by parasitic movement, and mucous increase as a defense mechanism from the host to overcome the infection, as reported by Abdel-Mawla et al. [29].

The present study recorded the isolation of *L. kroyeri* from the gills of *M. labrax*. Likewise, Toksen et al. [30], Henry et al. [31], and Eissa et al. [32] isolated the same parasite from the same host and the same site. Meanwhile, El-Deen et al. [33] and Hassanin [34] isolated *L. kroyeri* from the gills of other fish species such as *Mugil cephalus* and *Moolgarda seheli.*

In the current prospective study, the prevalence of *L. kroyeri* was 81%, concurrent with a previous study by Aneesh et al. [35] that recorded 81.4% infection of *Strongylura strongylura* by *L. kroyeri*. Additionally, Toksen [5] reported a higher infection rate (100%) by *L. kroyeri* in *Dicentrarchus labrax*. Nevertheless, Manera and Dezfuli [6] obtained a lower infection rate (35%) with *L. kroyeri* in *D. labrax*. Our paper reports that *L. kroyeri* infection was the highest during spring (94%), followed by summer (90%), then autumn (78%), and finally winter (31%). This sequence is nearly in agreement with Eissa [25], who also reported that the infection rate with *L. kroyeri* reached its maximum rate during spring and summer, while the lowest infection was recorded during autumn. These results were inconsistent with Samak and Said [36], who reported that the infection rates with the same parasite reached their maximum rates in autumn and winter (42.5% and 35%), respectively, while their minimum value was 7.5% in spring. These variances in the total infection and seasonal dynamics could be a result of the difference in fish species and the difference in the locality of fish collection.

Zn is an essential heavy metal with a permissible limit in the fish muscle of 40 mg/kg [37] or 100 mg/kg [38]. The toxic effect of zinc on aquatic animals depends on several environmental factors, especially temperature, water hardness, and dissolved oxygen concentration. An acute toxic concentration of zinc kills fish by destroying gill tissue and at a chronic toxic level, it induces stress that results in the death of fish [39]. Certain fish parasites can accumulate heavy metals at concentrations significantly higher than those in host tissues or the environment [40–44]. The data of our study revealed that there was a high concentration of Zn in the collected samples, while the concentrations of Cu, Cd, and Co were under the detection limit. In general, the accumulation of Zn was significantly higher in the non-infested tissue in comparison with the infested tissue samples. It is thought that *L. kroyeri* can absorb Zn from the fish tissue through its alimentary canal and that it accumulates in the parasite tissue, and this finding was verified by analysis of Zn in the parasite tissue. In the same manner, a recent study by Hassanine and Al-Hasawi [45] reported that acanthocephalan accumulates higher concentrations of heavy metals. Concurrent with another study, Szefer et al. [46] suggested that the bioaccumulation of parasites may reflect the higher ability of the host to clear heavy metals. In addition, Thielen et al. [44], Sures and Siddall [47], and Malek et al. [48] considered the parasites beneficial and that they could act as a heavy metal sanitizer for the host. Gills accumulated a higher Zn value compared with the edible part of its fish host. The low ratio of Zn concentration in the host muscle could be a result of the longer exposure time as metal uptake occurs faster in parasites, as stated by Sures [40].

Considering the histopathological findings, we illustrated sections of *L. kroyeri* were distributed in the gills. Similarly, a recent study by Eissa et al. [7] reported the occurrence of *L. kroyeri* fragments in the gills of *D. labrax*. The destruction of the secondary lamellar epithelium, goblet cell metaplasia with hemorrhage, and excess mucous secretion could be induced as a tissue reaction to decrease the irritation against the infestation. Concurrent with previous studies, Abdel-Mawla et al. [29], Lester and Hayward [49], Manera and Dezfuli [6], and Ragias et al. [50] reported extensive hemorrhage due to the feeding activity of this parasite. Lymphocytes and eosinophils were found in the gill filaments and arches, and these outcomes have been previously reported [4–6,51,52]. In addition, erosion of the gill raker as well as necrosis of the muscles was seen; likewise, Vinoth et al. [53] reported pale gills induced by copepod parasites due to the loss of the gill raker.

Our investigation concluded that, although *L. kroyeri* has a negative effect on the infected *M. labrax*, it also plays an important role in the elimination of heavy metals from the tissue of the infected fish through its ability to accumulate heavy metals in its body, which can be advantageous for the infected hosts, allowing them to tolerate much higher concentrations of certain metals. The present results also confirm that *L. kroyeri* seems to be a good indicator of environmental pollution.

5. Conclusions

To date, our perspective study represents a premier work to report on the efficacy of *L. kroyeri* to uptake and accumulate heavy metals (zinc). However, *L. kroyeri* infests *M. labrax* with a high prevalence in spring and summer and demonstrates excessive mucous secretion, ulceration, marbling appearance of gills, and various histopathological changes in the gills of the infested fish. By detecting various heavy metals (Zn, Co, Cu, and Cd) in the tissues of *L. kroyeri* and *M. labrax*, surprisingly, *L. kroyeri* was found to uptake the highest concentration of Zn in its tissues. Conclusively, the parasitic infestation is an eco-friendly method to uptake heavy metals, and *L. kroyeri* can be utilized as a natural antitoxic agent, as well as be considered a bio-indicator of toxicity with heavy metals and to lessen the hazardous impact on the aquatic environment for sustaining aquaculture. Future studies are needed to test the activity of other parasites to chelate heavy metals, as well as studies on various fish species.

Author Contributions: Conceptualization, A.A.A.Z., R.R.A.E.M., N.R., D.M.M., and H.H.M.; methodology, A.A.A.Z., R.R.A.E.M., N.R., D.M.M., and H.H.M.; formal analysis, A.A.A.Z., R.R.A.E.M., N.R., D.M.M., and H.H.M.; investigation, A.A.A.Z., R.R.A.E.M., N.R., D.M.M., and H.H.M.; resources, A.A.A.Z., R.R.A.E.M., N.R., D.M.M., and H.H.M.; writing—original draft preparation, A.A.A.Z., R.R.A.E.M., N.R., D.M.M., and H.H.M.; editing and responding to reviewers' comments, H.M.A.E.-L., J.-M.S., H.M.S., G.E.-S.B., and M.D.W. All authors have read and agreed to the published version of the manuscript.

Funding: M.D.W. thanks the French Agence Nationale de la Recherche and the Région Pays de la Loire for financial support on COVID-19 research (ANR Flash COVID 19 call—name: CoV2-E-TARGET—grant number: 2020 07132).

Institutional Review Board Statement: This research was reviewed and approved by the Institutional Aquatic Animal Care and Use Committee (IAACUC), Faculty of Aquatic and Fisheries Sciences, Kafrelsheikh University, Kafrelsheikh, Egypt. Approval Code: IAACUC-KSU-038-2022.

Informed Consent Statement: Not applicable.

Data Availability Statement: All data available in this manuscript.

Acknowledgments: The authors acknowledge the Deanship of Scientific Research, Vice Presidency for Graduate Studies and Scientific Research at King Faisal University, Saudi Arabia, for financial support under the annual funding track (GRANT 2136).

Conflicts of Interest: The authors declare no conflict of interest.

References

1. Mahboub, H.H.; Shaheen, A. Prevalence, diagnosis and experimental challenge of Dermocystidium sp. infection in Nile tilapia (Oreochromis niloticus) in Egypt. *Aquaculture* **2020**, *516*, 734556. [CrossRef]
2. Mahboub, H.H. Mycological and histopathological identification of potential fish pathogens in Nile tilapia. *Aquaculture* **2021**, *530*, 735849. [CrossRef]
3. Rameshkumar, G.; Ravichandran, S. Lernaeenicus sprattae (Crustacea: Copepoda) on Hemiramphus far. *Middle-East J. Sci. Res.* **2012**, *11*, 1212–1215.
4. KORUN, J.; TEPECİK, R. Gill lesions caused by infection of Lernanthropus spp. Blainville, 1822 on cultured sea bass, *Dicentrarchus labrax* (L.). *İstanbul Üniversitesi Vet. Fakültesi Derg.* **2005**, *31*, 1–8.
5. Toksen, E. Lernanthropus kroyeri van Beneden, 1851 (Crustacea: Copepoda) infections of cultured sea bass (*Dicentrarchus labrax* L.). *Bull. Eur. Assoc. Fish Pathol.* **2007**, *27*, 49.
6. Manera, M.; Dezfuli, B.S. Lernanthropus kroyeri infections in farmed sea bass Dicentrarchus labrax: Pathological features. *Dis. Aquat. Org.* **2003**, *57*, 177–180. [CrossRef]
7. Eissa, I.; Dessouki, A.; Abdel-Mawla, H.; Qorany, A. Prevalence of Lernanthropus Kroyeri in Seabass (Dicentrarchus Labrax) and spotted seabass (Dicentrarchus Punctatus) from Suez Canal, Egypt. *Int. J. Fisher. Aquat. Res* **2020**, *5*, 1–6.
8. Mbeh, G.M.; Kamga, F.T.; Kengap, A.K.; Atem, W.E.; Mbeng, L.O. Quantification of heavy metals (Cd, Pb, Fe, Mg, Cu, and Zn) in seafood (fishes and crabs) and evaluation of health risks to consumers in Limbe, Cameroon. *J. Mater. Environ. Sci.* **2019**, *10*, 948–957.

9. Abiona, O.O.; Anifowose, A.J.; Awojide, S.H.; Adebisi, O.C.; Adesina, B.T.; Ipinmoroti, M.O. Histopathological biomarking changes in the internal organs of Tilapia (Oreochromis niloticus) and catfish (Clarias gariepinus) exposed to heavy metals contamination from Dandaru pond, Ibadan, Nigeria. *J. Taibah Univ. Sci.* **2019**, *13*, 903–911. [CrossRef]
10. Abdelhiee, E.Y.; Elbialy, Z.I.; Saad, A.H.; Dawood, M.A.O.; Aboubakr, M.; El-Nagar, S.H.; El-Diasty, E.M.; Salah, A.S.; Saad, H.M.; Fadl, S.E. The impact of Moringa oleifera on the health status of Nile tilapia exposed to aflatoxicosis. *Aquaculture* **2021**, *533*, 736110. [CrossRef]
11. Mahmoud, N.E.; Alhindy, M.K.; Fahmy, M. Trypanorhynch cestodes infecting Mediterranean Sea fishes, Egypt: Callitetrarhynchus gracilis larvae (Pintner, 1931) as a bio-indicator of heavy metals pollution. *Oceanography* **2015**, *3*, 2.
12. Ismail, H.T.H.; Mahboub, H.H.H. Effect of acute exposure to nonylphenol on biochemical, hormonal, and hematological parameters and muscle tissues residues of Nile tilapia; Oreochromis niloticus. *Vet. World* **2016**, *9*, 616. [CrossRef] [PubMed]
13. Mahboub, H.H.; Beheiry, R.R.; Shahin, S.E.; Behairy, A.; Khedr, M.H.; Ibrahim, S.M.; Elshopakey, G.E.; Daoush, W.M.; Altohamy, D.E.; Ismail, T.A. Adsorptivity of mercury on magnetite nano-particles and their influences on growth, economical, hemato-biochemical, histological parameters and bioaccumulation in Nile tilapia (Oreochromis niloticus). *Aquat. Toxicol.* **2021**, *235*, 105828. [CrossRef]
14. Amini, Z.; Pazooki, J.; Abtahi, B.; Shokri, M.R. Bioaccumulation of Zn and Cu in Chasar bathybius (Gobiidae) tissue and its nematode parasite Dichelyne minutus, southeast of the Caspian Sea, Iran. *Indian J. Geo-Mar. Sci.* **2013**, *42*, 196–200.
15. Sabra, F.S.; Mehana, E.-S.E.-D. Pesticides toxicity in fish with particular reference to insecticides. *Asian J. Agric. Food Sci.* **2015**, *3*. Available online: https://www.ajouronline.com/index.php/AJAFS/article/view/2156 (accessed on 25 October 2022).
16. El-Bouhy, Z.M.; Reda, R.M.; Mahboub, H.H.; Gomaa, F.N. Bioremediation effect of pomegranate peel on subchronic mercury immunotoxicity on African catfish (Clarias gariepinus). *Environ. Sci. Pollut. Res. Int.* **2021**, *28*, 2219–2235. [CrossRef]
17. El-Bouhy, Z.M.; Reda, R.M.; Mahboub, H.H.; Gomaa, F.N. Chelation of mercury intoxication and testing different protective aspects of Lactococcus lactis probiotic in African catfish. *Aquac. Res.* **2021**, *52*, 3815–3828. [CrossRef]
18. Diamant, A. Ecology of the acanthocephalan Sclerocollum rubrimaris Schmidt and Paperna, 1978 (Rhadinorhynchidae: Gorgorhynchinae) from wild populations of rabbitfish (genus Siganus) in the northern Red Sea. *J. Fish Biol.* **1989**, *34*, 387–397. [CrossRef]
19. Sures, B.; Dezfuli, B.S.; Krug, H.F. The intestinal parasite Pomphorhynchus laevis (Acanthocephala) interferes with the uptake and accumulation of lead (210Pb) in its fish host chub (Leuciscus cephalus). *Int. J. Parasitol.* **2003**, *33*, 1617–1622. [CrossRef] [PubMed]
20. Luckenbach, T.; Triebskorn, R.; Müller, E.; Oberemm, A. Toxicity of waters from two streams to early life stages of brown trout (*Salmo trutta f. fario* L.), tested under semi-field conditions. *Chemosphere* **2001**, *45*, 571–579. [CrossRef]
21. Sures, B. How parasitism and pollution affect the physiological homeostasis of aquatic hosts. *J. Helminthol.* **2006**, *80*, 151–157. [CrossRef] [PubMed]
22. Najm, M.; Fakhar, M. Helminthic parasites as heavy metal bioindicators in aquatic ecosystems. *Med. Lab. J.* **2015**, *9*, 26–32. [CrossRef]
23. Khaleghzadeh-Ahangar, H.; Malek, M.; McKenzie, K. The parasitic nematodes Hysterothylacium sp. type MB larvae as bioindicators of lead and cadmium: A comparative study of parasite and host tissues. *Parasitology* **2011**, *138*, 1400–1405. [CrossRef] [PubMed]
24. Nachev, M.; Schertzinger, G.; Sures, B. Comparison of the metal accumulation capacity between the acanthocephalan Pomphorhynchus laevis and larval nematodes of the genus Eustrongylides sp. infecting barbel (Barbus barbus). *Parasites Vectors* **2013**, *6*, 1–8. [CrossRef]
25. Eissa, A.E. *Clinical and Laboratory Manual of Fish Diseases*; Lap Lambert Academic Publishing: Saarbrücken, Germany, 2016.
26. Lucky, Z.; Lucký, Z.k. Methods for the diagnosis of fish diseases. *Mar. Life Sci. Technol.* **1977**, *1*, 41–49.
27. Raef, A.; El-Ashram, A.; El-Sayed, N. Crustacean parasites of some cultured freshwater fish and their control in Sharkia. *Egypt. Vet. J.* **2000**, *28*, 180–191.
28. Suvarna, K.S.; Layton, C.; Bancroft, J.D. *Bancroft's Theory and Practice of Histological Techniques E-Book*; Elsevier Health Sciences: Amsterdam, The Netherlands, 2018.
29. Abdel-Mawla, H.I.; El-Lamie, M.M.; Dessouki, A.A. Investigation on ectoparasitic crustacean diseases in some Red sea fishes and their associated pathological lesions. *Benha Vet. Med. J.* **2015**, *28*, 301–309.
30. Toksen, E.; Nemli, E.; Degirmenci, U. The morphology of Lernanthropus kroyeri van Beneden, 1851 (Copepoda: Lernanthropidae) parasitic on sea bass, Dicentrarchus labrax (L., 1758), from the Aegean Sea, Turkey. *Turk. Soc. Parasitol.* **2008**, *32*, 386–389.
31. Henry, M.; Alexis, M.; Fountoulaki, E.; Nengas, I.; Rigos, G. Effects of a natural parasitical infection (Lernanthropus kroyeri) on the immune system of European sea bass, *Dicentrarchus labrax* L. *Parasite Immunol.* **2009**, *31*, 729–740. [CrossRef]
32. Eissa, I.; El-Lamie, M.; Zakai, M. Studies on Crustacean Diseases of Seabass, Morone Labrax, in Suez Canal, Ismailia Governorate. *Life Sci. J.* **2012**, *9*, 512–518.
33. El-Deen, A.N.; Mahmoud, A.; Hassan, A. Field studies of caligus parasitic infections among cultured seabass (Dicentrarchus labrax) and mullet (Mugil cephalus) in marine fish farms with emphasis on treatment trials. *Glob. Vet.* **2013**, *11*, 511–520.
34. Hassanin, D.A. Studies on prevailing problems affecting cultured marine fishes at port-said governorate. *M. Sc. Fac. Vet. Med. (Dept. Fish Dis. Manag.) Suez. Canal. Univ.* **2016**, *22*, 165–183. [CrossRef]

35. Aneesh, P.-T.; Sudha, K.; Helna, A.K.; Anilkumar, G.; Trilles, J.-P. Multiple parasitic crustacean infestation on belonid fish Strongylura strongylura. *ZooKeys* **2014**, *457*, 339–353.
36. Samak, O.A.A.; Said, A.E. Population Dynamics of the Monogeneans, Diplectanum Aequans and d. Laubieri and the Copepod, Lernanthropus Kroyeri Infesting the Gills of the Sea Bass, Dicentrarchus labrax in Egypt. *Res. Gate* **2008**, *56*, 47–50.
37. Joint FAO/WHO Expert Committee on Food Additives; Agriculture Organization of the United Nations; World Health Organization. In Proceedings of the Evaluation of Certain Food Additives and Contaminants: Thirty-Third Report of the Joint FAO/WHO Expert Committee on Food Additives, Geneva, Switzerland, 21–30 March 1989. Available online: https://apps.who.int/iris/handle/10665/39252 (accessed on 25 October 2022).
38. World Health Organization. *Lead: Environmental Aspects-Environmental Health Criteria 85*; WHO: Geneva, Switzerland, 1989.
39. Skidmore, J. Toxicity of zinc compounds to aquatic animals, with special reference to fish. *Q. Rev. Biol.* **1964**, *39*, 227–248. [CrossRef]
40. Sures, B. The use of fish parasites as bioindicators of heavy metals in aquatic ecosystems: A review. *Aquat. Ecol.* **2001**, *35*, 245–255. [CrossRef]
41. Sures, B. Accumulation of heavy metals by intestinal helminths in fish: An overview and perspective. *Parasitology* **2003**, *126*, S53–S60. [CrossRef]
42. Schludermann, C.; Konecny, R.; Laimgruber, S.; Lewis, J.; Schiemer, F.; Chovanec, A.; Sures, B. Fish macroparasites as indicators of heavy metal pollution in river sites in Austria. *Parasitology* **2003**, *126*, S61–S69. [CrossRef]
43. Tekin-Özan, S.; Kir, İ. Comparative study on the accumulation of heavy metals in different organs of tench (*Tinca tinca* L. 1758) and plerocercoids of its endoparasite Ligula intestinalis. *Parasitol. Res.* **2005**, *97*, 156–159. [CrossRef]
44. Thielen, F.; Zimmermann, S.; Baska, F.; Taraschewski, H.; Sures, B. The intestinal parasite Pomphorhynchus laevis (Acanthocephala) from barbel as a bioindicator for metal pollution in the Danube River near Budapest, Hungary. *Environ. Pollut.* **2004**, *129*, 421–429. [CrossRef]
45. Hassanine, R.; Al-Hasawi, Z. Acanthocephalan Worms Mitigate the Harmful Impacts of Heavy Metal Pollution on Their Fish Hosts. *Fishes* **2021**, *6*, 49. [CrossRef]
46. Szefer, P.; Rokicki, J.; Frelek, K.; Skóra, K.; Malinga, M. Bioaccumulation of selected trace elements in lung nematodes, Pseudalius inflexus, of harbor porpoise (Phocoena phocoena) in a Polish zone of the Baltic Sea. *Sci. Total Environ.* **1998**, *220*, 19–24. [CrossRef] [PubMed]
47. Sures, B.; Siddall, R. Pomphorhynchus laevis: The intestinal acanthocephalan as a lead sink for its fish host, chub (Leuciscus cephalus). *Exp. Parasitol.* **1999**, *93*, 66–72. [CrossRef] [PubMed]
48. Malek, M.; Haseli, M.; Mobedi, I.; Ganjali, M.; MacKenzie, K. Parasites as heavy metal bioindicators in the shark Carcharhinus dussumieri from the Persian Gulf. *Parasitology* **2007**, *134*, 1053–1056. [CrossRef] [PubMed]
49. Lester, R.J.; Hayward, C.J. Phylum arthropoda. In *Fish Diseases and Disorders. Volume 1: Protozoan and Metazoan Infections*; CABI: Wallingford, UK, 2006; pp. 466–565.
50. Ragias, V.; Tontis, D.; Athanassopoulou, F. Incidence of an intense Caligus minimus Otto 1821, C. pageti Russel, 1925, C. mugilis Brian, 1935 and C. apodus Brian, 1924 infection in lagoon cultured sea bass (*Dicentrarchus labrax* L.) in Greece. *Aquaculture* **2004**, *242*, 727–733. [CrossRef]
51. Jithendran, K.; Natarajan, M.; Azad, I. Crustacean parasites and their management in brackishwater fi nfi sh culture. *Aquac. Asia* **2008**, *13*, 1–60.
52. Yardimci, B.; Pekmezci, G.Z. Gill histopathology in cultured sea bass (*Dicentrarchus labrax* (L.) coinfected by Diplectanum aequans (Wagener, 1857) and Lernanthropus kroyeri (van Beneden, 1851). *Ank. Üniv. Vet. Fakültesi Derg.* **2012**, *59*, 61–64.
53. Vinoth, R.; Kumar, T.A.; Ravichandran, S.; Gopi, M.; Rameshkumar, G. Infestation of Copepod parasites in the food fishes of Vellar estuary, Southeast coast of India. *Acta Parasitol. Glob.* **2010**, *1*, 1–5.

pathogens

MDPI

Article

Scanning Electron Microscopy and First Molecular Data of Two Species of *Lamproglena* (Copepoda: Lernaeidae) from *Labeo victorianus* (Cyprinidae) and *Clarias gariepinus* (Clariidae) in Kenya

Nehemiah M. Rindoria [1,2,*], Zipporah Gichana [3], George N. Morara [4], Coret van Wyk [5], Willem J. Smit [1], Nico J. Smit [5,6] and Wilmien J. Luus-Powell [1]

[1] DSI-NRF SARChI Chair (Ecosystem Health), Department of Biodiversity, University of Limpopo, Private Bag X1106, Sovenga 0727, South Africa; wilmien.powell@ul.ac.za (W.J.L.-P.)
[2] Department of Biological Sciences, Kisii University, P.O. Box 408, Kisii 40200, Kenya
[3] Department of Environment, Natural Resources and Aquatic Sciences, Kisii University, P.O. Box 408, Kisii 40200, Kenya
[4] Kenya Marine and Fisheries Research Institute, P.O. Box 837, Naivasha 20117, Kenya; g_morara@yahoo.com
[5] Water Research Group, Unit for Environmental Sciences and Management, North-West University, Private Bag X6001, Potchefstroom 2520, South Africa; nico.smit@nwu.ac.za (N.J.S.)
[6] South African Institute for Aquatic Biodiversity, Makhanda 6140, South Africa
* Correspondence: mrindoria84@yahoo.com; Tel.: +254-727442299

Abstract: A parasitological study carried out in May 2022 and March 2023 in the Nyando River of Lake Victoria Basin, Kenya, disclosed two parasitic lernaeid copepods: *Lamproglena cleopatra* Humes, 1957, from the gills of a cyprinid, the Ningu *Labeo victorianus* Boulenger, 1901, endemic to the Lake Victoria drainage system, and *Lamproglena clariae* Fryer, 1957, from a clariid, the North African catfish *Clarias gariepinus* (Burchell, 1822). The copepods were studied and supplementary taxonomic information was presented using scanning electron micrographs and genetic data. Scanning electron microscopy (SEM) provided information on the morphology of *L. cleopatra*'s antennae, oral region, thoracic legs (2–5), and furcal rami not previously reported. Analyses of the partial fragments of 18S and 28S rDNA and cytochrome *c* oxidase subunit 1 (*cox*1) of the two parasites showed them to be distinct from all other *Lamproglena* taxa retrieved from GenBank. This study presents new taxonomic information on morphology using SEM and provides the first ribosomal (18S and 28S rDNA) and mitochondrial (mtDNA) data for these two parasite species. The *cox*1 data provided are the first for all 38 nominal species of *Lamproglena*. Notably, the study also provides a new host record for *L. cleopatra* and extends the geographical information of this species to Kenya.

Keywords: freshwater fish parasites; Lake Victoria Basin; mitochondrial gene; Ningu; North African catfish; Nyando River; ribosomal gene

1. Introduction

Lernaeidae Cobbold, 1879 comprises among other things the cosmopolitan parasitic freshwater copepods *Lamproglena* von Nordmann, 1832. This genus, comprising 38 nominal species, is regarded as the oldest and second-largest member of this family [1–3]. Out of the 38 valid species only 12 (31.59%) have been reported from Africa (*Lamproglena hemprichii* von Nordmann, 1832 (Zambia, Zimbabwe, Sudan, Egypt, Nigeria, Niger, and South Africa); *Lamproglena werneri* Zimmermann, 1923 (Sudan); *Lamproglena angusta* Wilson, 1924 (Egypt and Sudan); *Lamproglena monodi* Capart, 1944 (Malawi, Kenya, Zimbabwe, and Egypt); *Lamproglena wilsoni* Capart, 1956 (Sudan); *Lamproglena clariae* Fryer, 1956 (Malawi, Sudan, Zimbabwe, and South Africa); *Lamproglena elongata* Capart, 1956 (Sudan); *Lamproglena cleopatra* Humes, 1957 (Egypt and South Africa); *Lamproglena barbicola* Fryer, 1961; (South

Africa and Kenya); *Lamproglena cornuta* Fryer, 1965 (South Sudan and South Africa); *Lamproglena hoi* Dippenaar, Luus-Powell & Roux, 2001 (South Africa); and *Lamproglena hepseti* Van As & Van As, 2007 (Botswana)). Three of the African lamproglenoids have been recorded from Lake Victoria Basin, Kenya, namely *L. barbicola*, *L. monodi,* and *L. clariae* [4–7].

Humes [8] described *L. cleopatra* from the cyprinid *Labeo forskalii* Rüppell, 1835 obtained from the Giza market in Cairo, Egypt, but this fish was presumed to have come from the Nile River in Egypt. The description of Humes [8] employed the use of light microscopy (LM) with detailed line drawings of every taxonomic structure. Six decades later, Kunutu et al. [2] gave an expanded description of this lernaeid copepod from two cyprinids from South Africa (*Labeo rosae* Steindachner, 1894 from Flag Boshielo Dam and the Leaden labeo, *Labeo molybdinus* du Plessis, 1963 from Nwanedi-Luphephe Dam) and one cyprinid Silver labeo *Labeo ruddi* Boulenger, 1907 from the River Bubye in Zimbabwe. Line drawings, scanning electron micrographs, morphometric measurements of the taxonomic features of this parasite, and a key to adult females of *Lamproglena* species were also provided [2].

Fryer [5] provided the first description of *L. clariae*, a species endemic to Africa from Mudfish *Clarias anguillaris* (Linnaeus, 1758) collected from Lake Malawi. Fryer [6,9,10] recorded the same parasite from Lake Victoria, the White Nile, Lake Albert, and Lake Malawi and provided additional taxonomic features on the number of setae on the legs and furcal rami. Thurston [11], Shötter [12], and Euler and Avenant-Oldewage [13] recorded this parasite from clariid fishes in Lake George-Edward (Uganda), the Galma River (Nigeria), and the Olifants River (South Africa), respectively. Later, Marx and Avenant-Oldewage [14] provided a comprehensive redescription of morphological features using LM and scanning electron microscopy (SEM) on specimens collected from the gills of *C. gariepinus* sampled in the Olifants River in Kruger National Park, South Africa, and the Cuando River in the Caprivi Strip, Namibia.

The present study, carried out in May 2022 and March 2023 along the Nyando River of Lake Victoria Basin in Kenya, resulted in the collection of two *Lamproglena* species, *L. cleopatra* and *L. clariae*, from the gills of the cyprinid Ningu *L. victorianus* and the clariid *C. gariepinus (*the North African catfish), respectively. The study used SEM to add new taxonomic information on the morphology of *L. cleoptra* and provided the first ribosomal DNA (18S and 28S) and mitochondrial (mtDNA) genetic data for these two parasitic copepods. The study also provided a new host record and extended the geographical report for *L. cleopatra* to Kenya.

2. Materials and Methods

2.1. Sample Collection, Examination, and Identification

In May 2022 and March 2023, 34 *L. victorianus* and 2 *C. gariepinus* were collected from the Nyando River near Ahero town [15] using an Electrofisher (SAMUS 1000, Samus Special Electronics, RX 28371, China). The fish were identified using Okeyo and Ojwang's photographic guide [16]. The common names and nomenclature of fishes in this study followed FishBase [17].

Fish were killed by cervical dislocation [18] and gills were parasitologically examined in situ using a Leica Zoom 2000 Stereo microscope (model no. Z30V Shanghai, China). All female lernaeids found were removed using a Camel's hair paintbrush and identified as species of *Lamproglena* using the Boxshall and Halsey [19] key. The specific species identities were determined using the Kunutu et al. [2] key. The recovered *Lamproglena* species were transferred to 70% ethanol for morphological and 96% ethanol for molecular studies. The samples were transported to the parasitology laboratory in the Department of Biodiversity, University of Limpopo, South Africa, for further examination and analysis.

2.2. Morphological Analyses

Five specimens preserved in 70% ethanol were prepared for LM. The specimens were cleared in lactic acid for 24 h and examined with an Olympus U-DA 0C13617 compound microscope (model BX50F no. 4C05604 Olympus Optical Co., Ltd., Tokyo, Japan) fitted

with a digital camera and a drawing tube. Measurements of the body regions of the parasite were recorded (Table 1) for comparisons with previous descriptions. All measurements were expressed in millimetres (mm) unless otherwise indicated and presented as a mean with range in parentheses.

Table 1. Measurements in millimetres with mean followed by standard deviation and range in parentheses of various taxonomic features of *Lamproglena cleopatra* Humes, 1957 for the present study and comparisons with previous studies.

		Humes [8]	Kunutu et al. [2]	Present Study
Country/fish species/no. measured		Egypt: *L. forskalii* n = 5	SA: *L. rosae* and *L. molybdinus* ZIM: *L. ruddi* n = 40	KEN: *L. victorianus* n = 5
Taxonomic feature				
Total length		2.60 (2.43–2.77)	2.79 ± 0,39 (1.66–3.38)	2.71 ± 0.30 (2.41–3.20)
Cephalothorax	L	0.504	-	0.43 ± 0.07 (0.36–0.54)
	W	0.375	0.58 ± 0.07 (0.41–0.71)	0.56 ± 0.05 (0.51–0.62)
Second thoracic segment	L	-	0.28 ± 0.07 (0.16–0.41)	0.26 ± 0.05 (0.19–0.31)
	W	0.291	0.32 ± 0.05 (0.19–0.40)	0.35 ± 0.07 (0.24–0.42)
Third thoracic segment	L	-	0.38 ± 0.06 (0.15–0.48)	0.42 ± 0.07 (0.35–0.53)
	W	0.422	0.43 ± 0.08 (0.20–0.59)	0.52 ± 0.08 (0.39–0.59)
Fourth thoracic segment	L	-	0.41 ± 0.07 (0.16–0.51)	0.50 ± 0.07 (0.37–0.54
	W	0.413	0.43 ± 0.08 (0.20–0.59	0.50 ± 0.06 (0.41–0.56)
Fifth leg-bearing segment	L	-	0.09 ± 0.02 (0.06–0.14)	0.096 ± 0.02 (0.07–0.13)
	W	0.212	0.22 ± 0.03 (0.16–0.30)	0.242 ± 0.05 (0.15–0.29)
Genital segment	L	-	0.17 ± 0.03 (0.13–0.22)	0.194 ± 0.04 (0.13–0.24)
	W	0.343	0.35 ± 0.06 (0.16–0.43)	0.354 ± 0.02 (0.31–0.40)
Egg sac	L	1.32	1.22 ± 0.23 (0.92–1.46)	0.976 (n = 1)
	W	0.171	-	0.24 (n = 1)
Abdomen	L	0.975	0.96 ± 0.16 (0.56–1.22)	0.94 ± 0.13 (0.79–1.10)
	W	-	0.19 ± 0.02 (0.14–0.25)	-
% of the abdomen to total body length		37	34	34
Furcal rami	L	0.039	0.04 ± 0.01 (0.03–0.06)	0.037 (0.03–0.04)
	W	0.026		0.028 (0.02–0.03)

Abbreviations: SA, South Africa; KEN, Kenya; ZIM, Zimbabwe; -, not reported.

For SEM, four specimens fixed in 70% ethanol were prepared by dehydrating through graded ascending ethanol concentrations. The dehydration process consisted of 20 min sequential exchanges in increasing ethanol concentrations of 80%, 90%, 96%, 96%, 99.98%, and 99.98%. The samples were then dried for a 20 min sequential exchange using graded ascending series of Bis(trimethylsilyl)amine 30%, 40%, 50%, 60%, 70%, 80%, 90%, 100%, 100%, and 100% based on the procedures outlined by Nation [20] and Dos Santos et al. [21] with adjustments on the concentrations of ethanol and Bis(trimethylsilyl)amine and timing. Following this, the copepods were transferred into a glass desiccator for 24 h at room temperature and gold coated using a Quorum ™ Q150T Emscope sputter coater (Quorum Technologies Ltd., Newhaven, U.K.). The copepods were then examined using a Zeiss Sigma 500VP scanning electron microscope (Jena, Germany) at 4 kV acceleration voltages at the University of Limpopo. Photomicrographs from LM and SEM aided in the morphometric redescription of the copepods.

2.3. DNA Extraction, PCR, and Sequencing

Total genomic DNA was extracted from the isolated egg strings of two *L. cleopatra* and two *L. clariae* specimens. This was conducted using a NucleoSpin® Tissue Genomic DNA Tissue Kit (Macherey-Nagel, Düren, Germany) following the manufacturer's instructions. Two partial fragments of the 18S rDNA and 28S rDNA genes were amplified using the primer combinations 18SF (5′–AAGGTGTGMCCTATCAACT–3′) with 18SR (5′–TTACTTCCTCTAAACGCTC–3′) and 28SF (5′–ACAACTGTGATGCCCTTAG–3′) with

28SR (5′– TGGTCCGTGTTTCAAGACG–3′). The partial fragment of the cytochrome *c* oxidase subunit 1 (*cox*1) mitochondrial gene region (mtDNA) was amplified using the primer sets LCO1490 (5′–GGTCAACAAATCATAAAGTATTGG–3′) and HCO2198 (5′ TAAACTTCAGGGTGACAAAAAATCA–3′) [22]. PCR reactions were performed in a total volume of 25 µL containing 1.25 µL of each primer (10 µM), 7 µL of molecular-grade water, 12.5 µL of DreamTaqTM Hot Start Green PCR Master Mix (2X) (ThermoFisher Scientific, Waltham, Massachusetts, USA), and 3 µL of the DNA template, following the thermocycler conditions described in Song et al. [23] for the 18S and 28S rDNA genes. The thermal cycling profile for *cox*1 mtDNA had an initial denaturation of 95 °C for 5 min, followed by 37 cycles of 95 °C for 30 s, 47 °C for 30 s, 72 °C for 1 min, and final extension at 72 °C for 7 min. Successful amplification products were verified using a 1% agarose gel electrophoresis and sent for purification and sequencing to Inqaba Biotechnical Industries (Pty) Ltd. (Pretoria, South Africa).

2.4. Phylogenetic Analyses

The novel sequence data obtained were assembled and inspected using the built-in De Novo Assembly tool in Geneious Prime v2022.2. (https://www.geneious.com). The resulting consensus sequences, 18S, 28S rDNA, and *cox*1, were subjected to a Basic Local Alignment Search Tool (BLAST, https://blast.ncbi.nlm.nih.gov/Blast.cgi, accessed on 10 July 2023) [24] to identify the closest congeners. Alignments for each gene/region fragment were constructed under the default parameters of MAFFT in Geneious and trimming of the 28S alignment was performed in trimAL v.1.2. using the "*gappyout*" parameter selection under default settings to remove gaps in the alignment [25]. There were no comparable sequences in GenBank for *Lamproglena* for the *cox*1 sequences generated in this study. The species used in the phylogenetic trees are outlined in Table 2. For all the alignments the parasitic copepod *Lernea cyprinacea* Linnaeus, 1758 was selected as the outgroup. The best fitting model selected for 18S and 28S rDNA alignments according to the Akaike Information Criterion (AIC) from jModelTest v2.1.4. [26] was the GTR + I + G (general time-reversible model with invariant sites and gamma distribution) model. Maximum Likelihood (ML) analyses were computed in phyML using ATGC Montpellier Bioinformatics Platform specifying AIC criterion, model selection, and a bootstrap value of 100 (http://www.atgc-montpellier.fr/, accessed on 10 July 2023) [27]. Bayesian Inference (BI) analyses were performed in MrBayes using the CIPRES [28] computational resource. The BI analyses were generated by implementing a data block criterion running two independent Markov Chain Monte Carlo (MCMC) chains of four chains for 1 million generations. A sampling of the MCMC chain was set at every 1000th generation and a burn-in was set to the first 25% of the sample generations. Phylogenetic trees generated were visualised in FigTree v1.4.4. [29]. The uncorrected pairwise distances (*p*-distances) were estimated in MEGA 7.0 [30] and the number of base pair differences was calculated in Geneious.

Table 2. Information for the species, hosts, families, geographical localities, and accession numbers of 18S, 28S, and *cox*1 used from Lernaeidae used in molecular analyses.

Species	Host	Family	Locality	18S	28S	*cox*1	Reference
Lamproglena orientalis	*Squaliobarbus curriculus*	Xenocyprididae	Dangjiangkou Reservoir, China	DQ107552	DQ107544	—	Song et al. [2]
Lamproglena orientalis	*Chanodichthys erythropterus*	Xenocyprididae	Tangxun Lake, China	DQ107551	DQ107541		Song et al. [2]
Lamproglena orientalis	*Chanodichthys mongolicus*	Xenocyprididae	E-zhou farm, China	DQ107550	DQ107543	—	Song et al. [2]
Lamproglena orientalis	*Chanodichthys dabryi*	Xenocyprididae	Tangxun Lake, China	DQ107549	DQ107542	—	Song et al. [2]
Lamproglena hemprichii	*Hydrocynus vittatus*	Alestidae	Lake Kariba, Zimbabwe	OP277526	OP277527	—	Mabika et al. [28]
Lamproglena cleopatra Isolate UL236	*Labeo victorianus*	Cyprinidae	Nyando River, Kenya	OR242501	OR338169	—	Present study
Lamproglena cleopatra Isolate UL237	*Labeo victorianus*	Cyprinidae	Nyando River, Kenya	OR242502	OR338170	OR232207	Present study
Lamproglena clariae Isolate UL241	*Clarias gariepinus*	Clariidae	Nyando River, Kenya	OR242503	OR338195 OR338196	OR232208	Present study
Lamproglena clariae Isolate UL242	*Clarias gariepinus*	Clariidae	Nyando River, Kenya	OR242504	—	OR232209	Present study
Lamproglena monodi	*Oreochromis niloticus*	Cichlidae	Kibos Fish Farm, Kenya	ON419439	ON419422	—	Rindoria et al. [7]
Lamproglena monodi	*Oreochromis niloticus*	Cichlidae	Kibos Fish Farm, Kenya	ON419444	ON419428	—	Rindoria et al. [7]
Lamproglena monodi	*Oreochromis niloticus*	Cichlidae	Sharqia, Egypt	ON419450	ON419435	—	Rindoria et al. [7]
Lamproglena monodi	*Oreochromis niloticus*	Cichlidae	El-Minia, Egypt	ON419448	ON419432	—	Rindoria et al. [7]
Lamproglena chinensis	*Channa argus*	Channidae	Dangjiangkou Reservoir	DQ107553	DQ107545	—	Song et al. [2]
Lernea cyprinacea	*Chanodichthys erythropterus*	Xenocyprididae	Lake Dongxi, China	DQ107556	DQ107548	—	Song et al. [2]

— not available.

3. Results

A total of 20 female *L. cleopatra* occurred on the gills of 34 *Labeo victorianus.*

3.1. Taxonomic Summary

Lamproglena cleopatra Humes, 1957.
Host: *Labeo victorianus* Boulenger, 1901 (Cypriniformes: Cyprinidae).
Site of infection: Gills.
Locality/collection date: Nyando River-Ahero (Lake Victoria drainage system), Kisumu-County, Kenya (0°0′ 0°22′ S, 34°51′ E 35°11′ E), collected 10 May 2022 and 10 March 2023 by Drs. Nehemiah M. Rindoria and George N. Morara.
Materials studied: 14 specimens (5 for morphometrics, 4 for SEM, and 5 for molecular analysis).
Deposition of voucher specimens: A total of six voucher female specimens were deposited in the Helminthological Collection of the Institute of Parasitology, the Biology Centre of the Czech Academy of Sciences, České Budějovice, Czech Republic (IPCAS Cr-38).
Deposition of sequences: Sequence data obtained were deposited in GenBank: 18S rDNA (OR242501, OR242502), 28S rDNA (OR338169, OR338170), and *cox*1 (OR232207).
Redescription (Figure 1) *Female* (based on nine specimens, five morphometrics (all measurements in millimetres), and four SEM): Body elongated, slender, cylindrical, total length (excluding caudal rami) 2.71 (2.41–3.20) (Figure 1A,B). Body divided into cephalothorax, thorax, and abdomen (Figure 1A,B). Cephalothorax length 0.43 (0.36–0.54), width 0.56 (0.51–0.62), width represents 20.20% of total length, laterally indented; wider posterior part than thorax; U-shaped ridge on dorsal surface (Figure 1A,B). First thoracic segment fused with the head (Figure 1A–D). Second, third, and fourth thoracic segments free, with pedigerous segments distinct and well separated with indentations laterally (Figure 1A,B). Second segment 0.35 (0.24–0.42) wide, 0.26 (0.19–0.31) long. Third and fourth segments 0.42 (0.35–0.53) and 0.50 (0.37–0.54) long, respectively; width subequal 0.51 (0.39–0.59) and 0.50 (0.41–0.56), respectively, wider than the second segment (Figure 1A,B). Fifth thoracic segment narrower 0.24 (0.15–0.27), shorter 0.096 (0.07–0.13), bearing tiny fifth legs (Figure 1A,B,K). Genital segment free, wider 0.354 (0.31–0.40) than fifth thoracic segment, 0.19 (0.13–0.24) long, with egg sacs attached laterally (Figure 1A); other specimens with chitinous, kidney-shaped spermatophores attached ventrally (Figure 1A,B,L). Abdomen length 0.94 (0.79–1.10) (about 34.23% (29.43–37.69) of the total body length) composed of three approximately equal, poorly demarcated segments (Figure 1A,B). Furcal rami (Figure 1A,B,M,N) minute, 0.028 (0.02–0.03) wide, 0.037 (0.03–0.04) long. Each ramus with one long seta, one pore on inner and outer margins, and terminally with four setae, one blunt process, and two pores (Figure 1N). Antennules uniramous, indistinctly two-jointed with long swollen basal podomere bearing 11–14 naked setae and small distal podomere with 5 naked setae, 1 lateral and 4 terminal. Dorsal side of antennule with circular pores (Figure 1C–E). Antenna uniramous, indistinctly four-jointed, distal segment with five small terminal setae (Figure 1C–E). Oral region consisting of distinct projecting sucker-like with two lateral lobes from which arises two long setae and two finger-like posterior lobes (Figure 1C–E). Mandible not observed. Maxilla uniramous, rigid, covered with a thin layer through which distinct terminal spine projects, basal region finely granulated (Figure 1A–E). Maxilliped equipped with three roughly equal, curved claws, with a minute spine-like protrusion on the proximal part (Figure 1F). Legs 1–4 biramous, rami of legs indistinctly two-jointed. Endopodites of legs 1–4 all similar, terminating in a minute, rather blunt seta. Protopodite of legs 1–4 with one lateral long seta at the base before exopodite (Figure 1G–J). Exopodite of first leg first podomere with one smaller seta and four long terminal setae on the second podomere (Figure 1G). Second leg first exopodite podomere with one basal seta, second exopodite podomere with two small setae and a minute knob, an opening between setae and knob (Figure 1H). Second exopodite podomere of third and fourth legs with four setae: two long, one medium, one min (Figure 1I,J). Fifth leg made of small lobe with two long distal and one lateral seta (Figure 1K). Spermatophore observed (Figure 1I,L). Egg sac 0.98 × 0.24, containing about 20 eggs (19–22) (Figure 1A).

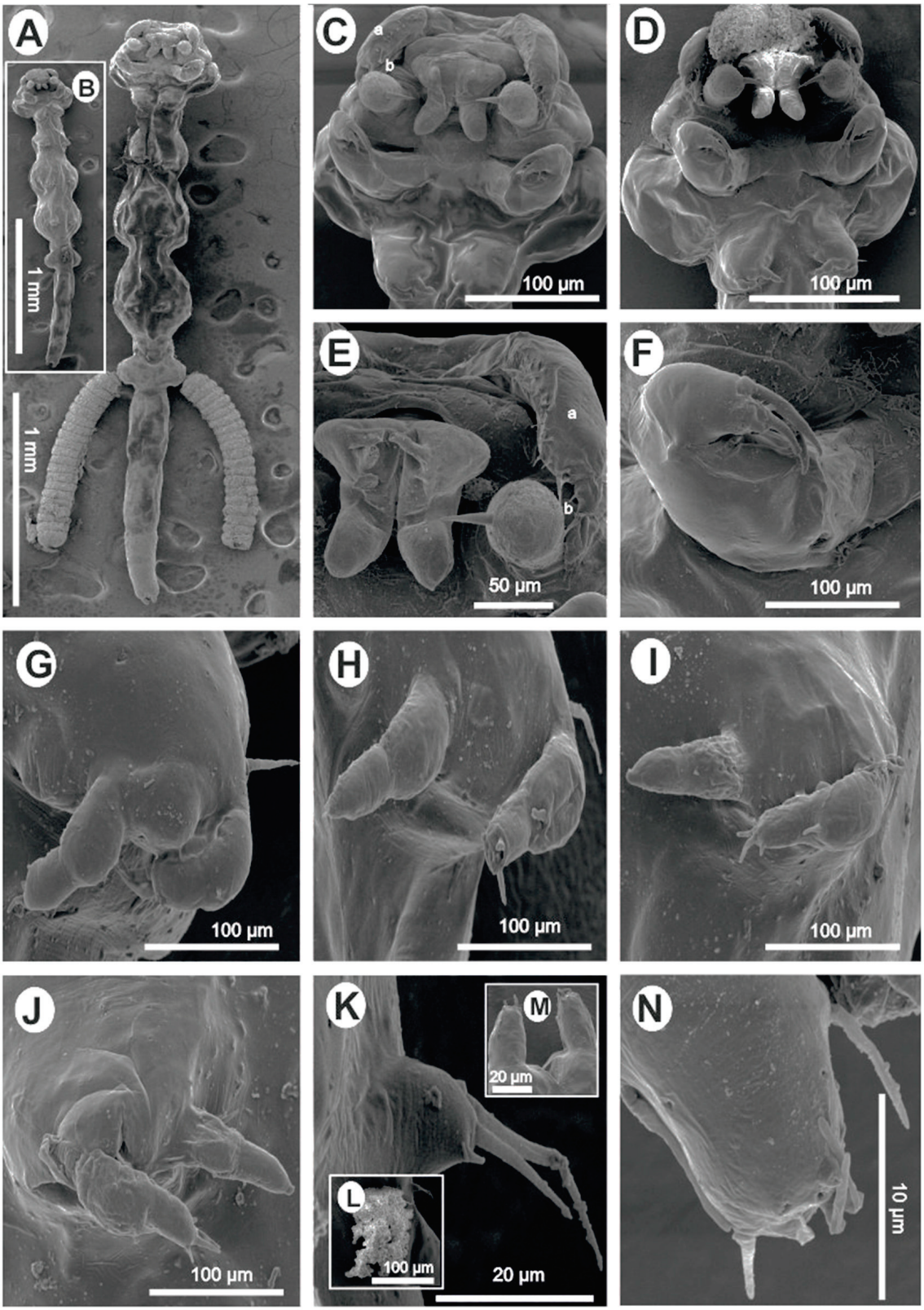

Figure 1. Scanning electron micrographs of a *Lamproglena cleopatra* Humes, 1957 female: (**A**,**B**) ventral view of the adult; (**C**–**E**) ventral view of cephalothorax showing antennules, antennae, oral region, and maxillae; (**F**) maxilliped; (**G**) first leg; (**H**) second leg; (**I**) third leg; (**J**) fourth leg; (**K**) fifth leg; (**L**) spermatophore; (**M**) furcal rami, showing the anal opening; (**N**) furcal rami. Abbreviations: a, antennules; b, antenna.

Remarks: The parasitic copepods studied here were indistinguishable from *L. cleopatra* as per the available morphological information published by Humes [8] and Kunutu et al. [2] and clearly distinct from other species of this genus. The indistinguishable features were as follows: body elongated, cylindrical and divided into a cephalothorax, thorax, and abdomen; cephalothorax broader than neck; first thoracic legs fused with the head; thoracic segments marked by lateral constrictions; indistinctly segmented abdomen; three clawed maxilliped; genital somite laterally protruding and distinctly demarcated from the rest of the thorax by a deep indent; antennule larger than antenna; biramous legs; and furcal rami with long lateral processes and terminal setae. Slight variations were noted between the present material and previous records of Humes [8] and Kunutu et al. [2], but the additional taxonomic features observed in the present material were as follows: two long setae on lateral lobes of the oral region (Figure 1C–E) and four circular pores on the furcal rami (Figure 1N).

Lamproglena clariae Fryer, 1956 (Figure 2).
Host: *Clarias gariepinus* (Burchell, 1822) (Siluriformes, Clariidae).
Site of infection: Gills.
Locality/collection date: Nyando River-Ahero (Lake Victoria drainage system), Kisumu County, Kenya (0°0′ 0°22′S, 34°51′E 35°11′E), collected 10 May 2022 and 10 March 2023 by Drs. Nehemiah M. Rindoria and George N. Morara.
Materials examined: Two specimens, one for SEM and one for molecular analysis.
Deposition of voucher specimens: Not deposited.
Deposition of sequences: Sequence data obtained were deposited in GenBank: 18S rRNA (OR242503, OR242504), 28S rRNA (OR338195, OR338196), and *cox*1 (OR232208, OR232209).
Remarks: Based on the morphological data available from the reports of Fryer [5] and Marx and Avenant-Oldewage [14], the present material was identical to *L. clariae*. Following a detailed redescription of this parasite using LM and SEM by Marx and Avenant-Oldewage [14], the present study only provided the SEM images to confirm the identity of our specimen and most importantly provided genetic sequences using 18S, 28S, and *cox*1 markers.

3.2. Molecular Identification

This study generated a total of 11 novel sequences of the three genetic markers: 5 sequences for *L. cleopatra* and 6 sequences for *L. clariae*. The Bayesian Inference and Maximum Likelihood analyses of the 18S alignment yielded similar hypotheses (nt = 1325) (Figure 3). The newly generated sequences for *L. clariae* and *L. cleopatra* fell into the clade of *Lamproglena* species previously reported from Africa with strong support. The sequences for *L. clariae* clustered together with high nodal support and formed a separate branch to the *L. monodi* clade with no nodal support. The novel sequences for *L. cleopatra* clustered together and formed a separate clade with *L. hemprichii* (OP277526) at the basal position of the African clade with no nodal support. The BI and ML analyses for the 28SrDNA dataset showed similar topologies (nt = 696) (Figure 4). A clear distinction between *Lamproglena* species from Africa and Asia clades were observed. The sequences for *L. clariae* fell at the basal position of the African clade with strong nodal support. The *L. cleopatra* sequences clustered with the *L. hemprichii* (OP277527) previously reported from Zimbabwe with strong nodal support.

The results from the analysis of the 18S and 28S rDNA haplotypes showed a distinct match with all sequences of the four *Lamproglena* species present in GenBank. There were no *cox*1 mtDNA sequences available in GenBank for this genus for species comparisons. The pairwise distances (*p*-distances) and number of base pair differences of *L. cleopatra* and *L. clariae* for small (18S) and large (28S) subunit rDNA and all sequences belonging to the Lernaeidae used in this analysis are presented in Tables 3 and 4, respectively.

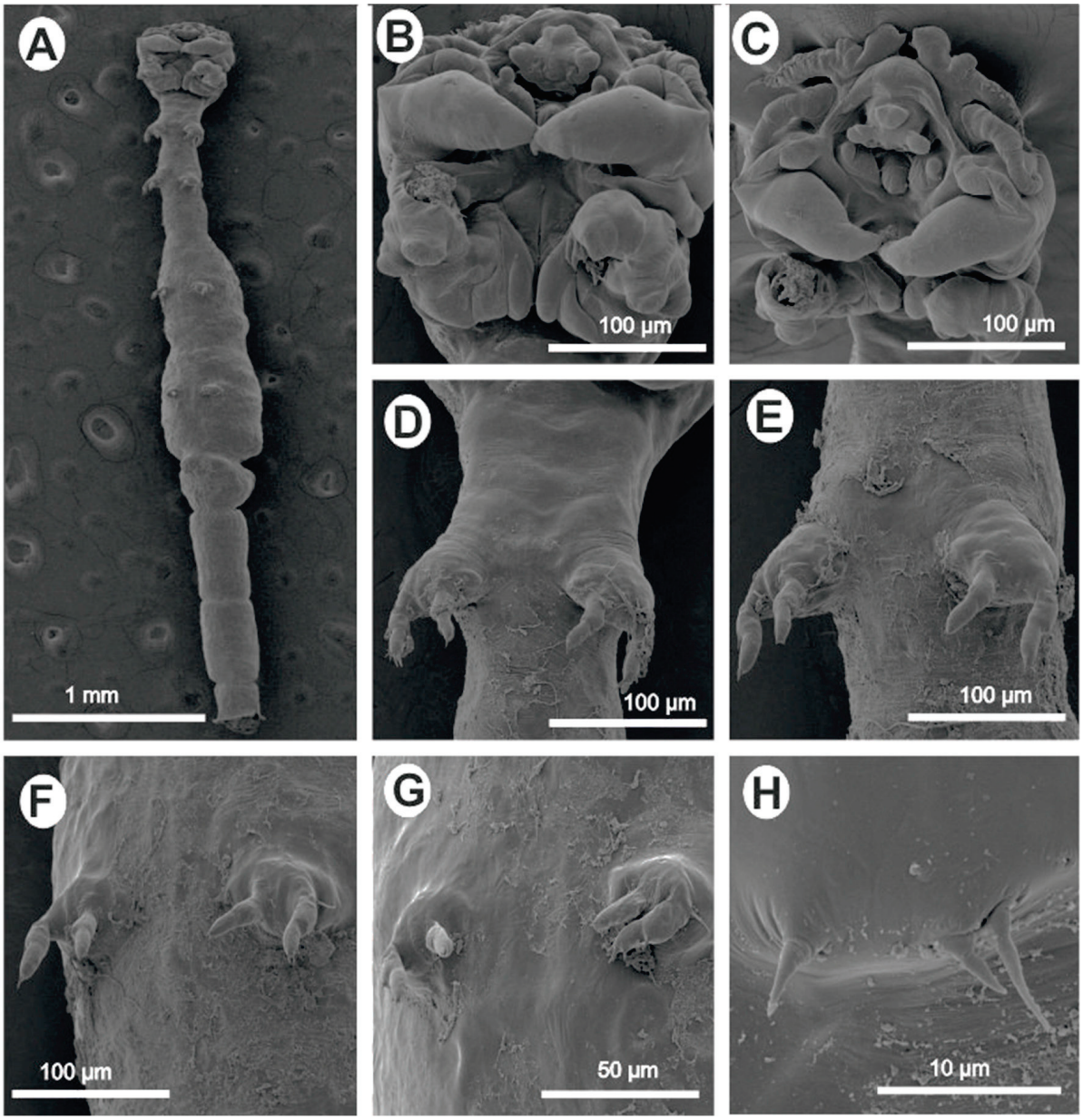

Figure 2. *Lamproglena clariae* Fryer, 1956 female: (**A**) ventral view of a mature adult; (**B**,**C**) ventral view of cephalothorax showing antennules, antennae, oral region, maxillae, and maxillipeds; (**D**) first leg; (**E**) second leg; (**F**) third leg; (**G**) fourth leg; (**H**) fifth leg.

The two copepods in the present study, *L. clariae* and *L. cleopatra*, were distinct from other *Lamproglena* species by *p*-distances of 0.9–2.1% (13–29 bp) and 0.1–2.0% (1–30 bp) based on 18S rDNA (Table 3). For the 28S rDNA, the results showed *p*-distances of 16.8–23.7% (120–167 bp) and 7.1–23.3% (46–156 bp), respectively (Table 4). The two ribosomal DNA (18S and 28S) markers produced nearly similar topologies with insignificant intraspecific branching. The unavailability of mitochondrial (*cox*1) marker sequences in GenBank made it impossible to construct any phylogeny tree; therefore, the *p*-distance and number of base pair differences are provided for *cox*1 sequences (nt = 683) generated from the present study (Table 5).

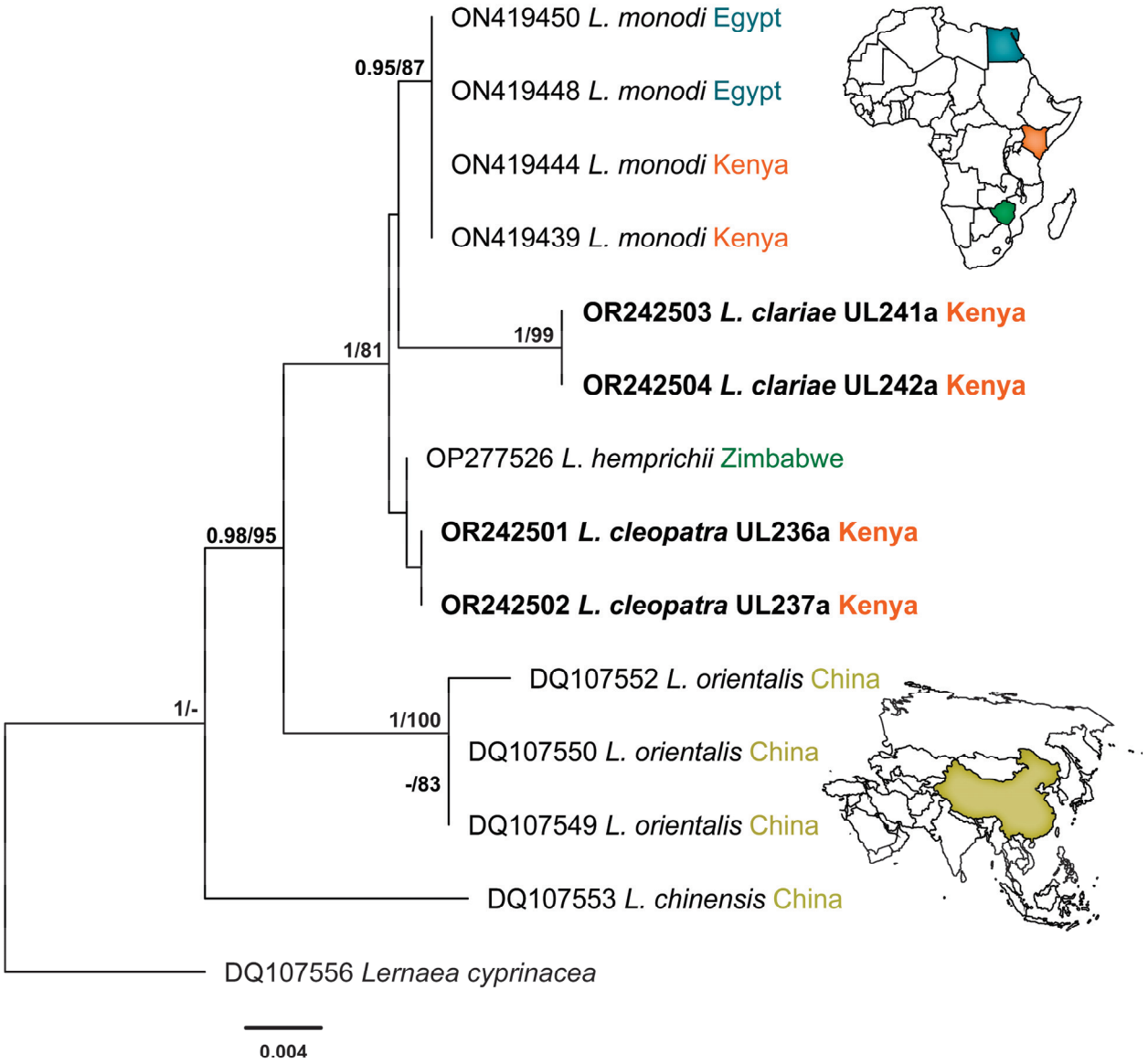

Figure 3. Phylogenetic relationship of *Lamproglena cleopatra* Humes, 1957 and *Lamproglena clariae* Fryer, 1956 to other Lernaeidae based on 18S rDNA. Phylogenies were reconstructed using Bayesian Inference (BI) and Maximum Likelihood (ML) with *Lernaea cyprinacea* designated as the outgroup. Sequences of the present study are highlighted in bold. Nodal support for BI and ML is indicated along the branch nodes (BI/ML); values < 0.90 (BI) and < 70 (ML) are not shown.

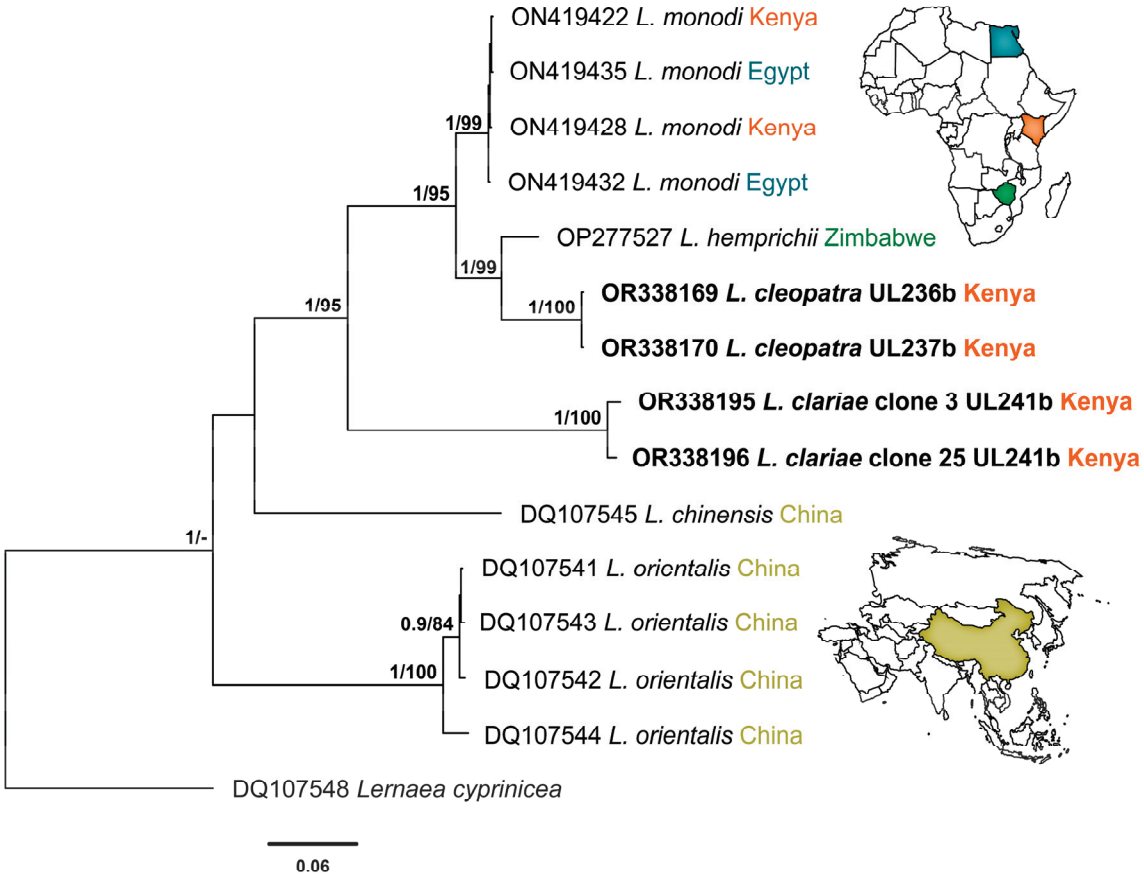

Figure 4. Phylogenetic relationship of *Lamproglena cleopatra* Humes, 1957 and *Lamproglena clariae* Fryer, 1956 to other Lernaeidae based on 28S rDNA. Phylogenies were reconstructed using Bayesian Inference (BI) and Maximum Likelihood (ML) with *Lernaea cyprinacea* designated as the outgroup. Sequences of the present study are highlighted in bold. Nodal support for BI and ML is indicated along the branch nodes (BI/ML); values < 0.90 (BI) and < 70 (ML) are not shown.

Table 3. Pairwise distances (%, unshaded diagonal) and the number of base pair differences (shaded diagonal) between *Lamproglena cleopatra* Humes, 1957, *Lamproglena clariae* Fryer, 1957, other *Lamproglena* species, and *Lernaea cyprinacea* Linnaeus, 1758 based on 18S rDNA (present study species % and base pairs are in bold).

		Accession Number	1	2	3	4	5	6	7	8	9	10	11	12	13	14
1	***L. cleopatra* UL236**	**OR242501**		**0.0**	**1.0**	**1.0**	**0.1**	**0.2**	**0.2**	**0.2**	**0.2**	**1.2**	**1.2**	**1.4**	**2.0**	**2.3**
2	***L. cleopatra* UL237**	**OR242502**	**0**		**1.0**	**1.0**	**0.1**	**0.2**	**0.2**	**0.2**	**0.2**	**1.2**	**1.2**	**1.4**	**2.0**	**2.3**
3	***L. clariae* UL241**	**OR242503**	**14**	**14**		**0.0**	**0.9**	**0.9**	**0.9**	**0.9**	**0.9**	**1.7**	**1.7**	**1.9**	**2.0**	**2.4**
4	***L. clariae* UL242**	**OR242504**	**14**	**14**	**0**		**1.0**	**1.0**	**1.0**	**1.0**	**1.0**	**1.9**	**1.9**	**1.9**	**2.1**	**2.6**
5	*L. hemprichii*	OP277526	**1**	**1**	**13**	**13**		0.3	0.3	0.3	0.3	1.1	1.1	1.4	2.0	2.4
6	*L. monodi*	ON419439	**3**	**3**	**13**	**13**	4		0.0	0.0	0.0	1.3	1.3	1.5	2.0	2.4
7	*L. monodi*	ON419444	**3**	**3**	**13**	**13**	4	0		0.0	0.0	1.3	1.3	1.5	2.0	2.4
8	*L. monodi*	ON419448	**3**	**3**	**13**	**13**	4	0	0		0.0	1.3	1.3	1.5	2.0	2.4
9	*L. monodi*	ON419450	**3**	**3**	**13**	**13**	4	0	0	0		1.3	1.3	1.5	2.0	2.4
10	*L. orientalis*	DQ107549	**16**	**16**	**24**	**24**	15	17	17	17	17		0.0	0.3	2.2	2.6
11	*L. orientalis*	DQ107550	**16**	**16**	**24**	**24**	15	17	17	17	17	0		0.3	2.2	2.6
12	*L. orientalis*	DQ107552	**19**	**19**	**26**	**25**	19	20	20	20	20	4	4		2.4	2.8
13	*L. chinensis*	DQ107553	**30**	**30**	**29**	**28**	29	29	29	29	29	32	32	35		2.5
14	*Lernaea cyprinacea*	DQ107556	**33**	**33**	**35**	**35**	34	34	34	34	34	37	37	39	38	

Table 4. Pairwise distances (%, unshaded diagonal) and the number of base pair differences (shaded diagonal) between *Lamproglena cleopatra* Humes, 1957, *Lamproglena clariae* Fryer, 1957, other *Lamproglena* species, and *Lernaea cyprinacea* Linnaeus, 1758 based on 28S rDNA (present study species % and base pairs are in bold).

		Accession Number	1	2	3	4	5	6	7	8	9	10	11	12	13	14	15
1	***L. cleopatra* UL236**	**OR338169**		**0.0**	**19.2**	**19.4**	**7.7**	**9.9**	**9.9**	**9.9**	**10.1**	**20.8**	**21.0**	**21.2**	**20.9**	**21.7**	**22.2**
2	***L. cleopatra* UL237**	**OR338170**	**0**		**20.4**	**20.4**	**7.1**	**9.1**	**9.1**	**9.1**	**9.2**	**22.4**	**22.6**	**22.7**	**22.5**	**23.3**	**23.0**
3	***L. clariae* UL241 c3**	**OR338195**	**115**	**135**		**1.3**	**18.4**	**16.8**	**16.8**	**16.8**	**16.9**	**23.5**	**23.7**	**23.5**	**23.3**	**21.1**	**24.0**
4	***L. clariae* UL242 c25**	**OR338196**	**116**	**135**	**9**		**17.9**	**16.8**	**16.8**	**16.8**	**16.9**	**23.2**	**23.4**	**23.2**	**23.0**	**20.7**	**24.0**
5	*L. hemprichii*	OP277527	**46**	**47**	**131**	**128**		6.6	6.6	6.6	6.8	19.9	20.0	20.1	19.9	19.9	22.5
6	*L. monodi*	ON419422	**59**	**60**	**120**	**120**	48		0.0	0.0	0.0	18.7	18.8	19.0	18.9	19.4	22.4

Table 4. *Cont.*

		Accession Number	1	2	3	4	5	6	7	8	9	10	11	12	13	14	15
7	*L. monodi*	ON419428	**59**	**60**	**120**	**120**	48	0		0.0	0.0	18.7	18.8	19.0	18.9	19.4	22.4
8	*L. monodi*	ON419432	**59**	**60**	**120**	**120**	48	0	0		0.0	18.7	18.8	19.0	18.9	19.4	22.4
9	*L. monodi*	ON419435	**59**	**60**	**120**	**120**	48	1	1	1		18.7	18.8	19.0	18.9	19.4	22.5
10	*L. orientalis*	DQ107541	**122**	**146**	**166**	**164**	139	131	131	131	130		0.1	0.3	2.5	21.0	22.2
11	*L. orientalis*	DQ107543	**123**	**147**	**167**	**165**	140	132	132	132	131	1		0.4	2.6	21.2	22.4
12	*L. orientalis*	DQ107542	**124**	**148**	**166**	**164**	141	133	133	133	132	2	3		2.7	21.3	22.5
13	*L. orientalis*	DQ107544	**125**	**149**	**167**	**165**	142	135	135	135	134	20	21	22		20.7	22.0
14	*L. chinensis*	DQ107545	**132**	**156**	**154**	**151**	144	141	141	141	140	151	152	153	151		22.7
15	*Lernaea cyprinacea*	DQ107548	**155**	**176**	**195**	**195**	182	183	183	183	183	181	182	183	182	180	

Table 5. Pairwise distances (%, unshaded diagonal) and the number of base pair differences (shaded diagonal) between *Lamproglena cleopatra* Humes, 1957, *Lamproglena clariae* Fryer, 1957, other *Lamproglena* species, and *Lernaea cyprinacea* Linnaeus, 1758 based on *cox*1 (present study species % and base pairs are in bold).

	Accession Number	**OR232207** ***L. cleopatra***	**OR232208** ***L. clariae***	**OR232209** ***L. clariae***	**NC 025239** ***Lernaea cyprinacea***
***L. cleopatra* UL237**	**OR232207**		**20.1**	**19.9**	26.8
***L. clariae* UL241**	**OR232208**	**137**		**0.1**	26.2
***L. clariae* UL242**	**OR232209**	**136**	**1**		26.4
Lernaea cyprinacea	NC 025239	183	179	180	

4. Discussion

In the present study, lamploglenoids collected in the Nyando River, Kenya, from *L. victorianus* and *C. gariepinus* were identified as *L. cleopatra* and *L. clariae*, respectively. To a large extent, the parasites bore resemblance to the original descriptions of *L. cleopatra* by Humes [8] and *L. clariae* by Fryer [5], respectively.

For *L. cleopatra*, the original description by Humes [8] and the redescription by Kunutu et al. [2] gave illustrations with morphological and morphometric information which forms a basis for comparison with the current study. The morphometrics given in the present study (see Table 1) are within the ranges provided by Humes [8] and Kunutu et al. [2]. It is worth noting that the present study failed to compare the SEM images provided by Kunutu et al. [2] as the images provided do not conform with the original description of Humes [8] especially on the position of the first thoracic segment. The SEM images of Kunutu et al. [2] show the first thoracic segment just after the cephalothorax, which differs from the same authors' line micrographs. The line micrographs presented by these authors are in agreement with the original description of *L. cleopatra* (see Humes [8]), which also corresponds with the morphology of the present study material (Figure 1A–D). Kunutu et al. [2] collected their study materials from three cyprinid species, *L. rosae*, *L. ruddi*, and *L. molybdinus*, from Flag Boshielo Dam, Nwanedi-Luphephe Dam, and River Bubye, respectively, the first two from South Africa and the latter from Zimbabwe, both in the Limpopo River System. We assume that the authors might have had more than one *Lamproglena* species hence the discrepancy in their line drawings and SEM images. Kunutu et al. [2] failed to provide SEM images of thoracic legs 1–4 but only provided this in the form of line micrographs, and interestingly the descriptions of the thoracic legs correspond well with the present study specimens, in which the four thoracic legs have been well illustrated (Figure 1G–J). Based on morphology, the present study recorded additional taxonomic features which were conspicuous and had not been previously recorded by Humes [8] and Kunutu et al. [2], including two long setae on lateral lobes of the oral region (Figure 1C–E) and four circular pores on the caudal region (Figure 1N).

The morphological study of the second species identified as *L. clariae* (Figure 2A–H) received little attention in the current study because Marx and Avenant-Oldewage [14] provided detailed morphological studies giving both line drawings and SEM images in addition to the original description by Fryer [5]. In this material, the present study provided an SEM image (for morphological identification) and a genetic description.

The analyses of both 18S and 28S rDNA sequence data for *L. clariae* and *L. cleopatra* proved to be distinct from all comparable Lernaeidae and the four *Lamproglena* sequences available in GenBank. Despite this, the pairwise distances calculated for all the *Lamproglena* species used in our analysis are from African 18S rDNA (0.9–1.0% 13 bp for *L. clariae* and 0.1–1.0% 1–14 bp for *L. cleopatra*) and 28S rDNA (1.3–18.4% 9–131 bp for *L. clariae* and 7.1–20.4% 46–135 bp for *L. cleopatra*). These pairwise distances from Africa suggest the conspecificity of *L. cleopatra* and *L. hemprichii*. Mabika et al. [31] noted that such a suggestion is improbable because of the distinctive morphology and host specificity of these two species (Cyprinidae and Alestidae, respectively). Rindoria et al. [7] found no variation

in the 18S rDNA gene region for *L. monodi* collected from Egypt and Kenya, confirming the marker's stability in distinguishing the taxa as also suggested by Mabika et al. [31]. For the mitochondrial marker (*cox*1), the present study was not able to construct any phylogeny tree due to the unavailability of sequences in GenBank for comparison. However, the study was able to give a comparison of *L. clariae* and *L. cleopatra* with *p*-distances (19.9–20.1%) and the number of base pair differences (136–137 bp) (Table 5), which confirms the distinctness of the two species.

Based on the results found in this study, the importance of global genetic data from the highly variant *cox*1 gene is highlighted, and more sequences need to be generated to help resolve the taxonomic position of all *Lamproglena* species. This study shows molecular advances in our knowledge of the diversity of *Lamproglena* and represents a significant milestone, as it is the first study to provide supplementary genetic data for *L. clariae* and *L. cleopatra* (the first ribosomal (18S and 28S rDNA) and the first mitochondrial (*cox*1 mtDNA) data for any of the 38 nominal species of *Lamproglena*). It also adds new taxonomic information on morphology using SEM for *L. cleopatra*. Furthermore, the study provides a new host record for *L. cleopatra* and extends the geographical information of this species to Kenya. We believe that both the morphological and molecular approaches during the classification of *Lamproglena* species are vital in expanding our understanding of their taxonomic position.

Author Contributions: Conceptualization, N.M.R. and W.J.L.-P.; methodology, N.M.R. and C.v.W.; software, N.M.R. and C.v.W.; validation, N.M.R., Z.G., G.N.M., W.J.S. and W.J.L.-P.; formal analysis, N.M.R., G.N.M. and C.v.W.; investigation, N.M.R., Z.G. and G.N.M.; resources, W.J.L.-P. and N.J.S.; data curation, N.M.R., C.v.W. and Z.G.; writing—original draft preparation, N.M.R.; writing—review and editing, N.M.R., Z.G., G.N.M., C.v.W., W.J.S., N.J.S. and W.J.L.-P.; visualization, N.M.R., Z.G. and C.v.W.; supervision, W.J.L.-P.; project administration, N.M.R. and W.J.L.-P.; funding acquisition, W.J.L.-P. All authors have read and agreed to the published version of the manuscript.

Funding: This work is based on the research supported in part by the Department of Science and Innovation and the National Research Foundation of South Africa (Grant Numbers 101054 and 146162). The funder had no role in the manuscript writing, editing, approval, or decision to publish.

Institutional Review Board Statement: The authors confirm that the ethical policies of the journal, as noted on the journal's author guidelines page, have been adhered to. No permit and ethical approval were required for this specific study as fish were collected as part of the routine aquatic research surveys of the Kenya Marine and Fisheries Research Institute (KMFRI), the government agency mandated to conduct research in fisheries and aquatic ecology of all water bodies in Kenya.

Informed Consent Statement: Not applicable.

Data Availability Statement: The data presented in this study are openly available in GenBank (accession number OR232207-OR232209; OR242501-OR242504; OR338169 and OR338170; OR338195 and OR338196) and the Helminthological Collection of the Institute of Parasitology, the Biology Centre of the Czech Academy of Sciences, České Budějovice, Czech Republic (voucher numbers IPCAS Cr-38).

Acknowledgments: The authors would like to thank Elijah M. Kembenya and his team from KMFRI-Sangoro station for their assistance during sample collections. Special thanks are given to Joan M. Maraganga and Gladys N. J. Rindoria from the Kisii University Department of Fisheries and Aquaculture and Judy K. Rindoria (Wildlife and Fisheries Research Institute—Naivasha campus) for their support in the collection and examination of the specimens in the laboratory.

Conflicts of Interest: The authors declare no conflict of interest.

References

1. Jirsa, F.; Zitek, A.; Schachner, O. First record of *Lamproglena pulchella* Nordmann, 1832 in the Pielach and Melk rivers, Austria. *J. Appl. Ichthyol.* **2006**, *22*, 404–406. [CrossRef]
2. Kunutu, K.D.; Tavakol, S.; Halajian, A.; Baker, C.; Paoletti, M.; Heckmann, R.A.; Luus-Powell, W.J. Expanded description of *Lamproglena cleopatra* Humes, 1957 (Lernaeidae: Copepoda) from *Labeo* spp. (Cyprinidae) with a key to species of *Lamproglena* von Nordmann, 1832. *Syst. Parasitol.* **2018**, *95*, 91–103. [CrossRef]

3. Piasecki, W. Comparative morphology of the three species of *Lamproglena* (Copepoda, Cyclopoida, Lernaeidae) described by von Nordmann, based on re-examination of the types. *Mitt. Zool. Mus. Berl.* **1993**, *69*, 307–315. [CrossRef]
4. Capart, A. Notes sur les Copépodes parasites. III. Copépodes parasites des poissons d'eau douce du Congo Belge. *Bull. Mus. R. Hist. Nat. Belg.* **1944**, *20*, 1–24.
5. Fryer, G. A report on the parasitic Copepoda and Branchiura of the fishes of Lake Nyasa. *Proc. Zool. Soc. Lond.* **1956**, *127*, 29–44. [CrossRef]
6. Fryer, G. The parasitic Copepoda and Branchiura of the fishes of Lake Victoria and the Victoria Nile. *Proc. Zool. Soc. Lond.* **1961**, *137*, 41–60. [CrossRef]
7. Rindoria, N.M.; Dos Santos, Q.M.; Ali, S.E.; Ibraheem, M.H.; Avenant Oldewage, A. *Lamproglena monodi* Capart, 1944 infecting *Oreochromis niloticus* (Linnaeus, 1758): Additional information on infection, morphology and genetic data. *Afr. Zool.* **2022**, *57*, 98–110. [CrossRef]
8. Humes, A.G. Two new caligoid copepods from Egyptian fishes. *J. Parasitol.* **1957**, *43*, 201–208. [CrossRef]
9. Fryer, G. Further studies on the parasitic Crustacea of African freshwater fishes. *Proc. Zool. Soc. Lond.* **1964**, *143*, 79–102.
10. Fryer, G. The parasitic Crustacea of African freshwater fishes; their biology and distribution. *J. Zool.* **1968**, *156*, 45–95. [CrossRef]
11. Thurston, P. The incidence of Monogenea and parasitic Crustacea on the gills of fish in Uganda. *Rev. Zool. Bot. Afric.* **1970**, *82*, 111–130.
12. Shotter, R.A. Copepod parasites of fishes from northern Nigeria. *Bull. I.F.A.N.* **1977**, *39*, 583–600.
13. Uler, C.; Avenant-Oldewage, A. Die biologie van verteenwoordiges van die genus *Lamproglena*. *Suid-Afrik. Tydskr. Nat. Wet. Tegnol.* **1992**, *11*, 72–73.
14. Marx, H.M.; Avenant-Oldewage, A. Redescription of *Lamproglena clariae* Fryer, 1956 (Copepoda: Lernaeidae) with notes on its occurrence and distribution. *Crustaceana* **1996**, *69*, 509–523.
15. Rindoria, N.M.; Moraa, G.N.; Smit, W.J.; Truter, M.; Smit, N.J.; Luu-Powell, W.J. Integrated morphological and molecular characterization of the fish parasitic nematode *Rhabdochona (Rhabdochona) gendrei* Campana-Rouget, 1961 infecting *Labeobarbus altianalis* (Boulenger, 1900) in Kenya. *IJP-PAW* **2023**, *21*, 201–209. [CrossRef] [PubMed]
16. Okeyo, D.O.; Ojwang, W.O. *A Photographic Guide to Freshwater Fishes of Kenya*; 2015; p. 66. Available online: www.seriouslyfish.com/publications/ (accessed on 1 March 2022).
17. Froese, R.; Pauly, D. (Eds.) *FishBase. World Wide Web Electronic Publication*; 2013. Available online: www.fishbase.org (accessed on 3 August 2022).
18. Schäperclaus, W. *Fischkrankheiten*; Akademie Verlag: Berlin, Germany, 1990.
19. Boxshall, G.A.; Halsey, S.H. *An Introduction to Copepod Diversity*; Part II; Ray Society: London, UK, 2004.
20. Nation, J.L. A new method using hexamethyldisilazane for preparation of soft insect tissues for scanning electron microscopy. *Stain Technol.* **1983**, *58*, 347–351. [CrossRef]
21. Dos Santos, Q.M.; Avenant-Oldewage, A. Soft tissue digestion of *Paradiplozoon vaalense* for SEM of sclerites and simultaneous molecular analysis. *J. Parasitol.* **2015**, *101*, 94–97. [CrossRef]
22. Folmer, O.; Black, M.; Hoeh, W.; Lutz, R.; Vrijenhoek, R. DNA primers for amplification of mitochondrial cytochrome *c* oxidase subunit I from diverse metazoan invertebrates. *Mol. Mar. Biol. Biotechnol.* **1994**, *3*, 294–299.
23. Song, Y.; Wang, G.T.; Yao, W.J.; Gao, Q.; Nei, P. Phylogeny of freshwater parasitic copepods in the Ergasilidae (Copepoda: Poecilostomatoida) based on 18S and 28S rDNA sequences. *Parasitol. Res.* **2008**, *102*, 299–306. [CrossRef]
24. Altschul, S.F.; Gish, W.; Miller, W.; Myers, E.W.; Lipman, D.J. Basic Local Alignment Search Tool. *J. Mol. Biol.* **1990**, *215*, 403–410. [CrossRef]
25. Capella-Gutiérrez, S.; Silla-Martínez, J.M.; Gabaldón, T. trimAl: A tool for automated alignment trimming in large-scale phylogenetic analyses. *Bioinformatics* **2009**, *25*, 1972–1973. [CrossRef] [PubMed]
26. Darriba, D.; Taboada, G.L.; Doallo, R.; Posada, D. jModelTest 2: More models, new heuristics and parallel computing. *Nat. Methods.* **2012**, *9*, 772. [CrossRef] [PubMed]
27. Guindon, S.; Gascuel, O. A simple, fast, and accurate algorithm to estimate large phylogenies by maximum likelihood. *Syst. Biol.* **2003**, *52*, 696–704. [CrossRef] [PubMed]
28. Miller, M.A.; Pfeiffer, W.; Schwartz, T. Creating the CIPRES Science Gateway for inference of large phylogenetic trees. In Proceedings of the 2010 Gateway Computing Environments Workshop (GCE), New Orleans, LA, USA, 14 November 2010; pp. 1–8.
29. Rambaut, A. FigTree v. 1.4. In *Molecular Evolution, Phylogenetics and Epidemiology*; University of Edinburgh, Institute of Evolutionary Biology: Edinburgh, UK, 2012. Available online: http://tree.bio.ed.ac.uk/software/figtree/ (accessed on 1 August 2022).
30. Kumar, S.; Stecher, G.; Tamura, K. MEGA7: Molecular evolutionary genetics analysis version 7.0 for bigger datasets. *Mol. Biol. Evol.* **2016**, *33*, 1870–1874. [CrossRef]
31. Mabika, N.; Barson, M.; Dos Santos, Q.M.; van Dyk, C.; Avenant-Oldewage, A. Additional Taxonomic Information for *Lamproglena hemprichii* (Copepoda: Lernaeidae) Based on Scanning Electron Microscopy and Genetic Characterization, Alongside Some Aspects of its Ecology. *Zool. Sci.* **2023**, *40*. [CrossRef]

pathogens

MDPI

Opinion

Are We Ready to Get Rid of the Terms "Chalimus" and "Preadult" in the Caligid (Crustacea: Copepoda: Caligidae) Life Cycle Nomenclature?

Wojciech Piasecki [1,*], Balu Alagar Venmathi Maran [2] and Susumu Ohtsuka [3]

[1] Institute of Marine and Environmental Sciences, University of Szczecin, ul. Adama Mickiewicza 16, 70-383 Szczecin, Poland
[2] Borneo Marine Research Institute, Universiti Malaysia Sabah, Jalan UMS, Kota Kinabalu 88400, Malaysia; bavmaran@ums.edu.my
[3] Takehara Station, Setouchi Field Science Center, Graduate School of Integrated Sciences for Life, Hiroshima University, Takehara 725-0024, Japan; ohtsuka@hiroshima-u.ac.jp
* Correspondence: wojciech.piasecki@usz.edu.pl

Abstract: In view of recent studies, we suggest that the term "preadult" should not be used in scientific reports on Copepoda parasitic on fishes as having no explicit meaning or further justification. Consequently, the term "chalimus" with its use currently restricted in the Caligidae to at most two instars in the life cycles of species of *Lepeophtheirus*, also becomes redundant. In our new understanding, both the chalimus and preadult stages should be referred to as the respective copepodid stages (II through V, in integrative terminology). The terminology for the caligid copepod life cycle thereby becomes consistent with that for the homologous stages of other podoplean copepods. We see no justification for keeping "chalimus" and "preadult" even as purely practical terms. To justify this reinterpretation, we comprehensively summarize and reinterpret the patterns of instar succession reported in previous studies on the ontogeny of caligid copepods, with special attention to the frontal filament. Key concepts are illustrated in diagrams. We conclude that, using the new integrative terminology, copepods of the family Caligidae have the following stages in their life cycles: nauplius I, nauplius II (both free-living), copepodid I (infective), copepodid II (chalimus 1), copepodid III (chalimus 2), copepodid IV (chalimus 3/preadult 1), copepodid V (chalimus 4/preadult 2), and adult (parasitic). With this admittedly polemical paper, we hope to spark a discussion about this terminological problem.

Keywords: caligid; nauplius; copepodid; chalimus; preadult; ontogeny; life cycle; larva; juvenile

1. Background of This Review

The class Copepoda, one of the most prominent taxa of the phylum Arthropoda, accommodates some 14,600 accepted species [1], and this number has been growing at a relatively fast pace. Copepods are ecologically very diverse and are almost equally represented by free-living as well as symbiotic species [2] (although this proportion may differ in most recent estimates). Many of the latter group, about 2400 valid species, are parasites of fishes [1]. Two factors indicate that this number is just the tip of the iceberg. The first is host specificity, which is usually narrow enough to allow individual fish species to have their own "private" parasite species, some of which are copepods. Less specific parasites can be found on hosts representing the same genus or a family. By the end of 2022, FishBase reported 34,900 valid fish species [3], only a small percentage of which have been examined by parasitologists. Unfortunately, the majority of those researchers have focused on internal parasites (helminths) whereas externally occurring copepods, if present, have usually been overlooked or misidentified. Consequently, thousands of species of parasitic copepods potentially remain to be discovered and described. Until

recently, progress in studies of those copepods was slow because of the limited practical effects of parasitic copepods on the economy. This situation changed with the onset of mariculture operations between the 1970s and 1990s. Formerly low-intensity infections of copepods occurring on individual fish, sparsely distributed in the ocean, received new horizons of opportunity. Crowding of fish in marine net pens provided excellent conditions for parasite transmission. The first copepods to take advantage of this situation were *Lepeophtheirus salmonis* (Krøyer, 1837) and *Caligus elongatus* von Nordmann, 1832 which began to excessively infect cultured Atlantic salmon, *Salmo salar* Linnaeus, 1758. When introduced to non-native areas (e.g., Chile), the latter fish species attracted local parasites that had earlier been unknown to science (e.g., *Caligus rogercresseyi* Boxshall et Bravo, 2000). Consumers' demand to diversify seafood products in the marketplace has broadened the range of cultured fish species, thereby lengthening the list of problematic parasites, especially externally attached copepods collectively known as sea lice that belong to the family Caligidae. Currently, 517 valid species represent the family Caligidae [1]. It should be emphasized that the caligids differ substantially from other families of the Siphonostomatoida in the extent of their sexual dimorphism. Other siphonostomatoids tend to have dwarf males, of rather limited pathological effect on the host. Both sexes are usually permanently or semi-permanently attached to the fish. Conversely, adult males and females of many caligid copepods are relatively large and free-swimming. They are capable of changing host individuals and the location on a fish. This, in turn, increases their pathogenic potential. Differences between the sexes become visible at the stage of chalimus 3 or even earlier. Massive sea lice infections, resulting in serious economic losses, were initially combatted using organophosphate compounds, but when these proved to be environmentally harmful, political decision-makers allocated substantial funds to basic research on Copepoda in the hope of developing alternative control measures. This represented a serious boost for copepod science, especially benefitting researchers who were studying sea lice biology.

For centuries, the free-living copepods and the symbiotic ones were studied in isolation, utilizing different methodologies and terminology. Notable examples of publications that have recently contributed to the standardization of copepod terminology include those by Kabata [4], Dudley [5], Huys and Boxshall [6], and Boxshall and Halsey [7], which all dealt with many aspects of copepodology but mainly focused on morphology, taxonomy, and phylogeny. We believe the time has come to integrate also the nomenclatural systems that have been applied to the ontogenetic studies of Copepoda, a goal we will pursue herein.

We were motivated to write this polemical article by a statement of Z. Kabata, one of the doyens of copepodology who wrote, "The unceasing progress of science moves in an uncoordinated manner, more often than not following the lines of least resistance, or exploiting opportunities provided by technological breakthroughs. Stimuli are indiscriminately provided to various fields of science by new concepts or theories. Rapid progress on narrow fronts leaves behind lacunae of ignorance. It is advisable, therefore, to pause occasionally and to take stock, to marshal our achievements, assess our failures, and—hopefully—plot rational paths ahead." (p. 2, [8]).

In this paper, we review all available literature on the life cycles of caligid copepods parasitic on fishes. We carefully analyze the descriptions and the terminology used. Our main goal is to understand the role and significance of some terms in relation to the most recent discoveries. Our intention is to reconcile the terminology used in ontogenetic studies on both free-living and symbiotic copepods and thereby challenge the validity of two terms: "chalimus" and "preadult", that are only used with reference to the ontogeny of certain fish-parasitic copepods.

2. Materials and Methods

The principal publications which prompted us to propose changes in the terminology of caligid life-history studies were Anstensrud [9], Ferrari and Dahms [10], Venmathi Maran

et al. [11], and Hamre et al. [12]. Those papers have indeed inspired us but they represented the traditional paradigm [9,11,12]. Ferrari and Dahms [10] opted for the reconciliatory terminology but without further discussion or explicit motion.

The introduced corrections in the accepted names of fishes were aided by the World Register of Marine Species [1].

We believe that the cited and analyzed scientific literature on the subject is complete for the past 40 years or so. We are confident to say that our literature search for other decades of the 19th and 20th centuries was also complete for the sources written in the Latin alphabet. We cannot exclude, however, that we missed some minor, unknown, and uncited sources written in a non-Latin script.

The names used for the developmental stages exhibit variability in the original literature (e.g., second chalimus, chalimus II, or chalimus 2). Therefore, in this paper, we will denote all the previously reported stages in a unified way, using Arabic numbers (e.g., chalimus 4). In the proposed new integrative nomenclature, we will use Roman numerals (e.g., copepodid V).

3. Early Studies on Caligid Ontogeny

A juvenile stage of a caligid copepod was first observed by Burmeister [13], who described a specimen collected from a mackerel captured off Helgoland in the North Sea. The copepod was relatively small and attached by "ein Fortsatz eigenthümlicher Art" [an extension of a peculiar kind] (p. 295, [13]). Burmeister described and illustrated this "extension" in detail as having a tripartite proximal part and a thread. Burmeister described his finding not only as a new species but he has also erected a new genus *Chalimus* for it. Krøyer [14] sustained the genus *Chalimus*, although not without hesitation, suggesting that it might be just a young *Caligus* and that further observations were necessary to confirm the situation. Milne-Edwards [15] repeated the information provided by Burmeister and Krøyer. Goodsir [16] observed a nauplius of a *Caligus*. Baird [17] described a nauplius of a *Caligus*, a chalimus stage, and its filament. He depicted the chalimus in dorsal view attached to an adult "*Caligus Mulleri*" [accepted as *Caligus curtus* Müller, 1785], and referred to the filament as a "rostrum". He again treated *Chalimus* as a valid genus. Müller [18], observing the molt of a chalimus into an adult, was the first to prove that *Chalimus* is a juvenile stage of a *Caligus*. Subsequent authors, such as Hesse [19] and von Nordmann [20], accepted the findings of Müller. Gadd [21] reported and illustrated a chalimus 4? of *Caligus lacustris* Steenstrup et Lütken, 1861. Scott [22] described and depicted a nauplius and a chalimus stage of *Lepeophtheirus pectoralis* (Müller, 1776) and two chalimi of *Caligus rapax* Milne Edwards, 1840. Wilson [23] devoted more than 20 pages to the ontogeny of *Caligus rapax* and *Caligus bonito* Wilson, 1905 providing a wordy description and a selection of drawings. His narrative, however, was poorly structured and was not always consistent and/or complete. He also made some reference to *Lepeophtheirus pectoralis* and *Lepeophtheirus edwardsi* Wilson, 1905 and referred to the copepodid stage as the metanauplius. Gurney [24] described and illustrated two consecutive naupliar stages and the copepodid of *Lepeophtheirus thompsoni* Baird, 1850 and four (?) chalimus stages of *Lepeophtheirus* sp. from whiting. Unfortunately, the stages were not illustrated, so their identification is not possible. Similarly, as Wilson, Gurney was uncertain about the number of chalimus stages or even copepodid stages.

4. Advanced Research on Caligid Life Cycles

Early researchers, despite their determined attitude, were not always able to record all molts, observe all stages, and correctly interpret their findings. It is also difficult to discriminate between "early studies" and "advanced research". One such "advanced" work was that of Russel [25], whose description and illustration of a new species *Caligus pageti* Russell, 1925, also covered the larval and juvenile stages. These included the nauplius and two (?) "metanauplius" (=copepodid) stages, the latter being followed by the chalimus, concerning which he wrote, "Among these there were three sizes, showing at least three moults." (p. 615, [25]). The life cycle of the same copepod species was soon

restudied by Argilas [26]. He reported the nauplius, with a series of intermediate states, the "cyclopoid stage" (=copepodid; secreting a long brown frontal cord), and the chalimus stage (undergoing numerous metamorphoses). He considered the copepodid's "rostrum", which he illustrated, to be homologous to the frontal filament of the chalimus. He also mentioned a chalimus structured like an adult but bearing a frontal cord. In 1934 Gurney [27] published an interesting paper that summarized previous ontogenetic studies on caligid copepods while also providing his own original contribution to this issue. Observing *Caligus centrodonti* Baird, 1850, he noted two nauplius stages, illustrated a molting nauplius 2, and observed a molting copepodid with extruded and attached frontal filament. In each subsequent molts Gurney observed that a "new portion" is added to the filament base. In "Stage III" he reported three bases of the filament. In "Stage IV" (male and female dealt with separately) he reported and illustrated four filament bases, lunulae, and a sternal furca. Confusingly, his illustrations referred to "chalimus" (1 through 4), whereas his descriptions referred to "stage" (I through IV). Nominally, the work of Gurney [27] constituted the first account presenting four chalimus stages, although the true identity of those stages may be debated and challenged. It now seems clear that Gurney [27], biased by his observation that the number of filament bases corresponds to the chalimus stage, missed or misinterpreted early chalimus stages. It is also evident that his "chalimus 4/stage IV" was in fact a young adult.

The first description of the life cycle of *Lepeophtheirus salmonis* (Krøyer, 1837) [now considered to consist of the two subspecies *L. salmonis salmonis* (Krøyer, 1837) and *L. salmonis oncorhynchi* Skern-Mauritzen, Torrissen et Glover, 2014] was published by White [28]. Despite its promising title, this was more of a preliminary study, in which the following developmental stages were reported: "metanauplius, (=copepodid) (p. 26, [24]), "first chalimus stage", "second chalimus stage", "several other chalimus moults", "final chalimus stage", and "numerous moults before the parasites attain their maximum size" (pp. 27–28, [28]). The "final chalimus stage" featured a marginal membrane and a filament. All stages were depicted in a dorsal view. The author was not able to obtain the nauplius.

White's article was soon followed by the treatise of Heegaard [29], who appears to be one of the very few researchers who have purposely planned a career as an expert on parasitic copepods (personal communication of Z. Kabata to WP, 1987). In his book, Heegaard included a historical review of the previous studies on the biology of Caligidae, as well as original contributions including the description of the life cycle of *Caligus curtus*. The text, however, was verbose and the results were not separated from the discussion. Some parts are confusing, multi-threaded, and difficult to follow (e.g., pp. 39–40). Nevertheless, Heegaard's [29] treatise is still the most extensive published account of caligid copepod biology and should be carefully (though in some aspects also critically) studied by students of copepodology. Heegaard included all details of his observations, even those that seemed insignificant. The presented life-cycle study included aquarium and in vitro observations of the behavior of the fish and copepods, the timing of events, and the external morphology and anatomy (including histology) of the copepod's ontogenetic stages. Heegaard described in detail all the steps in the copepod's development that he was able to observe and interpret: nauplius 1, nauplius 2, copepodid 1, copepodid 2, pupa, and 5 chalimi preceding the adult. Kabata [30] noticed that Heegaard's "pupa" stage was comparable to chalimus 1 of other species. Copepodid 1 had a rostrum that was probably used for emerging from the second naupliar cuticle and copepodid 2 was attached to a fish by means of its frontal filament. It differed from copepodid 1 in having a new frontal filament already formed within its cephalothorax. The pupa, which was also attached to its host fish by a frontal filament and additionally had a full-sized new filament visible within its body, was evidently really a chalimus 1. Heegaard's chalimus 2 was probably a chalimus 3 and his chalimus 3 was probably chalimus 4; It is likely that he missed chalimus 2. His chalimus 4 and chalimus 5, which were probably actually young adults, were both still attached to their host fish by a filament.

Kozikowska [31] studied the developmental stages of *Caligus lacustris*, the only freshwater representative of its genus, as part of a study on copepods parasitic on fishes in the estuary of the Odra/Oder River, mostly in the Polish part of the Szczecin Lagoon. The author also broadly reviewed historical references related to the collected copepods' hitherto reported host fishes and geographical distribution. Kozikowska collected *C. lacustris* from a juvenile pikeperch, "*Lucioperca lucioperca*" [accepted as *Sander lucioperca* (Linnaeus, 1758)], captured in Wicko Lake. Having a total of 14 specimens, she described and illustrated the copepodid, chalimi 1, 2, and 3, and the adult female attached by a filament. The author was probably misled by the number of filament bases, so her "chalimus 3" was probably chalimus 4 judging by its morphological advancement and the filament base structure. Similarly, her "chalimus 2" was probably chalimus 3.

Lewis's [32] work on the life cycle of *Lepeophtheirus dissimulatus* Wilson, 1905 represented a substantially more complex kind of ontogenetic study of these parasitic copepods. He not only illustrated the morphology of the successive stages but also plotted the basic morphometric data against time. His study describing and illustrating the nauplius 1, nauplius 2, copepodid, chalimus 1, chalimus 2, chalimus 3, chalimus 4, chalimus 5, chalimus 6, and adult was well organized and well structured. A special feature, presented by Lewis [32] for the first time and rarely followed in subsequent copepod life-cycle studies, was to show the ontogenetic changes of selected appendages. This approach dominated his description of the life cycle. No separate sections describing individual stages were provided; instead, the author focused his attention on the ontogenetic changes of the appendages. He also suggested that the filament can be re-attached. Ohtsuka et al. [33] and Venmathi Maran et al. [11] later revived his idea of counting the setae of the proximal segment of the antennule.

Hwa [34] studied the life history of *Caligus orientalis* Gusev, 1951. He collected developmental stages of the copepod from cultured "*Tilapia mossambica*" [accepted as *Oreochromis mossambicus* (Peters, 1852)] and determined that the life cycle consists of the following stages: nauplius 1, nauplius 2, copepodid, chalimus 1, chalimus 2, chalimus 3, chalimus 4, chalimus 5, and adult. A copepodid with an extruded filament was illustrated, as well as all other stages with details of their appendages and—something that must be emphasized—their frontal filament structure. Chalimus 5 had a marginal membrane and lunulae and its frontal filament had four extension lobes; therefore, we believe it was a young adult.

Izawa [35] studied the life cycle of *Caligus spinosus* Yamaguti, 1939 obtained from cultured yellowtail, *Seriola quinqueradiata* Temminck et Schlegel, 1845. In this important work, he distinguished, described, and illustrated the following stages: nauplius 1, nauplius 2, copepodid, chalimus 1, chalimus 2, chalimus 3, preadult 1, preadult 2, and adult. Both the first and the second preadult featured lunulae and a marginal membrane. One of the specimens of the first preadult had a frontal filament. This was the first paper to introduce the term "preadult" to denote juvenile adult specimens that are not obligatorily attached to the host by a filament. The structure of the frontal filament of this particular species was totally different from that of the filaments of other described *Caligus* species. No regularity in this respect was observed in sequential stages and it appears that the extension elements of new stages were rod-like rather than lobe-like structures. It is likely that the two preadult stages were actually young adults. The author plotted body length and width for the individual stages and, quite importantly, showed that the lengths of chalimus 3 and preadult 1 do not overlap. This gap suggests that one stage, chalimus 4, was overlooked.

Another advanced study on caligid development was that of Voth [36], who wrote a doctoral thesis on the life history of *Lepeophtheirus hospitalis* Fraser, 1920. This thesis was not officially published, but it has been widely disseminated in paper as well as electronic form. The following stages were described and illustrated: nauplius 1, nauplius 2, copepodid, chalimus 1, chalimus 2, chalimus 3, chalimus 4, chalimus 5, chalimus 6, and adult. Even though Voth knew of Izawa's paper [35], he decided not to use the term "preadult". His "fifth chalimus" and "sixth chalimus" were quite advanced morphologically, both having a sternal furca and a marginal membrane, so they may have been young adults.

An important paper by Kabata [30] became a trend-setting publication. The author was already a leading specialist of copepods parasitic on fishes, and in the cited article he not only reported on the developmental stages of *Caligus clemensi* Parker et Margolis, 1964 but also analyzed and compared the hitherto described life cycles of caligid species and created a paradigm for an ontogenetic sequence consisting of four chalimi followed by two preadults. Although Kabata described only one preadult, he concluded that he must have missed the second one in his study. He admitted, however, that his "preadult" in general appearance differed from the adult only in having "a relatively poorly developed genital complex". Kabata commented on the diversity of ontogenetic patterns in the published descriptions of known caligid life cycles, but he attributed the differences to "semantic misunderstandings". Unfortunately, Kabata did not describe or adequately illustrate the proximal filament base. In a later review paper [8], Kabata further emphasized the existence of a "preadult" phase in caligid development.

Quite soon thereafter, Boxshall [37] published a paper on the developmental stages of *Lepeophtheirus pectoralis*. He described and illustrated the following stages: nauplius 1, nauplius 2, copepodid, chalimus 1, chalimus 2, chalimus 3, chalimus 4, preadult 1, preadult 2, and adult. In the copepodid, he observed a rostrum on the frontal plate. The male preadult 1 was attached to the host by a filament while also featuring a marginal membrane and sternal furca, and the preadult 2 had no filament. Both preadult stages were morphologically advanced and differed from the adults mainly in the body proportions.

In 1979 Caillet [38] wrote a doctoral thesis on the comparative biology of two species of parasitic copepods, one of which was *Caligus minimus* Otto, 1821. He described two nauplius stages, a copepodid, and five chalimus stages, but was not able to discriminate a separate preadult stage separated by molt. The copepodid had a rostrum as well as a filament visible within the cephalothorax. Chalimi 4 and 5 had lunulae, a sternal furca, an H-suture, and a marginal membrane and were attached to the host fish by a filament. Chalimus 3 showed primordia of the H-suture and thus was probably really chalimus 4. His chalimus 1 and 2 were probably really chalimus 2 and 3, respectively, and it is possible that he missed chalimus 1 altogether. The author dedicated several figure plates to a comparison of the ontogeny of individual appendages. Although fully aware of the "preadult" described earlier by authorities like Kabata, Caillet [38], he admitted that no preadult was observed in the life cycle of *Caligus minimus*.

The work of Wootten et al. [39] was an example of the acceptance of a 10-stage life cycle (including two preadult stages) for caligids based on the examples of *Lepeophtheirus salmonis* and *Caligus elongatus* on farmed salmonids.

In a dissertation, Ben Hassine [40] presented her studies on the life cycle of *Caligus pageti*. She reported two nauplius stages, one copepodid, four chalimi, one preadult, and the adult. Her chalimus 3 was probably really chalimus 4 because of the presence of an H-suture, a frontal filament with 3(?) lobes, and lunulae visible beneath the cuticle. Her chalimus 4 with a marginal membrane and functional lunulae was probably a young adult, and it was attached by a filament with 4(?) lobes. Misled by the standing paradigm, she apparently missed chalimus 2 because her chalimus 2 with a bilobate(?) proximal end of the filament looks like chalimus 3. Her preadult 1 was clearly a more advanced young adult without a frontal filament.

The end of the 1980s and the beginning of the 1990s marked the beginning of intensive sea lice studies. Aquaculture operations for Atlantic salmon not only began to increase in numbers, but also spread to regions nonnative to *Salmo salar* (e.g., Chile, British Columbia, Tasmania, and New Zealand [41]). In some countries, previously unreported sea lice species became problematic in the aquaculture of local fish species [42]. The losses attributed to sea lice were estimated to be millions of dollars [41]. Therefore, intensive efforts were focused on finding an effective remedy for sea lice. Unfortunately, the most effective organophosphate treatment methods were quickly criticized for their adverse environmental effects. This situation resulted in the allocation of research funds to study the biology of these parasitic crustaceans in the hope of finding alternative, non-chemical treatment methods.

As a result, by the end of the 1980s and the beginning of the 1990s unprecedented numbers of papers on sea lice were published. In September 1992, the first big sea lice workshop with some 85 participants took place in Paris, France [43]. The topics discussed there included the life cycle stages, developmental factors, anatomy, behavior, epidemiology, and control of sea lice, with this last topic covering fallowing, chemotherapy, vaccination, biological control, and pathology. Around this time the most intensively targeted species were *Lepeophtheirus salmonis* and *Caligus elongatus* because of their particularly deleterious effects on salmon aquaculture.

Hogans and Trudeau [44] published a preliminary description of the life cycle of *Caligus elongatus*. They reported two naupliar stages, one copepodid, four chalimi, one preadult, and the adult, all nicely illustrated but unfortunately showing only the overall appearance of the individual stages. In all chalimus stages the frontal filament was surprisingly unnaturally short, and it supposedly became shorter in sequential stages. Their chalimus 2 was probably actually chalimus 3 because of its morphological advancement, developed H-suture, filament structure, and dramatic increase in size in relation to the preceding stage; consequently, their chalimus 3 was probably chalimus 4. Their chalimus 4 (featuring a marginal membrane) and "preadults" were definitely young adults representing two steps in morphological advancement. It is clear that these authors missed chalimus 2 altogether.

A fundamental and highly cited, but surprisingly poorly appreciated and/or understood, work was that of Anstensrud [9]. He observed that "during the ecdysis, all preadult and adult *Lepeophtheirus pectoralis* were observed attached to the host by a frontal filament." (p. 271, [9]). "Within 1–2 h, moulting is completed. After another 2–3 h, the new exoskeleton has hardened, and the newly moulted individual detaches itself from the frontal filament and can move freely on the body surface of the host." (pp. 271–272, [9]). What is also important, Anstensrud [9] illustrated the frontal organ of an adult female, which was very similar to the structure depicted by Piasecki and MacKinnon [45] for *C. elongatus* and by Ohtsuka et al. [46] for *C. undulatus* Shen et Li, 1959. This means that both the so-called preadult that up to then (and, unfortunately, also subsequently) had been reported in the life cycles of species of the genus *Lepeophtheirus*, and also the adults, need and use the filament as an indispensable element of their post-ecdysial period of life! The so-called preadults are in fact chalimi, and in light of Anstensrud's [9] findings the concept of "preadult" could no longer be sustained. Unfortunately, this brilliant copepod biologist died the same year in a tragic diving accident [47], and his important observations were effectively ignored for the next 32 years!

Bron et al. [48] studied the settlement and attachment of early stages of the salmon louse, *Lepeophtheirus salmonis*. This work was well illustrated with SEM micrographs. Describing the attachment process they stated, "Filament production must be rapidly followed by the moult to the first chalimus stage, since no copepodites were found attached by a filament." (p. 203, [48]) They also noticed that the "basal plate" used to glue the filament to the fish stains differently than the filament stem. The latter "stained similarly to the rest of the exoskeleton, indicating that might be cuticular in origin". Bron et al. [48] demonstrated the presence of an "axial duct" in the filament stem and described in detail the filament-producing apparatus. They suggested that the "axial duct" might deliver a cement substance to the distal end of the filament. The nature of the "filament duct" depicted on one of their SEM micrographs is, however, unclear.

At the beginning of the 1990s, when the intensity of the sea lice studies increased, Johnson and Albright [49,50] provided a description of the life cycle and all developmental stages of *Lepeophtheirus salmonis*. They distinguished the following stages: nauplius 1, nauplius 2, copepodid, chalimus 1, chalimus 2, chalimus 3, chalimus 4, preadult 1, preadult 2, and adult. The copepodid featured a rostrum and the preadult stages were quite advanced morphologically. They differed from the adults in their body proportions and some details of the appendage morphology.

Ogawa [51] studied the developmental stages of *Caligus longipedis* Bassett-Smith, 1898. The early stages were reared in the lab, whereas the more advanced stages were collected

from their host. The author described and illustrated the nauplius 1, nauplius 2, copepodid, chalimus 1, chalimus 2, chalimus 3, chalimus 4, preadult, and adult. The preadult had lunulae and a marginal membrane and it was attached by a filament. The author stated that the preadult differed from the adult in having a thinner cuticle and a poorly developed genital complex; we interpret this stage as a young adult.

In the proceedings of the 1992 Paris Sea Lice conference [43], three papers dealt with life cycles and or developmental stages, namely Lin and Ho [52], Kim [53], and Schram [54]. Lin and Ho [52] studied the ontogeny of *Caligus epidemicus* Hewitt, 1971 parasitic on tilapia (*Oreochromis mossambicus*) cultured in brackish water. They observed and described a record high number of stages: nauplius 1, nauplius 2, copepodid, chalimus 1, chalimus 2, chalimus 3, chalimus 4, chalimus 5, chalimus 6, preadult, and adult. Unfortunately, the stages were not illustrated, and this account should, therefore, be considered preliminary. Kim [53] described and illustrated the nauplius 1, nauplius 2, copepodid, chalimus 1, chalimus 2, chalimus 3, chalimus 4, and adult of *Caligus punctatus* Shiino, 1955 collected from "*Chaenogobius castaneus*" [accepted as *Gymnogobius castaneus* (O'Shaughnessy, 1875)] in Korea. Some young adults were attached by a filament but Kim [53] refrained from discussing the number of developmental stages in the Caligidae. Schram [54] probably worked concurrently with but independently of Johnson and Albright [49,50] in another attempt to determine the life cycle of *Lepeophtheirus salmonis*. He was late in publishing, however, and his paper's title ("Supplementary descriptions . . . ") acknowledged Johnson and Albright's priority. Schram's [54] description was nonetheless of high quality and his illustrations (including SEM) were supreme. Acknowledging the standing paradigm of Kabata [30], Schram listed the following stages: nauplius 1, nauplius 2, copepodid, chalimus 1, chalimus 2, chalimus 3, chalimus 4, preadult 1, preadult 2, and adult. He noted, however, that the two preadult stages differed from the adult only in the relative proportions of the genital complex.

Other important papers in the proceedings of the 1992 Paris Sea Lice conference [43] were those of Pike et al. [55,56] on the ultrastructure of the frontal filament in chalimus stages of *Caligus elongatus* and *Lepeophtheirus salmonis* from Atlantic salmon. Using TEM, they effectively described and compared the inner structure of the filament while, however, disregarding the changes in the filament structure of *Caligus elongatus* that occur during the course of its ontogeny. One of their papers [56] also contains some SEM micrographs, although Figure 3 in that work is either mislabeled or was misunderstood by the authors. It shows the proximal end of the filament of an adult *Caligus elongatus* but is labeled "chalimus 1". A similar study was carried out concurrently by Piasecki and MacKinnon [45], but only in relation to the filament structure of *Caligus elongatus*. Their results are discussed in detail below.

Lin et al. [57] elaborated on their preliminary report [52] on the developmental stages of *Caligus epidemicus* parasitizing tilapia cultured in brackish water. They described the highest number of larval and juvenile stages amounting to 10: nauplius 1, nauplius 2, copepodid, chalimus 1, chalimus 2, chalimus 3, chalimus 4, chalimus 5, chalimus 6, preadult, and adult. This time they were hesitant and clearly stated that "no moult was observed between the preadult and the adult stage". (p. 661, [57]) They illustrated a rostrum on the frontal plate of the copepodid. Chalimi 5 and 6 were advanced morphologically and had a marginal membrane and lunulae. The armature differences between these two stages were small. On the exopod of leg 4 "terminal inner seta increased greatly in length" between chalimus 4 and chalimus 5 (p. 681, [57]), and the ramus "becomes more elongated" between chalimus 5 and chalimus 6 (p. 681, [57]).

The life cycle of *Caligus elongatus*—later shown to be a collective name that has been applied to a number of separate genotypes and/or cryptic species [58–61]—was described by Piasecki and MacKinnon [62], and the morphology of its developmental stages by Piasecki [63]. Those observations, supported by those of Piasecki and MacKinnon [45], conclusively proved that no preadult is present in this species and that the cycle includes only the nauplius 1, nauplius 2, copepodid, chalimus 1, chalimus 2, chalimus 3, chalimus 4,

and adult (Figure 1). The details were first presented in 1993 at the 5th International Conference on Copepoda in Baltimore, MD, USA.

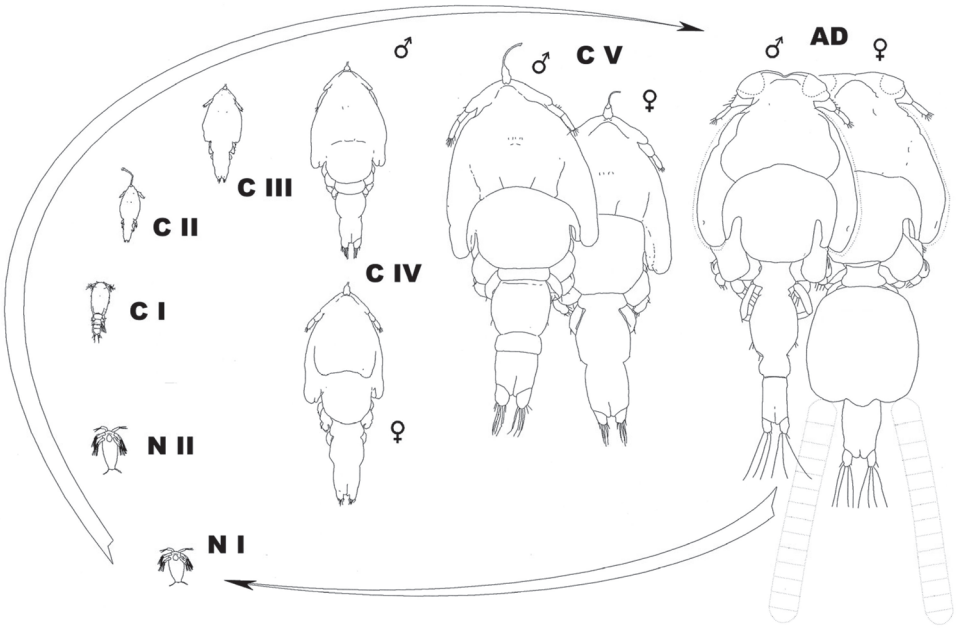

Figure 1. Diagrammatic representation of the life cycle of *Caligus elongatus*. Silhouettes of all stages are on the same scale. Stage numbers referring to the new interpretation of the present paper (with old nomenclature in the parentheses): N I = nauplius I, N II = nauplius II, C I = copepodid I, C II = copepodid II (chalimus 1), C III = copepodid III (chalimus 2), C IV = copepodid IV (chalimus 3), C V = copepodid V (chalimus 4), AD = adult. (Reprinted from Piasecki 1995 [64]; Piasecki©).

Lin et al. [65] studied the development of supposed "*Caligus multispinosus* Shen, 1957" from black sea bream, *Acanthopagrus schlegelii* (Bleeker, 1854), cultured in Taiwan. As was later demonstrated by Ho et. al. [66], the copepod was actually *Caligus rotundigenitalis* Yü, 1933. Lin et al. [65] identified two nauplii, one copepodid, four chalimus stages, one preadult, and the adult. The early copepodid was illustrated with a rostrum and the "advanced" copepodid was illustrated in the process of molting. The proximal part of the frontal filament was well described and illustrated, and it was consistent with the pattern described by Piasecki and MacKinnon [45]. The preadult was attached by a filament and was rather advanced morphologically, having a marginal membrane, lunulae, and a sternal furca; this preadult was, therefore, actually a young adult.

Gonzalez-Alanis et al. [67] described the morphogenesis of the frontal filament in the salmon louse *Lepeophtheirus salmonis*. This study was a continuation and a progressive development of the research reported by Bron et al. [48]. González and Carvajal [68] studied the life cycle of *Caligus rogercresseyi* infecting cultured salmonids in Chile. They found and described two nauplii, one copepodid, four chalimus stages, and the adult. No preadult stage was observed. Unfortunately, the developmental stages were not illustrated in detail. The development of the frontal filament followed the pattern described by Piasecki and MacKinnon [45].

In their book "Sea lice of Taiwan", Ho and Lin [69] repeated the information on the ontogeny of *Caligus epidemicus* and *C. rotundigenitalis* provided in the two earlier works by Lin et al. [57,65]. They discussed not only the morphology of the instars but also emphasized the different structures of the frontal filament in *Caligus epidemicus*, arguing that in this particular species, each stage has a different frontal filament and at each molt, a new filament must be formed. It is worth mentioning that a frontal filament with a similar rod-like structure was observed in *Caligus spinosus* by Izawa [35].

In their monograph on the post-embryonic development of the Copepoda, Ferrari and Dahms [10] wrote, "chalimus 1 of caligid-like copepods resembles CII of other copepods in

the number and kind of somites: a cephalon with five limbs, six thoracic somites, and a posterior abdominal somite." (p. 55, [10]). They explicitly stated that "the four chalimus stages correspond to the second to fifth copepodid stages." (p. 217, [10]).

Ohtsuka et al. [33] studied the developmental stages and growth of "*Pseudocaligus fugu*" (accepted as *Caligus fugu* Yamaguti, 1936). They described and illustrated two nauplii, one copepodid, four chalimus stages, and the adult. They reviewed all known life cycles including 11 full life cycles for *Caligus* and 4 for *Lepeophtheirus*. They also summarized and discussed the hitherto published information on the frontal filament and emphasized the importance of the setation of the antennule's proximal segment for discriminating the juvenile stages.

Madinabeitia and Nagasawa [70] studied the chalimus stages, but not the nauplius or copepodid stages, of *Caligus latigenitalis* Shiino, 1954 parasitic on blackhead seabream, *Acanthopagrus schlegelii* (Bleeker, 1854), from Japan. They introduced the term "semaphoront" to denote a functional (i.e., morphologically different) stage that is not necessarily separated by a molt. Within the copepodid stage, they distinguished two semaphoronts (the infective copepodid and the chalimus copepodid), which were followed by four chalimus stages (=semaphoronts) and the adult stage (with two semaphoronts: the chalimus adult and the mobile adult). They amended the definition of "chalimus", distinguishing between the stage and the semaphoront [71]. Accordingly, a "chalimus" may be either a post-naupliar stage corresponding to copepodids II through V [10] or a semaphoront with a frontal filament used for attachment to the host.

Venmathi Maran et al. [11] described the life cycle of *Lepeophtheirus elegans*. They determined that the traditionally recognized chalimus 1 and 2 should be merged into a single stage—chalimus 1—and similarly that chalimus 3 and 4 represent a single stage—chalimus 2. Consequently, they listed the following stages in the life history: nauplius 1, nauplius 2, copepodid, chalimus 1, chalimus 2, preadult 1, preadult 2, and adult. Like Ohtsuka et al. [33], Venmathi Maran et al. [11] used the number of setae on the proximal segment of the antennule to differentiate between the post-naupliar stages. Their new model of the caligid life cycle reconciled the sequences of development of *Caligus* and *Lepeophtheirus* for the first time and will be very important for the final conclusions of the present paper.

Hamre et al. [12], probably working concurrently with and independently of Venmathi Maran et al. [11], studied *Lepeophtheirus salmonis* and achieved comparable results. They also observed chalimus 1 (merging the former chalimus 1 and 2) and chalimus 2 (merging the former chalimus 3 and 4). They emphasized that their study was the first to be based on direct observation of molts and/or shed exuviae of all the developmental stages. The "external lamina" of the frontal filament (as defined by Bron et al. [48]), which had been supposed to be a remnant of the shed exuvium of chalimus 1, is in fact an extension of the chalimus's cuticle. Hamre et al.'s [12] direct molt observations were backed up by the morphometric clustering analysis. Their study marked an important step in the advancement of the methodology for life-cycle research on caligid copepods. The same team developed this methodology further, as published by Eichner et al. [72], to study instar growth and molt increments in the chalimus stages of *Lepeophtheirus salmonis* and to provide additional important observations regarding the frontal filament.

Khoa et al. [73] studied the life cycle of the species identified as *Caligus minimus* infecting seabass, *Lates calcarifer* (Bloch, 1790), in floating cage culture. They recognized eight developmental stages: nauplius 1, nauplius 2, copepodid, chalimus 1, chalimus 2, chalimus 3, chalimus 4, preadult, and adult. The authors were apparently unaware of the unpublished thesis of Caillet [38], who had studied the ontogeny of the same species. The authors provided photographs of the various stages but no morphological details, and some of the stages appear to be mislabeled.

Hamre et al. [74] monitored the development of parasitic stages of *Lepeophtheirus salmonis* reared in temperatures ranging from 3 to 24 °C.

Hemmingsen et al. [75] provided a comprehensive review of *Caligus elongatus* and other sea lice of the genus *Caligus* infecting farmed salmonids. They summarized the available literature

but for unknown reasons perpetuated the preliminary and erroneous results of Hogans and Trudeau [44], especially by reproducing their figures with unrealistic frontal filaments.

Under controlled conditions, Bravo et al. [42] compared the life cycles of *Lepeophtheirus mugiloidis* Villalba et Duran, 1986 and *Caligus rogercresseyi*, parasites of the Patagonian blenny *Eleginops maclovinus* (Cuvier, 1830). They reported the existence of nauplius 1, nauplius 2, copepodid, chalimus 1, chalimus 2, preadult 1, preadult 2, and the adult in *L. mugiloidis* and nauplius1, nauplius 2, copepodid, chalimus 1, chalimus 2, chalimus 3, chalimus 4, and the adult in *C. rogercresseyi*. This paper was very brief, and no details of the developmental stages were provided.

One of the most recent papers on this subject was that of Jeong et al. [76], who quantified key parameters related to the life cycle of *Caligus rogercresseyi* and reported a developmental sequence of nauplius1, nauplius 2, copepodid, chalimus 1, chalimus 2, chalimus 3, chalimus 4, and adult.

Tables 1 and 2 summarize the main morphological characters of the developmental stages of *Lepeophtheirus* and *Caligus*, and Table 3 provides a summary of "advanced" life cycle studies.

Table 1. Comparison of diagnostic features of developmental stages of *Caligus elongatus* (based on Piasecki [63]).

	Copepodid I	**Copepodid II (Ch 1)**	**Copepodid III (Ch 2)**	**Copepodid IV (Ch 3)**	**Copepodid V (Ch 4)**	**Adult**
Filament	1-lobed	1-lobed	1-lobed *	2-lobed	3-lobed	4-lobed
3rd leg	Vestigial	Vestigial	Biramous	Biramous	Biramous	Biramous
4th leg			Uniramous	Uniramous	Uniramous	Uniramous
5th leg				Vestigial	Vestigial	Vestigial
Sternal furca					Vestigial	Present
H-suture					Vestigial?	Present
Lunulae						Present
Marginal membrane	Absent	Absent	Absent	Absent	Absent	Present
Pinnate setae on swimming legs						Present
Post-antennary process						Present

* Extension lobe of chalimus 2 completely engulfing the lobe of chalimus 1.

Table 2. Comparison of diagnostic features of developmental stages of female *Lepeophtheirus elegans* (based on Venmathi Maran et al. [11]).

Features	**Copepodid I**	**Copepodid II (=Chalimus 1)**	**Copepodid III (=Chalimus 2)**	**Copepodid IV (=Preadult 1)**	**Copepodid V (=Preadult 2)**	**Adult**
Body	Highly pigmented, no frontal filament	No pigmentation; short frontal filament	No pigmentation; developed frontal filament	Well-developed frontal plates	Fully developed cephalothorax	Typical caligiform cephalothorax
Cephalothorax	About 1.5 times longer than free posterior somites	About 2.5 to 3 times longer than free posterior somites	About 3.5 times longer than free posterior somites	Typical H-shaped suture	About 2 times longer than free posterior somites	As in preceding stage

Table 2. *Cont.*

Features	Copepodid I	Copepodid II (=Chalimus 1)	Copepodid III (=Chalimus 2)	Copepodid IV (=Preadult 1)	Copepodid V (=Preadult 2)	Adult
Antennule (2 segments)	Proximal: 3 setae Distal: 11 setae + 2 Aesthetascs (A)	Proximal: 7 Distal: 12 + 2A	Proximal: 13; Distal: 12 + 2A	Proximal: 20; Distal: 12 + 2A	Proximal: 27 Distal: 12 + 2A	Proximal: 27 Distal: 12 + 2A
Antenna	Three-segmented; second segment with rugose process; third segment with recurved claw	Modified from that of preceding copepodid stage; third segment with curved distal claw	Middle segment with rudiment of dorsal adhesion pad	Second segment with reniform adhesion pad; terminal claw strongly curved	As in preceding stage	Terminal part forming strong, recurved claw
Maxilliped	Distal segment separated by partial suture, carrying terminal claw and trifid setal element	Distal segment of subchela bearing curved claw and short inner seta	Segments comprising subchela more completely fused than in preceding stage	As in preceding stage	As in preceding stage	Distal subchela with trace of suture separating short apical claw
Sternal furca	Absent	Absent	Present	Broad box and divergent, slightly tapering tines	As in preceding stage	As in preceding stage

Table 3. Overview of life cycle studies of caligid copepod species of the genera *Caligus* and *Lepeophtheirus*. Stage interpretation was confirmed by reference to Tables 1 and 2.

Reference	Species	Stages Originally Found/Determined	Stages Interpreted and Comments
Russel [25]	*C. pageti*	N, C1, C2, Ch ("three sizes")	N I, C I, C II, [—], [—], C V, Ad
Argilas [26]	*C. pageti*	N, C, Ch	N I, C I, [—], [—], CIV, Ad
Gurney [24]	*C. centrodonti*	N1, N2, C, Ch1, Ch2, Ch3, Ch4, Ad	N I, N II, C I, C II, [—], C IV, C V, Ad
Heegaard [29]	*C. curtus*	N1, N2, C 1, C2, pupa, Ch1, Ch2, Ch3, Ch4, Ch5, Ad	N I, N II, C I, C II, [—], C IV(?), C V(?), Ad
Kozikowska [31]	*C. lacustris*	C, Ch1, Ch2, Ch3, Ch4, Ad	[N I?], [N II?], C I, C II, [—], C IV(?), C V(?), Ad
Hwa [34]	*C. orientalis*	N1, N2, C, Ch1, Ch2, Ch3, Ch4, Ch5, Ad	N I, N II, C I, C II, C III, C IV, CV, Ad
Izawa [35]	*C. spinosus*	N1, N2, C, Ch1, Ch2, Ch3, pAd1, pAd2, Ad	N I, N II, C I, C II, C III, C IV, [–], Ad
Kabata [30]	*C. clemensi*	N1, N2, C, Ch1, Ch2, Ch3, Ch4, pAd1, Ad	N I, N II, C I, C II, C III, C IV, CV, Ad
Caillet [38]	*C. minimus*	N1, N2, C, Ch1, Ch2, Ch3, Ch4 Ch5, Ad	N I, N II, C I, [—], C III, C IV, CV, Ad
Ben Hassine [40]	*C. pageti*	N1, N2, C, Ch1, Ch2, Ch3, Ch4 pAd1, Ad	N I, N II, C I, C II, [—], C IV, CV, Ad
Hogans and Trudeau [44]	*C. elongatus*	N1, N2, C, Ch1, Ch2, Ch3, Ch4 pAd1, Ad	N I, N II, C I, C II, [—], C IV, CV, Ad

Table 3. *Cont.*

Reference	Species	Stages Originally Found/Determined	Stages Interpreted and Comments
Ogawa [51]	*C. longipedis*	N1, N2, C, Ch1, Ch2, Ch3, Ch4 pAd1, Ad	N I, N II, C I, C II, C III, C IV, CV, Ad
Kim [53]	*C. punctatus*	N1, N2, C, Ch1, Ch2, Ch3, Ch4, Ad	N I, N II, C I, C II, C III, C IV, CV, Ad
Lin et al. [57]	*C. epidemicus*	N1, N2, C, Ch1, Ch2, Ch3, Ch4, Ch5, Ch6, pAd, Ad	N I, N II, C I, C II, C III, C IV, CV, Ad
Piasecki [63]	*C. elongatus*	N1, N2, C, Ch1, Ch2, Ch3, Ch4, Ad	N I, N II, C I, C II, C III, C IV, CV, Ad
Lin et al. [65]	*C.rotundigenitalis*	N1, N2, C, Ch1, Ch2, Ch3, Ch4, pAd, Ad	N I, N II, C I, C II, C III, C IV, CV, Ad
González and Carvajal [68]	*C. rogercresseyi*	N1, N2, C, Ch1, Ch2, Ch3, Ch4, Ad	N I, N II, C I, C II, C III, C IV, CV, Ad
Ohtsuka et al. [33]	*C. fugu*	N1, N2, C, Ch1, Ch2, Ch3, Ch4, Ad	N I, N II, C I, C II, C III, C IV, CV, Ad
Madinabeitia and Nagasawa [70]	*C. latigenitalis*	C, Ch1, Ch2, Ch3, Ch4, Ad	[N I], [N II], C I, C II, C III, C IV, CV, Ad
Khoa et al. [73]	*C. minimus*	N1, N2, C, Ch1, Ch2, Ch3, Ch4, Ad	N I, N II, C I, C II, C III, C IV, CV, Ad
Bravo et al. [42]	*C. rogercresseyi*	N1, N2, C, Ch1, Ch2, Ch3, Ch4, Ad	N I, N II, C I, C II, C III, C IV, CV, Ad
White [28]	*L. salmonis*	C, Ch1, Ch2, [. . .], Ch(final), [. . .], Ad	C I, C II, [—], C IV(?), C V(?), Ad
Lewis [32]	*L. dissimulatus*	N1, N2, C, Ch1, Ch2, Ch3, Ch4, Ch5, Ch6, Ad	N I, N II, C I, C II, C III, C IV, CV, Ad
Voth [36]	*L. hospitalis*	N1, N2, C, Ch1, Ch2, Ch3, Ch4, Ch5, Ch6, A	N I, N II, C I, C II, C III, C IV, CV, Ad
Boxshall [37]	*L. pectoralis*	N1, N2, C, Ch1, Ch2, Ch3, Ch4 pAd1, pAd2, Ad	N I, N II, C I, C II, C III, C IV, CV, Ad
Johnson and Albright [49]	*L. salmonis*	N1, N2, C, Ch1, Ch2, Ch3, Ch4 pAd1, pAd2, Ad	N I, N II, C I, C II, C III, C IV, CV, Ad
Schram [54]	*L. salmonis*	N1, N2, C, Ch1, Ch2, Ch3, Ch4 pAd1, pAd2, Ad	N I, N II, C I, C II, C III, C IV, CV, Ad
Venmathi Maran et al. [11]	*L. elegans*	N1, N2, C, Ch1, Ch2, pA1, pA2, Ad	N I, N II, C I, C II, C III, C IV, CV, Ad
Hamre et al. [12]	*L. salmonis*	N1, N2, C, Ch1, Ch2, pA1, pA2, Ad	N I, N II, C I, C II, C III, C IV, CV, Ad
Bravo et al. [42]	*L. mugiloidis*	N1, N2, C, Ch1, Ch2, Ch3, Ch4 pAd1, pAd2, Ad	No details available. Interpretation not possible

[—] denotes stages apparently overlooked by the cited author. [N I] and [N II] denote stages apparently known to the author but not studied. [. . .] denotes stages that were not explicitly defined and/or named.

5. Reports on Individual Developmental Stages

A number of people have published papers concerning individual developmental stages of caligids. Among them was Markewitsch [77], who found and illustrated (in dorsal view) a "metanauplius" (=copepodid) and a "chalimus" (probably chalimus 3) of *Caligus lacustris* infecting many different fish species in the Caspian Sea. While studying fish-parasitic copepods of the Gulf of Mexico, Bere [78] found, described, and illustrated chalimus stages of a newly discovered species, *Caligus praetextus* Bere, 1936, which had

been collected from the tail of a hogfish, *Orthopristis chrysoptera* (Linnaeus, 1766). Among Bere's "chalimus a", "chalimus b", and "chalimus c", the latter two might represent either chalimus 4 or young adults still attached by a very short and thick filament; unfortunately, the structure of the filament's proximal end was not illustrated. Gnanamuthu [79] described sex differences in the advanced chalimus stages (possibly including young adults) of *Caligus polycanthi* Gnanamuthu, 1950 parasitic on "*Balistes maculatus*" [accepted as *Canthidermis maculata* (Bloch, 1786)] from Madras, India. His drawings were quite superficial and the filament structure was not shown. Kaj [80] found chalimus stages of *Caligus lacustris* on *Alburnus alburnus* (Linnaeus, 1758) from Górzyń Lake, Poznań Voivodship, Poland. His description was only general, and his drawings do not permit stage identification. Hewitt [81] described a new species, *Caligus epidemicus* Hewitt, 1971, while also covering some of its developmental stages, which he labeled as A, B, C, D, and E. Stage A was the copepodid. Stages B and C had lunulae visible beneath the cuticle, so they probably represented chalimus 4. Stage D was a young adult (probably male) with a filament, and stage E was an adult (female) without a filament. The author illustrated not only the respective habiti in dorsal view, but also compared the morphology of the appendages of stages A, B, C, and D. Hewitt's descriptions and images reveal very little about the nature and structure of the frontal filament. Lopez [82] incubated egg-strings of "*Lepeophtheirus kareii*" (accepted as *Lepeophtheirus hospitalis* Fraser, 1920, the same species that Voth [36] studied) and managed to obtain two naupliar stages and the copepodid. Lopez documented their general appearance in photographs and their appendages in microscopic drawings. Johannessen [83] studied the early stages of *Lepeophtheirus salmonis*, describing and illustrating nauplius 1 and 2 and only briefly mentioning the copepodid, providing its length and width. Pike et al. [55] studied the naupliar stages and the copepodid of *Caligus elongatus* in relation to temperature. Izawa [84] described the copepodid, chalimus 2, and chalimus 4 of *Caligus latigenitalis* Shiino, 1954 parasitic on black sea bream, *Acanthopagrus schlegelii*, from Japan. The filament was reported as having a structure similar to that of *Caligus elongatus* as described by Piasecki and MacKinnon [45]. Izawa [84] also contended that the preadult described by some authors was not a true instar separated by a molt but simply a young adult. Jones [85] studied *Caligus patulus* Wilson, 1937 from a fish farm in the Philippines. He found the copepodid, chalimus 2, two preadult stages, and the adult female and male. Both of his preadult stages had lunulae, a marginal membrane, and a sternal furca, so they were probably young adults. Eichner et al. [72] studied instar growth and molt increments in chalimi of *Lepeophtheirus salmonis* and provided important observations regarding the frontal filament (see Section 7 below). Ohtsuka et al. [46] reported chalimus 3, chalimus 4, and the ovigerous female of *Caligus undulatus*. The ovigerous female was attached to its host fish by a frontal filament. Montory et al. [86] studied the early development of *Caligus rogercresseyi* under combined salinity and temperature gradients and recognized nauplius 1, nauplius 2, and the copepodid.

6. Frontal Filament in Species of *Caligus*

We usually understand the term "chalimus" to denote a juvenile copepod stage that is attached to its host by a frontal filament. To define it better, however, we need to describe this structure in detail stage-by-stage. In most cases, our understanding of copepod juveniles attached permanently by a filament (or cord, thread, or tether) is overly simplified and limited to selected stages only. In reality, it is not that straightforward. A good example is *Caligus elongatus*, studied by Piasecki and MacKinnon [45,62] and Piasecki [63]. According to those sources (and WP's unpublished information), the first traces of the frontal filament appear within the cephalothorax of older copepodids in the form of irregular particles of a dark-staining substance. During the next few hours, the filament becomes more developed and elongated. It is very likely that the filament is produced at the bottom of the cuticular pocket that extends from the frontal area to the center of the cephalothorax. The filament's distal end is permanently attached to the fish, and the proximal end is the filament's base. When the copepodid contacts the fish, the

cuticular pocket evaginates in such a way that the copepodid carries the filament's proximal end (the evaginated cuticular pocket) on its frontal area and the distal end of the filament becomes attached to the host [63]. This activity will be discussed in more detail below. The original filament will be "inherited" by all subsequent stages including the adult. The frontal organ, which is responsible for secreting the filament and its extension lobes, is originally (at the copepodid stage) located at the bottom of a cuticular pocket and migrates to the frontal area, where it remains in all subsequent stages. Each of the consecutive stages modifies the proximal end of the filament. Namely, before a molt the new instar prepares a filament extension lobe beneath its cuticle. During the molt, the old cuticle remains attached to the filament's base. The newly emerging stage leaves the old cuticle behind, but its first action is to secure its own attachment to the host. To do this, it glues the new extension lobe, which is firmly attached to the frontal organ, to the filament base. The old cuticle eventually wears away and detaches, but its remnants are sometimes visible, attached to the connection pads of the previous stage's filament extension lobe (Figure 2A).

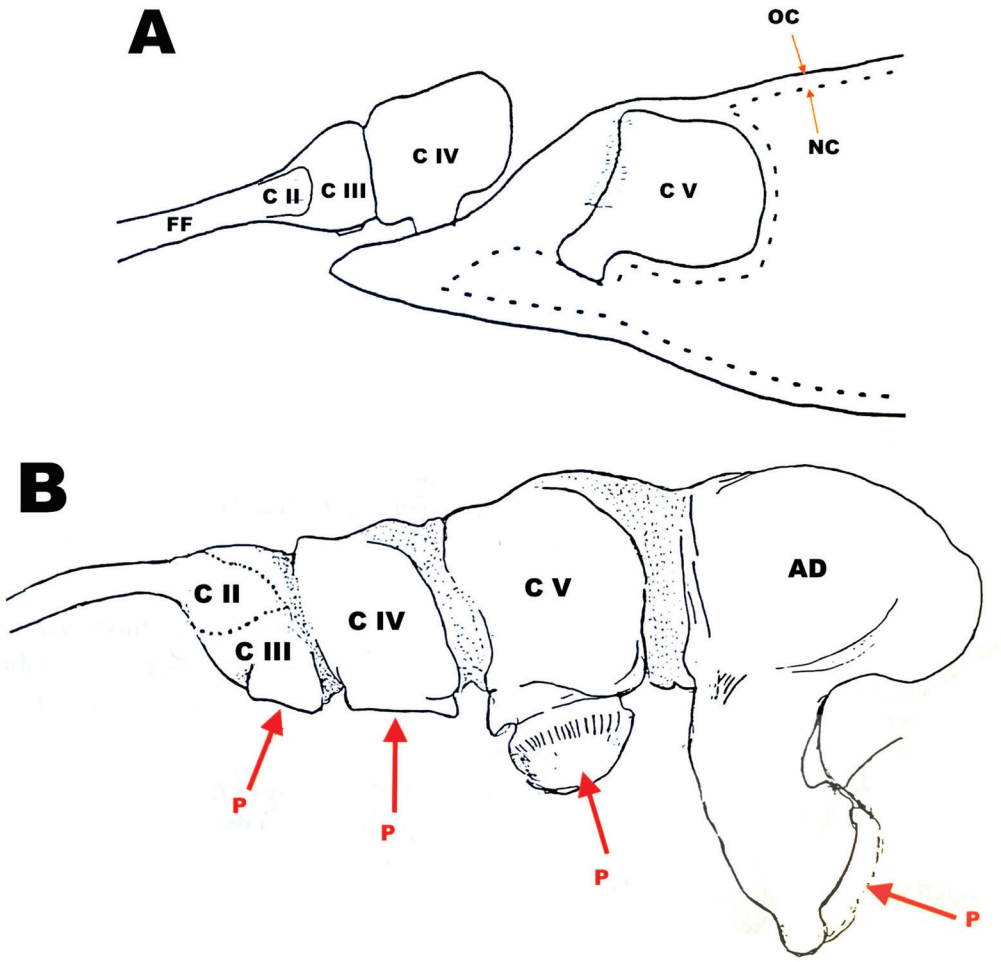

Figure 2. (**A**) Hypothetical, diagrammatic representation of the frontal filament extension lobes in a sagittal section of a pre-molt copepodid IV (chalimus 3) of *Caligus elongatus*; lateral view of the anterior part of the body. (**B**) Diagrammatic representation of the proximal part of the frontal filament in an adult of *Caligus elongatus*; lateral view. P denotes connecting pads of the consecutive stages. Abbreviations: C II = copepodid II (ch1), C III = copepodid III (ch2), C IV = copepodid IV (ch3), C V = copepodid V (ch4), AD = adult; FF = frontal filament shaft; OC = old cuticle, NC = new cuticle.

The number of filament-base elements is directly related to the numbering of the chalimus stages; however, in chalimus 2, only one element of this base is visible; in chalimus 3, two such elements; in chalimus 4, three; and in the young adult, four. This

increment in the number of the elements of the proximal end of the filament was understood literally by some researchers who believed, for example, that three elements identified the stage as chalimus 3 (etc.) This is because the smallest and earliest element belonging to chalimus 1, including its attachment pad, becomes completely engulfed by the element added by chalimus 2 and is thus completely obscured. Each subsequent filament extension piece is slightly larger than the previous one. Disregarding the engulfed element, the filament base has a single, semi-triangular lobe in chalimus 2, a bipartite lobe in chalimus 3, a tripartite lobe in chalimus 4, and finally a four-lobed base in the young adult (Figure 2B).

It is evident from the observations of Piasecki and MacKinnon [45] presented above that a frontal filament is possessed by all post-naupliar stages, namely the chalimus 1, chalimus 2, chalimus 3, chalimus 4, and adult. This means that the existing definition of "chalimus" is not consistent, because of the arbitrary elimination of the copepodid and the adult from the concept. Cases of a copepodid attached by a filament, as has been reported by many authors, will be discussed below.

According to Piasecki and MacKinnon [45,62], adults need the filament to complete their last molt (chalimus to adult). Those authors also reported that ovigerous females were still attached by the filament. Also important, in conjunction with this last molt the filament receives its final lobe. If we stick to an unqualified definition of "chalimus", we would need to refer to the adult as chalimus 5. Also, the advanced (attached) copepodid appears to be attached by a filament. Therefore, we must regard the copepodid as a chalimus 1, and then the adult female still attached by a filament as chalimus 6? Remember that Izawa [35] illustrated the first preadult of *Caligus spinosus* as still being attached by a filament. This first preadult seems to be homologous with chalimus 5 of Piasecki and MacKinnon [45] and also with the adult of Piasecki [63]. Non-filament-mediated attachment of newly molted adults (preadults?) or any other stage seems impossible because of the soft post-molt cuticle. We believe that the condition of being attached by a filament does not define the stage but is rather a functional characteristic of several developmental stages, which are really copepodids in integrative terminology.

The filament structure of *Caligus epidemicus* described by Lin et al. [57] is totally different from that described for *C. elongatus* by Piasecki and MacKinnon [45], although very similar to that of *C. spinosus* reported by Izawa [35]. The differences are so profound that the different filament structures could potentially serve as important taxonomic traits. The extension element in *C. epidemicus* is rod-like and very elongate, so much so that it might be used as either an extension lobe or a brand-new filament if something goes wrong. Lin et al. [57] believed that only chalimus 4, not every post-naupliar stage as in *C. elongatus*, reuses the old filament of the preceding stage. The filaments of *C. spinosus* and *C. epidemicus* should be restudied with a focus on the consistency of the filament's structure in successive stages.

7. Frontal Filament in Species of *Lepeophtheirus*

The filament in species of the genus *Lepeophtheirus* has a different structure from that in species of *Caligus*. Also, the strategy of attachment, its details, and changes during the sequence of developmental stages seems to be different. The filament is relatively short and stout, and no modification of its proximal end is observed during ontogeny [49]. The first comprehensive study on this subject was that of Bron et al. [48]. Using light microscopy for histological observations and a scanning electron microscope (SEM) to obtain external views of the structures, they determined that the filament consists of a fibrous stem with an axial duct and that the basal plate is attached to the epithelial basement membrane of the host fish. The filament is covered by "external lamina" supposedly continuous with the integument of the chalimus. The basal plate is formed from a secretion produced in the cephalothorax by the A-group gland cells they discovered; the secretion is delivered to the distal portion of the stem through the axial duct. B- and C-group gland cells were also defined, but their function was not characterized. The spatial locations of the three groups of gland cells were presented in diagrams.

Pike et al. [56] soon published a set of SEM and TEM observations including five micrographs of the filament of *Lepeophtheirus salmonis*, but they were rather hesitant to interpret them in detail. They did state, however, that the filament of *Lepeophtheirus salmonis* is an integral part of the chalimus body.

Gonzalez-Alanis et al. [67] used high-resolution light microscopy to study histological sections of juvenile *Lepeophtheirus salmonis* and proposed the following sequence of events in filament development. First, the B-groups cells release secretion 1 (S1) (substance 1?), which forms the basal plate. Then the C-group cells produce S2, which becomes the stem of the external frontal filament. The A-cells secrete a glue-like substance, delivered to the distal part of the frontal filament through the axial duct. In pre-molt specimens, S1 and S2 are tightly enclosed within a cuticular invagination, first described by Bron et al. [48] as the "external lamina". The spatial location of the three groups of gland cells was shown in very informative diagrams (Figure 3). Most importantly, Gonzalez-Alanis et al. [67] provided strong evidence that *Lepeophtheirus salmonis* produces a brand-new filament with each molt.

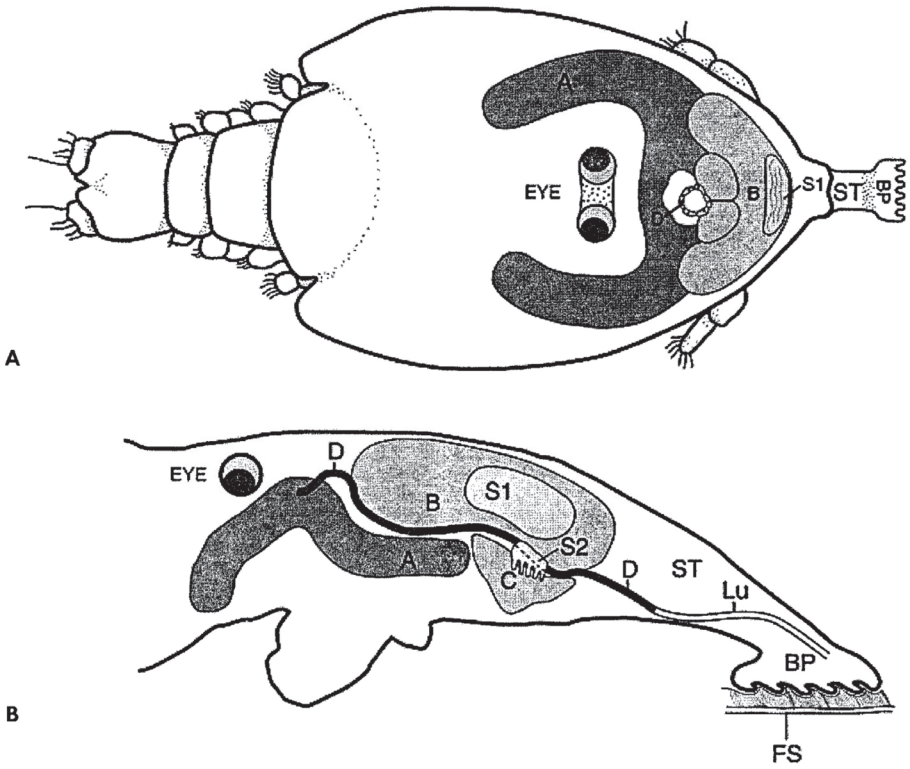

Figure 3. Diagrammatic representation and the arrangement of cell groups A, B, and C responsible for the secretion of the frontal filament and internal filament material S1, S2, and duct D, in chalimus of *Lepeophtheirus salmonis* at 7 dpi. Reproduced from Gonzalez-Alanis et al. [67] under the permission of the Journal of Parasitology. (**A**) Dorsal view; (**B**) Sagittal view; BP, basal plate; FF, frontal filament; FS, fish scale (Other abbreviations were not explained by [67].

Anstensrud [9] determined that the frontal filament is present in each post-molt stage of *Lepeophtheirus pectoralis*, including the adults. This is very important for understanding the conclusions of the present paper. Eichner et al. [72] not only studied the growth and molt increments in chalimi of *Lepeophtheirus salmonis* but also made important observations on the frontal filament. They stated that Hamre et al. [12] had observed a frontal filament on the exuvium of chalimus 1. This statement is not precisely correct because it is evident from Figure 4 in [12] that the exuvium featured only the cuticular sheath of the filament, that is, Bron et al.'s [48] "external lamina". Although Eichner et al. (71) observed no such structure in the exuvium of chalimus 2, Figure 4 in [12] apparently shows that the exuvium of this stage does indeed have an "external lamina". Eichner et al. [72] also noticed that

filaments are visible inside pre-molt juveniles. Based on other studies [9,49,67] as well as their own, they stated that "a total of five separate filaments are formed during the *L. salmonis* life cycle, that is, the filaments produced prior to molting by the copepodid, chalimus 1, chalimus 2, preadult 1 and preadult 2." It is very possible that the "external lamina" does not occur in preadult 1 and 2, nor the adult, during their period of temporary attachment by the filament. The "external lamina" is a continuation of the integument, and it would be unlikely for such a structure to be discarded long before the actual molt (which does not occur in the adult). If it is present in preadults, we would expect to see its remnants around the frontal organ, but no such remnants are visible in Anstensrud's [9] figures.

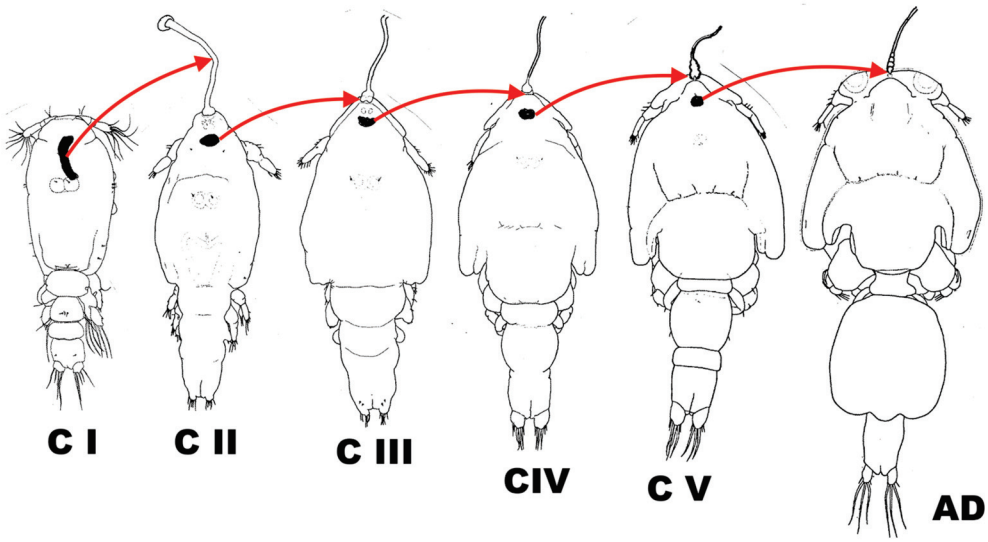

Figure 4. The sequence of events in the formation of the frontal filament in consecutive developmental stages of *Caligus elongatus*. In pre-molt specimens, extension lobes (black) are visible beneath the old cuticle (in the copepodid it is the future frontal filament). Abbreviations: C I = copepodid I, C II = copepodid II (ch1), C III = copepodid III (ch2), C IV = copepodid IV (ch3), C V = copepodid V (ch4), AD = adult. Silhouettes of the stages are based on those from Piasecki 1995 [64] (Piasecki©).

8. "Copepodid Attached by the Frontal Filament"?

In *Caligus* life cycles, a "copepodid attached by the frontal filament" has been observed and illustrated by Gurney [27], Hwa [34], Hogans and Trudeau [44], Piasecki [63], and Khoa et al. [73]. Such reports may prove deceptive when the course of events is analyzed carefully. For example, Izawa [35] stated that chalimus 1 is the stage that first attaches to the host by the filament; but this is also an oversimplification. It is quite reasonable to believe that alternating actions of the clawed appendages and the frontal filament are needed for securing the attachment of consecutive instars in the life history of caligid copepods. We interpret the course of events during the post-naupliar phase of the ontogeny as follows:

- The copepodid finds a suitable place on the surface of the host and firmly attaches there using the claws of the antennae and the maxillipeds;
- Through intensive scraping by some appendages it removes a portion of the host's epithelium, thereby exposing a suitable place for permanent attachment;
- Molting starts with a rupture of the copepod's larval cuticle in the frontal area;
- The cuticular pocket containing fully formed frontal filament, previously visible within the cephalothorax, evaginates to become a frontal extremity;
- The filament is released and its proximal end becomes firmly attached to the tip of the frontal extremity;
- The distal end of the filament is glued to the previously exposed part of the host's body;
- After the hardening of the filament has assured that the attachment to the host is secure, the organism continues its molting process;

- The next stage—copepodid II (chalimus 1)—withdraws from the copepodid I exuvium and hangs from the host, attached only by the frontal filament. The exuvium itself is discarded.

An alternative course of events whereby the copepodid is already attached to its host by a filament is rather unlikely. This is because every molt is preceded by the formation of the next-stage filament element beneath the cuticle (Figure 4). Copepodid I produces the entire frontal filament. Copepodid II (chalimus 1) produces the extension lobe of copepodid III (chalimus 2), copepodid III (chalimus 2) produces the extension lobe of copepodid IV (chalimus 3), etc. If copepodid I was already attached by the filament it would also need to produce the extension lobe of the next stage, something which has never been observed and it is unlikely to occur considering the extremely short time before the attachment of the original filament and the first occurrence of copepodid II (chalimus 1). The so-called "copepodid attached by a filament" is definitely not a stage but it may be treated as a "semaphoront" representing a copepodid I in the process of molting into a copepodid II (chalimus 1).

9. The Concept of "Preadult"

The term 'preadult' was first introduced by Izawa [35], who distinguished two nauplii, a copepodid, three chalimi, and two preadults in the life cycle of *Caligus spinosus*. The preadults had lunulae, a marginal membrane, and a sternal furca. Some specimens of preadult 1 were even attached by a frontal filament. The preadults differed from the adult in their body proportions, mainly those of the genital complex. While the body lengths of the preadult 1 and adult did not overlap, the mean values for carapace length of the two preadult stages were similar (0.96/0.96 mm vs. 1.19/1.16 mm for females/males). Izawa doubted whether the preadult 2 and adult were really distinct stages.

The concept of the "preadult" became institutionalized in the wake of Kabata [30], who suggested that regardless of the genus, the caligid life cycle should contain two nauplii, a copepodid, four chalimi, and two preadults. Even though Kabata himself observed only one preadult, his model became the standing paradigm for the next 50 years. The term 'preadult' has been used to denote young adults of species belonging to both *Caligus* [8,39–41,44,51,52,57,65,85,87] and *Lepeophtheirus* [8,37,39,41,49,50,54,87–94], and very few researchers have admitted to observing no preadult [38,45,51,62,63]. Ho and Lin [69] nonetheless concluded that the so-called preadults described in *Caligus* species are freshly molted, young adults, and some subsequent life cycle studies did not report preadult stages for *Caligus* [33,70]. Only recently was the term "preadult" redefined to denote stages separated by one or more molts from the adult [11]. By this definition, the preadults (1 and 2) of *Lepeophtheirus elegans* [11] and *Lepeophtheirus salmonis* [12] were revealed as homologous, respectively, with chalimus 3 and 4 of *Caligus* and copepodid IV and V of all podoplean copepods [8,10].

Preadults 1 and 2 reported by Venmathi Maran et al. [11] and Hamre et al. [12] were in fact advanced juvenile stages, most probably already using their frontal filament within hours after a molt. Such a phenomenon was observed by Anstensrud [9], and it is very likely that this is a common pattern among *Lepeophtheirus* spp. Use of a filament makes them chalimi. If we also consider the adult's temporary use of the filament in *Caligus* and *Lepeophtheirus*, we might have to extend the term "chalimus" to the adult as well. We believe that no molt in caligid ontogeny occurring on the host is possible without (at least) temporary attachment by a filament. In view of the above, it would be difficult to define preadult explicitly.

10. Recapitulation

The preadult stage reported in species of the genus *Caligus* [30,35,40,44,51,57,65] turns out to be young adults mostly differing in the proportions of the genial complex (Table 3). Such preadults have all the morphological attributes of the adult (e.g., lunulae, marginal membrane, sternal furca, H-suture) and are not separated by a molt from the adult. In the

genus *Lepeophtheirus*; however, the so-called preadults are indeed separated by a molt from the adult [11,12]. As was noted above, several authors have demonstrated that the four preceding chalimus stages in this genus should be merged into only two. The *Lepeophtheirus* life-cycle thus became reconciled with that of *Caligus* in terms of the number of post-naupliar stages (Figure 5), but not in terms of their terminology. Venmathi Maran et al. [11] and Hamre et al. [12] for some reason did not reconcile the two life cycles completely. Although they both cited Anstensrud [9], they were apparently deceived by the notion that preadults and adults have only a "temporary filament". The apparent actual similarities between the life cycles of *Lepeophtheirus* and *Caligus* were obscured by semantic differences. If we insist that preadult 1 and 2 are not homologous with chalimus 3 and 4, respectively, then what are they? A chalimus is a copepodid attached by a filament. If it loses the filament or uses it only temporarily, does it become a copepodid again? If so, the life cycle of *Lepeophtheirus* spp. should be amended to contain only two real chalimi. We believe, to the contrary, that the validity of the term "preadult" cannot be defended any longer and that the life cycle of both *Caligus* and *Lepeophtheirus* includes a nauplius 1, nauplius 2, copepodid 1, chalimus 1, chalimus 2, copepodid 4, copepodid 5, and adult. This still does not represent a full reconciliation of the two life cycle patterns (Figure 6). Why should chalimus 2 be followed by copepodid 4? And what has happened to "stage 3"? The best solution might be to abandon the term "chalimus" altogether for life-history stages of these copepods. It might still remain in use by field researchers for making practical observations, but only as a "semaphoront" [70] because the actual "stage" cannot be determined in the field. Used as a semaphoront, the term "chalimus" may refer to any filament-bearing stage from the copepodid to the adult (inclusive), but such use cannot be easily interpreted and converted to precise life-cycle stages.

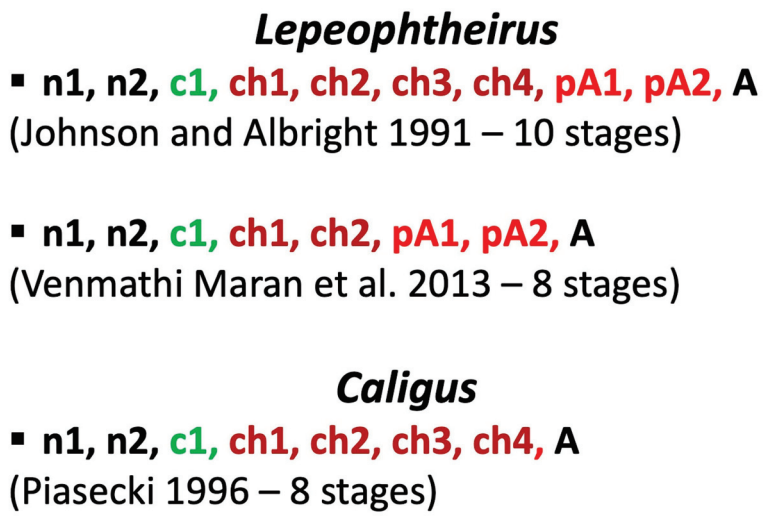

Figure 5. Alternative terminological sequences in the development of copepods of the family Caligidae based on examples from the genera *Lepeophtheirus* and *Caligus*. Abbreviations: n1 = nauplius 1, n2 = nauplius 2, c1 = copepodid 1, ch1 = chalimus 1, ch2 = chalimus 2, ch3 = chalimus 3, ch4 = chalimus 4, A = adult.

Kabata [8] wrote "The life cycles of copepods belonging to Gymnoplea, which comprise only the almost exclusively free-living Calanoida, consist of 12 stages other than adult: six nauplii and six copepodids. In contrast, the free-living Podoplea, ancestors of the parasitic copepods, often have only five nauplius stages (although that number may be reduced) and six copepodid stages. Since parasitic copepods descended from podoplean ancestors, they can be expected to have not more, possibly fewer, than five nauplius stages." (p. 20, [8]). Also "Remembering that our copepods have descended from the free-living Podoplea, we would expect that the species least modified by their pursuit of a parasitic way of life would have life cycles differing only slightly from those of their ancestors." (p. 21, [8]).

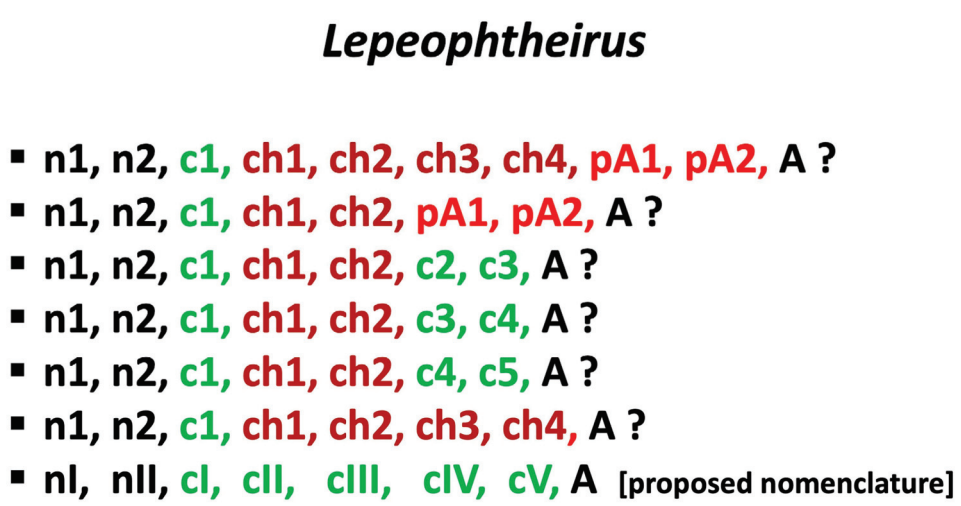

Figure 6. Alternative terminologies for ontogenetic sequences in the development of copepods representing the family Caligidae. The last row (using Roman numerals) is the proposed new terminology. Abbreviations: n1 = nauplius 1, n2 = nauplius 2, c1 = copepodid 1, ch1 = chalimus 1, ch2 = chalimus 2, ch3 = chalimus 3, ch4 = chalimus 4, c2 = copepodid 2, c3 = copepodid 3, c4 = copepodid 4, c5 = copepodid 5, A = adult, nI = nauplius I, nII = nauplius II, cI = copepodid 1, cII = copepodid II, cIII = copepodid III, cIV = copepodid IV, cV = copepodid V.

If the number of copepodid stages in Caligidae is (almost) consistent with that of the podoplean ancestors, why the number of naupliar stages is so much reduced? The answer was suggested by Pedaschenko [95] who observed exuviae within the egg of *Lernaeocera branchialis* (Linnaeus, 1767). This phenomenon should be studied further, but if proven, it might explain why there are only two naupliar stages are in caligid life cycles. A further reduction of the naupliar phase can be observed in fish-parasitic copepods of the family Lernaeopodidae [96,97], in with only single nauplius stage that hatches from the egg and is immediately ready to molt into the copepodid.

As we mentioned earlier, Ferrari and Dahms [10] explicitly stated that "the four chalimus stages correspond to the second to fifth copepodid stages." Consequently, we believe that the terms "preadult" and "chalimus" are no longer justified in studies on the biology of caligid copepods as they only contribute to confusion and should be abandoned. We suggest that copepods of the family Caligidae be deemed to have the following stages in their life cycle: nauplius I, nauplius II, copepodid I (infective), copepodid II (chalimus 1), copepodid III (chalimus 2), copepodid IV (chalimus 3), copepodid V (chalimus 4), and adult. An alternative, practical terminology may also contain an indication (F) of the presence of the frontal filament: nauplius I, nauplius II, copepodid I, copepodid II/F, copepodid III/F, copepodid IV/F, copepodid V/F, and the adult. Alternatively, a lower case "f" may be used for those stages where the filament is only temporary. For example, "adult f" means young one with a frontal filament.

This is a polemical paper, and our intention is to spark a discussion on this terminological problem. The general concept presented here may be extended to the life cycle of other siphonostomatoid copepods. According to Boxshall and Halsey [7], the following families are known to have "chalimus" stages with a frontal filament: Cecropidae, Lernaeopodidae, Nicothidae, and Pennellidae. Considering the phylogenetic placement of the Caligidae among other caligiforms [98], the families Dissonidae, Pandaridae, Sphyriidae, and Trebidae may also have "chalimi". If so, our reinterpretation of the developmental stages can be extended to all these families. According to a recent molecular phylogenetic analysis on the order Siphonostomatoida [99], the family Nicothidae, which may not be monophyletic, seems to have developed frontal filaments independently of the caligiform group. A final hypothesis, that siphonostomatoids other than caligiforms and "nicothoids" might have secondarily lost the frontal filament cannot be ruled out.

Author Contributions: Conceptualization, W.P., B.A.V.M. and S.O.; writing, review, and editing, W.P., B.A.V.M. and S.O. All authors have read and agreed to the published version of the manuscript.

Funding: This study was partially supported by a grant (subwencja naukowa) of the University of Szczecin, Poland (Institute of Marine and Environmental Studies; 503-0013-230000-01) awarded to WP and a grant-in-aid from the Japan Society for the Promotion of Science (KAKEN, No. 19H03032, awarded to SO. Additionally, UMS Project SDN0073-2019 was awarded to BAVM.

Institutional Review Board Statement: Not applicable.

Informed Consent Statement: Not applicable.

Data Availability Statement: Not applicable.

Acknowledgments: We are thankful to those anonymous reviewers who through their constructive criticism helped to improve this paper.

Conflicts of Interest: The authors declare no conflict of interest.

References

1. WoRMS Editorial Board. World Register of Marine Species. 2022. at VLIZ (Vlaams Instituut voor de Zee = Flanders Marine Institute, Oostende, Belgium). Available online: https://www.marinespecies.org (accessed on 29 November 2022).
2. Piasecki, W.; Avenant-Oldewage, A. Diseases caused by Crustacea. In *Fish Diseases*; Eiras, J., Segner, H., Wahli, T., Kapoor, B.G., Eds.; Science Publishers: Enfield, NH, USA, 2008; pp. 1115–1200.
3. Froese, R.; Pauly, D. (Eds.) FishBase. Version 08/2022. 2022. Available online: https://www.fishbase.org (accessed on 29 November 2022).
4. Kabata, Z. *Parasitic Copepoda of British Fishes*; No. 152; Ray Society: London, UK, 1979.
5. Dudley, P.L. Aspects of general body shape and development in Copepoda. *Syllogeus* **1986**, *58*, 7–25.
6. Huys, R.; Boxshall, G.A. (Eds.) *Copepod Evolution*; No. 159; Ray Society: London, UK, 1991.
7. Boxshall, G.A.; Halsey, S.H. *An Introduction to Copepod Diversity*; No. 166; Ray Society: London, UK, 2004.
8. Kabata, Z. Copepoda (Crustacea) parasitic on fishes: Problems and perspectives. *Adv. Parasitol.* **1981**, *19*, 1–71.
9. Anstensrud, M. Moulting and mating in *Lepeophtheirus pectoralis* (Copepoda, Caligidae). *J. Mar. Biol. Assoc. UK* **1990**, *70*, 269–281. [CrossRef]
10. Ferrari, F.D.; Dahms, H.U. *Post-Embryonic Development of the Copepoda*; Crustacean Monographs 8; Brill: Leiden, The Netherlands, 2007.
11. Venmathi Maran, B.A.; Moon, S.Y.; Ohtsuka, S.; Soh, H.Y.; Myoung, J.G.; Oh, S.-Y.; Iglikowska, A.; Boxshall, G.A. The caligid life cycle: New evidence from *Lepeophtheirus elegans* reconciles the cycles of *Caligus* and *Lepeophtheirus*. *Parasite* **2013**, *20*, e15. [CrossRef]
12. Hamre, L.A.; Eichner, C.; Caipang, C.M.A.; Dalvin, S.T.; Bron, J.E. The salmon louse *Lepeophtheirus salmonis* (Copepoda: Caligidae) life cycle has only two chalimus stages. *PLoS ONE* **2013**, *8*, e73539. [CrossRef] [PubMed]
13. Burmeister, H. Beschreibung einiger neuen oder weniger bekannten Schmarotzerkrebse: Nebst allgemeinen Betrachtungen über die Gruppe, welcher sie angehören. *Acad. Caes. Leop. Nova Acta.* **1835**, *17*, 269–336. [CrossRef]
14. Krøyer, H. Om Snyltekrebsene, isaer med Hensyn til den danske Fauna. *Naturhist. Tidsskr.* **1837**, *2*, 172–208.
15. Milne-Edwards, H. *Histoire Naturelle des Crustacés: Comprenant L'anatomie, la Physiologie et la Classification de ces Animaux*; Tome Troisième; Librairie Encyclopedique de Roret: Paris, France, 1840. [CrossRef]
16. Goodsir, H.D.S. On a new genus and six new species of Crustacea with observations on the development of the egg, and on the metamorphosis of *Caligus*, *Carcinus* and *Pagurus*. *Edinb. New Phil. J.* **1842**, *33*, 174–192.
17. Baird, W. *The Natural History of British Entomostraca*; No. 17; Ray Society: London, UK, 1850. [CrossRef]
18. Müller, F. Eine Beobachtung über die Beziehung der Gattungen *Caligus* und *Chalimus*. *Arch. Naturgesch.* **1852**, *18*, 91–92.
19. Hesse, E. Mémoire sur les moyens à l'aide desquels certaines Crustacés parasites assurent la conservation de leurs espèces. *Ann. Sci. Nat. Zool. Botan. Anatom. Phys.* **1858**, *4*, 120–125.
20. Von Nordmann, A. Neue Beiträge zur Kenntnis parasitischer Copepoden. *Bull. Soc. Imp. Natur. Moscou* **1864**, *37*, 461–520.
21. Gadd, P. Parasit-Copepoder i Finland. Master's Thesis, University of Helsinki, Helsinki, Finland, 1901.
22. Scott, A., VI. *Lepeophtheirus and Lernaea*; LMBC Memoirs: London, UK, 1901.
23. Wilson, C.B. North American parasitic copepods belonging to the family Caligidae—Part I. The Caliginae. *Proc. U. S. Natl. Mus.* **1905**, *28*, 479–672. [CrossRef]
24. Gurney, R. *British Fresh-Water Copepoda*; No. 3; Ray Society: London, UK, 1933.
25. Russell, F.S. LXX.—A new species of *Caligus* from Egypt, *Caligus pageti*, sp. n. *Ann. Mag. Nat. Hist.* **1925**, *9*, 611–618. [CrossRef]
26. Argilas, A. Un Copépode parasite de *Mugil auratus* Risso, nouveau pour l'Algerie: *Caligus pageti* Russel. *Bull. Trav. Sta. Aquic. Alger.* **1931**, *2*, 93–106.
27. Gurney, R. The development of certain parasitic Copepoda of the families Caligidae and Clavellidae. *Proc. Zool. Soc. Lond.* **1934**, *105*, 177–217. [CrossRef]
28. White, H.C. Life history of *Lepeophtheirus salmonis*. *J. Fish. Res. Board Can.* **1942**, *6*, 24–29. [CrossRef]

29. Heegaard, P. Contribution to the phylogeny of the arthropods; Copepoda. *Spolia Zool. Mus. Haun.* **1947**, *8*, 1–227.
30. Kabata, Z. Developmental stages of *Caligus clemensi* (Copepoda: Caligidae). *J. Fish. Res. Board. Can.* **1972**, *29*, 1571–1593. [CrossRef]
31. Kozikowska, Z. Skorupiaki pasożytnicze (*Crustacea parasitica*) Polski. Część I. Pasożyty ryb wód ujściowych Odry. *Zool. Polon.* **1957**, *8*, 217–270.
32. Lewis, A.G. Life history of the caligid copepod *Lepeophtheirus dissimulatus* Wilson, 1905 (Crustacea: Caligoida). *Pac. Sci.* **1963**, *17*, 195–242.
33. Ohtsuka, S.; Takami, I.; Venmathi Maran, B.A.; Ogawa, K.; Shimono, T.; Fujita, Y.; Asakawa, M.; Boxshall, G.A. Developmental stages and growth of *Pseudocaligus fugu* Yamaguti, 1936 (Copepoda: Siphonostomatoida: Caligidae) host-specific to puffer. *J. Nat. Hist.* **2009**, *43*, 1779–1804. [CrossRef]
34. Hwa, T.-K. Studies on the life history of a fish louse. *Acta Zool. Sin.* **1965**, *17*, 48–57. (In Chinese)
35. Izawa, K. Life history of *Caligus spinosus* Yamaguti, 1939 obtained from cultured yellow tail, *Seriola quinqueradiata* T. & S. (Crustacea: Caligoida). *Rep. Fac. Fish. Prefect. Univ. Mie* **1969**, *9*, 127–157.
36. Voth, D.R. Life history of the caligid copepod *Lepeophtheirus hospitalis* Fraser, 1920 (Crustacea: Caligoida). Ph.D. Thesis, Oregon State University, Corvallis, OR, USA, 1972.
37. Boxshall, G.A. The developmental stages of *Lepeophtheirus pectoralis* (Müller, 1776) (Copepoda: Caligidae). *J. Nat. Hist.* **1974**, *8*, 681–700. [CrossRef]
38. Caillet, C. Biologie Comparée de *Caligus minimus* Otto, 1848 et de *Clavellodes Macrotrachelus* (Brian, 1906), Copépods Parasites de Poissons Marins. Ph.D. Thesis, Université de Montpellier II (Université des Sciences et Techniques du Languedoc), Montpellier, France, 1979.
39. Wootten, R.; Smith, J.W.; Needham, E.A. Aspects of the biology of the parasitic copepods *Lepeophtheirus salmonis* and *Caligus elongatus* on farmed salmonids, and their treatment. *Proc. R. Soc. B* **1982**, *81*, 185–197. [CrossRef]
40. Ben Hassine, O.K. Les Copépodes Parasites de Poissons Mugilidae en Méditerranée Occidentale (Côtes Françaises et Tunisiennes); Morphologie, Bio-Écologie, Cycles Évolutifs. Ph.D. Thesis, Université de Montpellier II (Université des Sciences et Techniques du Languedoc), Montpellier, France, 1983.
41. Costello, M.J. The global economic cost of sea lice to the salmonid farming industry. *J. Fish Dis.* **2009**, *32*, 115–118. [CrossRef]
42. Bravo, S.; Erranz, F.; Silva, M.T. Comparison under controlled conditions of the life cycle of *Lepeophtheirus mugiloidis* and *Caligus rogercresseyi*, parasites of the Patagonian blenny *Eleginops maclovinus*. *Aquac. Res.* **2021**, *52*, 4198–4204. [CrossRef]
43. Boxshall, G.A.; Defaye, D. (Eds.) *Pathogens of Wild and Farmed Fish: Sea Lice*; Ellis Horwood: Chichester, UK, 1993.
44. Hogans, W.E.; Trudeau, D.J. Preliminary studies on the biology of sea lice, *Caligus elongatus*, *Caligus curtus* and *Lepeophtheirus salmonis* (Copepoda: Caligoida) parasitic on cage-cultured salmonids in the Lower Bay of Fundy. *Can. Tech. Rep. Fish. Aquat. Sci.* **1989**, *1715*, 14.
45. Piasecki, W.; MacKinnon, B.M. Changes in structure of the frontal filament in sequential developmental stages of *Caligus elongatus* von Nordmann, 1832 (Crustacea, Copepoda, Siphonostomatoida). *Can. J. Zool.* **1993**, *71*, 889–895. [CrossRef]
46. Ohtsuka, S.; Nawata, M.; Nishida, Y.; Nitta, M.; Hirano, K.; Adachi, K.; Kondo, Y.; Venmathi Maran, B.A.; Suárez-Morales, E. Discovery of the fish host of the 'planktonic' caligid *Caligus undulatus* Shen & Li, 1959 (Crustacea: Copepoda: Siphonostomatoida). *Biodivers. Data. J.* **2020**, *8*, e52271. [CrossRef]
47. Schram, T.A. 1990. Morten Anstensrud; 30 December 1957–27 March 1990. *J. Crustac. Biol.* **1990**, *10*, 751–752.
48. Bron, J.; Sommerville, C.; Jones, M.; Rae, G.H. The settlement and attachment of early stages of the salmon louse, *Lepeophtheirus salmonis* (Copepoda: Caligidae) on the salmon host, *Salmo salar*. *J. Zool.* **1991**, *224*, 201–212. [CrossRef]
49. Johnson, S.C.; Albright, L.J. The developmental stages of *Lepeophtheirus salmonis* (Krøyer, 1837) (Copepoda: Caligidae). *Can. J. Zool.* **1991**, *69*, 929–950. [CrossRef]
50. Johnson, S.C.; Albright, L.J. Development, growth, and survival of *Lepeophtheirus salmonis* (Copepoda: Caligidae) under laboratory conditions. *J. Mar. Biol. Assoc. UK* **1991**, *71*, 425–436. [CrossRef]
51. Ogawa, K. *Caligus longipedis* infection of cultured striped jack, *Pseudocaranx dentex* (Teleostei: Carangidae) in Japan. *Gyobyo Kenkyu* **1992**, *27*, 191–205. [CrossRef]
52. Lin, C.-L.; Ho, J.-S. Life history of *Caligus epidemicus* Hewitt parasitic on tilapia (*Oreochromis mossambicus*) cultured in brackish water. In *Pathogens of Wild and Farmed Fish: Sea Lice*; Boxshall, G.A., Defaye, D., Eds.; Ellis Horwood: Chichester, UK, 1993; pp. 5–15.
53. Kim, I.-H. Developmental stages of *Caligus punctatus* Shiino, 1955 (Copepoda: Caligidae). In *Pathogens of Wild and Farmed Fish: Sea Lice*; Boxshall, G.A., Defaye, D., Eds.; Ellis Horwood: Chichester, UK, 1993; pp. 16–29.
54. Schram, T.A. Supplementary descriptions of the developmental stages of *Lepeophtheirus salmonis* (Krøyer, 1837) (Copepoda: Caligidae). In *Pathogens of Wild and Farmed Fish: Sea Lice*; Boxshall, G.A., Defaye, D., Eds.; Ellis Horwood: Chichester, UK, 1993; pp. 30–47.
55. Pike, A.W.; Mordue (Luntz), A.J.; Ritchie, G. The development of *Caligus elongatus* Nordmann from hatching to copepodid in relation to temperature. In *Pathogens of Wild and Farmed Fish: Sea Lice*; Boxshall, G.A., Defaye, D., Eds.; Ellis Horwood: Chichester, UK, 1993; pp. 51–60.

56. Pike, A.W.; MacKenzie, K.; Rowand, A. Ultrastructure of the frontal filament in chalimus larvae of *Caligus elongatus* and *Lepeophtheirus salmonis* from Atlantic salmon, *Salmo salar*. In *Pathogens of Wild and Farmed Fish: Sea Lice*; Boxshall, G.A., Defaye, D., Eds.; Ellis Horwood: Chichester, UK, 1993; pp. 99–113.
57. Lin, C.-L.; Ho, J.-S.; Chen, S.-N. Developmental stages of *Caligus epidemicus* Hewitt, a copepod parasite of tilapia cultured in brackish water. *J. Nat. His.* **1996**, *30*, 661–684. [CrossRef]
58. Øines, Ø.; Heuch, P.A. Identification of sea louse species of the genus *Caligus* using mtDNA. *J. Mar. Biol. Assoc. UK* **2005**, *85*, 73–79. [CrossRef]
59. Øines, Ø.; Heuch, P.A. *Caligus elongatus* Nordmann genotypes on wild and farmed fish. *J. Fish Dis.* **2007**, *30*, 81–91. [CrossRef]
60. Øines, Ø.; Simonsen, J.H.; Knutsen, J.A.; Heuch, P.A. Host preference of *Caligus elongatus* Nordmann in the laboratory and its implications for Atlantic cod aquaculture. *J. Fish Dis.* **2006**, *29*, 167–174. [CrossRef]
61. Øines, Ø.; Schram, T. Intra- or inter-specific difference in genotypes of *Caligus elongatus* Nordmann 1832. *Acta Parasitol.* **2008**, *53*, 93–105. [CrossRef]
62. Piasecki, W.; MacKinnon, B.M. Life cycle of a sea louse, *Caligus elongatus* von Nordmann, 1832 (Copepoda, Siphonostomatoida, Caligidae). *Can. J. Zool.* **1995**, *73*, 74–82. [CrossRef]
63. Piasecki, W. The developmental stages of *Caligus elongatus* von Nordmann, 1832 (Copepoda: Caligidae). *Can. J. Zool.* **1996**, *74*, 1459–1478. [CrossRef]
64. Piasecki, W. *Cykl Rozwojowy Caligus elongatus von Nordmann, 1832 (Crustacea, Coepoda, Siphonostomatoida)*; Rozprawy No. 165; Akademia Rolnicza w Szczecinie: Szczecin, Poland, 1995; 69p.
65. Lin, C.-L.; Ho, J.-S.; Chen, S.N. Development of *Caligus multispinosus* Shen, a caligid copepod parasitic on the black sea bream (*Acanthopagrus schlegeli*) cultured in Taiwan. *J. Nat. Hist.* **1997**, *31*, 1483–1500. [CrossRef]
66. Ho, J.-S.; Lin, C.-L.; Chen, S.-N. Species of *Caligus* Müller, 1785 (Copepoda: Caligidae) parasitic on marine fishes of Taiwan. *Syst. Parasitol.* **2000**, *46*, 159–179. [CrossRef]
67. Gonzalez-Alanis, P.; Wright, G.M.; Johnson, S.C.; Burka, J.F. Frontal filament morphogenesis in the salmon louse *Lepeophtheirus salmonis*. *J. Parasitol.* **2001**, *87*, 561–574. [CrossRef]
68. González, L.; Carvajal, J. Life cycle of *Caligus rogercresseyi*, (Copepoda: Caligidae) parasite of Chilean reared salmonids. *Aquaculture* **2003**, *220*, 101–117. [CrossRef]
69. Ho, J.-S.; Lin, C.-L. *Sea Lice of Taiwan (Copepoda: Siphonostomatoida: Caligidae)*; Sueichan Press: Keelung, Taiwan, 2004.
70. Madinabeitia, I.; Nagasawa, K. Chalimus stages of *Caligus latigenitalis* (Copepoda: Caligidae) parasitic on blackhead seabream from Japanese waters, with discussion of terminology used for developmental stages of caligids. *J. Parasitol.* **2011**, *97*, 221–236. [CrossRef]
71. Hawksworth, D.L. Terms Used in Bionomenclature: The Naming of Organisms (and Plant Communities). Global Biodiversity Information Facility, Copenhagen Publication. 2010. Available online: http:/www.gbif.org/document/80577 (accessed on 29 November 2022).
72. Eichner, C.; Hamre, L.A.; Nilsen, F. Instar growth and molt increments in *Lepeophtheirus salmonis* (Copepoda: Caligidae) chalimus larvae. *Parasitol. Int.* **2015**, *64*, 86–96. [CrossRef]
73. Khoa, T.N.D.; Mazelan, S.; Muda, S.; Shaharom-Harrison, F. The life cycle of *Caligus minimus* on seabass (*Lates calcarifer*) from floating cage culture. *Thalassas* **2019**, *35*, 77–85. [CrossRef]
74. Hamre, L.A.; Bui, S.; Oppedal, F.; Skern-Mauritzen, R.; Dalvin, S. Development of the salmon louse *Lepeophtheirus salmonis* parasitic stages in temperatures ranging from 3 to 24 °C. *Aquac. Environ. Interact.* **2019**, *11*, 429–443. [CrossRef]
75. Hemmingsen, W.; MacKenzie, K.; Sagerup, K.; Remen, M.; Bloch-Hansen, K.; Imsland, A.K.D. *Caligus elongatus* and other sea lice of the genus *Caligus* as parasites of farmed salmonids: A review. *Aquaculture* **2020**, *522*, e735160. [CrossRef]
76. Jeong, J.; McEwan, G.F.; Arriagada, G.; Gallardo-Escárate, C.; Revie, C.W. Quantifying key parameters related to the life cycle of *Caligus rogercresseyi*. *J. Fish Dis.* **2022**, *45*, 219–224. [CrossRef] [PubMed]
77. Markewitsch, A.P. Les Crustacés parasites des poissons de la Mer Caspiènne. *Bull. l'Inst. Océanograph. Monaco* **1933**, *638*, 1–27.
78. Bere, R. Parasitic copepods from Gulf of Mexico fish. *Amer. Midl. Nat.* **1936**, *17*, 577–625. [CrossRef]
79. Gnanamuthu, C.P. Sex differences in the chalimus and adult forms of *Caligus polycanthi* sp. nov. (Crustacea: Copepoda) parasitic on *Balistes maculatus* from Madras. *Rec. Indian Mus.* **1950**, *47*, 159–170. [CrossRef]
80. Kaj, J. *Caligus lacustris* Stp. et Ltk. Materiały do znajomości pasożytniczych widłonogów Polski. *Pol. Arch. Hydrobiol.* **1953**, *1*, 45–48.
81. Hewitt, G.C. Two species of *Caligus* (Copepoda, Caligidae) from Australian waters, with a description of some developmental stages. *Pac. Sci.* **1971**, *25*, 145–164.
82. Lopez, G. Redescription and ontogeny of *Lepeophtheirus kareii* Yamaguti, 1936 (Copepoda, Caligoida). *Crustaceana* **1976**, *31*, 203–207. [CrossRef]
83. Johannessen, A. early stages of *Lepeophtheirus salmonis* (Copepoda, Caligidae). *Sarsia* **1978**, *63*, 169–176. [CrossRef]
84. Izawa, K. The copepodid and two chalimus stages of *Caligus latigenitalis* Shiino, 1954 (Copepoda, Siphonostomatoida, Caligidae), parasitic on Japanese black sea bream, *Acanthopagrus schlegeli*. *Contrib. Biol. Lab. Kyoto Univ.* **2004**, *29*, 329–341.
85. Jones, J.B. A redescription of *Caligus patulus* Wilson, 1937 (Copepoda: Caligidae) from a fish farm in the Philippines. *Syst. Parasitol.* **2004**, *2*, 103–116. [CrossRef]

86. Montory, J.A.; Cumillaf, J.P.; Cubillos, V.M.; Paschke, K.; Urbina, M.A.; Gebauer, P. Early development of the ectoparasite *Caligus rogercresseyi* under combined salinity and temperature gradients. *Aquaculture* **2018**, *486*, 68–74. [CrossRef]
87. Tully, O. The succession of generations and growth of the caligid copepods *Caligus elongatus* and *Lepeophtheirus salmonis* parasitizing farmed Atlantic salmon smolts (*Salmo salar* L.). *J. Mar. Biol. Assoc. UK* **1989**, *69*, 279–287. [CrossRef]
88. Boxshall, G.A. *Lepeophtheirus pectoralis* (O. F. Müller, 1776): A description, a review and some comparisons with the genus *Caligus* Müller, 1785. *J. Nat. Hist.* **1974**, *8*, 445–468. [CrossRef]
89. Jónsdóttir, H.; Bron, J.E.; Wootten, R.; Turnbull, J.F. The histopathology associated with the pre-adult and adult stages of *Lepeophtheirus salmonis* on the Atlantic salmon, *Salmo salar* L. *J. Fish Dis.* **1992**, *15*, 521–527. [CrossRef]
90. Johnson, S.C. Comparison of development and growth rates of *Lepeophtheirus salmonis*(Copepoda: Caligidae) on naive Atlantic (*Salmo salar*) and Chinook (*Oncorhynchus tshawytscha*) salmon. In *Pathogens of Wild and Farmed Fish: Sea Lice*; Boxshall, G.A., Defaye, D., Eds.; Ellis Horwood: Chichester, UK, 1993; pp. 68–142.
91. Bjørn, P.; Finstad, B. The development of salmon lice (*Lepeophtheirus salmonis*) on artificially infected post smolts of sea trout (*Salmo trutta*). *Can. J. Zool.* **1998**, *76*, 970–977. [CrossRef]
92. Pike, A.W.; Wadsworth, S. Sealice on salmonids: Their biology and control. *Adv. Parasitol.* **1999**, *44*, 233–337. [CrossRef]
93. Schram, T.A. Practical identification of pelagic sea lice larvae. *J. Mar. Biol. Assoc. UK* **2004**, *84*, 103–110. [CrossRef]
94. Beamish, R.; Neville, C.M.; Sweeting, R.M.; Jones, S.R.M.; Ambers, N.; Gordon, E.K.; Hunter, K.L.; McDonald, T.E. Proposed life history strategy for the salmon louse, *Lepeophtheirus salmonis* in the subarctic Pacific. *Aquaculture* **2007**, *264*, 428–440. [CrossRef]
95. Pedaschenko, D.D. Èmbrional'noe razvitie i metamorfoz" *Lernaea branchialis*. Die Embryonalentwicklung und Metamorphose von *Lernaea branchialis*. *Trudý Imp. St.-Petersbg. Obshch. Estest. Zoolog.* **1898**, *26*, 1–307.
96. Piasecki, W. Life cycle of *Tracheliastes maculatus* Kollar, 1835 (Copepoda, Siphonostomatoida, Lernaeopodidae). *Wiad. Parazytol.* **1989**, *35*, 187–245. [PubMed]
97. Piasecki, W.; Kuźmińska, E. Developmental stages of *Achtheres percarum* (Crustacea: Copepoda), parasitic on European perch, *Perca fluviatilis* (Actinopterygii: Perciformes). *Acta Ichthyol. Piscat.* **2007**, *37*, 117–128. [CrossRef]
98. Huys, R.; Llewellyn-Hughes, J.; Conroy-Dalton, S.; Olson, P.D.; Spinks, J.N.; Johnston, D.A. Extraordinary host switching in siphonostomatoid copepods and the demise of the Monstrilloida: Integrating molecular data, ontogeny and antennulary morphology. *Mol. Phylogenetics Evol.* **2007**, *43*, 368–378. [CrossRef] [PubMed]
99. Kakui, K.; Munakata, M. A new *Sphaeronella* species (Copepoda: Siphonostomatoida: Nicothoidae) parasitic on *Euphilomedes* sp. (Ostracoda: Myodocopa: Philomedidae) from Hokkaido, Japan, with an 18S molecular phylogeny. *Syst. Parasitol.* **2023**, *100*, 121–131. [CrossRef]

pathogens

MDPI

Article

Limnotrachelobdella hypophthalmichthysa n. sp. (Hirudinida: Piscicolidae) on Gills of Bighead Carp *Hypophthalmichthys nobilis* in China

Lin Lin [1,2], Houda Cheng [2,3], Wenxiang Li [2,3], Ming Li [2], Hong Zou [2] and Guitang Wang [2,3,*]

[1] College of Fisheries, Huazhong Agricultural University, Wuhan 430070, China
[2] State Key Laboratory of Freshwater Ecology and Biotechnology and Key Laboratory of Aquaculture Disease Control, Ministry of Agriculture, Institute of Hydrobiology, Chinese Academy of Sciences, Wuhan 430072, China
[3] College of Advanced Agricultural Science, University of Chinese Academy of Sciences, Beijing 100049, China
* Correspondence: gtwang@ihb.ac.cn

Abstract: We describe the characterization of a novel fish leech species found on the gills of bighead carp (*Hypophthalmichthys nobilis*) from lakes and reservoirs in China. This leech is morphologically similar to *Limnotrachelobdella sinensis* recorded on goldfish and common carp. However, there are 0–2 pairs of symmetrical or asymmetrical eyes and 10 pairs of pulsatile vesicles in the newly discovered leech, in remarkable contrast to *L. sinensis*. Except for bighead carp, where it demonstrated a higher than 90% prevalence, and silver carp (*H. molitrix*), where there was low infection, this leech was not detected on any other fish from the Qiandao reservoir in China that were examined during this investigation. Molecular analyses indicated 87.8% ITS sequence identity with *L. sinensis* and 85.0 and 86.1% COX1 sequence identity with *L. sinensis* and *L. okae*, respectively. The uncorrected p-distance based on the COX1 sequence was found to be 15.1 and 14.0% for *L. sinensis* and *L. okae*, respectively, suggesting interspecific variation. Phylogenetic analyses based on the combination of 18S and COX1 sequences showed that the newly discovered leech groups with *Limnotrachelobdella* species. Histopathological observation indicated that attachment of the leech on the gill rakers and gill arches causes a loss of connective tissue, hemorrhage, and ulceration. Based on the morphology, molecular analyses, and host specificity, we conclude that this leech is a new species of *Limnotrachelobdella* and named it *Limnotrachelobdella hypophthalmichthysa* n. sp.

Keywords: fish leech; species identification; *Hypophthalmichthys nobilis*; *Limnotrachelobdella hypophthalmichthysa*

1. Introduction

Leeches (Annelida: Hirudinida) are usually found in freshwater, estuarine, terrestrial, and marine ecosystems [1]. Species of leeches of the genera *Piscicola* and *Limnotrachelobdella* (Rhynchobdellida: Piscicolidae) tend to parasitize marine and freshwater fish [2–5]. Fish leeches have been suggested as pathogens to hosts [6], causing severe epidermal erosion on the attachment and secondary infection of viruses or bacteria [5,7]. The heavy infestation of leeches can even cause the mortality of hosts [8,9].

It has traditionally been accepted that there are three subfamily members in Piscicolidae: Piscicolinae Johnston, 1865; Platybdellinae Epshtein, 1970; and Pontobdellinae Llewellyn, 1966. However, according to the latest phylogenetic analyses, Piscicolinae and Platybdellinae are both now considered to be polyphyletic groups based on their nuclear and mitochondrial gene sequences and morphology [10,11]. *Limnotrachelobdella*, belonging to Piscicolidae, comprises five nominal species: *L. sinensis* (Blanchard, 1896) [12], *L. okae* (Moore, 1924) [13], *L. taimeni* (Epstein 1957) [14], *L. fujianensis* (Yang, 1987) [15], and

L. turkestanica (Stschegolew, 1912) [16]. The first four species have been previously found in China [17].

In recent years, a kind of leech was only found on the bighead carp, *Hypophthalmichthys nobilis* (Richardson, 1845), in reservoirs and lakes in China. A preliminary investigation showed that this leech is morphologically similar to *L. sinensis*, which has been recorded on goldfish (*Carassius auratus*) and common carp *(Cyprinus carpio)* in China [15]. However, the leech found on bighead carp is distinct from *L. sinensis* and has not been found on goldfish or common carp during investigations. Therefore, the leech on bighead carp was identified by its morphological characteristics and further characterized based on molecular sequence analyses as well histopathological observation.

2. Materials and Methods

2.1. Sample Collection and Preservation

Fish were collected for the examination of leeches in the Qiandao reservoir (29°33′44.32″ N, 119°01′51.98″ E), Zhejiang province, China, during 2021–2022. Leeches were detached from fish gills using forceps. Living leeches were stocked in fresh water for morphological analyses. Some leeches were preserved in 100% ethanol and stored at −20 °C for DNA extraction, including one specimen each from Hubei and Jiangxi provinces. In addition, gills infected with leeches were preserved in 4% paraformaldehyde for histopathological observation.

2.2. Morphological Identification

First, living leeches were examined for the number of eyes within 48 h after detachment from gills. Then, specimens were anesthetized by adding ethanol in a dropwise manner for a subsequent observation of the digestive and reproductive system under a stereomicroscope. The epidermis of the slack leech was separated using a scalpel applied along the longitudinal centerline dorsally or ventrally. The ventral nerve cord was then separated from the epidermis using ophthalmic forceps to determine its positional relationship to the reproductive and digestive systems. The digestive system was directly observed in small leeches collected from December to February when it has thinner and more transparent muscle layers. In addition, specimens fixed in 4% paraformaldehyde were photographed using a Panasonic DMC-GX85CGK digital camera. The materials were deposited in the collection of the Institute of Hydrobiology, Chinese Academy of Science, Hubei, China [Holotype (accession no. LH-Z3) and four paratypes (accession nos. LH-Z2, Z4, H1, and J1)].

2.3. Histopathological Observation

Gills fixed in 4% paraformaldehyde were trimmed into 1 cm × 1 cm tissue blocks and dehydrated using a series of graded ethanol solutions and cleared in xylene. After the paraffin wax solidified, 4 μm paraffin sections were taken and mounted on slides for hematoxylin and eosin (H and E) staining. The slides were subsequently examined under a stereomicroscope.

2.4. DNA Extraction, Amplification, and Sequencing

Muscles of the lateral body and caudal sucker were removed for DNA extraction to avoid the presence of host blood in the leech gut. Genomic DNA was isolated using an Aidlab Genomic DNA extraction kit (Aidlab Co., Beijing, China) according to the manufacturer's instructions. Ribosomal encoded genes, including the 18S DNA gene, internal transcribed spacer 1–5.8S rDNA—internal transcribed spacer 2 (ITS) and fragments of the mitochondrial gene, cytochrome c oxidase subunit I (COX1), were amplified from the genomic DNA. All the genes used, following polymerase chain reaction (PCR) condition, were according to the manufacturer's instructions (Takara Bio, China): 98 °C for 2 min, 40 cycles of 98 °C for 10 s, 50 °C for 15 s, and 68 °C for 1 min, and final extension at 68 °C for 10 min. Primer pairs were designed according to the sequence in similar species (Table 1). PCR products were sequenced using an ABI 3730 automatic sequencer (Sanger

Sequencing). The sequences were assembled manually using DNAstar software v7.1 (Madison, Wisconsin, USA).

Table 1. List of the primers and accession numbers of genes used in this study.

Gene or Region	Primer Name	Sequence (5′-3′)	Accession Number (Gene Length)		
			Limnotrachelobdella hypophthalmichthysa n. sp.		
			Z1	H1	J1
18S	18SF 18SR	5′-GATTAAGCCATGCATGTCTA-3′ 5′-ACTTCCTCTAGATGATCAAG-3′	OP595730 (1712 bp)	OP709950 (1712 bp)	OP709959 (1713 bp)
ITS	ITSF ITSR	5′-TCGCGTTGATTACGTCCCTG-3′ 5′-GCATTCTCAAACAACCCGAC-3′	OP723914 (1495 bp)	OP723913 (1490 bp)	OP723912 (1489 bp)
COX1	COX1F COX1R	5′-GCTTCTAACTTTTAGTRGRTAG-3′ 5′-CTTCTARTTAACAGTTAGRTGCA-3′	OP711958 (1537 bp)	OP712182 (1537 bp)	OP712183 (1537 bp)

2.5. Molecular Identification and Phylogenetic Analyses

Fish were collected for leech examination in the Qiandao reservoir (29°33′44.32″ N, 119°01′51.98″ E), Zhejiang province, China, during 2021–2022. For molecular analyses, ITS and COX1 were chosen to compare specimens collected from three places: Zhejiang, Hubei, and Jiangxi provinces. In addition, the new species' similarity to *L. sinensis* and *L. okae* was verified in the NCBI GenBank database. The uncorrected p-distance was used to examine COX1 genetic variation among *Limnotrachelobdella* species with 1000 replicates in MEGA11 [18].

Phylogenetic analyses were performed, combining 18S and COX1 gene datasets using 29 sequences of Piscicolidae leech species from GenBank (Table 2). All of the sequences were imported into PhyloSuite [19] and aligned using MAFFT 7.149 [20] with auto strategy and normal alignment mode; further adjustments to sequence alignments were manually applied. Then, the 18S and COX1 sequences were concatenated using the "concatenate sequence" function in PhyloSuite. The best partitioning scheme and evolutionary models for 2 predefined partitions were selected using PartitionFinder2 [21] with a greedy algorithm. Bayesian inference (BI) phylogenies were inferred using MrBayes 3.2.6 [22] under the partition model (2 parallel runs, 100,000 generations), with the initial 25% of sampled data discarded as burn-in and sampling frequency of 3000.

Table 2. Species used in phylogenetic analyses with details of their environment and GenBank accession number. *L. hypophthalmichthysa* n. sp. Z1, H1, and J1 were collected from Zhejiang, Hubei, and Jiangxi, respectively.

Species	Environment	GenBank Accession Number	
		18S	COX1
Ingroup			
Piscicolidae			
Stibarobdella macrothela	Brackish to marine	DQ414295	DQ414340
Pontobdella muricata	Marine	AF099945	AY336029
Aestabdella abditovesiculata	Marine	DQ414254	DQ414300
Austrobdella bilobata	Marine	DQ414255	DQ414301
Bathybdella sawyeri	Marine	DQ414265	DQ414311
Beringobdella rectangulata	Marine	DQ414264	DQ414310
Heptacyclus virgatus	Brackish to marine	DQ414273	DQ414319
Janusion virida	Marine	DQ414281	N/A
Myzobdella lugubris	Freshwater to marine	DQ414278	DQ414324
Notobdella nototheniae	Marine	DQ414283	DQ414328
Oceanobdella khani	Marine	DQ414286	DQ414331
Oxytonostoma typica	Marine	DQ414288	DQ414333
Piscicolaria reducta	Freshwater	DQ414294	DQ414339
Platybdella anarrhichae	Marine	DQ414290	DQ414335
Pterobdella amara	Brackish	DQ414289	DQ414334
Trulliobdella capitis	Marine	N/A	AY336030

Table 2. *Cont.*

Species	Environment	GenBank Accession Number	
		18S	COX1
Zeylanicobdella arugamensis	Brackish to marine	DQ414299	DQ414344
Alexandrobdella makhrovi	Freshwater	MN312187	MN295413
Baicalobdella torquata	Freshwater	N/A	AY336018
Branchellion lobata	Marine	DQ414261	DQ414307
Calliobdella lophii	Marine	DQ414268	DQ414314
Caspiobdella fadejewi	Freshwater	N/A	AY336019
Cystobranchus meyeri	Freshwater	DQ414269	DQ414315
Gonimosobdella vivida	Freshwater	AF115992	AF003260
Johanssonia arctica	Marine	DQ414274	DQ414320
Limnotrachelobdella hypophthalmichthysa n. sp. Z1	Freshwater	OP595730	OP711958
Limnotrachelobdella hypophthalmichthysa n. sp. H1		OP709950	OP712182
Limnotrachelobdella hypophthalmichthysa n. sp. J1		OP709959	OP712183
Limnotrachelobdella okae	Freshwater to marine	N/A	AY336022
Limnotrachelobdella sinensis	Freshwater to brackish	LC275139	LC275140
Piscicola geometra	Freshwater to marine	AF115995	AF003280
Trachelobdellina glabra	Marine	N/A	EF405597
Outgroup			
Ozobranchidae			
Ozobranchus branchiatus	Marine	KF728214	KF728213
Ozobranchus margoi	Marine	AF115991	AF003268

3. Results

3.1. Infection by Fish Leeches

In total, 16 species of fish from the Qiandao reservoir were examined, including *Carassius auratus*, *Megalobrama amblycephala*, and *Opsariichthys bidens*. Fish leeches were found on bighead carp at higher than 90% prevalence and silver carp (*Hypophthalmichthys molitrix*) at extremely low prevalence (only one silver carp infected with one leech).

3.2. Description

External morphology: The body distinctly divides into trachelosome and urosome, with a total length of 4.6–70.3 mm and width of 0.9–16.2 mm (Figure 1A). Body skin is smooth, but with numerous brown pigments on the surface of the trachelosome region (Figure 2B). Body color of the living leech is reddish or reddish brown (Figure 1B). Eyes, 0–2 pairs, symmetrical or asymmetrical or degenerated eyes on oral sucker (Figure 2B–F). Clitellum is ring-like, sharply distinct from pre-clitellum and urosome. In the urosome region, the body musculature is well developed. Complete somite is composed of six annuli, but the external appearance suggests it is divided into fourteen annuli, which is consistent with *L. sinensis*. Grape-like tissue is present in the area before somite XXII in the mature individuals. Pulsatile vesicles are of 10 pairs, present separately on each somite of somites XIV–XXIII and matched against sequential numbers of the ventral nerve cord ganglion, respectively. Caudal sucker is deep cup-like, thick, and ventrally directed, and its diameter is smaller than the maximum body width. Anal is separated by the last two annuli of somite XXVII and is difficult to be observed.

Figure 1. Whole view of preserved and fresh *Limnotrachelobdella hypophthalmichthysa* n. sp. (**A**) Specimen preserved in 4% paraformaldehyde, ventral (left) and dorsal (right) view. Numbers indicate 10 pairs of pulsatile vesicles. Scale bar, 1 cm. (**B**) Fresh *L. hypophthalmichthysa* n. sp. attached to gill rakers and arches of bighead carp *Hypophthalmichthys nobilis*.

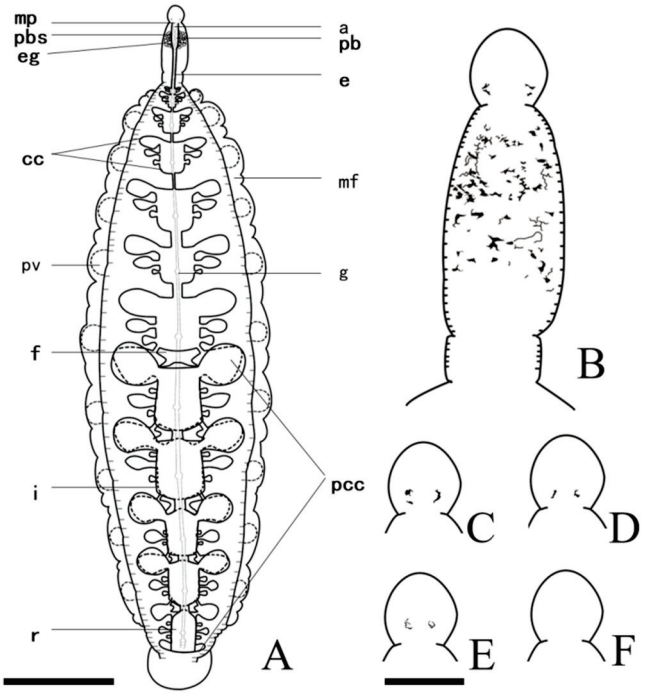

Figure 2. Digestive system, eyes, and pigment of *Limnotrachelobdella hypophthalmichthysa* n. sp. (**A**) Digestive system and overall structure. Patterns of eyes and pigment: (**B**) 2 pairs of eyes, (**C**) right eyes of 2 pairs slightly fused, (**D**) 1 pair of eyes, (**E**) degenerated eyes, and (**F**) no eyes (**F**). Abbreviations: cc, crop chamber; e, esophagus; eg, esophageal gland; f, fenestrae; g, ganglion of ventral nerve cord; a, anterior nerve mass; i, intestine; mf, margin fold; mp, mouthpore; pb, proboscis; pcc, posterior crop caeca; r, rectum; pbs, proboscis sheath; pv, pulsatile vesicle. Parts of digestive system shown in bold type. Scale bar: A, 1 cm; B–F; 2 mm.

Internal morphology: Esophagus passes posteriorly from the proboscis to somite XI. Crop extends from somite XIII, and with seven chambers, each with three pairs of pouches (the first two bigger than the last). Posterior crop caeca fused with five fenestraes, forming

five well-developed chambers similar to crop chambers. Intestine consists of four chambers without lateral pouches (Figure 2A). Male gonopore is large, round and crinkled. Female gonopore is below the male gonopore, particularly smaller, and elliptical (Figure 3C). Because of the smooth skin of the clitellum, it was difficult to determine the number of annuli between the two gonopores. Testisacs are five pairs, elliptical in shape, located on somites XIV–XVIII and alternating with crop caeca, slightly posterior to the ganglion of the ventral nerve cord (Figure 3A). Ejaculatory duct and atrial cornua are both in kidney-like shape. Accessory gland cells are absent. Common atrium is near-spherical, connecting a thick and large bursa that leads to the male gonopore. The ejaculatory duct, atrial cornua, and common atrium are all semitranslucent and threaded before fixation and are often wrapped by the brusa, then evert out of the male gonopore (Figure 3B). Conducting tissue and vector tissue are absent. Paired ovisacs are sac-like, extending to somite XV. Each ovisac consists of three lobes with the third lobe the largest.

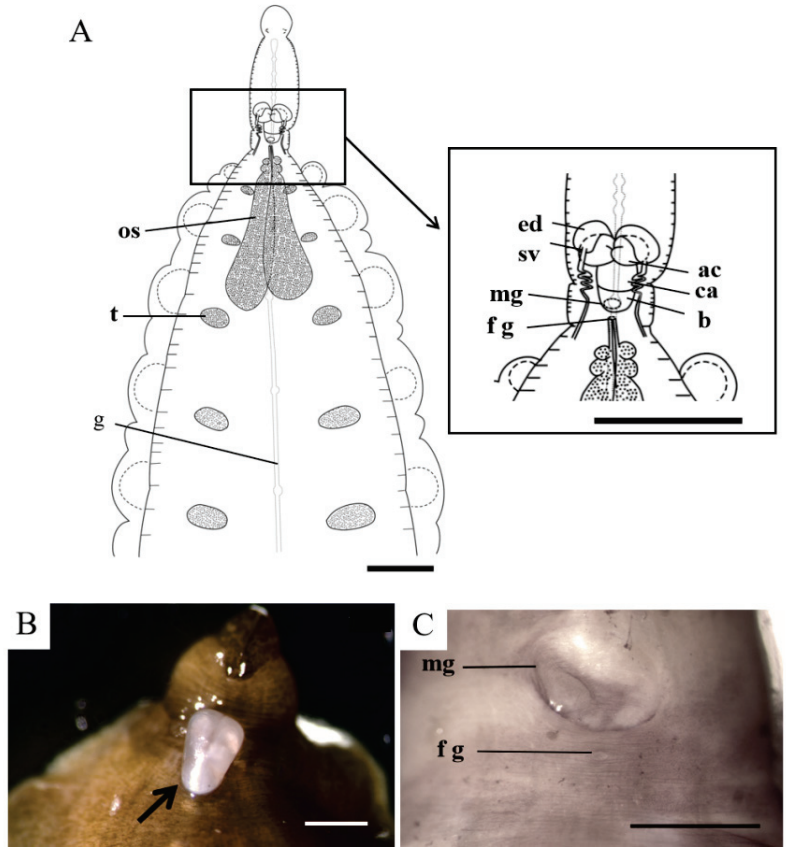

Figure 3. Reproductive system of *Limnotrachelobdella hypophthalmichthysa* n. sp. (**A**) Overall dorsal view of reproductive system (left) and reproductive organs in trachelosome region (right). (**B**) Ejaculatory duct, atrial cornua, and common atrium, wrapped by bursa, evert out of male gonopore (arrow). (**C**) Male and female gonopores. Abbreviations: ac, atrial cornua; b, bursa; ca, common atrium; ed, ejaculatory duct; fg, female gonopore; g, ganglion of ventral nerve cord; os, ovisac; mp, male gonopore; t, testisac; sv, seminal vesicle. Part of reproductive system shown in bold type. Scale bars: A, 3 mm; B, 2 mm; C, 1 mm.

3.3. Molecular Identification and Phylogenetic Analyses

From the three specimens (Z1, H1 and J1), the 18S rDNA (1712–1713 bp), ITS (1489–1495 bp), and COX1 (1537 bp) genes sequence were obtained. Molecular analyses indicate that the ITS and COX1 sequence identity of the three specimens (collected from Zhejiang, Hubei, and Jiangxi) ranges from 98.6 to 99.7%. The new leech shares 87.8% of ITS sequence identity with *L. sinensis* and 85.0 and 86.1% of COX1 sequence identity with *L. sinensis* and *L. okae*, respectively. The uncorrected p-distance of COX1 sequence was found to be 0.3%

for the three specimens in pairwise comparison, and 15.1 and 14.1% with *L. sinensis* and *L. okae*, respectively.

The phylogenetic tree produced by BI analyses of a combination of 18S and COX1 sequences indicates that *L. hypophthalmichthysa* n. sp. groups with *L. sinensis* and *L. okae* (Figure 4).

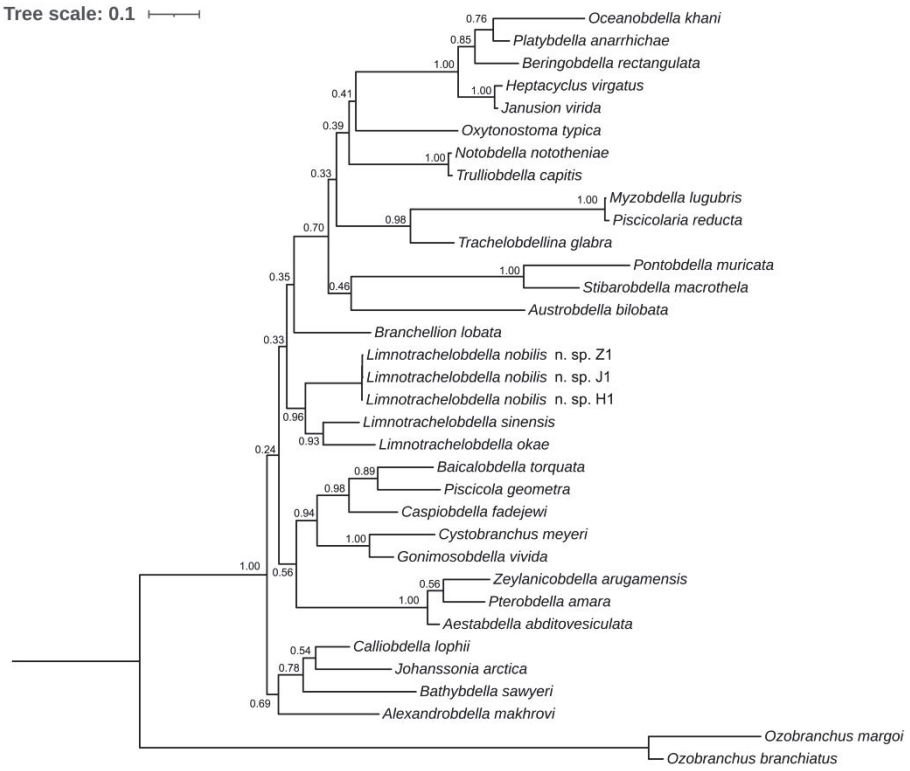

Figure 4. BI tree resulting from the analyses of combined 18S rDNA and COX1 data containing *Limnotrachelobdella hypophthalmichthysa* n. sp. and related species of the Piscicolidae family. *Ozobranchus margoi* and *O. branchiatus*, of the same suborder, and Oceanobdelliformes are chosen as outgroups. Node numbers represent Bayesian posterior probabilities. *L. hypophthalmichthysa* n. sp. specimens were collected from three places (Z1 from Zhejiang, H1 from Hubei, J1 from Jiangxi).

3.4. Taxonomic Summary

Family: Piscicolidae Johnston, 1865.

Genus: *Limnotrachelobdella* Epshtein, 1968.

Species: *Limnotrachelobdella hypophthalmichthysa* n. sp.

Type host: *Hypophthalmichthys nobilis* (Richardson, 1845).

Type locality: Qiandao reservoir (29°33′44.32″ N, 119°01′51.98″ E), Zhejiang province, China.

Type material: Holotype (accession no. LH-Z3) and four paratypes (accession nos. LH-Z2, Z4, H1, and J1) were deposited in the Museum of the Institute of Hydrobiology, Chinese Academy of Sciences, China.

Infection site on host: Gill arch and gill raker.

ZooBank registration: The Life Science Identifier (LSID) for *Limnotrachelobdella hypophthalmichthysa* n. sp. is urn:lsid:zoobank.org:act:5996B408-EB5E-4470-974C-30962DF5D041.

Etymology: The species name is derived from the genus name of fish hosts *Hypophthalmichthys nobilis* (Richardson, 1845) and *Hypophthalmichthys molitrix* (Valenciennes, 1844).

3.5. Histopathological Analyses

Attachment of the leeches on gill rakers and gill arches with the caudal sucker causes loss of connective tissue (Figure 5A). Hemorrhage and ulceration were also observed on gills infected by leeches (Figure 5B).

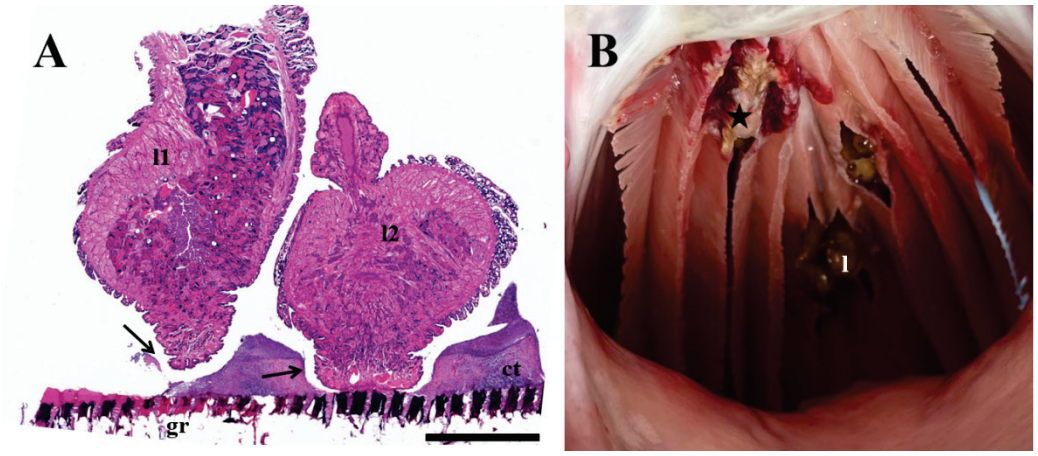

Figure 5. Histopathology of bighead carp *Hypophthalmichthys nobilis* parasitized by *Limnotrachelobdella hypophthalmichthysa* n. sp. (**A**) Gill raker section (H and E stained) infected by two *L. hypophthalmichthysa* n. sp. (l1, l2), with eroded connective tissue (arrows). Scale bar: 200 mm. (**B**) Ulceration and hemorrhage at attachment site of leeches (star). Abbreviations: ct, connective tissue; gr, gill raker; l, leech.

4. Discussion

Yang [17] presented identification keys for the genus *Limnotrachelobdella*: the distinction between trachelosome and urosome, deeply cup-shaped caudal sucker with a smaller diameter than the maximum width of the body, six annuli in each complete somite, ten to thirteen pairs of pulsatile vesicles on the urosome, a fused posterior crop caeca, and five to six pairs of testisacs. The morphological identification of the fish leeches we collected revealed conformance to these features. So far, five nominal species of *Limnotrachelobdella* have been recorded: *L. sinensis* (Blanchard, 1896), *L. okae* (Moore, 1924), *L. taimeni* (Epshtein, 1957), *L. fujianensis* (Yang, 1987), and *L. turkestanica* (Stschegolew, 1912). Owing to its similar appearance, fish leech *L. hypophthalmichthysa* n. sp. collected from bighead carp can be easily mistaken for *L. sinensis*. However, it has 10 pairs of pulsatile vesicles, while the latter has 11 pairs. Meanwhile, the following characteristics are helpful in distinguishing it from five known species: no eyes or one to two pairs of symmetrical, asymmetrical, or degenerated eyes, seven pairs of crop caeca, and five pairs of testisacs (Table 3). In addition, there are numerous brown pigments on the surface of the trachelosome region, and the appearance of the atrial cornua, which extends dorsally, is typical.

Table 3. Comparison of morphological differences among six species of *Limnotrachelobdella*.

	***L. hypophthalmichthysa* n. sp.**	***L. sinensis***	***L. okae***	***L. taimeni***	***L. fujianensis***	***L. turkestanica***
Eyes	0–2	2	2	0 *	2	N/A
Pulsatile vesicles	10	11	11–13	10	12	11
Testisacs	5	6	6	N/A	6	5

* Uncertain. N/A, not available.

L. hypophthalmichthysa n. sp. is also different from other *Limnotrachelobdella* species in terms of its host range. *L. sinensis* has been recorded on goldfish/silver crucian carp such as *Carassius auratus* and *C. cuvieri* in Korea [23–25], *C. cuvieri* and *C. auratus langsdorfii* in

Japan [7,26], and *C. gibelio* in Russia [17,27]. *L. sinensis* has also been found on common carp such as *Cyprinus carpio* in China [15] and Japan [28] and *C. carpio haematopterus* in Russia [20,27]. Meanwhile, *L. taimeni* was found on *Hucho taimen* (Pallas, 1773) [14] and *L. fujianensis* was found on *Epinephelus akaara* (Temminck and Schlegel, 1842) and *Planiliza affinis* (Gunther, 1861) [15,17], respectively. However, *L. okae* was recorded on fish in the Acipenseridae, Cyprinidae, Salmonidae, Lateolabracidae, Carangidae, Paralichthyidae, and Tetraodontidae families [29,30], exhibiting a wide host range. *L. turkestanica* was also considered to have a wide range of fish hosts [31,32]. Therefore, unlike *L. okae* and *L. turkestanica*, *L. sinensis*, *L. taimeni*, and *L. fujianensis* are fish leeches with high host specificity. *L. hypophthalmichthysa* n. sp. has only been found on *Hypophthalmichthys nobilis* and *H. molitrix*, which suggests that it is a highly host-specific species. In addition, *L. sinensis* was found on the operculums of goldfish and common carp [7,26,28], whereas the leech representing the focus of this study has been found on gill arches and gill rakers of bighead carp. Therefore, its different host species and infection sites compared with *L. sinensis* suggests that this leech is a new species.

The ITS sequences of the species in genus *Whitmania* (Hirudinida: Haemopidae) (*W. acranulata*, JX885692; *W. laevis*, JX885693; *W. plgra*, EU652726) was obtained on Genbank database and the 92.7 to 98.4% of sequence identity could be calculated easily. In this study, the high ITS sequence identity of 98.6 to 99.5% of the specimens from Zhejiang, Hubei, and Jiangxi indicates that they are of the same species. However, only 87.8% ITS sequence identity was found between the new leech and *L. sinensis*, which was smaller than the range of interspecific divergence in genus *Whitmania*. Based on the COX1 sequence, the uncorrected p-distance is 15.1% with *L. sinensis* and 14.0% with *L. okae*, which are higher than the intraspecific divergence of 0.3% for specimens of the new leech from Zhejiang, Hubei, and Jiangxi. For COX1, a 2.0% genetic distance was found to be indicative of intraspecific divergence [33–35], with interspecific divergence of 13.3 to 23.6% between *Helobdella blinni* (Hirudinidea: Glossiphoniidae) and other species in the genus *Helobdella* [36]. In the present study, the p-distance of 14.0 to 15.1% is within this range of interspecific divergence. Therefore, the low ITS sequence identity and high genetic distance between the new leech and other species in *Limnotrachelobdella* provides molecular evidence that the leech found on bighead carp is a novel species of the genus *Limnotrachelobdella*.

Williams and Burreson [11] attempted to sequence 18S rDNA, COX1, and ND1 gene data of a large number of species in Piscicolidae and illuminated the phylogeny of the family by considering the sequences above in combination with morphological data. In this study, the BI tree is consistent with our expectations, implying that *L. hypophthalmichthysa* n. sp. groups together with *L. sinensis* and *L. okae*.

In summary, based on the morphology, molecular analyses, host specificity, and infection site, the leech infecting bighead carp is a novel species of *Limnotrachelobdella*, which we named *Limnotrachelobdella hypophthalmichthysa* n. sp.

Author Contributions: L.L. and G.W. designed the experiments. L.L. performed the experiments, analyzed the data, and wrote the paper. H.C. assisted with data analyses. W.L., M.L. and H.Z. reviewed and revised the paper. All authors have read and agreed to the published version of the manuscript.

Funding: This work was funded by an earmarked fund for CARS (CARS-45), the National Natural Science Foundation of China (No. 32230109), and the Qiandao Reservoir Fish Parasitic Disease Prevention and Control Project (No. E141030101).

Institutional Review Board Statement: The animal study protocol was approved by the Animal Ethics Committee of the Institute of Hydrobiology, Chinese Academy of Sciences (project identification code: IHB/LL/2020025; date of approval: 27 July 2022).

Informed Consent Statement: Written informed consent has been obtained from the patient(s) to publish this paper.

Data Availability Statement: Data are available from the authors upon reasonable request.

Acknowledgments: The authors would like to thank Qiandao Lake Development Group Co., Ltd., Hangzhou, P.R. China, for assistance with the collection of leeches. We are also very grateful to an anonymous reviewer for helpful suggestions.

Conflicts of Interest: The authors declare no conflict of interest.

References

1. Bottari, T.; Profeta, A.; Rinelli, P.; Gaglio, G.; La Spada, G.; Smedile, F.; Giordano, D. On the presence of *Pontobdella muricata* (Hirudinea: Piscicolidae) on some elasmobranchs of the Tyrrhenian Sea (Central Mediterranean). *Acta Adriat.* **2017**, *58*, 225–234. [CrossRef]
2. SIDDALL, M.E. Phylogeny of adeleid blood parasites with a partial systematic revision of the haemogregarine complex. *J. Eukaryot. Microbiol.* **1995**, *42*, 116–125. [CrossRef]
3. Karlsbakk, E. A trypanosome of Atlantic cod, Gadus morhua L., transmitted by the marine leech *Calliobdella nodulifera* (Malm, 1863) (Piscicolidae). *Parasitol. Res.* **2004**, *93*, 155–158. [CrossRef]
4. Siddall, M.E.; Desser, S.S. Ultrastructure of merogonic development of *Haemogregarina* (sensu lato) *myoxocephali* (Apicomplexa: Adeleina) in the marine leech *Malmiana scorpii* and localization of infective stages in the salivary cells. *Eur. J. Protistol.* **1993**, *29*, 191–201. [CrossRef]
5. Karlsbakk, E.; Haugen, E.; Nylund, A. Morphology and aspects of growth of a trypanosome transmitted by the marine leech *Johanssonia arctica* (Piscicolidae) from Northern Norway. *Folia Parasitol.* **2005**, *52*, 209. [CrossRef]
6. Burreson, E.M. Phylum Annelida: Hirudinea as vectors and disease agents. In *Fish Diseases and Disorders. Volume 1: Protozoan and Metazoan Infections*; CABI: Wallingford, UK, 2006.
7. Kazuo, O.; Olga, R.; Masaharu, T. New Record of the Leech *Limnotrachelobdella sinensis* Infecting Freshwater Fish from Japanese Waters. *Fish Pathol.* **2007**, *42*, 85–89. [CrossRef]
8. Kua, B. Marine leech isolated from cage-cultured sea bass (*Lates calcarifer*) fingerlings: A parasite or vector? *Malay. Fish. J.* **2009**. Available online: https://cir.nii.ac.jp/crid/1571417126167425280 (accessed on 1 January 2020).
9. Cruz-Lacierda, E.R.; Toledo, J.D.; Tan-Fermin, J.D.; Burreson, E.M. Marine leech (*Zeylanicobdella arugamensis*) infestation in cultured orange-spotted grouper, *Epinephelus coioides*. *Aquaculture* **2000**, *185*, 191–196. [CrossRef]
10. Utevsky, S.Y.; Trontelj, P. Phylogenetic relationships of fish leeches (Hirudinea, Piscicolidae) based on mitochondrial DNA sequences and morphological data. *Zool. Scr.* **2004**, *33*, 375–385. [CrossRef]
11. Williams, J.I.; Burreson, E.M. Phylogeny of the fish leeches (Oligochaeta, Hirudinida, Piscicolidae) based on nuclear and mitochondrial genes and morphology. *Zool. Scr.* **2006**, *35*, 627–639. [CrossRef]
12. Blanchard, R. Description de quelques Hirudinees asiatiques. *Mem. Soc. Zool. Fr.* **1896**, *9*, 316–330.
13. Moore, J.P. Notes on some Asiatic leeches (Hirudinea) principally from China, Kashmir, and British India. *Proc. Acad. Nat. Sci. USA* **1924**, *76*, 343–388. Available online: https://www.jstor.org/stable/4063928 (accessed on 14 February 2023).
14. Epshtein, V. A new species of leech from the Amur Basin. *Zool. Zhurnal* **1957**, *36*, 1414-141.
15. Yang, T. On the genus *Limnotrachelobdella* Epstein, 1968 and a new species from South China Sea. *Acta Hydrobiol. Sin.* **1987**, *11*, 268–273. Available online: http://ir.ihb.ac.cn/handle/152342/6212 (accessed on 14 February 2023).
16. Epstein, V. From morphology to phylogeny (on the example of study of the fish leeches of Palearctic). *Вісник Харківського Національного Університету Імені Вн Каразіна. Серія Біологія* **2013**, *18*, 144–150. Available online: https://periodicals.karazin.ua/biology/article/view/13754 (accessed on 14 February 2023).
17. Yang, T. *Fauna Sinica, Annelida: Hirudinea*; Science Press: Beijing, China, 1996.
18. Tamura, K.; Stecher, G.; Kumar, S. MEGA11: Molecular evolutionary genetics analysis version 11. *Mol. Biol. Evol.* **2021**, *38*, 3022–3027. [CrossRef]
19. Zhang, D.; Gao, F.; Jakovli, I.; Zou, H.; Wang, G.T. PhyloSuite: An integrated and scalable desktop platform for streamlined molecular sequence data management and evolutionary phylogenetics studies. *Mol. Ecol. Resour.* **2020**, *20*, 348–355. [CrossRef]
20. Katoh, K.; Standley, D.M. MAFFT multiple sequence alignment software version 7: Improvements in performance and usability. *Mol. Biol. Evol.* **2013**, *30*, 772–780. [CrossRef]
21. Lanfear, R.; Frandsen, P.B.; Wright, A.M.; Senfeld, T.; Calcott, B. PartitionFinder 2: New methods for selecting partitioned models of evolution for molecular and morphological phylogenetic analyses. *Mol. Biol. Evol.* **2017**, *34*, 772–773. [CrossRef]
22. Ronquist, F.; Huelsenbeck, J.; Huelsenbeck, J. MrBayes version 3.0: Bayesian phylogenetic inference under mixed models. *Bioinformatics* **2003**, *19*, 1572–1574. [CrossRef]
23. Park, M.A.; Kim, S.R.; Kim, M.S.; Kim, J.H.; Park, J.J. Histopathological observation of the gill of the crucian carp, *Carassius auratus* by the leech, *Limnotrachelobdella sinensis*. *J. Fish Pathol.* **2010**, *23*, 399–407.
24. Rhee, J.K. *Trachelobdella sinensis* Blanchard, 1896 found from *Cyprinus carpio nudus* in Korea. *Kisaengchunghak Chapchi* **1986**, *24*, 216–217. [CrossRef] [PubMed]
25. Nagasawa, K.; Park, S.-W.; Kim, Y.-G.; Kim, H.J. *Limnotrachelobdella sinensis*, a leech associated with mortality in a wild population of Japaneses curcian carp *Carassius cuvieri* in Korea. *J. Grad. Sch. Biosph. Sci.* **2009**, *48*, 49–53. [CrossRef]
26. Nagasawa, K.; Tanaka, M. The fish leech *Limnotrachelobdella sinensis* (Hirudinida, Piscicolidae) invaded Kyoto Prefecture, central Japan. *Biogeography* **2009**, *11*, 17–21. Available online: http://ir.lib.hiroshima-u.ac.jp/00030959 (accessed on 14 February 2023).

27. Bauer, O.N. Key to the parasites of freshwater fish of the USSR, Volume 3, Parasitic Metazoa (part 2). In *Opredelitel' Parezitov Presnovodnykh Ryb Fauny SSSR, Tom 3, Parazitichеskie Mnogokletochnye (Vtoraya Chast')*; Nauka: Leningrad, Russia, 1987.
28. Nagasawa, K.; Tanaka, M. Common carp (*Cyprinus carpio carpio*) as a host for the fish leech *Limnotrachelobdella sinensis* (Hirudinida: Piscicolidae) in Japan <Short Communication>. *Biogeography* **2011**, *13*, 111–113. Available online: https://ir.lib.hiroshima-u.ac.jp/00031800 (accessed on 14 February 2023).
29. Nagasawa, K.; Sasaki, M.; Matsubara, H. *Limnotrachelobdella okae* (Hirudinida: Piscicolidae) Parasitic on Big-scaled Redfin, *Pseudaspius hakonensis* (Cypriniformes: Leuciscidae), in Two Brackish Water Lakes, Hokkaido, Japan. *Species Divers.* **2022**, *27*, 279–284. [CrossRef]
30. Nagasawa, K.; Izumikawa, K.; Yamanoi, H.; Umino, T. New Hosts, Including Marine Fishes Cultured in Japan, of *Limnotrachelobdella okae* (Hirudinida: Piscicolidae). *Comp. Parasitol.* **2009**, *76*, 127–129. [CrossRef]
31. Bielecki, A.; Kapusta, A.; Cichocka, J. Atlantic sturgeon, Acipenser oxyrinchus Mitchill, infected by the parasitic leech, *Caspiobdella fadejewi* (Epshtein) (Hirudinea; Piscicolidae), in the Drwęca River. *Arch. Pol. Fish.* **2011**, *19*, 87–93. [CrossRef]
32. Bauer, O.; Pugachev, O.; Voronin, V. Study of parasites and diseases of sturgeons in Russia: A review. *J. Appl. Ichthyol.* **2002**, *18*, 420–429. [CrossRef]
33. Folmer, O.; Black, M.; Wr, H.; Lutz, R.; Vrijenhoek, R. DNA primers for amplification of mitochondrial Cytochrome C oxidase subunit I from diverse metazoan invertebrates. *Mol. Mar. Biol. Biotechnol.* **1994**, *3*, 294–299.
34. Kaygorodova, I.; Matveenko, E. Diversity of the *Piscicola* Species (Hirudinea, Piscicolidae) in the Eastern Palaearctic with a Description of Three New Species and Notes on Their Biogeography. *Diversity* **2023**, *15*, 98. [CrossRef]
35. Hebert, P.D.; Cywinska, A.; Ball, S.L.; DeWaard, J.R. Biological identifications through DNA barcodes. *Proc. R. Soc. B Biol. Sci.* **2003**, *270*, 313–321. [CrossRef] [PubMed]
36. Beresic-Perrins, R.K.; Govedich, F.R.; Banister, K.; Bain, B.A.; Rose, D.; Shuster, S.M. *Helobdella blinni* sp. n. (Hirudinida, Glossiphoniidae) a new species inhabiting Montezuma Well, Arizona, USA. *Zookeys* **2017**, *661*, 137–155. [CrossRef] [PubMed]

pathogens

MDPI

Article

Dual RNA-Seq of *Flavobacterium psychrophilum* and Its Outer Membrane Vesicles Distinguishes Genes Associated with Susceptibility to Bacterial Cold-Water Disease in Rainbow Trout (*Oncorhynchus mykiss*)

Pratima Chapagain [1,†], Ali Ali [2,†] and Mohamed Salem [2,*]

[1] Department of Biology and Molecular Biosciences Program, Middle Tennessee State University, Murfreesboro, TN 37132, USA
[2] Department of Animal and Avian Sciences, University of Maryland, College Park, MD 20742, USA
* Correspondence: mosalem@umd.edu
† These authors contributed equally to this work.

Abstract: *Flavobacterium psychrophilum* (*Fp*), the causative agent of Bacterial Cold-Water disease in salmonids, causes substantial losses in aquaculture. Bacterial outer membrane vesicles (OMVs) contain several virulence factors, enzymes, toxins, and nucleic acids and are expected to play an essential role in host–pathogen interactions. In this study, we used transcriptome sequencing, RNA-seq, to investigate the expression abundance of the protein-coding genes in the *Fp* OMVs versus the *Fp* whole cell. RNA-seq identified 2190 transcripts expressed in the whole cell and 2046 transcripts in OMVs. Of them, 168 transcripts were uniquely identified in OMVs, 312 transcripts were expressed only in the whole cell, and 1878 transcripts were shared in the two sets. Functional annotation analysis of the OMV-abundant transcripts showed an association with the bacterial translation machinery and histone-like DNA-binding proteins. RNA-Seq of the pathogen transcriptome on day 5 post-infection of *Fp*-resistant versus *Fp*-susceptible rainbow trout genetic lines revealed differential gene expression of OMV-enriched genes, suggesting a role for the OMVs in shaping the host–microbe interaction. Interestingly, a cell wall-associated hydrolase (CWH) gene was the most highly expressed gene in OMVs and among the top upregulated transcripts in susceptible fish. The CWH sequence was conserved in 51 different strains of *Fp*. The study provides insights into the potential role of OMVs in host–pathogen interactions and explores microbial genes essential for virulence and pathogenesis.

Keywords: cell wall hydrolase; ribosome; translation; DNA-binding proteins; methyltransferases

1. Introduction

Flavobacterium psychrophilum (*Fp*) is a harmful pathogen that causes Bacterial Cold-Water Disease (BCWD) in salmonids [1,2]. *Fp* is a Gram-negative bacterium affecting all species of salmonids, and infections occur worldwide. The high mortality caused by *Fp* is due to the ability of the pathogen to survive in harsh environmental conditions, multiple transmission routes, and the unavailability of effective vaccines [3]. This bacterium can be detected in water samples and can form biofilms on environmental and host surfaces, which aids bacteria in pathogenesis [4]. The bacterium primarily affects fry with an underlying immune system, whereas upon infection in adult fish, necrotic lesions are developed, resulting in hemorrhagic septicemia [5], and because of this, the salmonid aquaculture industries suffer from considerable losses annually.

Several breeding approaches have been used to assist in the genetic improvement of hosts for BCWD resistance [6]. Moreover, some efforts have been made to understand the role of bacterial genes in causing the disease. Previous studies on *Flavobacterium columnare* and *Flavobacterium johnsoniae* identified several peptidase enzymes and cell surface adhesin

genes involved in causing the disease [5,7,8]. To some extent, virulence factors, such as extracellular proteases, are associated with host tissue destruction [9]. Similarly, an iron-uptake-associated gene has also been studied as a virulence gene because iron acquisition allows the pathogenic bacteria to scavenge iron and grow inside the host; *Fp* strains that lack these genes are less virulent [10].

Evidence has emerged that the bacterial outer membrane vesicle-mediated delivery of virulence factors, proteins, and nucleic acids embedded inside nanoparticles is a novel mechanism of host–pathogen communication [11,12]. OMVs and their inner content can be transferred to host cells either via endocytosis or attachment to host cell receptors, as proposed for *Pseudomonas aeruginosa* [12]. The presence of proteins and nucleic acids within the prokaryotic OMVs may be explained through the protein synthesis process since OMVs entrap the protein synthesis machinery, including the mRNAs, during vesicle formation. Alternatively, the free-floating inner cargos in the cytoplasm or the cytoplasmic constituents might be entrapped during vesicle formation [13].

The mechanism of cell lysis during cargo transfer to the host has not been explained yet in animals. Studies showed that OMVs contain several enzymes, including cell wall-associated hydrolase (CWH). These hydrolases are enzymes associated with bacterial cell wall degradation and biosynthesis during bacterial growth. They are also involved in cell autolysis and cleavage, which might mediate the transfer of inner cargos to the host cell during the interaction. These enzymes participate in cell lysis during cell division and intercellular communication [14]. In bacteria, cell wall hydrolase enzymes are primarily associated with cell division, cell wall degradation, and biosynthesis during bacterial growth. Bacteriophages use hydrolases to destroy bacterial cell membranes and walls during host–pathogen communication [15].

In this study, we aimed to investigate mRNA transcript abundance in *Fp* OMVs versus *Fp* whole cells, which will help explain the functions of *Fp* genes involved in host–pathogen interactions. A high enrichment of histone-like DNA-binding protein and ribosomal transcripts in OMV was the primary finding of our study. A CWH transcript was the most abundant in OMVs. We also identified protein-coding genes enriched in OMVs and associated their expression with BCWD resistance in two selectively bred rainbow trout genetic lines. The study provides insight into the role of OMVs in the host–pathogen interaction during infection and warrants further physiological and omics studies.

2. Results and Discussion

2.1. OMV Isolation and TEM

Isolated *Fp* OMVs were observed via TEM as spherical-shaped particles having an average diameter between 50 and 300 nm (Figure 1A), while *Fp* was observed as having a rod-shaped morphology with a size of approximately 2–5 μm. (Figure 1B).

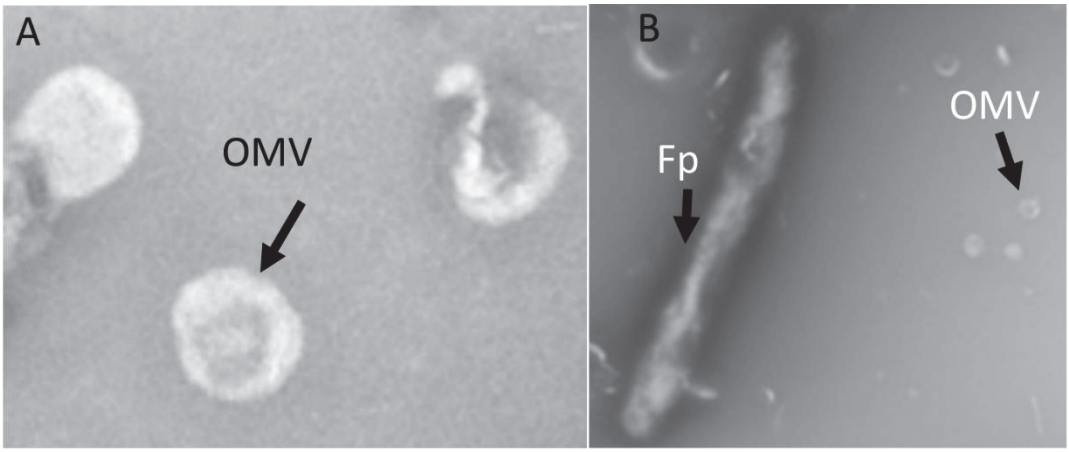

Figure 1. (**A**) Transmission electron microscopy (TEM) of *Fp* OMVs. OMVs appeared as spherical, nano-shaped particles. (**B**) TEM of *Fp*; bacteria appeared rod-shaped with OMVs.

2.2. RNA-Seq of Fp Whole Cells and OMVs Identify Protein-Coding Genes Associated with Bacterial Virulence and Pathogenesis

RNA-seq identified 2190 transcripts expressed in the whole cell and 2046 transcripts expressed in OMVs with an RPKM >0.45. The list of transcripts with their expression values is included in Supplementary File S1. Among these transcripts, 1878 were found in both OMVs and *Fp* whole cells, whereas 312 transcripts were uniquely expressed in the whole cell, and 168 were OMV-unique transcripts (Figure 2A). Several of those OMV-specific transcripts are essential for bacterial virulence. These transcripts included cold shock domain-containing protein (CSPs), threonine ammonia-lyase IlvA (threonine dehydratase), integration host factor (IHF) subunit beta, and co-chaperone GroES (Table 1). The bacterial CSPs function as regulators of the expression of stress resistance and virulence genes, thereby promoting host pathogenicity [16]. Threonine dehydratase is essential for pneumococcal virulence in mice [17], and IHF is a positive regulator of virulence gene expression in Gram-negative bacteria [18].

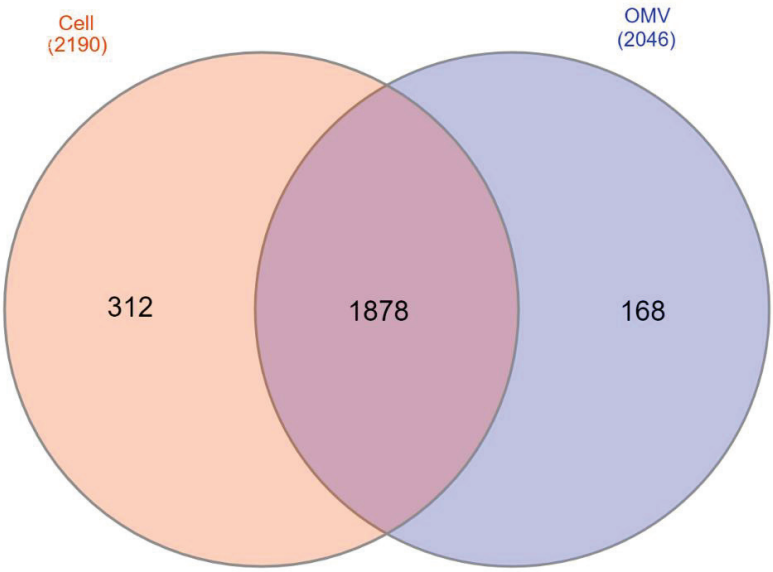

(**A**)

ClassID	Term name	−log10 adj pvalue
IPR	Histone-like DNA-binding protein, conserved site	2.80
IPR	Histone-like DNA-binding protein	2.60
GO:0006412	translation	2.24
KEGG	Pantothenate and CoA biosynthesis [PATH:ko00770]	2.22
GO:0008168	methyltransferase activity	2.20
GO:0005840	ribosome	2.16
KEGG	Ribosome [PATH:ko03010]	2.15
GO:0003735	structural constituent of ribosome	2.13
GO:0009086	methionine biosynthetic process	2.10
GO:0009229	thiamine diphosphate biosynthetic process	1.98
GO:0006364	rRNA processing	1.97
GO:0016757	transferase activity, transferring glycosyl groups	1.93
GO:0009228	thiamine biosynthetic process	1.92
KEGG	Glycine, serine and threonine metabolism [PATH:ko00260]	1.89
GO:0032259	methylation	1.85
KEGG	Two-component system [PATH:ko02020]	1.67

(**B**)

Figure 2. (**A**) Venn diagram showing OMV- and cell-unique and overlapping transcripts. (**B**) Enrichment analysis of abundant transcripts in the bacterial OMVs. Negative log10 adj *p*-values were plotted to show over-represented KEGG pathways, IPRs, and GO terms.

Table 1. OMV-versus whole cell-unique mRNA transcripts. Several OMV-unique transcripts are essential for bacterial virulence.

Feature ID	Gene Description	Differential Abundance (OMVs/*Fp* Whole Cell)
FE46_RS03875	Hypothetical protein IA03_02225	258.63
FE46_RS01465	Cold shock domain-containing protein	236.83
FE46_RS04325	DUF3820 family protein	40.87
FE46_RS03890	Co-chaperone GroES	28.51
FE46_RS08245	Putative membrane spanning protein	25.95
FE46_RS05500	Integration host factor subunit beta	23.18
FE46_RS05600	CDP-alcohol phosphatidyltransferase family protein	18.81
FE46_RS02350	Threonine ammonia-lyase IlvA	18.17
FE46_RS04330	OsmC family protein	15.54
FE46_RS02255	Cadmium-translocating P-type ATPase	−223.61
FE46_RS12900	Leucine-rich repeat protein	−193.17
FE46_RS10250	Family transcriptional regulator	−186.12
FE46_RS11155	Ketoacyl-ACP synthase III	−127.88
FE46_RS02245	Acetyl-hydrolase transferase family	−117.56
FE46_RS12880	Leucine-rich repeat protein	−100.47
FE46_RS12920	Leucine-rich repeat protein	−82.91
FE46_RS12885	Leucine-rich repeat protein	−79.44
FE46_RS03485	Division cell wall cluster transcriptional repressor	−60.93
FE46_RS03530	UDP-N-acetylmuramate–L-alanine ligase	−59.90
FE46_RS11460	NADH-quinone oxidoreductase subunit B	−53.92
FE46_RS04540	DUF2147 domain-containing	−51.66

Transcripts, common to both OMVs and whole cells showed differential abundance. A total of 214 transcripts were more abundant in OMVs, whereas 1143 transcripts were more expressed in the whole cell (fold-change $\geq$2). Remarkably, ribosome-related transcripts were the dominant differentially abundant transcripts in the OMV compared to levels in the whole cell (Table 2).

To gain insights into the biological function of the cell- versus OMV-unique and most significantly enriched transcripts (fold-change $\geq$15), we performed gene enrichment analysis (Figure 2B). Abundant transcripts in the *Fp* whole cell were significantly enriched in energy production and conversion (Table 2). The list included NAD (P) FAD-dependent oxidoreductase, cytochrome-c cbb3-type subunit I, and 4Fe-4S dicluster domain-containing. Conversely for OMVs, the analysis showed an over-representation of genes mapped to four KEGG pathways, ribosome, pantothenate and CoA biosynthesis, glycine, serine and threonine metabolism, and two-component system. Furthermore, the analysis showed the enrichment of GO terms associated with methyltransferase activity, rRNA processing, structural constituent of ribosome, translation, methionine biosynthetic process, and thiamine diphosphate biosynthetic process. Some of the important OMV-enriched pathways and GO terms will be discussed in the following sections.

Table 2. Differentially abundant transcripts between the *Fp* whole cells and OMVs. Pervasive enrichment of transcripts involved in translation, ribosomal structure, and biogenesis was observed in OMVs. In contrast, energy production and conversion genes were enriched in the whole cell.

Feature ID	Gene Description	Differential Abundance (OMVs/*Fp* Whole Cell)
FE46_RS03770	HU family DNA-binding protein	250.39
FE46_RS09040	30S ribosomal protein S20	236.37
FE46_RS03985	KTSC domain-containing protein	124.10
FE46_RS03320	Family outer membrane	61.13
FE46_RS09965	Type B 50S ribosomal L31	43.71
FE46_RS09215	50S ribosomal L33	37.49
FE46_RS12230	50S ribosomal L32	33.37
FE46_RS01825	30S ribosomal S16	30.62
FE46_RS01795	Inorganic pyrophosphatase	29.61
FE46_RS12455	Copper resistance	28.99
FE46_RS11385	50S ribosomal L27	23.06
FE46_RS05880	3,4-Dihydroxy-2-butanone-4-phosphate synthase	22.28
FE46_RS04555	30S ribosomal S6	21.17
FE46_RS04560	30S ribosomal S18	19.11
FE46_RS02470	Ribosome assembly cofactor	16.53
FE46_RS05480	NAD(P) FAD-dependent oxidoreductase	−158.95
FE46_RS10070	Cytochrome-c cbb3-type subunit I	−149.66
FE46_RS08120	4Fe-4S dicluster domain-containing	−125.13
FE46_RS10110	Aconitate hydratase	−59.32
FE46_RS10085	Cytochrome c oxidase accessory	−56.74
FE46_RS01775	Electron transfer flavo subunit alpha family	−40.12
FE46_RS12380	2-Oxoglutarate dehydrogenase complex dihydrolipoyllysine-residue succinyltransferase	−37.85
FE46_RS01970	4Fe-4S dicluster domain-containing	−33.28
FE46_RS12375	2-Oxoglutarate dehydrogenase E1 component	−26.94
FE46_RS02175	L-glutamate gamma-semialdehyde dehydrogenase	−25.98
FE46_RS06595	Succinate–ligase subunit alpha	−24.98
FE46_RS01780	Electron transfer flavo subunit beta family	−24.12
FE46_RS05145	Dihydrolipoyl dehydrogenase	−23.63
FE46_RS08480	FAD-binding	−22.90
FE46_RS05800	Class II fumarate hydratase	−22.35
FE46_RS11950	Aldehyde dehydrogenase family	−21.72
FE46_RS00480	Succinate dehydrogenase/fumarate reductase iron-sulfur subunit	−17.80

2.3. Ribosome

Remarkably, several ribosomal RNAs were among the most enriched in the OMVs compared to levels in the whole cell, suggesting the continuation of protein synthesis in the OMVs and most likely in the host cell following infection. The enriched ribosomal subunits included 30S ribosomal protein S16, 30S ribosomal protein S6, 30S ribosomal protein S18, 30S ribosomal protein S20, 50S ribosomal protein L33, 50S ribosomal protein L27, and 50S

ribosomal protein L32. For instance, the transcript encoding 30S ribosomal protein S20 (FE46_RS09040) was ranked second among the most enriched in the OMVs (enrichment fold-change ~236). The enrichment of the ribosome components perhaps facilitates the production of more virulence factors necessary to hijack the host immune system. Previous reports showed that disrupting the optimal arrangement of the bacterial ribosomal components can lead to a loss of function and resistance to pathogens. Ribosome-targeting antibiotics lodge between the crucial ribosomal components to disrupt the synthesis of new proteins [19]. Our results suggest the bacterial ribosome as an interesting area of research to develop novel strategies that can contain the disease, such as the development of new ribosome-inhibiting antimicrobial drugs [20].

2.4. Two-Component System

Two-component signal transduction systems facilitate bacterial responses and adaptation to environmental or intracellular changes. Each two-component system includes a sensor histidine kinase protein, which receives a signal and transmits it to a response regulator. The latter transmits the signal to the target and induces changes in transcription [21]. Genes involved in the two-component system were uniquely represented in the OMVs. These genes included glycosyltransferase, LytTR family DNA-binding domain-containing protein, and the response regulator transcription factor (GerE).

Glycosyltransferase plays a crucial role in the assembly of peptidoglycan, which surrounds most bacteria and confers a stress-bearing shell [22]. Many Gram-negative bacteria interact with host cells by injecting proteins, such as glycosyltransferases, into infected host cells to post-translationally modify the structure and function of host proteins. Glycosyltransferases can modify protein substrates on arginine residues, which disrupts the normal functioning of the innate immune system [23]. Thus, glycosyltransferases have been suggested as great potential targets for anti-virulence compounds and the future of antibiotic discovery [22].

Furthermore, LytTR family DNA-binding domain-containing protein is a transcriptional regulator that controls the production of virulence factors in some bacterial pathogens [24], whereas GerE is a DNA-binding protein that works with σ^K to activate or repress gene expression. GerE binds to the promoter region of σ^K-dependent genes; however, the mechanism by which GerE affects promoter activity is not known yet [25].

2.5. Pantothenate and CoA Biosynthesis

Pantothenate (vitamin B5) is the critical precursor for the biosynthesis of coenzyme A (CoA). CoA is a cofactor essential for the growth of pathogenic microorganisms and is implicated in various metabolic reactions, such as the tricarboxylic acid cycle, synthesis of phospholipids, and synthesis and degradation of fatty acids [26]. Genes involved in pantothenate and CoA biosynthesis were unique to the OMVs. These genes included the pantetheine-phosphate adenylyltransferase (PPAT) and biotin–acetyl-CoA-carboxylase ligase (BirA).

PPAT is essential in the CoA biosynthetic pathway to catalyze the reversible transfer of an adenylyl group from ATP to 4′-phosphopantetheine [27]. PPAT has been previously suggested as a candidate drug target to overcome antibiotic resistance [28]. The biotin protein ligase BirA represses the transcription of the biotin synthetic operon. BirA was identified as an essential component of a virulence-regulating pathway to allow bacterial adherence in a low biotin environment [29]. In addition, BirA regulates the expression of genes encoding heat and cold shock proteins perhaps to allow for bacterial survival under harsh environmental conditions [30].

2.6. Glycine, Serine, and Threonine Metabolism

Genes involved in glycine, serine, and threonine metabolism were enriched in the OMVs. These genes included aspartokinase and threonine ammonia-lyase IlvA (threonine dehydratase). Aspartate is an essential metabolite for bacterial virulence. Enzymes involved

in aspartate metabolism, such as the aspartokinase, are suggested as promising targets for novel antibacterial compounds [31]. Moreover, threonine dehydratase *Streptococcus pneumoniae* mutants demonstrated in vitro decreased colonization, adhesion inability, and subsequently less virulence [17].

2.7. Genes with Enriched GO Terms

GO terms linked to ribosome, structural constituent of ribosome, translation, methionine biosynthetic process, thiamine diphosphate biosynthetic process, methylation, and methyltransferase activity were enriched in the OMVs.

Genes involved in the methionine biosynthetic process, such as aspartokinase and O-acetyl-L-homoserine sulfhydrolase, were significantly enriched in OMVs. Methionine is indispensable for many cellular processes, such as the initiation of protein synthesis and methylation of DNA, RNA, and proteins. The de novo methionine biosynthetic pathway is conserved in prokaryotes but absent in vertebrates, which makes methionine a potential antimicrobial target [32–34]. Previous studies demonstrated that the combined disruption of methionine biosynthesis and transport affected the growth and virulence of Salmonella [35].

Genes mapped to the thiamine diphosphate biosynthetic pathway encode hydroxymethylpyrimidine/phosphomethylpyrimidine kinase and HesA/MoeB/ThiF family protein. Thiamine (Vitamin B1) functions in the form of thiamine pyrophosphate (TPP) [36]. Bacteria synthesize the TPP or acquire it via the transportation of exogenous thiamine [37]. Deletion of the thiamine transporter (TT) operon in *Edwardsiella piscicida*, the causative agent of the edwardsiellosis disease in fish, resulted in attenuated pathogenicity, reduced host cell adhesion, and impaired abilities associated with motility [38].

Interestingly, GO terms associated with methylation and methyltransferase activity were also enriched in OMVs. Methyltransferase enzymes regulate the epigenetic landscape in prokaryotes and eukaryotes. Bacterial methyltransferases play an essential role in controlling the epigenetic information at the microbe level and in host–microbe interactions [39]. Methyltransferase activities target the host DNA and histone proteins, resulting in transcriptional changes in the host cell to enhance bacterial colonization [39]. Our results suggest that methyltransferases are promising targets to fight bacterial pathogenesis.

2.8. RNA-Seq of Pathogen on Day 5 Post-Infection of Fish from Resistant and Susceptible Genetic Lines

To identify potential bacterial transcript markers associated with disease susceptibility, we sought to investigate the variation in abundance of bacterial transcripts, in vivo, on day 5 following the infection of rainbow trout with *Fp*. For this purpose, we used fish collected from selectively bred resistant (ARS-*Fp*-R) and susceptible (ARS-*Fp*-S) genetic lines challenged with *Fp* as previously described in [40]. RNA-Seq from infected resistant and susceptible genetic lines yielded 372,100,715 raw sequence reads (average of 46,512,589 reads/sample). To identify differentially expressed (DE) bacterial transcripts, sequence reads were mapped to the pathogen's reference genome [2]. A total of 4,870,725 reads (1.31%) were mapped to the *Fp* reference genome. Notably, 97.82% of the *Fp* mapped reads were generated from the susceptible genetic line, which is explained by a higher bacterial load as reported in the susceptible line compared to that in the resistant line [40]. Normalized gene expression was used to account for differences across samples by converting raw count data to RPKM values. A total of 576 bacterial transcripts were DE with a false discovery rate (FDR) <0.05 and a minimum fold-change value ≥ 2 or ≤ -2 (Figure 3A,B and Supplementary File S2). Notably, 87 OMV-enriched transcripts were among the DE transcripts between the two genetic lines. Most of the DE bacterial transcripts (96.4%) were downregulated in the resistant line. More information about DE transcripts is given in Supplementary File S2.

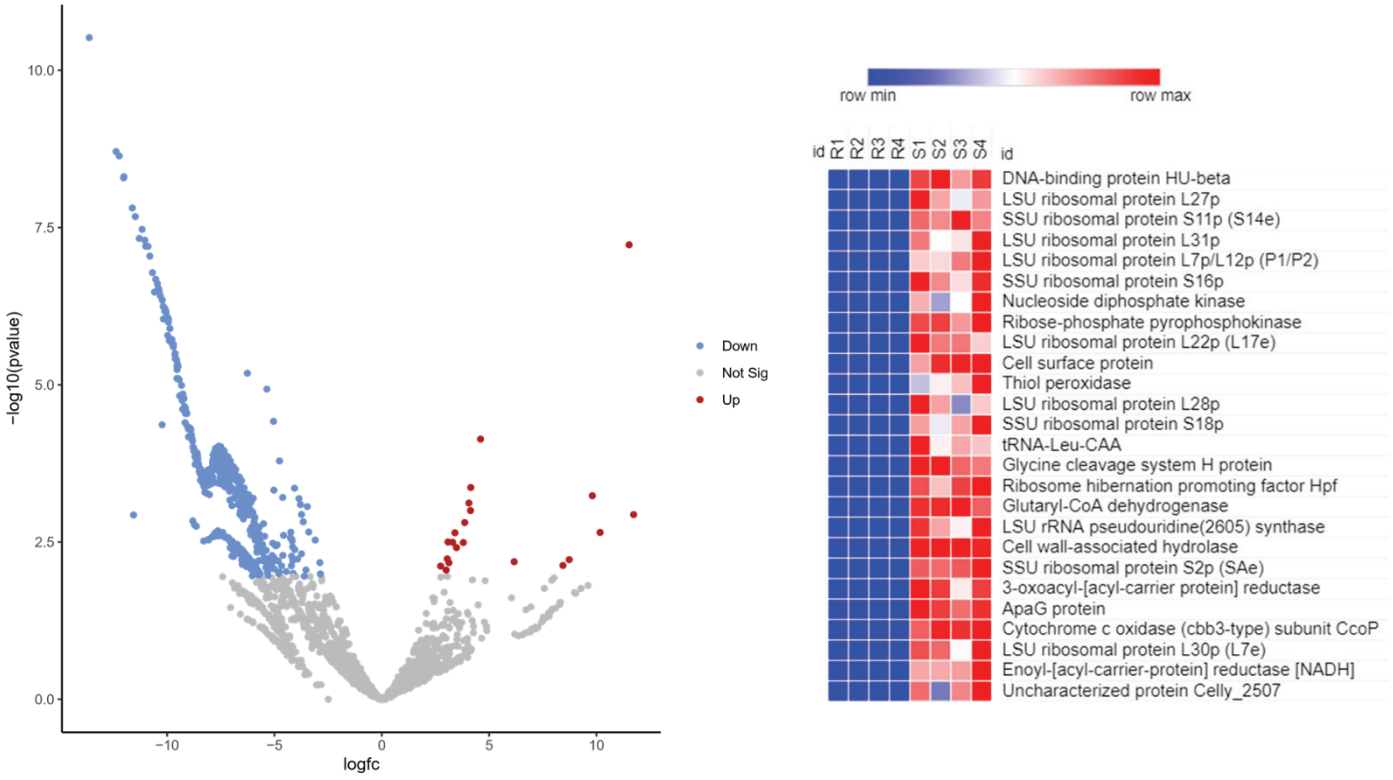

(**A**) (**B**)

Figure 3. (**A**) Volcano plot showing DE bacterial transcripts between susceptible and resistant fish on day 5 post-infection (R/S). Upregulated transcripts in the resistant line are represented with red dots, whereas the downregulated transcripts are represented with blue dots (FDR $\leq$ 0.05). (**B**) Heat map showing the expression profile of the top DE transcripts (fold-change <−1000) between the susceptible and resistant fish on day 5 post-infection (R/S). The numbers at the top represent replicates per genetic line.

In total, 555 bacterial transcripts were downregulated in resistant fish on day 5 post-infection. Functional enrichment analysis was conducted to gain insights into the biological functions of the downregulated transcripts (Figure 4A). Transcripts encoding Fe-S cluster assembly ATPase, FeS assembly SUF system protein, Ferredoxin, Ferredoxin–NADP reductase, ferritin-like domain-containing protein, and nitrogen fixation were downregulated in *Fp* when the resistant fish genetic line was infected. Iron-sulfur clusters have a primary role in electron transfer and act as "molecular switches" for gene regulation [41]. Iron is a necessity for virulence in most pathogenic bacteria, and heme/iron transport is a virulence determinant of *Fp* [42,43]. Moreover, bacteria require nitrogen to synthesize core cell constituents, such as purines, pyrimidines, and amino sugars [44]. Genes involved in DNA replication and the synthesis of RNA primer were significantly underrepresented in the resistant fish. Consistently, genes promoting ribosome structure and biogenesis or enhancing the efficiency of translation machinery were among the most downregulated in resistant fish (Figures 3B and 4B). Twenty-seven genes were mapped to the ribosome KEGG pathway. Ribosome and translation-related genes were also identified among the most over-represented genes in OMVs (Table 2). Our results provide initial evidence for the potential crucial role of the bacterial ribosome and translation machinery in hijacking the host immune response and rendering the fish susceptible to disease.

ClassID	Term name	−log10 adj pvalue
IPR	Histone-like DNA-binding protein, conserved site	6.37
IPR	Histone-like DNA-binding protein	6.20
IPR	Methylated DNA-protein cysteine methyltransferase	6.17
GO:0003735	structural constituent of ribosome	5.50
GO:0006412	translation	5.03
GO:0005840	ribosome	4.91
KEGG	Ribosome [PATH:ko03010]	4.45
COG	Translation, ribosomal structure and biogenesis	3.89
GO:0045454	cell redox homeostasis	1.62
IPR	Fe-S cluster assembly domain superfamily	1.61
GO:0006979	response to oxidative stress	1.45
GO:0016740	transferase activity	1.41
GO:0006364	rRNA processing	1.38

(**A**)

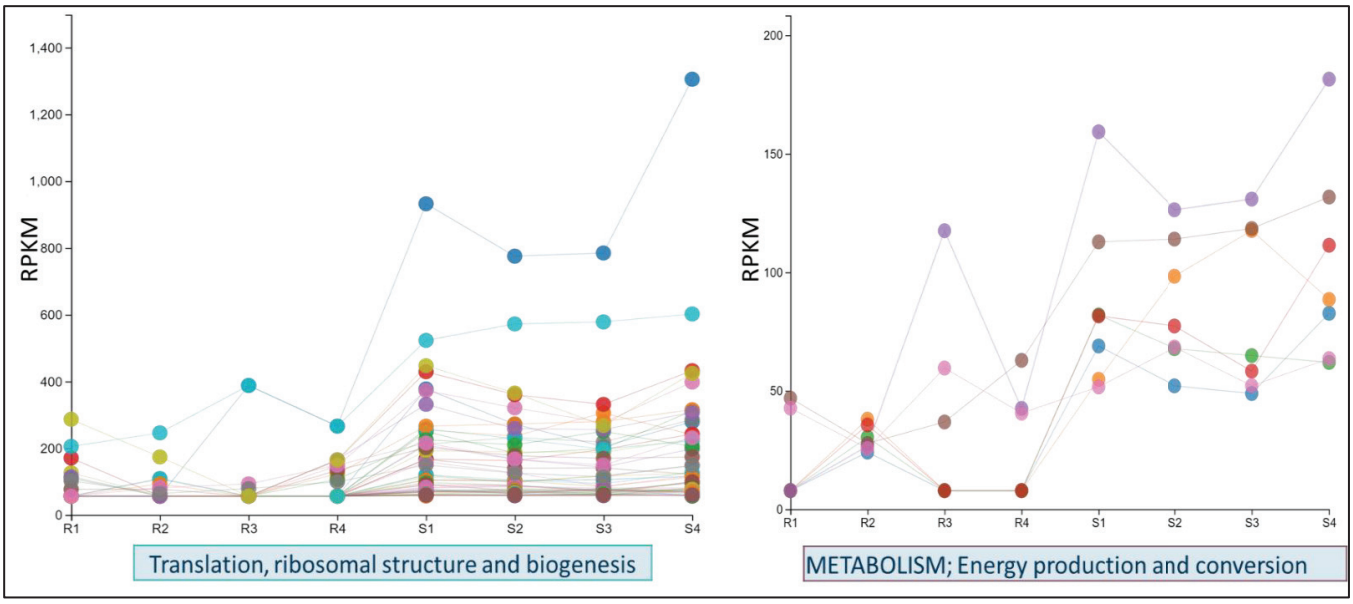

(**B**)

Figure 4. (**A**) Enrichment analysis of DE bacterial transcripts in susceptible and resistant fish on day 5 post-infection. Negative log10 adj *p*-values were plotted to show over-represented KEGG pathways, IPRs, and GO terms. (**B**) Line chart of the normalized expression values of genes involved in the translation machinery (**left** panel) and energy production/conversion (**right** panel) in the resistant and susceptible genetic lines. R1–R4 and S1–S4 represent replicates of the resistant and susceptible genetic lines. Each color represents one gene.

In resistant fish, we noticed an under-representation of bacterial genes implicated in the response to oxidative stress, such as thiol peroxidase, glutathione peroxidase, peptide-methionine (R)-S-oxide reductase, and alkyl hydroperoxide reductase. This suggests that bacteria in the resistant fish are more vulnerable to oxidative stress, as the production of a complex mixture of oxidants is a major host defense mechanism against invading pathogens [45]. In addition, several bacterial genes involved in DNA methylation were under-represented in resistant fish. The list includes methylated-DNA–protein-

cysteine methyltransferase, 23S rRNA (guanosine (2251)-2′-O)-methyltransferase, and tRNA (guanosine (18)-2′-O)-methyltransferase. Methylation is one of the mechanisms by which pathogens can control host functions [46]. Besides their role in microbial epigenetic regulation, bacterial methyltransferase enzymes have a crucial role in host–microbe interactions [39].

Histone-like DNA-binding proteins, such as integration host factor (IHF) alpha/beta and DNA-binding protein HU-beta, were under-represented in resistant fish. IHF alpha/beta binds the minor groove of DNA to induce a large bend, which stabilizes distinct DNA conformations essential for bacterial recombination, transposition, replication, and transcription. IHF contributes to bacterial survival in highly competitive environments [47]. Notably, DNA-binding protein HU-beta was the most downregulated bacterial transcript in resistant fish (fold-change −12,667.9) (Figure 3B). DNA-binding protein HU-beta wraps the DNA to stabilize it under extreme environmental conditions [48].

Remarkably, *Fp* genes with hydrolase activity were significantly downregulated in resistant fish on day 5 following infection (Table 3). These *Fp* genes included CWH, GTP cyclohydrolase I, isopentenyl-diphosphate delta-isomerase, NUDIX hydrolase, and Rhs-family protein. *Fp* CWH was the most downregulated hydrolase (fold-change −1204.8) in the resistant fish (Supplementary File S2). GTP cyclohydrolase I is the first enzyme of the de novo tetrahydrofolate biosynthetic pathway in bacteria [49], whereas isopentenyl diphosphate (IPP) isomerase catalyzes the conversion of IPP to dimethylallyl diphosphate (DMAPP), an essential step in the isoprenoid biosynthetic pathway [50]. Several in vivo and in vitro studies linked isoprenoid synthesis to the intracellular survival of pathogenic bacteria. Consequently, isoprenoid synthesis was suggested as a target to inhibit bacterial growth [51]. Furthermore, nudix proteins catalyze the hydrolysis of pyrophosphate bonds and have a demonstrated role in bacterial fitness and virulence. Mutants of *Pseudomonas aeruginosa* devoid of individual nudix hydrolases were more sensitive to killing by oxidative stress/H_2O_2 and showed less virulence [52]. Moreover, Rhs proteins play a crucial role in the interaction between bacteria and host cell. The Rhs protein has anti-phagocytosis activities and facilitates bacterial adhesion and invasion abilities. Rhs mutants showed a significant decrease in bacterial ability for multiplication in vivo [53]. Taken together, this study helps in understanding the mechanism governing *Fp* pathogenesis and establishing a foundation for further research.

Table 3. Differentially expressed *F. psychrophilum* transcripts, with hydrolase activities, in susceptible and resistant rainbow trout fish on day 5 post-infection.

Feature ID	Fold Change (R/S)	*p*-Value FDR	Gene Description
FE46_RS09020	−1204.81	0.002	Cell wall-associated hydrolase
FE46_RS07385	−348.46	0.003	TIGR00730 family Rossman fold protein
FE46_RS11855	−306.96	0.003	Rhs-family protein
FE46_RS04860	−291.40	0.003	Isopentenyl-diphosphate delta-isomerase
FE46_RS08365	−288.91	0.003	GTP cyclohydrolase
FE46_RS08015	−116.46	0.022	NUDIX domain-containing protein
FE46_RS08160	−84.13	0.006	GTP cyclohydrolase I
FE46_RS11250	−8.59	0.018	Cell wall-associated hydrolase

2.9. Cell Wall Hydrolase (CWH)

CWH, a hydrolytic enzyme, was the most abundant transcript in OMVs (RPKM = 55,688) (Supplementary File S1). Cell wall hydrolases are enzymes involved in cell lysis during bacterial cell division [54]. *Fp* contains several other enzymes besides cell wall hydrolase involved in host invasion. Genome-wide prediction in *Fp* determined another hydrolytic enzyme similar to an elastinolytic enzyme, which resembles an enzyme

present in pathogenic bacteria, such as *Pseudomonas*, *Vibrio*, and *Leptospiria,* and these enzymes enable invasion, tissue necrosis, and increased vascular permeability in the host [55]. However, the role of the hydrolytic enzymes, specifically cell wall hydrolase, in pathogenesis has not been explained clearly yet in most bacteria. The enrichment of the CWH gene in OMVs compared to that in the transcriptome of the whole bacterial cells (3.56-fold) and CWH downregulation in resistant fish on day 5 following infection (Table 3) might suggest a specific function of this gene in lysing the bacterial or host cell during the bacterial–host interaction. Some studies indicated a cell wall hydrolase role in bacterial growth and division by controlling the degradation of the peptidoglycan layer in bacteria, and that are thus referred to explicitly as peptidoglycan hydrolases [56,57]. A recent study on Gram-positive bacteria detected proteomic enrichment of four cell wall hydrolases in OMVs and suggested the involvement of CWH in the formation of the OMV [58].

2.10. CWH Is Conserved among Many Strains of Fp

The CWH transcript was conserved in 51 out of 64 studied strains of *Fp* with a sequence identity ≥99% and query coverage >99%. In the genome of *Fp* CSF 259-93, the strain used for sequencing in this study, there were four copies of this gene [2]. We investigated CWH conservation in seven highly virulent versus three less virulent strains of *Fp.* The highly virulent strains were *Fp* G10, *Fp* G101, JIP02-86, *Fp* S-S6, OSU THCO2-90, JIP 08/99, JIP 16/00, 950106-1, and *Fp* G3 [55,59–61], and the less virulent strains were CR, *Fp* GIW08, and NCIMB 1947 [59,60,62]. The CWH transcript was conserved in six (highly virulent) strains with 100% sequence identity and three (low virulence strains) (Supplementary File S3). As these enzymes are primarily involved in cell lysis during bacterial cell division, cell wall synthesis, development [63], and OMV formation [58], they might be crucial for bacterial survivability, which might explain the evolutionary conservation of this gene in a vast number of *Fp* strains.

2.11. Genetic Manipulation of the Cell Wall Hydrolase Gene Failed in Fp

To investigate the role of the CWH in the pathogenesis of *Fp*, we tried to delete this gene in *Fp*. For this, we used a pyt313 suicide vector carrying the sacB, Amp^r (Em^r) gene generated by Barbier et al. [64]. We incorporated an insert in this plasmid and then subjected it to conjugation. After cell plating, patches of pale-yellow colonies were observed, and those patches were screened via PCR using Srn primers, and an expected 1.1 kb band was observed upon running the gel electrophoresis. However, no bacterial growth was observed in erythromycin tryptone yeast extract agar plates. This might be due to difficulties in transferring the plasmid to *Fp* based on the strain used, which might be due to restriction enzymes produced by the bacteria used in our study.

3. Conclusions

The current study characterized and functionally annotated the OMV and *Fp* whole-cell transcriptomes and investigated variation in the bacterial transcript abundance on day 5 following infection of resistant and susceptible fish with *Fp*. Interestingly, ribosome-related transcripts were highly enriched in the OMV and susceptible fish indicating an essential role for the bacterial translation machinery in pathogenesis. The study revealed a potential role for the histone-like DNA-binding proteins and bacterial methyltransferases in the host–microbe interaction. The CWH was the most abundant transcript in OMVs and among the top upregulated transcripts in susceptible fish on day 5 following infection, suggesting this gene's role in lysing the bacterial cell and host cell, forming and merging OMV with host cells during the host–microbe interaction. The CWH was subjected to gene silencing; however, it could not be accomplished in the *Fp* strain CSF-259-93. This might be because the restriction enzymes produced by *Fp* cause difficulties in the conjugal transfer of a plasmid. Further molecular characterization should be performed to understand the function of CWH in mediating cell lysis in the host.

4. Materials and Methods

4.1. Bacterial Strain and Growth Condition

Fp strain CSF-259-93, kindly provided by Dr. Gregory Wiens, NCCCWA/ARS/USDA, was used in our study. A frozen stock culture of *Fp* was cultured on tryptone yeast extract agar with an agar percentage of 1.5%, with a 0.02% beef extract [65] plate, and the plate was incubated at 15 °C for one week. *Fp* colonies were then transferred to tryptone yeast extract broth, and absorbance (525 nm wavelength) was measured every day for 2 weeks to determine the log phase of the cultures. Measurement of *Fp* density by measuring the OD in the broth culture indicated that the log phase existed between days 5 and 11 (Supplementary File S4), and day 8 was used for OMV isolation. Tryptone yeast extract broth culture without *Fp* was used as a negative control.

4.2. Isolation of OMVs

Fp broth culture was used to increase the bacterial mass, and OMVs were isolated from *Fp* broth culture on day 8 of bacterial growth. OMVs were isolated from bacterial cells for downstream RNA sequencing and the prediction of bacterial genes. The experimental design is shown in Supplementary File S4. A loopful of culture was subcultured on a plate on day 7 of bacterial growth to ensure that the broth was contamination-free. For OMV isolation, broth culture from a flask was distributed into several 50 mL tubes. Each tube was centrifuged at 2800× *g* for 1 h at 4 °C to pellet the bacterial cells. The supernatant was collected and filtered through a 250 mL sterile 0.22 µm PES membrane filter (EMD Millipore Corporation, Billerica, MA, USA) to filter any remaining bacterial cells. The filtrate was then subjected to ultracentrifugation (Beckman Coulter Optima L-90K, 40 Ti rotor) for 3 h at 40,000 rpm (285,000× *g*) at 4 °C to pellet the OMVs. The OMV pellet was then washed with phosphate-buffered saline (PBS) buffer and again subjected to ultracentrifugation for 2 h at 40,000 rpm at 4 °C to re-pellet the OMVs. The OMV pellet was then resuspended in nuclease-free (NF) water and stored at −20 °C. The protein concentration of the OMVs was quantified using a BCA Protein assay kit (Thermo Fisher Scientific, Waltham, MA, USA). To ensure that the suspension containing OMVs was free from bacteria, 30 µL of the suspension was cultured on a tryptone yeast extract agar plate and incubated for 10 days at 18 degrees Celsius.

4.3. Transmission Electron Microscopy (TEM) of OMVs

Transmission electron microscopy (TEM) was performed on *Fp* OMVs and *Fp* bacterial cell samples. For *Fp* bacterial cells, a single colony from a tryptone yeast extract agar plate was suspended in nuclease-free water. For *Fp* OMVs, TEM was performed using OMV suspensions. Using a dropper, 2 drops of OMVs suspended in nuclease-free water were deposited on carbon-coated grids and incubated for 2 min. The excess sample was removed from the grid using blotting paper. Nuclease-free water and tryptone yeast extract broth were used as a negative control. All samples (*Fp* whole cells and *Fp* OMVs) were subjected to negative staining using uranyl acetate. Briefly, samples were deposited on TEM carbon coated grids (80 mesh square grid, EMS, TED PELLA, Inc., Redding, CA, USA) and incubated for 2 min. Samples were blotted dry, and grids were washed with sterile deionized water three times (30 s each) to remove the salt buffer. Before the samples were stained, excess water from grids was removed with blotting paper. To stain the samples, 5 µL of 1% uranyl acetate was added onto the grid and incubated for about 1 min. The stain was then washed with sterile deionized water and dried, and finally, the grids were observed under a Hitachi H-7650-II instrument (Schaumburg, IL, USA) for TEM.

4.4. RNA Extraction, Library Preparation, and Sequencing

RNA was extracted from *Fp* colonies isolated from a tryptone yeast extract agar plate for whole *Fp* cells and from OMVs isolated from *Fp* broth culture using TriZol reagent (Invitrogen, Carlsbad, CA, USA). OMV RNA, RNase-treated, and untreated OMV RNA samples were run based on agarose gel electrophoresis for confirmation. For RNAse

treatment, 4 µL of the RNA samples was treated with RNase (Invitrogen RNase Cocktail Enzyme mix) (Thermo Fisher Scientific, Waltham, MA, USA) (2 µg/µL) and incubated in a water bath at 37 °C for 30 min. RNA samples were stored at −80 °C until subjected to further processing.

For library preparation and sequencing, samples were sent to BGI Genomics (Cambridge, MA, USA). The library preparation was performed using a Trio RNA-seq kit (NuGEN, San Carlos, CA, USA) according to the manufacturer's recommendations. Briefly, an rRNA depletion step was performed for mRNA enrichment. The enriched mRNA was then fragmented into small pieces using a fragmentation buffer and purified using a QiaQuick PCR extraction kit, the solution was resuspended in EB buffer, and cDNA was then subjected to end repair and poly (A) tail addition. The fragments were then connected with adaptors. The library was then purified using a MiniElute PCR Purification kit before PCR amplification. The libraries were amplified via PCR, and then, the yield was quantified. Sequencing was performed using 100 bp-paired end sequencing on an Illumina Miseq.

4.5. Data Processing and Functional Prediction of Transcripts

After sequencing, raw reads were filtered, including removing adaptor sequences, contamination, and low-quality reads. A total of 60,352,578 *Fp* RNA clean reads and 55,722,742 OMVs clean reads were subjected to downstream analysis using the QIAGEN CLC Genomics workbench (version 12.0.3, CLC bio, Aarhus, Denmark; http://www.clcbio.com/products/clc-genomics-workbench/, accessed on 13 March 2019). Five base pairs from the forward ends and 5 bp from the reverse ends were trimmed to remove low-quality nucleotides. The trimmed reads were then mapped to the *Fp* CSF-259-93 reference genome, NCBI accession GCF_000739395.1 [2]. Mapping parameters included mismatch cost = 2, insertion/deletion cost = 3, minimum length fraction = 0.9, and similarity fraction = 0.9. To determine the abundance of genes, the expression values of transcripts were calculated in terms of reads per kilobase per million (RPKM).

4.6. Bacterial Challenge of BCWD-Resistant and BCWD-Susceptible Fish Population

Tissue samples from resistant and susceptible rainbow trout genetic lines were obtained from the USDA/NCCCWA (Provided by Dr. Gregory D Wiens). The genetic lines were developed by the USDA-NCCCWA via a family-based selection method as previously described [40,66]. In brief, within the genetic lines, single-sire × single-dam matings were established between 3-year-old dams and 1-year-old sires (neo-males). To enhance the disease-resistance phenotype, the resistant line dams and sires had undergone three and four generations of BCWD selection. In contrast, the susceptible line parents had undergone one generation of selection to allow for a higher susceptibility to infection. Significant differences in susceptibility to *Fp* were previously observed between the resistant and susceptible genetic lines [40,67].

As previously described by Marancik et al. [40], fish from resistant and susceptible genetic lines were challenged with *Fp* (49 days post-hatch). In brief, fifty fish from each genetic line were randomly allocated to two tanks (2.4 L min^{-1} of 12.5 ± 0.1 °C flow-through spring water supply), and then, fish were intraperitoneally injected with 4.2×10^6 CFU $fish^{-1}$ *Fp* suspended in 10 µL PBS. Similarly, two fish tanks were injected with PBS for each genetic line as a non-infected control. The fish survival was monitored for 21 days. Five fish from each tank were sampled on day 5 post-infection. All fish used in this study were certified as infection-free before injection with *Fp.*

4.7. Sequencing and Differential Gene Expression Analysis of BCWD-Resistant and BCWD-Susceptible Fish

RNA was isolated from the whole fish (1.1 g fry) using TriZol (Invitrogen, Carlsbad, CA, USA). Quantity and quality assessments were performed as previously described [68]. To eliminate potential DNA contamination, RNA samples were treated with DNAase

I (Fisher BioReagents, Hudson, NH, USA). Equal amounts of RNA were pooled from 2 fish, and 4 pools (2 samples/pool) from each resistant and susceptible genetic line were sequenced (i.e., a total of 8 libraries). RNA was sequenced at RealSeq Biosciences, Inc. (Santa Cruz, CA, USA). The Zymo Ribofree library prep kit (Irvine, CA, USA), targeting the host and bacterial RNAs, was used during the rRNA-depleted library preparation.

Raw RNA-Seq datasets were submitted to the NCBI Short Read Archive under BioProject ID PRJNA259860. As previously described, raw sequence reads generated from each genetic line were subjected to a quality check and trimming [68]. High-quality reads were mapped to the *Fp* reference genome [2] using a CLC genomics workbench to identify DE transcripts. Mismatch cost = 2, insertion/deletion cost = 3, minimum length fraction = 0.9, and similarity fraction = 0.9 were allowed during mapping. Unmapped reads, including rainbow trout reads, were filtered out. Supplementary File S4 shows sequence read counts and mapping statistics.

The expression value of each transcript was calculated in terms of RPKM, and then, the EDGE test was used to identify DE transcripts between resistant and susceptible genetic lines (p-value FDR < 0.05, fold change cutoff ± 2). Gene set enrichment analysis was performed using FUNAGE-Pro with an adj p-value < 0.05 [69]. Supplementary File S4 shows the principal component analysis of eight RNA-seq datasets generated from selectively bred, resistant- and susceptible-line rainbow trout on day 5 post-infection and the validation of RNA-Seq data via qPCR for selected genes.

4.8. Conservation of CWH Transcripts

To determine the conservation of CWH transcripts, genome sequences were downloaded from 64 strains of *Fp* from NCBI https://www.ncbi.nlm.nih.gov/genome/browse/#!/prokaryotes/1589/, accessed on 7 May 2020 (Supplementary File S3). CWH transcripts were blasted against all 64 *Fp* strains using a local BLAST in Bioedit [70]. The conservation of transcripts in more and less virulent strains was determined by blasting the transcript with their genomes, respectively. The cutoff value includes query coverage >99% and identity $\geq$99% of the matching sequencing.

4.9. Genetic Manipulation of CWH Gene

Construction of the CWH Deletion Mutant

Efforts to genetically manipulate CWH were conducted using a modified method of Barbier et al. [64]. For the effort to delete CWH from *F. pyschrophilum* (CSF-259-93), a ~3 Kbp fragment upstream of 2995 bp and downstream of 2947 bp was used to amplify the transcripts associated with the cell wall hydrolase gene using Green Taq polymerase and primers CWHus (introducing a BamHI site in the forward primer and SalI in the reverse primer) and CWHds (introducing a PstI sit in both forward and reverse primers). The CWHus fragment was then digested with BamHI and SalI and ligated into the suicide vector pYT313 (kindly provided by Dr. Mark J. McBride). The plasmid was digested with the same enzymes. To the vector, rSAP (shrimp alkaline phosphatase) was added to prevent recircularization during ligation. After ligation, the transformation was performed using competent cells of *E. coli*, strain S17-1 (λ-pir). The transformed cells were PCR-screened to confirm the transformation of the insert into the plasmid. The colonies were then cultured in LB broth with ampicillin in it. The plasmid containing the CWHus insert was then subjected to purification using a QIAprep Spin Miniprep Kit (Qiagen, Germantown, MD, USA). The procedure was repeated with the CWHds primer, which had been ligated with the PstI enzyme, and the vector PYT313 incorporated with the CWHus insert had also been digested with the same PstI enzyme. Since we used the same restriction enzyme at both ends of CWHds, to ensure proper orientation of the insert, we designed the primer upstream and downstream of CWHds, and colony screening of the transformants was performed using screening (CWHscrn) primers. A band size of approximately 1.1 kb was observed upon running gel electrophoresis. Plasmid incorporated with our insert CWHus and CWHds was then transferred to *Fp* CSF-259-93 via conjugation, and the

colonies having the plasmid incorporated into the chromosome through recombination were selected by screening for erythromycin resistance colonies. Resistant colonies were streaked on tryptone yeast extract agar.

4.10. Conjugative Transfer of Plasmid into F. psychrophilum

Conjugation was used to transfer the plasmid from *E. coli* strain S17-1 (λ-pir) into *Fp* strains. Briefly, *E. coli* strains were grown overnight in 5 mL LB broth with shaking at 37 °C. Similarly, *Fp* strains were also grown at 15 °C for 4 days in 5 mL tryptone yeast extract broth. Cells from *E. coli* and *Fp* cells were collected via centrifugation at ~10,000 rpm for 25 min and washed twice with 1 mL LB broth for *E. coli* cells and tryptone yeast extract broth for *Fp* cells. *E. coli* cells were resuspended in 500 µL LB broth, and *Fp* cells were resuspended in 500 µL of tryptone yeast extract broth. Both suspensions were mixed, cells were then spotted on tryptone yeast extract agar using a micropipette, and the plates were incubated at 17 °C for 4 days. After incubation, cells were removed from the plate using a scrapper and suspended in 2 mL tryptone yeast extract broth. From the suspension, 100 µL of the aliquots was spread on tryptone yeast extract agar containing erythromycin (10 ug/mL). The plates were then incubated for 7 days at 17 °C. The colonies were then PCR-screened using the CWH Scrn primer (upstream and downstream of CWH DS region). An isolated colony was inoculated in tryptone yeast extract broth without erythromycin, and the broth was incubated at 17 °C to allow for the loss of an integrated plasmid. Recombinant plasmids were screened by culturing on 50 g/L sucrose-containing tryptone yeast extract agar, and the plate was incubated at 17 °C. All primers used in this study are included in Table 4.

Table 4. Primers used in this study.

Restriction Enzyme	Primers	Tm (Degree C)
CWH1us(Bam)	5′ actactGGATCCTAAAAGACAAAATATGCTAGATGG 3′	61
CWH1us(Sal)	3′ actactGTCGACTTATGTACACACTTTTCCCGAG 5′	62
CWH1ds(Pst)	5′ actactCTGCAGTTTCTAGCCATTAGCCATTAG 3′	60
CWH1ds(Pst)	3′ actactCTGCAGTTATCAAATCCGTGTCATCTG 5′	60
CWH1ko(scrn)	5′ GAATTTAGAAATATTTATGAAGAAAC 3′	60
CWH1ko(scrn)	3′ TCTCGTAGCTCAGCTGGTTAG 5′	61

Supplementary Materials: The following supporting information can be downloaded at: https://www.mdpi.com/article/10.3390/pathogens12030436/s1, Supplementary File S1: Transcripts identified in the *Fp* whole cells and OMVs; Supplementary File S2: Differentially expressed bacterial transcripts in susceptible and resistant fish on day 5 post-infection (R/S); Supplementary File S3: CWH conservation in different *Fp* strains; Supplementary File S4: Method supporting materials.

Author Contributions: Conceptualization, M.S., P.C. and A.A.; methodology, P.C., A.A. and M.S.; formal analysis, A.A.and P.C.; writing, review and editing, A.A., P.C. and M.S.; supervision, M.S.; project administration, M.S.; funding acquisition, M.S. All authors have read and agreed to the published version of the manuscript.

Funding: This study was supported by competitive grants (Nos. 2020-67015-30770) from the United States Department of Agriculture, National Institute of Food and Agriculture (MS).

Institutional Review Board Statement: Fish were maintained at the NCCCWA, and animal procedures were performed under the guidelines of NCCCWA Institutional Animal Care and Use Committee Protocols #053 and #076.

Informed Consent Statement: Not applicable.

Data Availability Statement: The waw RNA-Req data that support the findings of this study are openly available in the NCBI Short Read Archive under BioProject ID PRJNA259860.

Acknowledgments: The authors acknowledge Gregory D. Wiens for providing *Fp* (CSF 259-93) for OMV isolation and tissues from BCWD-resistant and BCWD-susceptible genetic lines for RNA-Seq.

Conflicts of Interest: The authors declare no conflict of interest.

References

1. Starliper, C.E. Bacterial coldwater disease of fishes caused by *Flavobacterium psychrophilum*. *J. Adv. Res.* **2011**, *2*, 97–108. [CrossRef]
2. Wiens, G.D.; LaPatra, S.E.; Welch, T.J.; Rexroad, C., 3rd; Call, D.R.; Cain, K.D.; LaFrentz, B.R.; Vaisvil, B.; Schmitt, D.P.; Kapatral, V. Complete Genome Sequence of *Flavobacterium psychrophilum* Strain CSF259-93, Used To Select Rainbow Trout for Increased Genetic Resistance against Bacterial Cold Water Disease. *Genome Announc.* **2014**, *2*, e00889-14. [CrossRef] [PubMed]
3. Barnes, M.E. A review of *Flavobacterium psychrophilum* Biology, Clinical signs, and Bacterial Cold Water Disease Prevention and Treatment. *Open Fish Sci. J.* **2011**, *4*, 40–48. [CrossRef]
4. Levipan, H.A.; Avendano-Herrera, R. Different Phenotypes of Mature Biofilm in *Flavobacterium psychrophilum* Share a Potential for Virulence That Differs from Planktonic State. *Front. Cell Infect. Microbiol.* **2017**, *7*, 76. [CrossRef]
5. Nematollahi, A.; Decostere, A.; Pasmans, F.; Haesebrouck, F. *Flavobacterium psychrophilum* infections in salmonid fish. *J. Fish Dis.* **2003**, *26*, 563–574. [CrossRef]
6. Leeds, T.D.; Silverstein, J.T.; Weber, G.M.; Vallejo, R.L.; Palti, Y.; Rexroad, C.E., 3rd; Evenhuis, J.; Hadidi, S.; Welch, T.J.; Wiens, G.D. Response to selection for bacterial cold water disease resistance in rainbow trout. *J. Anim. Sci.* **2010**, *88*, 1936–1946. [CrossRef]
7. Shrivastava, A.; Johnston, J.J.; van Baaren, J.M.; McBride, M.J. Flavobacterium johnsoniae GldK, GldL, GldM, and SprA are required for secretion of the cell surface gliding motility adhesins SprB and RemA. *J. Bacteriol.* **2013**, *195*, 3201–3212. [CrossRef]
8. Duchaud, E.; Boussaha, M.; Loux, V.; Bernardet, J.F.; Michel, C.; Kerouault, B.; Mondot, S.; Nicolas, P.; Bossy, R.; Caron, C.; et al. Complete genome sequence of the fish pathogen *Flavobacterium psychrophilum*. *Nat. Biotechnol.* **2007**, *25*, 763–769. [CrossRef]
9. Secades, P.; Alvarez, B.; Guijarro, J.A. Purification and properties of a new psychrophilic metalloprotease (Fpp2) in the fish pathogen *Flavobacterium psychrophilum*. *FEMS Microbiol. Lett.* **2003**, *226*, 273–279. [CrossRef]
10. Alvarez, B.; Alvarez, J.; Menendez, A.; Guijarro, J.A. A mutant in one of two exbD loci of a TonB system in *Flavobacterium psychrophilum* shows attenuated virulence and confers protection against cold water disease. *Microbiology* **2008**, *154*, 1144–1151. [CrossRef]
11. Jan, A.T. Outer Membrane Vesicles (OMVs) of Gram-negative Bacteria: A Perspective Update. *Front. Microbiol.* **2017**, *8*, 1053. [CrossRef] [PubMed]
12. Koeppen, K.; Hampton, T.H.; Jarek, M.; Scharfe, M.; Gerber, S.A.; Mielcarz, D.W.; Demers, E.G.; Dolben, E.L.; Hammond, J.H.; Hogan, D.A.; et al. A Novel Mechanism of Host-Pathogen Interaction through sRNA in Bacterial Outer Membrane Vesicles. *PLoS Pathog.* **2016**, *12*, e1005672. [CrossRef] [PubMed]
13. Sjostrom, A.E.; Sandblad, L.; Uhlin, B.E.; Wai, S.N. Membrane vesicle-mediated release of bacterial RNA. *Sci. Rep.* **2015**, *5*, 15329. [CrossRef] [PubMed]
14. Wyckoff, T.J.; Taylor, J.A.; Salama, N.R. Beyond growth: Novel functions for bacterial cell wall hydrolases. *Trends Microbiol.* **2012**, *20*, 540–547. [CrossRef]
15. Grabowski, L.; Lepek, K.; Stasilojc, M.; Kosznik-Kwasnicka, K.; Zdrojewska, K.; Maciag-Dorszynska, M.; Wegrzyn, G.; Wegrzyn, A. Bacteriophage-encoded enzymes destroying bacterial cell membranes and walls, and their potential use as antimicrobial agents. *Microbiol. Res.* **2021**, *248*, 126746. [CrossRef]
16. Eshwar, A.K.; Guldimann, C.; Oevermann, A.; Tasara, T. Cold-Shock Domain Family Proteins (Csps) Are Involved in Regulation of Virulence, Cellular Aggregation, and Flagella-Based Motility in Listeria monocytogenes. *Front. Cell Infect. Microbiol.* **2017**, *7*, 453. [CrossRef]
17. Yan, W.; Wang, H.; Xu, W.; Wu, K.; Yao, R.; Xu, X.; Dong, J.; Zhang, Y.; Zhong, W.; Zhang, X. SP0454, a putative threonine dehydratase, is required for pneumococcal virulence in mice. *J. Microbiol.* **2012**, *50*, 511–517. [CrossRef]
18. Stonehouse, E.; Kovacikova, G.; Taylor, R.K.; Skorupski, K. Integration host factor positively regulates virulence gene expression in Vibrio cholerae. *J. Bacteriol.* **2008**, *190*, 4736–4748. [CrossRef]
19. Poehlsgaard, J.; Douthwaite, S. The bacterial ribosome as a target for antibiotics. *Nat. Rev. Microbiol.* **2005**, *3*, 870–881. [CrossRef]
20. Lin, J.; Zhou, D.; Steitz, T.A.; Polikanov, Y.S.; Gagnon, M.G. Ribosome-Targeting Antibiotics: Modes of Action, Mechanisms of Resistance, and Implications for Drug Design. *Annu. Rev. Biochem.* **2018**, *87*, 451–478. [CrossRef]
21. Zschiedrich, C.P.; Keidel, V.; Szurmant, H. Molecular Mechanisms of Two-Component Signal Transduction. *J. Mol. Biol.* **2016**, *428*, 3752–3775. [CrossRef] [PubMed]
22. Sauvage, E.; Terrak, M. Glycosyltransferases and Transpeptidases/Penicillin-Binding Proteins: Valuable Targets for New Antibacterials. *Antibiotics* **2016**, *5*, 12. [CrossRef] [PubMed]
23. El Qaidi, S.; Zhu, C.; McDonald, P.; Roy, A.; Maity, P.K.; Rane, D.; Perera, C.; Hardwidge, P.R. High-Throughput Screening for Bacterial Glycosyltransferase Inhibitors. *Front. Cell Infect. Microbiol.* **2018**, *8*, 435. [CrossRef] [PubMed]
24. Galperin, M.Y. Telling bacteria: Do not LytTR. *Structure* **2008**, *16*, 657–659. [CrossRef] [PubMed]
25. Crater, D.L.; Moran, C.P., Jr. Identification of a DNA binding region in GerE from Bacillus subtilis. *J. Bacteriol.* **2001**, *183*, 4183–4189. [CrossRef] [PubMed]
26. Leonardi, R.; Jackowski, S. Biosynthesis of Pantothenic Acid and Coenzyme A. *EcoSal Plus* **2007**, *2*. [CrossRef]

27. Izard, T. A novel adenylate binding site confers phosphopantetheine adenylyltransferase interactions with coenzyme A. *J. Bacteriol.* **2003**, *185*, 4074–4080. [CrossRef]
28. Gupta, A.; Sharma, P.; Singh, T.P.; Sharma, S. Phosphopantetheine Adenylyltransferase: A promising drug target to combat antibiotic resistance. *Biochim. Biophys. Acta Proteins Proteom.* **2021**, *1869*, 140566. [CrossRef]
29. Yang, B.; Feng, L.; Wang, F.; Wang, L. Enterohemorrhagic *Escherichia coli* senses low biotin status in the large intestine for colonization and infection. *Nat. Commun.* **2015**, *6*, 6592. [CrossRef]
30. Yang, B.; Jiang, L.; Wang, S.; Wang, L. Global transcriptional regulation by BirA in enterohemorrhagic *Escherichia coli* O157:H7. *Future Microbiol.* **2018**, *13*, 757–769. [CrossRef]
31. Gouzy, A.; Poquet, Y.; Neyrolles, O. A central role for aspartate in Mycobacterium tuberculosis physiology and virulence. *Front. Cell Infect. Microbiol.* **2013**, *3*, 68. [CrossRef] [PubMed]
32. Ferla, M.P.; Patrick, W.M. Bacterial methionine biosynthesis. *Microbiology* **2014**, *160*, 1571–1584. [CrossRef] [PubMed]
33. Neis, E.P.; Dejong, C.H.; Rensen, S.S. The role of microbial amino acid metabolism in host metabolism. *Nutrients* **2015**, *7*, 2930–2946. [CrossRef] [PubMed]
34. Murima, P.; McKinney, J.D.; Pethe, K. Targeting bacterial central metabolism for drug development. *Chem. Biol.* **2014**, *21*, 1423–1432. [CrossRef]
35. Husna, A.U.; Wang, N.; Cobbold, S.A.; Newton, H.J.; Hocking, D.M.; Wilksch, J.J.; Scott, T.A.; Davies, M.R.; Hinton, J.C.; Tree, J.J.; et al. Methionine biosynthesis and transport are functionally redundant for the growth and virulence of *Salmonella Typhimurium*. *J. Biol. Chem.* **2018**, *293*, 9506–9519. [CrossRef]
36. Jurgenson, C.T.; Begley, T.P.; Ealick, S.E. The structural and biochemical foundations of thiamin biosynthesis. *Annu. Rev. Biochem.* **2009**, *78*, 569–603. [CrossRef]
37. Maupin-Furlow, J.A. Vitamin B1 (Thiamine) Metabolism and Regulation in Archaea. In *B Group Vitamins—Current Uses and Perspectives*; LeBlanc, J.G., Ed.; IntechOpen Limited: London, UK, 2018; pp. 9–31.
38. Liu, X.; Wang, X.; Sun, B.; Sun, L. The Involvement of Thiamine Uptake in the Virulence of Edwardsiella piscicida. *Pathogens* **2022**, *11*, 464. [CrossRef]
39. Rolando, M.; Silvestre, C.D.; Gomez-Valero, L.; Buchrieser, C. Bacterial methyltransferases: From targeting bacterial genomes to host epigenetics. *microLife* **2022**, *3*, uqac014. [CrossRef]
40. Marancik, D.; Gao, G.; Paneru, B.; Ma, H.; Hernandez, A.G.; Salem, M.; Yao, J.; Palti, Y.; Wiens, G.D. Whole-body transcriptome of selectively bred, resistant-, control-, and susceptible-line rainbow trout following experimental challenge with *Flavobacterium psychrophilum*. *Front. Genet.* **2014**, *5*, 453. [CrossRef]
41. Ayala-Castro, C.; Saini, A.; Outten, F.W. Fe-S cluster assembly pathways in bacteria. *Microbiol. Mol. Biol. Rev.* **2008**, *72*, 110–125. [CrossRef]
42. Zhu, Y.; Lechardeur, D.; Bernardet, J.F.; Kerouault, B.; Guerin, C.; Rigaudeau, D.; Nicolas, P.; Duchaud, E.; Rochat, T. Two functionally distinct heme/iron transport systems are virulence determinants of the fish pathogen *Flavobacterium psychrophilum*. *Virulence* **2022**, *13*, 1221–1241. [CrossRef] [PubMed]
43. Bruce, T.J.; Ma, J.; Sudheesh, P.S.; Cain, K.D. Quantification and comparison of gene expression associated with iron regulation and metabolism in a virulent and attenuated strain of *Flavobacterium psychrophilum*. *J. Fish Dis.* **2021**, *44*, 949–960. [CrossRef] [PubMed]
44. Reitzer, L. Biosynthesis of Glutamate, Aspartate, Asparagine, L-Alanine, and D-Alanine. *EcoSal Plus* **2004**, *1*. [CrossRef]
45. Xie, K.; Bunse, C.; Marcus, K.; Leichert, L.I. Quantifying changes in the bacterial thiol redox proteome during host-pathogen interaction. *Redox Biol.* **2019**, *21*, 101087. [CrossRef] [PubMed]
46. Yao, Q.; Zhang, L.; Wan, X.; Chen, J.; Hu, L.; Ding, X.; Li, L.; Karar, J.; Peng, H.; Chen, S.; et al. Structure and specificity of the bacterial cysteine methyltransferase effector NleE suggests a novel substrate in human DNA repair pathway. *PLoS Pathog.* **2014**, *10*, e1004522. [CrossRef]
47. Pan, J.; Zhao, M.; Huang, Y.; Li, J.; Liu, X.; Ren, Z.; Kan, B.; Liang, W. Integration Host Factor Modulates the Expression and Function of T6SS2 in *Vibrio fluvialis*. *Front. Microbiol.* **2018**, *9*, 962. [CrossRef]
48. UniProt. hupB—DNA-Binding Protein HU-Beta—*Escherichia coli* (Strain K12) | UniProtKB | UniProt. Available online: https://www.uniprot.org/uniprotkb/P0ACF4/entry (accessed on 2 September 2022).
49. El Yacoubi, B.; Bonnett, S.; Anderson, J.N.; Swairjo, M.A.; Iwata-Reuyl, D.; de Crecy-Lagard, V. Discovery of a new prokaryotic type I GTP cyclohydrolase family. *J. Biol. Chem.* **2006**, *281*, 37586–37593. [CrossRef]
50. Wu, Z.; Wouters, J.; Poulter, C.D. Isopentenyl diphosphate isomerase. Mechanism-based inhibition by diene analogues of isopentenyl diphosphate and dimethylallyl diphosphate. *J. Am. Chem. Soc.* **2005**, *127*, 17433–17438. [CrossRef]
51. Heuston, S.; Begley, M.; Gahan, C.G.M.; Hill, C. Isoprenoid biosynthesis in bacterial pathogens. *Microbiology* **2012**, *158*, 1389–1401. [CrossRef]
52. Drabinska, J.; Ziecina, M.; Modzelan, M.; Jagura-Burdzy, G.; Kraszewska, E. Individual Nudix hydrolases affect diverse features of *Pseudomonas aeruginosa*. *MicrobiologyOpen* **2020**, *9*, e1052. [CrossRef]
53. Lu, W.; Tan, J.; Lu, H.; Wang, G.; Dong, W.; Wang, C.; Li, X.; Tan, C. Function of Rhs proteins in porcine extraintestinal pathogenic *Escherichia coli* PCN033. *J. Microbiol.* **2021**, *59*, 854–860. [CrossRef] [PubMed]
54. Do, T.; Page, J.E.; Walker, S. Uncovering the activities, biological roles, and regulation of bacterial cell wall hydrolases and tailoring enzymes. *J. Biol. Chem.* **2020**, *295*, 3347–3361. [CrossRef] [PubMed]

55. Rochat, T.; Perez-Pascual, D.; Nilsen, H.; Carpentier, M.; Bridel, S.; Bernardet, J.F.; Duchaud, E. Identification of a Novel Elastin-Degrading Enzyme from the Fish Pathogen *Flavobacterium psychrophilum*. *Appl. Environ. Microbiol.* **2019**, *85*, e02535-18. [CrossRef] [PubMed]
56. Vermassen, A.; Leroy, S.; Talon, R.; Provot, C.; Popowska, M.; Desvaux, M. Cell Wall Hydrolases in Bacteria: Insight on the Diversity of Cell Wall Amidases, Glycosidases and Peptidases Toward Peptidoglycan. *Front. Microbiol.* **2019**, *10*, 331. [CrossRef]
57. van Heijenoort, J. Peptidoglycan hydrolases of *Escherichia coli*. *Microbiol. Mol. Biol. Rev.* **2011**, *75*, 636–663. [CrossRef]
58. Kroniger, T.; Flender, D.; Schluter, R.; Kollner, B.; Trautwein-Schult, A.; Becher, D. Proteome analysis of the Gram-positive fish pathogen *Renibacterium salmoninarum* reveals putative role of membrane vesicles in virulence. *Sci. Rep.* **2022**, *12*, 3003. [CrossRef]
59. Castillo, D.; Christiansen, R.H.; Dalsgaard, I.; Madsen, L.; Espejo, R.; Middelboe, M. Comparative Genome Analysis Provides Insights into the Pathogenicity of *Flavobacterium psychrophilum*. *PLoS ONE* **2016**, *11*, e0152515. [CrossRef]
60. Jarau, M.; Di Natale, A.; Huber, P.E.; MacInnes, J.I.; Lumsden, J.S. Virulence of *Flavobacterium psychrophilum* isolates in rainbow trout *Oncorhynchus mykiss* (Walbaum). *J. Fish Dis.* **2018**, *41*, 1505–1514. [CrossRef]
61. Sundell, K.; Landor, L.; Nicolas, P.; Jorgensen, J.; Castillo, D.; Middelboe, M.; Dalsgaard, I.; Donati, V.L.; Madsen, L.; Wiklund, T. Phenotypic and Genetic Predictors of Pathogenicity and Virulence in *Flavobacterium psychrophilum*. *Front. Microbiol.* **2019**, *10*, 1711. [CrossRef]
62. Gliniewicz, K.; Wildung, M.; Orfe, L.H.; Wiens, G.D.; Cain, K.D.; Lahmers, K.K.; Snekvik, K.R.; Call, D.R. Potential mechanisms of attenuation for rifampicin-passaged strains of *Flavobacterium psychrophilum*. *BMC Microbiol.* **2015**, *15*, 179. [CrossRef]
63. Chodisetti, P.K.; Reddy, M. Peptidoglycan hydrolase of an unusual cross-link cleavage specificity contributes to bacterial cell wall synthesis. *Proc. Natl. Acad. Sci. USA* **2019**, *116*, 7825–7830. [CrossRef] [PubMed]
64. Barbier, P.; Rochat, T.; Mohammed, H.H.; Wiens, G.D.; Bernardet, J.F.; Halpern, D.; Duchaud, E.; McBride, M.J. The Type IX Secretion System Is Required for Virulence of the Fish Pathogen *Flavobacterium psychrophilum*. *Appl. Envrion. Microbiol.* **2020**, *86*, e01769-17. [CrossRef] [PubMed]
65. Cepeda, C.; Garcıa-Márquez, S.; Santos, Y. Improved growth of *Flavobacterium psychrophilum* using a new culture medium. *Aquaculture* **2004**, *238*, 75–82. [CrossRef]
66. Silverstein, J.T.; Vallejo, R.L.; Palti, Y.; Leeds, T.D.; Rexroad, C.E., 3rd; Welch, T.J.; Wiens, G.D.; Ducrocq, V. Rainbow trout resistance to bacterial cold-water disease is moderately heritable and is not adversely correlated with growth. *J. Anim. Sci.* **2009**, *87*, 860–867. [CrossRef] [PubMed]
67. Paneru, B.; Al-Tobasei, R.; Palti, Y.; Wiens, G.D.; Salem, M. Differential expression of long non-coding RNAs in three genetic lines of rainbow trout in response to infection with *Flavobacterium psychrophilum*. *Sci. Rep.* **2016**, *6*, 36032. [CrossRef] [PubMed]
68. Ali, A.; Al-Tobasei, R.; Kenney, B.; Leeds, T.D.; Salem, M. Integrated analysis of lncRNA and mRNA expression in rainbow trout families showing variation in muscle growth and fillet quality traits. *Sci. Rep.* **2018**, *8*, 12111. [CrossRef]
69. de Jong, A.; Kuipers, O.P.; Kok, J. FUNAGE-Pro: Comprehensive web server for gene set enrichment analysis of prokaryotes. *Nucleic Acids Res.* **2022**, *50*, W330–W336. [CrossRef]
70. Hall, T.A. BioEdit: A user-friendly biological sequence alignment editor and analysis program for Windows 95/98/NT. *Nucleic Acids Symp. Ser.* **1999**, *41*, 95–98.

pathogens

MDPI

Article

Application of Phyto-Stimulants for Growth, Survival Rate, and Meat Quality Improvement of Tiger Shrimp (*Penaeus monodon*) Maintained in a Traditional Pond

Esti Handayani Hardi [1,*], Rudi Agung Nugroho [2], Maulina Agriandini [3], Muhammad Rizki [1], Muhammad Eko Nur Falah [1], Ismail Fahmy Almadi [1], Haris Retno Susmiyati [4], Rita Diana [5], Nurul Puspita Palupi [6], Gina Saptiani [1], Agustina Agustina [1], Andi Noor Asikin [7] and Komsanah Sukarti [1]

[1] Department of Aquaculture, Faculty of Fisheries and Marine Science, University of Mulawarman, Samarinda 75242, Kalimantan Timur, Indonesia
[2] Department of Biology Science, Faculty of Science Mulawarman University, Samarinda 75123, Kalimantan Timur, Indonesia
[3] Study Program of Aquaculture, Polytechnic of Lingga, Lingga 29872, Kepulauan Riau, Indonesia
[4] Faculty of Law, University of Mulawarman, Samarinda 75119, Kalimantan Timur, Indonesia
[5] Faculty of Forestry, University of Mulawarman, Samarinda 75116, Kalimantan Timur, Indonesia
[6] Faculty of Agriculture, University of Mulawarman, Samarinda 75117, Kalimantan Timur, Indonesia
[7] Departement of Fisheries Product Technology, Faculty of Fisheries and Marine Science, University of Mulawarman, Samarinda 75242, Kalimantan Timur, Indonesia
* Correspondence: estie_hardie@fpik.unmul.ac.id

Abstract: The tiger shrimp culture in East Borneo is commonly performed using traditional pond system management. In this work, the objective was to evaluate the application of *Boesenbergia pandurata* and *Solanum ferox* extract supplemented as feed additives considering shrimp growth, survival rate, and meat quality culture in a traditional pond. There were three dietary groups that were stocked with 300 shrimp in this study. The shrimp were maintained in a pond, separated with a 3×3 m^2 net. The dietary treatment applied was divided into three types, namely P1, without the extracts; P2, 20 mL kg^{-1} dietary supplementation; and P3, 30 mL kg^{-1} dietary supplementation in the diet. The findings revealed that the herb extract influenced the growth rate, feed efficiency, survival rate, and meat quality of the shrimp, mainly the amino and fatty acid contents in the shrimp meat. The 30 mL kg^{-1} herb extract dose in group 3 showed a higher growth performance and survival rate. In group 3, 98% of the shrimp could survive until the final study period, while 96% of shrimp survived in group 2, and 70% of the shrimp survived in group 1. These findings indicate that the phytoimmune (*B. pandurata* and *S. ferox)* extract can be utilized as a feed additive to improve the growth, survival rate, and meat quality of the shrimp.

Keywords: amino acids; fatty acids; natural fish drug; plant extract; silvofishery; tiger shrimp

1. Introduction

Tiger shrimp (*Penaeus monodon*) has become an excellent aquaculture commodity in East Borneo. The data show that tiger shrimp comprises the world's second largest fishery sector [1,2]. In East Borneo, the production value of tiger shrimp reached 27,506 tons in 2020 [3]. Therefore, tiger shrimp culture is a sector that could increase the regional income in East Borneo, besides that from coal. Shrimp cultured with the silvofishery system has been applied in some countries, namely Vietnam, Taiwan, and Thailand [4]. Silvofishery is a cultivation system for brackish water that has a low input, sustainable aquaculture, and is integrated with mangrove [5]. The traditional shrimp ponds in Indonesia cover a larger area than intensive ponds, but only about 20% of the land is used for active aquaculture. It has numerous issues, including water quality supply, SPF larva, and lack of farmer technology knowledge. It is believed that by only using intensification, greater production

can be obtained, and amaranth management has no drawbacks for improving production performance, whereas most communities manage their ponds in an extensive system with 36 ha per plot [6]. Pond management still relies on tides for the culture production cycle, as well as depending on live feed availability without water management handling either before or after the culture production process [7]. The occurrence of harvest failures is commonly caused by disease incidence [8]; high water quality fluctuation, mainly in DO and pH parameters; a slow growth rate; and high mortality level due to less available feed. Based on these problems, the utilization of plant extracts can achieve meaningful application, as plant extracts can help improve the growth performance and immunity level, besides increasing the amino and fatty acid quality in the shrimp meat, as well as being an additional nutrition source in shrimp feed [9–14].

The Indonesian Government, through the Ministry of Marine and Fisheries, has established a regulation regarding plant extract development as a standardized natural fish drug, as well as antibiotic and growth promoter usage limitation and restriction actions for cultured animals [15,16]. As a further action to prove the efficacy of plant extracts in shrimp culture, it is necessary to conduct a field experiment of plant extract formulations that have passed limited laboratory tests on a wider culture scale. The natural fish drug candidates made from ginger (*Boesenbergia pandurata*) and hairy-fruited eggplant (*Solanum ferox*) extracts have several phytoimmune compounds, namely flavonoids, alkaloids, and steroids, which function as antibacterial agents [7,17–19], immunostimulants [20], growth promoters [21], survival rate improvement agents [22], and additive ingredients in order to improve feed efficiency and growth performance [23]. This article will explain how these phyto-stimulants from *S. ferox* and *B. pandurata* extracts improvement the growth performance, immunomodulatory effect, mortality suppression, and meat quality of tiger shrimp maintained in the pond.

2. Materials and Methods

2.1. Culture Location

The pond used for the shrimp culture was a 1 Ha silvofishery pond in Solo Palai Village, Muara Badak Subdistrict, Kutai Kartanegara District, East Borneo (0°21′54.702″ S and 117°26′45.5028″ E). The pond was formed as a ditch, surrounding a *Rhizophora apiculata* mangrove plant with 1 m spacing and 80% density. Pond management was carried out in a traditional way, whereas the water exchanges followed the tidal cycle with a stocking density of 20 shrimp m^{-3}.

2.2. Experimental Animal

The experimental activity was performed for 40 days in October 2021. The tiger shrimp seeds used originated from the Center for Brackish Water and Marine Hatchery, Manggar, Balikpapan, East Borneo. Before stocking the pond, shrimp seeds with an average weight of 0.01 g were first maintained in the hatchery in order to reach an average weight of 2.26 ± 0.04 g.

The shrimp were previously selected based on their organ completion, marked by a transparent body color and incurved tail, less pigmented spots, well-formed eyes and eye-stalks, active-swimmers with a straight body and highly responsive to shock cues, reddish or pale color absence, and no glows observed in a dark room condition.

The maintenance tank in the hatchery was a 1×3 m squared tank filled with water at 0.75 m. The tiger shrimp maintenance tank in the pond was a 1×1 m net. As each treatment contained four replications, 12 nets were used to stock 100 shrimp seeds per net ($n = 100 \times 3 \times 4 = 1200$).

2.3. Plant Extracts

The plant extract used in this study was derived from *Boesenbergia pandurata* and *Solanum ferox.* It was obtained from Sempayau Village, Kutai Timur District, East Borneo, and the extraction process was performed using 98% ethanol [10]. The ingredient concen-

trations used comprised *B. pandurata* at 900 mg L^{-1} and *S. ferox* at 400 mg L^{-1} with a ratio of 2:1. The diets were produced by mixing the plant extract in the formulation following the diet ingredient composition in Table 1.

Table 1. Tiger shrimp diet formulation (g kg^{-1}) with phytoimmune extract supplementation.

Composition	P0	P1	P2
Shrimp head meal (g)	180	180	180
Fish meal (g)	320	320	320
Wheat flour (g)	220	220	220
Gluten meal (g)	60	60	60
Rice flour (g)	60	60	60
Soybean meal	100	100	100
Fish oil (mL)	20	20	20
Strach (g)	20	20	20
Mineral mix (g)	20	20	20
Phytoimmune [1] (mL)	0	20	30
	Approximate feed composition		
Water content (%)	8.27	8.3	8.22
Ash (%)	15.18	16.13	17.42
Crude protein (%)	35.22	35.4	35.53
Crude lipid (%)	2.26	3.42	3.1
Carbohydrate (%)	39.07	36.75	35.73

[1] *B. pandurata* and *S. ferox*.

The diet ingredients are described in Table 1. The ingredients were mixed with warm water (38 °C) until forming a homogenous dough, before being supplemented with the phytoimmune extract based on the applied doses. Each diet was extruded with a mini-pelletizer and dried under sunlight. The dried pellets from different diet types were packed separately in airtight plastic containers and preserved in a refrigerator for further use.

The shrimp were maintained for 40 days and fed with the formulated diets at 5% of the shrimp weight. Feeding was performed three times a day. The diet treatment groups in this study were divided into the following groups:

P0 = tiger shrimp fed without dietary extract supplementation
P1 = tiger shrimp fed with 20 mL kg^{-1} phytoimmune-supplemented diet
P2 = tiger shrimp fed with 30 mL kg^{-1} phytoimmune-supplemented diet

2.4. The Mortality and Growth

The mortality and growth parameters were measured every 10 days during the maintenance period, containing the total living shrimp, average body weight (ABW), average daily growth (ADG), and specific growth rate (SGR), based on the Aftabuddin et al. (2017) method [1]. The immunostimulatory activity of the shrimp was also observed at the final maintenance period, containing the total hemocytes (TH), phenol oxidase activity (PO), and anion-superoxide concentration (SO).

2.5. The Hemolymph

The hemolymph sample was taken at 100 mL with a 1 mL syringe filled with 0.9 mL anticoagulant (trisodium citrate 30 mM, NaCl 115 mM, and EDTA 10 mM, pH 6–7). The total hemocytes (TH) were counted using a Neubaeur hemocytometer [24]. The hemolymph–anticoagulant mixture (100 mL) was dropped in a hemocytometer and the hemocytes were counted in four different squares under the microscope; each point was presented as cell mL 1 hemolymph.

2.6. The Phenol Oxidase Activity (PO)

The PO of the hemocytes was determined using a spectrophotometer and L-dihydroxyphenylalanine (L-DOPA) as a standard [25]. Then, 50 mL of the hemolymph–anticoagulant

mixture was mixed with 50 mL of SDS 10% and 1.0 mL of L-dihydroxyphenylalanine (0.19% L-DOPA in Tris-HCl buffer), and then incubated for 30 min at 25 °C on 96-microliter plates. The dopachrome formation was measured every 30 s for 3 min in a spectrophotometer at a 490 nm wavelength. The PO activity was presented as the dopachrome formation per 50 mL of hemolymph.

2.7. The Amino and Fatty Acids

The meat quality of the shrimp (amino and fatty acids) was determined at the final maintenance period, while the water quality of the shrimp culture was measured once every 4 days, including temperature (27 ± 2 °C), salinity (16 ± 2 ppt), pH (7.6 ± 0.3), and DO (3–5 ppm). The measurement was performed in situ using a Waterproof Meter-HI98196 tool once every 4 days, in the morning and afternoon.

2.8. Data Analysis

The statistical analysis was carried out using STATISTICA v 13.2 (Statsoft Inc., Tulsa, OK, USA). For growth performance and survival rate parameters, different diet treatment groups were compared with each other using two-way ANOVA, followed by Tukey's test. The alpha was determined at 0.05 for all of the analyses.

3. Results

3.1. The Mortality and Growth

The mortality level (%) of the tiger shrimp maintained in the pond was low, at 10–20% for the plant extract-supplemented diet treatment groups (Figure 1), but reached 34% for the control diet treatment group. These data represent low total mortality levels of the tiger shrimp culture in the pond. A significant difference ($p < 0.05$) between the plant extracts supplemented diet and the control diet treatment groups indicates that the plant extract of *B. pandurata* and *S. ferox* could help improve the body condition sustainably during the ongoing culture activity.

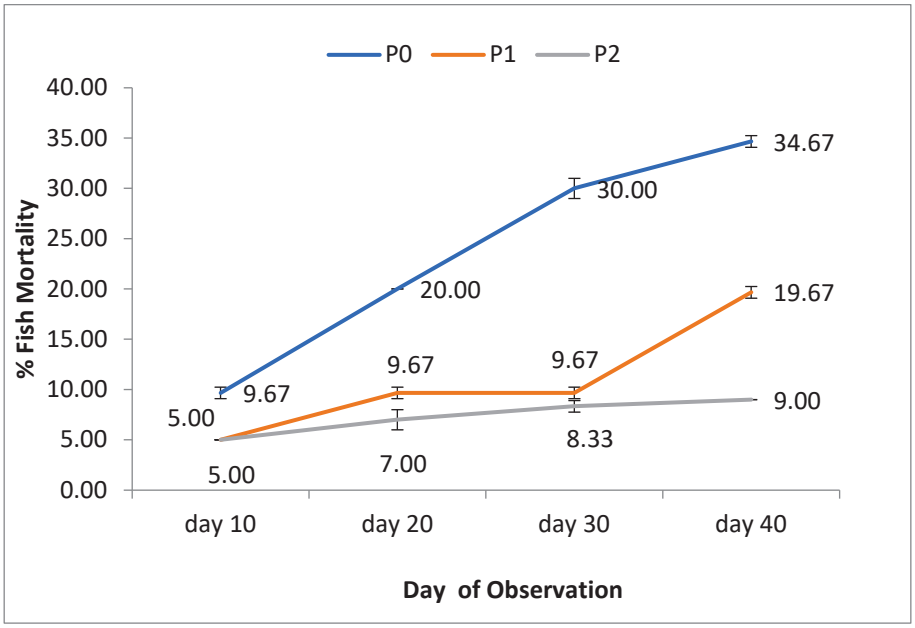

Figure 1. The *P. monodon* mortality percentage fed with phytoimmune supplemented diet and control diet for 40 days.

The shrimp growth performance (Table 2) was maintained for 40 days and those fed the 20-30 mL kg^{-1} plant extract supplemented diets weighed more than those without the plant extracts dietary supplementation, i.e., the average body weight, ABW; average

daily growth, ADG; and specific growth rate, SGR. These growth performance parameters were significantly different between the plant extracts supplemented diet and control diet treatment groups ($p < 0.05$). The 20 and 30 mL kg^{-1} diet dose had no significant difference ($p > 0.05$) on the ADG and SGR values, but showed a significant difference for the ABW value ($p < 0.05$).

Table 2. *P. monodon* growth performance after feeding with the diet treatment groups for 40 days.

Composition	Group	Observation Period			
		Day 10	**Day 20**	**Day 30**	**Day 40**
ABW (g)	P0	1.1 ± 0.1^{a}	2.1 ± 0.4^{b}	2.4 ± 0.1^{b}	3.9 ± 0.3^{c}
	P1	2.2 ± 0.2^{b}	4.1 ± 0.1^{c}	5.3 ± 0.0^{c}	6.2 ± 0.1^{d}
	P2	2.5 ± 0.2^{b}	4.8 ± 0.2^{c}	6.4 ± 0.2^{d}	7.2 ± 0.2^{e}
ADG (g day^{-1})	P0	0.11 ± 0.1^{a}	0.11 ± 0.1^{a}	0.08 ± 0.1^{a}	0.10 ± 0.1^{a}
	P1	0.22 ± 0.1^{b}	0.21 ± 0.1^{b}	0.18 ± 0.1^{b}	0.16 ± 0.1^{b}
	P2	0.25 ± 0.1^{c}	0.24 ± 0.1^{c}	0.21 ± 0.1^{c}	0.18 ± 0.1^{b}
SGR (%)	P0	0.95 ± 0.1^{a}	3.71 ± 0.1^{a}	2.92 ± 0.1^{a}	3.40 ± 0.1^{a}
	P1	7.88 ± 0.1^{b}	7.05 ± 0.1^{b}	5.56 ± 0.1^{b}	4.56 ± 0.1^{b}
	P2	9.16 ± 0.1^{b}	7.84 ± 0.1^{b}	6.19 ± 0.1^{b}	4.94 ± 0.1^{b}

Different superscript letters on the same line for each parameter show a significant difference ($p < 0.05$).

3.2. Immunomodulatory Activity

The total hemocytes of *P. monodon* after being fed with the phytoimmune-supplemented and controls diet are presented in Table 3. A significant difference ($p < 0.05$) was revealed among the different doses on the 10th day. A significant difference with the control diet treatment group was presented on the 20-th day in the 30 mL kg^{-1} diet dose, then the total hemocytes were found to be significantly different among the treatment groups on the 30th and 40th days.

Table 3. The immunomodulatory activity of shrimp fed with extract-supplemented diets and control diet. The total hemocytes (TH), phenol oxidase activity (PO), and anion superoxide concentration (SO).

Composition	Group	Observation Period			
		Day 10	**Day 20**	**Day 30**	**Day 40**
TH (10^5 cells mL^{-1})	P0	4.9 ± 0.4^{a}	4.7 ± 0.2^{a}	5.1 ± 0.2^{a}	5.1 ± 0.5^{a}
	P1	5.0 ± 0.2^{a}	5.1 ± 0.1^{a}	5.4 ± 0.1^{b}	5.4 ± 0.2^{b}
	P2	5.2 ± 0.3^{a}	5.5 ± 0.4^{b}	5.6 ± 0.4^{b}	5.7 ± 0.2^{b}
PO (OD 490 nm)	P0	0.19 ± 0.04^{a}	0.19 ± 0.04^{a}	0.19 ± 0.06^{a}	0.20 ± 0.02^{a}
	P1	0.18 ± 0.01^{a}	0.19 ± 0.04^{a}	0.20 ± 0.07^{a}	0.20 ± 0.01^{a}
	P2	0.20 ± 0.02^{b}	0.20 ± 0.02^{b}	0.21 ± 0.04^{b}	0.23 ± 0.03^{b}
SO (OD 630 nm)	P0	0.05 ± 0.01^{a}	0.06 ± 0.01^{a}	0.06 ± 0.02^{a}	0.06 ± 0.01^{a}
	P1	0.06 ± 0.01^{a}	0.07 ± 0.00^{a}	0.09 ± 0.01^{b}	0.08 ± 0.00^{b}
	P2	0.07 ± 0.00^{a}	0.07 ± 0.01^{a}	0.09 ± 0.01^{b}	0.09 ± 0.01^{b}

Different superscript letters on the same line for each parameter show a significant difference ($p < 0.05$).

The maximum phenol oxidase activity (PO) was found in the 30 mL kg^{-1} phytoimmune extract dose treatment group from the 10th to the 40th day of the observation period (Table 3). The anion superoxide concentration (SO) gradually increased in all treatment groups during the maintenance period (Table 3). The SO formation in the 20 and 30 mL kg^{-1} dose treatment groups was significantly higher on the 30th day of the maintenance period compared with in the control treatment group ($p < 0.05$).

3.3. Amino and Fatty Contents of Shrimp

The culture product quality, for example with shrimp, is mainly influenced by the culture process. The traditional maintenance system produces a more excellent product than the intensive system. The application of phytoimmune extracts made from *B. pandurata* and *S. ferox* can help improve several shrimp amino acids (body and head) (Table 4) and fatty acids (Table 5).

Table 4. Several amino acid contents (mg kg^{-1}) in shrimp meat and heads after feeding with 30 mL kg^{-1} of phytoimmune extracts and control diets.

Amino Acid Type (mg kg^{-1})	Shrimp Meat		Shrimp Head	
	Control	P2	Control	P2
L-Cystine	56,413.07	56,466.18	24,160.76	24,180.44
L-Methionine	8500.58	8520.86	2916.78	2918.05
L-Serine	24,633.41	24,716.14	14,953.73	14,999.02
L-Glutamic Acid	90,620.8	91,109.07	34,657.86	34,566.42
L-Phenylalanine	25,928.48	25,979.99	14,079.15	14,086.56
L-Isoleucine	24,248.84	24,341.69	11,318.36	11,345.83
L-Valine	25,367.82	25,549.14	14,749.06	14,810.70
L-Alanine	34,077.31	34,275.23	17,059.32	17,115.16
L-Arginine	52,698.91	52,975.34	16,568.30	16,625.57
Glycine	44,871.87	45,070.06	20,865.24	20,931.82
L-Lysine	51,634.89	51,881.43	16,421.97	16,475.75
L-Aspartic Acid	52,336.6	52,583.77	23,428.32	23,458.00
L-Leucine	43,825.49	44,013.44	17,229.53	17,268.10
L-Tyrosine	19,491.9	19,611.29	8731.65	8746.47
L-Proline	16,979.02	17,039.32	12,610.90	12,623.35
L-Threonine	27,163.5	27,301.99	14,497.80	14,522.81
L-Histidine	12,748.99	12,754.34	7409.95	7458.42
L-Tryptophan	2867.86	2873.6	2781.41	2795.45
Taurine	1349.4	1372.01	5609.91	5626.02

Table 5. Several fatty acid contents (%) in shrimp meat and head after feeding with 30 mL kg^{-1} of phytoimmune extracts and control diets.

Amino Acid Type (%)	Shrimp Meat		Shrimp Head	
	Control	P2	Control	P2
Linolenic Acid	0.0435	0.0452	0.0267	0.0272
Linoleic Acid	0.2582	0.2593	0.2632	0.2714
Oleic Acid	0.4290	0.4312	1.0678	1.0756
C 18:2 W6 (Linoleic Acid/W6)	0.2582	0.2593	0.2632	0.2714
C 18:2 W6C (C-Linoleic Acid)	0.2582	0.2593	0.2632	0.2714
C 18:1 W9C (C-Oleic Acid)	0.4290	0.4312	1.0678	1.0756
C 20:5 W3 (Eicosatpentaenoic Acid)	0.4188	0.4199	0.1193	0.1227
C 17:1 (Heptadecanoic Acid)	0.0365	0.0378	0.0454	0.0477
C 16:1 (Palmitoleic Acid)	0.0758	0.0788	0.0925	0.0947
C 20:4 W6 (Arachidonic Acid)	0.5616	0.5686	0.3444	0.3457
Omega 6 Fatty Acids	0.6234	0.8198	0.6089	0.6158
C 20:2 (Eicosadienoic Acid)	0.0290	0.0305	0.0268	0.0276
DHA	0.3070	0.3149	0.1243	0.1256
Omega 3 Fatty Acids	0.7721	0.7771	0.2720	0.2736
C 18:3 W3 (Linolenic Acid/W3)	0.0435	0.0452	0.0267	0.0272
C 24:0 (Lignoseric Acid)	0.0831	0.0849	0.0534	0.0543
Polyunsaturated Fat	1.7888	1.7917	1.0752	1.076
C 22:6 W3 (Docosahexanoic Acid)	0.307	0.3149	0.1243	0.1256
C 18:0 (Stearic Acid)	0.5055	0.5084	0.4736	0.4806
C 22:2 (Docosadinoic Acid)	0.1612	0.1628	0.1603	0.165
C 17:0 (Heptadecanoic Acid)	0.0968	0.1000	0.0702	0.0721
C 16:0 (Palmitic Acid)	0.5478	0.555	0.9938	1.0023
Unsaturated Fat	2.3324	2.3373	2.2832	2.2907
Omega 9 Fatty Acids	0.429	0.4312	1.0678	1.0756
C 15:0 (Pentadecanoic Acid)	0.0243	0.0251	0.0171	0.0171
AA	0.5616	0.5686	0.3444	0.3577
C 14:0 (Myristic Acid)	0.0244	0.025	0.036	0.038
EPA	0.4188	0.4199	0.1193	0.1227
C 12:0 (Lauraic Acid)	0.0099	0.0102	0.0337	0.0348
Monounsaturated Fat	0.5436	0.5456	1.208	1.2157
C 20:0 (Arachidic Acid)	0.00145	0.00156	0.0237	0.0241
Saturated Fat	1.2976	1.3027	1.7068	1.7193

Table 4 indicates that the amino acids in both the shrimp body and head fed with 30 mL kg-1 of a phytoimmune-extract-supplemented diet treatment were higher than for the control diet treatment, although there was a small difference in value for the L-Alanine content in shrimp meat for the P0 treatment as the control diet treatment at 34,077.31 mg kg^{-1} compared with the P2 treatment as the plant extract-supplemented diet treatment at 34,275.23 mg kg^{-1}. The attractive condition occurred in the L-Arginine and Taurine contents of the shrimp head, which were higher than the shrimp body meat.

Almost all of the fatty acids detected in the shrimp meat and head had a higher value in the 30 mL kg-1 phytoimmune-extract-dose treatment than in the control treatment. Several fatty acids were measured, but they remained undetected or showed a below threshold value, namely C 24:1 W9 (Nervonic Acid); C 18:1 W9T (T-Oleic Acid); C 23:0 (trichosanoic acid); C 8:0 (caprylic acid); C 15:1 (pentadecenoic acid); C 20:3 W6 (eicosatrienoic acid/W6); C 14:1 (miristoleic acid); C 13:0 (tridecanoic acid); C 18:3 W6 (linolenic acid/W6); C 11:0 (undecanoic acid); C 4:0 (butyric acid); C 18:2 W6T (T-linoleic acid); C 6:0 (caporic acid); C 20:3 W3 (eicosatrienoic acid/W3); C 22:1 (erucic acid); C 22:0 (behenic acid); C 21:0 (heneicosanoic acid); C 20:1 (eicocyanic acid); and C 10:0 (capric acid).

Similar to the amino acids, 10 fatty acids had a higher value in the shrimp head, such as C 18:2 W6C (C-linoleic acid); C 18:1 W9C (C-oleic acid); C 17:1 (heptadecanoic acid); C 16:1 (palmitoleic acid); C 16:0 (palmitic acid); omega 9 fatty acids; C 12:0 (lauraic acid); monounsaturated fat; C 20:0 (arachidic acid); and saturated fat.

4. Discussion

After the shrimp were maintained in the pond for 40 days, the tiger shrimp juveniles fed with dietary phytoimmune-extract product made from *B. pandurata* and *S. ferox* at a dose of 20 and 30 mL kg^{-1} showed a significant difference in value compared with the control treatment (P0) for the average body weight (g)/ABW, average daily growth/ADG, and SGR (%). The increased growth rate was caused by the application of non-isoenergic diet for shrimp juveniles. In addition, the increased growth rate of shrimp juveniles occurred as a result of the application of seaweed extract [8]. The plant extract could be utilized as a drug or a feed additive ingredient for fish and shrimp [26].

Shrimp fed with 30 mL kg^{-1} phytoimmune-extract-supplemented diet obtained the maximum average body weight (7.2 g) after 40 days of the maintenance period in the pond. This result was closed to the tiger shrimp growth rate after being fed with seaweed extract [26] and *Sargassum wightii* extract [27] at 7.09-8.54 g. Several plant extract applications, such as *Laurencia snyderiae*, *Hypnea cervicornis*, and *Crypto nemia,* also presented a positive effect on the growth of white shrimp *L. vannamei* [28,29]. The increased shrimp growth rate as mentioned above could be associated with the water quality of pond, vitamin and mineral contents, and the improvement in the diet nutrient absorption efficiency ratio in shrimp was found to be similar to that in [30]. The water quality of the traditional pond was in normal condition (Table 6). Its mean traditional management was preservation of the DO, pH, and salinity.

Table 6. Average pond water quality.

Parameter	Unit	Value
Temperature	°C	18–30
Salinity	‰	15–25
pH		5.5–8
Dissolved oxygen (DO)	mg L^{-1}	4–5
pH of pond substrate	-	6–8
Pyrite	‰	1.46–2.98

Crustacea such as shrimp have no adaptive or specific immune system, and thus only rely on the innate immunity (non-specific immune system), as an evolutionarily older immune strategy [31,32]. The most distinctive immune system in shrimp is a cellular

immune system [31,33]. The granular and agranular cells in shrimp are responsive cells against pathogens and other stressors [27].

The cellular immune response of *P. monodon* involves hemocytes, induced by the activation process of phenol oxidase (PO) through the phagocytosis process [1]. In this study, the application of 30 mL kg^{-1} phytoimmune extract could increase the maximum phenol oxidase activity (PO) significantly ($p < 0.05$). In addition, an increased SO level occurred significantly in the 20 and 30 mg L^{-1} phytoimmune-extract treatment groups on the 30th day of the maintenance period ($p < 0.05$). These data reveal a positive effect of *B. pandurata* and *S. ferox* (phytoimmune extracts) for improving the non-specific immunity of tiger shrimp. The cellular immune response is the primary immune response in shrimp against pathogens and stress. Both the PO and SO levels indicate the shrimp's health.

The dietary supplementation of the plant extract could increase the total hemocytes of the tiger shrimp [34], similar to the application of phytoimmune-extract dietary supplementation in this study, which gradually increased the total hemocytes. Another study that followed this result was found on the supplementation of red seaweed *Gracilaria fisheri* extract in *P. monodon*, which showed an increased THC value in the post-supplementation period [35]. In shrimp, hemocytes play an important role in cellular immune system, and are more sensitive to pathogens [36]. One of the effective immune responses in the invertebrates is the phenol oxidase system. When the phenol oxidase enzyme activity declines, the phagocytosis process will fail. The hemocytes activated will simultaneously produce other bactericidal substances, such as H_2O_2 and superoxide anion (O_2), and help induce the resistance level to infectious and non-infectious diseases [37]. Shrimp, unlike fish, lack leukocytes and must rely on hemocytes to transport nutrients. Hemocytes in shrimp contain granular, agranular, and hyaline cells. Increased THC levels indicate that the shrimp are in good health and are growing well.

The total hemocytes of tiger shrimp gradually increased from the first 10 days after the phytoimmune-extract dietary supplementation treatments, as the highest total hemocyte value was found in the 30 mL kg^{-1} diet dose at $5.7 \pm 0.2 \times 10^5$ cells mL^{-1}. The increased TH in shrimp also occurred in another dietary extract supplementation dose, which indicates that the cell performance improved well for producing TC compared with the control treatment without the dietary phytoimmune-extract supplementation.

Hemocytes have an important role in cellular immunity, although migrating continuously as in macrophages in fish, which have a high sensitivity level against pathogens [36]. The effective immune system in the invertebrates is a phenol oxidase system. When the phenol oxidase enzyme activity declines, the phagocytosis process will fail. As mentioned in this study, the increased TH was also followed by the increased PO and SO.

PO will be formed when the ProPO reacts with several compounds, such as zymosans (carbohydrates of yeast cell wall), bacterial lipopolysaccharides (LPS), urea, calcium ion, and tripsin [26]. In this study, shrimp fed with the 20 and 30 mL kg^{-1} phytoimmune-extract-supplemented diet showed a significantly higher PO concentration than the control diet group. The immunology parameter revealed the gradual increase in PO activity on the 10th day in the P2 treatment and the 20th day in the P1 treatment, which indicates that the shrimp larvae immune system was improved. The increased TH, PO, and SO levels has also been shown in *P. monodon* supplemented with the β-glucan immunostimulatory herbs [8,27,37].

The increased immune system in shrimp fed with the phytoimmune-extract-supplemented diets provided a good protection during the maintenance period in the pond, as a low mortality level at only 10-15% occurred in the phytoimmune extract application treatment groups. The tiger shrimp growth performance also significantly increased on the 40-th day of the maintenance period, although showing no significant difference between the 20 and 30 mL kg^{-1} doses. Only ABW obtained a significant different value between the different doses.

Shrimp contain an adequate amount of these omega-3 fats, and the fatty acid composition, as well as the MUFA/SFA, PUFA/SFA, w-3/w-6, and EPA/DHA fatty acid ratios,

differed between species and diet. The variation of shrimp culture method, shrimp feed, and water quality could be attributed to differences in shrimp amino acid and fatty acid composition. When comparing meat and poultry, we conclude that shrimp are one of the most nutritious foods. Thus, the current study emphasizes that the shrimp are nutritionally dense, containing all of the proteins, lipids, amino acids, and fatty acids, and can serve as an effective diet supplement, as well as be encouraged for aquaculture under controlled environmental conditions.

The amounts of AA, EPA, and DHA in tiger prawns with the extract were higher than those without the extract, with high DHA of 0.3149%, EPA of 0.4199%, and AA of 0.5686%. The amount of DHA (C22:6w-3) was higher than the amount of EPA (C20:5w-3) based on research of Bragagnolo and Rodriguez-Amaya, some species of shrimp *Xiphopenaeus kroyeri* [38], and pink shrimp, *Parapenaeus longirostris* [39] were similar. According to Oksuz et al. [40], the DHA content of *P. monodon* and *P. vannamei* was higher than that of EPA. The content of AA and EPA was higher than the DHA in this study, indicating that the fatty acid composition of *P. monodon* shrimp muscle was influenced by feed, size, salinity, temperature, season, and the Mahakam Delta's geographic location.

Traditional culture, using plant extracts, showed a satisfying yield. Besides shrimp growth and survival rate, the quality of meat containing amino acids and fatty acids was also increased. Shrimp farmers and local governments should reconsider using plant extract products in aquaculture because it provides more economic and environmental benefits.

5. Conclusions

Many factors influence the shrimp production level in ponds, specifically in the tradition pond system management performed by the community in East Borneo. This study presents an illustration and description of the phytoimmune extract supplementation efficacy, containing hairy-fruited eggplant and ginger extract at 2:1 ratio, for improving the growth performance (ABW, ADG, and SGR); inducing the TH, phenol oxidase activity (PO), anion superoxide (SO), and suppressing the shrimp mortality level when cultured in a pond. Both diets for 20 and 30 mL kg^{-1} dose of phytoimmune extract obtained a similar efficacy level. However, specific studies to identify the specific compounds in hairy-fruited eggplant and ginger that have an active role both in tiger shrimp growth performance and immunity response should be conducted further.

Author Contributions: Conceptualization, E.H.H. and G.S.; methodology, R.A.N.; software, M.A.; validation, E.H.H. and R.A.N.; formal analysis, M.R.; investigation, M.E.N.F. and I.F.A.; resources, H.R.S. and A.N.A.; data curation, R.D.; writing—original draft preparation, E.H.H.; writing—review and editing, E.H.H. and M.A.; visualization, A.A.; supervision, K.S.; project administration, N.P.P.; funding acquisition, E.H.H. All authors have read and agreed to the published version of the manuscript.

Funding: This research was funded by matching fund of Indonesian Sovereignty in Design (Kedaireka), Directorate General of Higher Education, Research, and Technology, Ministry of Education, Culture, Research, and Technology, grant number 2821/E3/SK.07/KL/2021.

Institutional Review Board Statement: The animal study protocol was approved by the Ethical Commission for Health Research, Mulawarman University (protocol code 89/KEPK-FK/VI/2022 and 24 June 2022).

Informed Consent Statement: Not applicable.

Data Availability Statement: Not applicable.

Acknowledgments: We would like to thank Peatland and Mangrove Restoration Agency of the Republic of Indonesia (BRGM RI), Ministry of Research, Technology, and Higher Education Indonesia, Faculty of Fishery and Marine Science, Faculty of Forestry, Faculty of Agriculture, and Faculty of Law for support, as well as all of the lecturers and students involved in the Kedaireka project in 2021.

Conflicts of Interest: The authors declare no conflict of interest.

References

1. Deris, Z.M.; Iehata, S.; Ikhwanuddin, M.; Sahimi, M.B.M.K.; Do, T.D.; Sorgeloos, P.; Sung, Y.Y.; Wong, L.L. Immune and bacterial toxin genes expression in different giant tiger prawn, *Penaeus monodon* post-larvae stages following AHPND-causing strain of *Vibrio parahaemolyticus* challenge. *Aquac. Res.* **2020**, *16*, 100248. [CrossRef]
2. FAO. *The State of World Fisheries and Aquaculture: Meeting the Sustainable Development Goals*; FAO Fisheries and Aquaculture Department: Italy, Rome, 2018.
3. BPS. *Statistical Yearbook of Indonesia*; BPS-Statistical Indonesia: Jakarta, Indonesia, 2020.
4. Belton, B.; Little, D. The development of aquaculture in central Thailand: Domestic demand versus export-led production. *J. Agrar. Chang.* **2008**, *8*, 123–143. [CrossRef]
5. Fitzgerald, W.J. Integrated mangrove forest and aquaculture systems in Indonesia. In *Mangrove-Friendly Aquaculture, Proceedings of the Workshop on Mangrove-Friendly Aquaculture, Iloilo City, Philippines, 11–15 January 1999*; Primavera, J.H., Garcia, L.M.B., Castaños, M.T., Surtida, M.B., Eds.; Southeast Asian Fisheries Development Center, Aquaculture Department: Tigbauan, Philippines, 2000; pp. 21–34.
6. Bosma, R.H.; Tendencia, E.A.; Bunting, S.W. Financial feasibility of green-water shrimp farming associated with mangrove compared to extensive shrimp culture in the Mahakam Delta, Indonesia. *Asian Fish. Sci.* **2012**, *25*, 258–269. [CrossRef]
7. Akber, M.A.; Aziz, A.A.; Lovelock, C. Major drivers of coastal aquaculture expansion in Southeast Asia. *Ocean. Coast. Manag.* **2020**, *198*, 105364. [CrossRef]
8. Aftabuddin, S.; Siddique, M.A.M.; Romkey, S.S.; William, S.L. Antibacterial function of herbal extracts on growth, survival and immunoprotection in the black tiger shrimp *Penaeus monodon*. *Fish Shellfish Immunol.* **2017**, *65*, 52–58. [CrossRef]
9. Citarasu, T.; Venkatramalingam, K.; Babu, M.; Sekar, R.R.; Petermarian, M. Influence of the antibacterial herbs, *Solamum trilobatum*, *Androgra phispaniculata* and *Psoralea corylifolia* on the survival, growth and bacterial load of *Penaeus monodon* post larvae. *Aquac. Int.* **2003**, *11*, 581–595. [CrossRef]
10. Galina, J.; Yin, G.; Ardo, L.; Jeney, Z. The use of immunostimulating herbs in fish. An overview of research. *Fish Physiol. Biochem.* **2009**, *35*, 669–676. [CrossRef]
11. Harikrishnan, R.; Kim, J.S.; Kim, M.C.; Balasundaram, C.; Heo, M.S. *Lactuca indica* extract as feed additive enhances immunological parameters and disease resistance in *Epinephelus bruneus* to *Streptococcus iniae*. *Aquaculture* **2011**, *318*, 43–47. [CrossRef]
12. Immanuel, G.; Uma, R.P.; Iyapparaj, P.; Citarasu, T.; Peter, S.M.P.; Babu, M.; Palavesam, A. Dietary medicinal plant extracts improve growth, immune activity and survival of tilapia *Oreochromis mossambicus*. *J. Fish Biol.* **2009**, *74*, 1462–1475. [CrossRef]
13. Sivaram, V.; Babu, M.; Immanuel, G.; Murugadass, S.; Citarasu, T.; Marian, M.P. Growth and immune response of juvenile greasy groupers (*Epinephelus tauvina*) fed with herbal antibacterial active principle supplemented diets against *Vibrio harveyi* infections. *Aquaculture* **2004**, *237*, 9–20. [CrossRef]
14. Vaseeharan, B.; Thaya, R. Medicinal plant derivatives as immunostimulants: An alternative to chemotherapeutics and antibiotics in aquaculture. *Aquacult. Int.* **2011**, *22*, 1079–1091. [CrossRef]
15. Ministry of Agriculture No 14. In *Klasifikasi Obat Hewan*; Menteri Pertanian Republik Indonesia: Jakarta, Indonesia, 2017; p. 25.
16. Ministry of Marine and Fisheries, No.1. In *Obat Ikan*; Menteri Kelautan dan Perikanan Republik Indonesia: Jakarta, Indonesia, 2019; p. 151.
17. Hardi, E.H.; Saptiani, G.; Kusuma, I.; Suwinarti, W.; Sudaryono, A. Inhibition of fish bacteria pathogen in tilapia using a concoction three of *Borneo plant* extracts. *IOP Conf. Ser. Earth Environ. Sci.* **2018**, *144*, 012015. [CrossRef]
18. Hardi, E.H.; Kusuma, I.W.; Suwinarti, W.; Agustina, A.; Nugroho, R.A. Antibacterial activity of *Boesenbergia pandurata*, *Zingiber zerumbet* and *Solanum ferox* extracts against *Aeromonas hydrophila* and *Pseudomonas* sp. *Nusant. Biosci.* **2016**, *8*, 18–21. [CrossRef]
19. Hardi, E.H.; Saptiani, G.; Nurkadina, M.; Kusuma, I.W.; Suwinarti, W. In Vitro test of concoction extracts *Boesenbergia pandurata*, *Solanum ferox*, *Zingimber zerumbet* against pathogen bacteria in tilapia. *J. Vet.* **2018**, *19*, 35–44.
20. Hardi, E.H.; Nugroho, R.A.; Kusuma, I.; Apriza, A. Immunomodulatory effect and disease resistance from concoction three of *Borneo plant* extracts in tilapia, *Oreochromis niloticus*. *J. Aquac. Indones.* **2019**, *20*, 41–47. [CrossRef]
21. Hardi, E.H.; Saptiani, G.; Nugroho, R.A.; Rahman, F.; Sulistyawati, S.; Rahayu, W.; Kusuma, I.W. *Boesenbergia pandurate* application un *Gold fish* feed to enhancing fish growth, immunity system, and resistance to bacterial infection. *F1000 Res.* **2021**, *10*, 766. [CrossRef]
22. Hardi, E.H.; Nugroho, R.A.; Kusuma, I.W.; Suwinarti, W.; Sudaryono, A.; Rostika, R. Borneo herbal plant extracts as a natural medication for prophylaxis and treatment of *Aeromonas hydrophila* and *Pseudomonas fluorescens* infection in tilapia (*Oreochromis niloticus*). *F1000 Res.* **2018**, *7*, 1847. [CrossRef]
23. Hardi, E.H.; Nugroho, R.A.; Rostika, R.; Mardliyaha, S.M.; Sukarti, K.; Rahayu, W.; Supriansyah, A.; Saptiani, G. Synbiotic application to enhance growth, immune system, and disease resistance toward bacterial infection in catfish. *Aquaculture* **2022**, *549*, 737794. [CrossRef]
24. Yeh, S.T.; Lee, C.S.; Chen, J.C. Administration of hot-water extract of brown seaweed Sargassum duplicatum via immersion and injection enhances the immune resistance of white shrimp *Litopenaeus vannamei*. *Fish Shellfish Immunol.* **2006**, *20*, 332–345. [CrossRef]
25. Gigi, P. Immune Response of *Penaeus Monodon* to the Inactivated White Spot Syndrome Virus Preparation. Ph.D. Thesis, Cochin University of Science and Technology, Kochi, India, 2011.
26. Chang, J. Medicinal herbs: Drugs or dietary supplements? *Biochem. Pharmacol.* **2000**, *59*, 211–219. [CrossRef]

27. Huxley, V.; Lipton, A. Immunomodulatory effect of *Sargassum wightii* on *Penaeus monodon* (Fab.). *Asian J. Anim. Sci.* **2009**, *4*, 192–196.
28. Da Silva, R.L.; Barbosa, J.M. Seaweed meal as a protein source for the white shrimp *Litopenaeus vannamei*. *J Appl. Phycol.* **2009**, *21*, 193–197. [CrossRef]
29. Dashtiannasab, A.; Yeganeh, V. The effect of ethanol extract of a macroalgae *Laurencia snyderia* on growth parameters and vibriosis resistance in shrimp *Litopenaeus vannamei*. *Iran. J. Fish. Sci.* **2017**, *16*, 210–221.
30. Cruz-Suarez, L.; Tapia-Salazar, M.; Nieto-Lopez, M.; Guajardo-Barbosa, C.; Ricque-Marie, D. Comparison of *Ulva clathrata* and the kelps *Macrocystis pyrifera* and *Ascophyllum nodosum* as ingredients in shrimp feeds. *Aqua. Nutri.* **2009**, *15*, 421–430. [CrossRef]
31. Loof, T.G.; Schmidt, O.; Herwald, H.; Theopold, U. Coagulation systems of invertebrates and vertebrates and their roles in innate immunity: The same side of two coins? *J. Innate Immun.* **2011**, *3*, 34–40. [CrossRef]
32. Chang, C.F.; Su, M.S.; Chen, H.Y.; Liao, I.C. Dietary b-1, 3-glu- can effectively improves immunity and survival of *Penaeus monodon* challenged with white spot syndrome virus. *Fish Shellfish Immunol.* **2003**, *15*, 297–310. [CrossRef]
33. Kimbrell, D.A.; Beutler, B. The evolution and genetics of innate immunity. *Nat. Rev. Genet.* **2001**, *2*, 256–267. [CrossRef]
34. Citarasu, T.; Sivaram, V.; Immanuel, G.; Rout, N.; Murugan, V. Influence of selected Indian immunostimulant herbs against white spot syndrome virus (WSSV) infection in black tiger shrimp, *Penaeus monodon* with reference to haematological, biochemical and immunological changes. *Fish Shellfish Immunol.* **2006**, *21*, 372–384. [CrossRef]
35. Kanjana, K.; Radtanatip, T.; Asuvapongpatana, S.; Withyachumnarnkul, B.; Wongprasert, K. Solvent extracts of the red seaweed *Gracilaria fisheri* prevent *Vibrio harveyi* infections in the black tiger shrimp *Penaeus monodon*. *Fish Shellfish Immunol.* **2011**, *30*, 389–396. [CrossRef]
36. Le Moullac, G.; Soyez, C.; Saulnier, D.; Ansquer, D.; Avarre, J.C.; Levy, P. Effect of hypoxic stress on the immune response and the resistance to vibriosis of the shrimp *Penaeus stylirostris*. *Fish Shellfish Immunol.* **1998**, *8*, 621–629. [CrossRef]
37. Ong, Y.L.; Hsieh, Y.T. Immunostimulation of tiger shrimp (*Penaeus monodon*) hemocytes for generation of microbicidal substances: Analysis of reactive oxygen species. *Dev. Comp. Immunol.* **1994**, *18*, 201–209.
38. Bragagnolo, N.; Rodriguez-Amaya, D.B. Total lipid, cholesterol, and fatty acids of farmed freshwater prawn (*Macrobrachium rosenbergii*) and wild marine shrimp (*Penaeus brasiliensis*, *Penaeus schimitti*, *Xiphopenaeus kroyeri*). *J. Food Comp. Anal.* **2021**, *14*, 359–369. [CrossRef]
39. Rosa, L.; Nunes, M.L. Nutritional quality of red shrimp, Aristeus antennatus (Risso), pink shrimp, *Parapenaeus longirostris* (Lucas) and *Norway lobster*, *Nephrops norvegicus* (Linnaeus). *J. Sci. Food. Agric.* **2004**, *84*, 89–94. [CrossRef]
40. Oksuz, A.; Ozyilmaz, A.; Aktas, M.; Gercek, G.; Motte, J. A comparative study on proximate, mineral and fatty acid compositions of deep seawater rose shrimp (*Parapenaeus longirostris*, Lucas 1846) and red shrimp (*Plesionika martia*, A. Milne-Edwards, 1883). *J. Anim. Vet. Adv.* **2009**, *8*, 183–189.

MDPI AG
Grosspeteranlage 5
4052 Basel
Switzerland
Tel.: +41 61 683 77 34

Pathogens Editorial Office
E-mail: pathogens@mdpi.com
www.mdpi.com/journal/pathogens

MDPI

Academic Open
Access Publishing

mdpi.com

ISBN 978-3-7258-5606-0